AGSO

Stream Sediment Geochemistry of the Red River Region, Cape York Peninsula, North Queensland

by

B. I. Cruikshank

Record 1997/21

AGSO

AUSTRALIAN
GEOLOGICAL SURVEY
ORGANISATION

Stream sediment geochemistry of the Red River Region, Cape York Peninsula, north Queensland

Record 1997/21

B I Cruikshank

DEPARTMENT OF PRIMARY INDUSTRIES AND ENERGY

Minister for Primary Industries and Energy: Hon. J. Anderson, M.P.
Minister for Resources and Energy: Senator the Hon. W.R. Parer
Secretary: Paul Barratt

AUSTRALIAN GEOLOGICAL SURVEY ORGANISATION

Executive Director: Neil Williams

ISSN: 1039-0073
ISBN: 0 642 25029 4

Contents

SUMMARY v

1. INTRODUCTION **1**
1.1 Survey Area 1
1.2 Climate 1
1.3 Physiography, Vegetation and Access 3

2. GEOLOGY and MINERALISATION **5**
2.1 Geology 5
2.1.1 Proterozoic Rocks 6
2.1.2 Palaeozoic Rocks 8
2.1.2.1 Silurian-Devonian Rocks 8
2.1.2.2 Carboniferous-Permian Rocks 8
2.1.3 Mesozoic Rocks 9
2.1.4 Cainozoic Rocks 10
2.2 Mineralisation 10
2.2.1 Gold and silver 10
2.2.2 Copper 10
2.2.3 Lead and Zinc 12
2.2.4 Tin and Tungsten 12
2.2.5 Uranium 12

3. SAMPLING, CHEMICAL ANALYSIS and DATA PROCESSING **13**
3.1 Sampling 13
3.2 Chemical Analysis 15
3.2.1 AGSO Analyses 15
3.2.2 ICP-MS Analyses 16
3.2.3 Bulk Cyanide Leach Analyses 16
3.3 Data Analysis 17

4. STATISTICAL ANALYSIS **19**
4.1 Duplicate Samples 19
4.2 Summary Univariate Statistics 19
4.3 Summary Multivariate Statistics 22
4.3.1 Correlations 22
4.3.2 Factor Analysis 22

5 INTERPRETATION **25**
5.1 Factor 1 (Ce, Nd, La, Th, Y, U, P and Nb) 25
5.2 Factor 2 (V, Fe, Ni, Sc, Cu, Cr, Ti, Zn and Mn) 36
5.3 Factor 3 (Rb, Tl, Be, Ga, Ba, Pb and Sr) 44
5.4 Factor 4 (Bi, Sn, Hf, W and Zr) 54
5.5 Factor 5 (Pt, Au and As) 62
5.6 Factor 6 (Cd and Ge) 67
5.7 Factor 7 (Sb and Mo) 69
5.8 Factor 8 (Pd) 69
5.9 Mineral Potential 69

5.9.1 Element Residuals..... 71
5.9.2 Additive Indices..... 71
5.9.2.1 Gold Index..... 73
5.9.2.2 Base Metal Index..... 73
5.9.2.3 Heavy Mineral Index..... 73
5.9.2.4 Porphyry Copper Index..... 76
5.9.2.5 Platinum Index..... 76
5.9.2.6 Uranium Index..... 76
6. CONCLUSIONS..... 76
7 ACKNOWLEDGMENTS..... 78
8 REFERENCES..... 79
APPENDIXES A, B and C

SUMMARY

A regional stream sediment sampling program in the Georgetown Region was carried out in association with geological and regolith mapping by the Australian Geological Survey Organisation and the Geological Survey of Queensland, under the National Geoscience Mapping Accord. The survey area covered parts of the RED RIVER, ATHERTON, GEORGETOWN and EINASLEIGH 1:250 000 map sheet areas. The samples were analysed for 39 elements, including Au by the bulk cyanide leach method, and image maps showing the spatial distribution of each element and a number of statistically derived parameters, including factor scores, element residuals and additive indices, have been prepared. The full dataset is available separately, and colour versions of all image maps are available in a separate atlas.

Variability in the data can be accounted for by 8 factors with the most important being the accumulation of resistant minerals such as monazite and xenotime in the stream sediment (Factor 1), Fe geochemistry, either as Fe-rich minerals in the bedrock or as Fe scavenging in the secondary environment (Factor 2), and the weathering of K-rich minerals (Factor 3). Residual values for Cu, Pb, U and Zn, for which bedrock lithochemical contributions have been removed, showed areas which may be prospective for these elements.

The greatest potential appears to be for gold, base metals and tin, with some possibility for uranium and Rare Earth-rich heavy minerals.

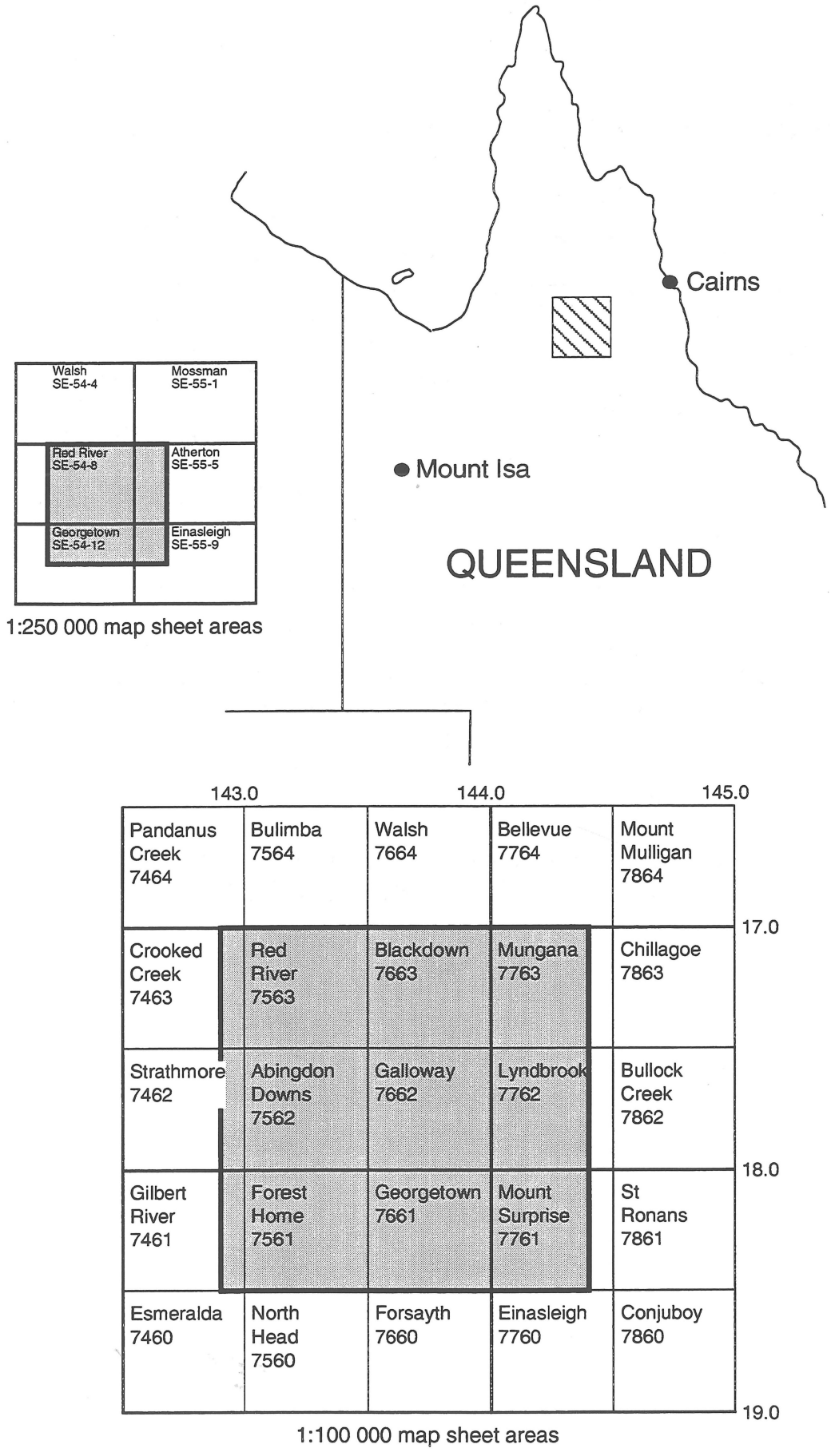

Figure 1. Location of Red River Region survey area.

INTRODUCTION

This study forms part of the North Queensland, National Geoscience Mapping Accord (NGMA) project undertaken by the Australian Geological Survey Organisation (AGSO) and the Geological Survey of Queensland (GSQ). The NGMA, endorsed by the Australian (now Australian and New Zealand) Minerals and Energy Council in August 1990, is a joint Commonwealth/State/Territory initiative to produce, using modern technology, a new generation of geoscientific maps, data sets, and other information on strategically important regions of Australia.

The study area covers Cape York Peninsula and extends from Charters Towers in the south to Normanton in the west and Cape York in the north, and includes the islands in the Torres Strait. The area has important mineral resources, for example the bauxite deposits at Weipa, but includes areas of world heritage value. The project was undertaken to provide the sound, current geoscientific data necessary for resolution of potentially conflicting land-use demands, and to facilitate efficient, effective exploration for mineral resources.

Activity during the 1992 field season centred on the RED RIVER Region, essentially the eastern part of the RED RIVER 1:250 000 map sheet and parts of neighbouring sheet areas (Figure 1). The 1992 sampling was supplemented by sampling carried out during the following (1993) field program, which completed work in the northern part of the survey area. This record describes the surficial (stream sediment) geochemical sampling program over the RED RIVER Region.

1.1 Survey Area

Stream sediment sampling was carried out over most of the ABINGDON DOWNS and GALLOWAY, and parts of the BLACKDOWN, MUNGANA, LYNDBROOK, FOREST HOME, GEORGETOWN and MOUNT SURPRISE 1:100 000 map sheet areas, which encompass the eastern part of the RED RIVER 1:250 000 sheet area (ABINGDON DOWNS, GALLOWAY and BLACKDOWN), and adjacent parts of the ATHERTON (LYNDBROOK and MUNGANA), EINASLEIGH (MOUNT SURPRISE) and GEORGETOWN (FOREST HOME and GEORGETOWN) 1:250 000 sheet areas. The survey area is bounded by latitudes 17.0° and 18.5°S, and longitudes 142.9° and 144.4°E.

Land tenure in the area is mostly pastoral holdings, including Abingdon Downs (plus Eden Vale Outstation), Blackdown, Bolwarra (plus Piccaninny Outstation), Dagworth, Eveleigh, Ironhurst, Mount Surprise, Mount Turner, Talaroo, Torwood and Van Lee stations (Figure 2(a)). The area also includes several small mining leases, the O'Briens Creek Mineral Field (mainly topaz) and a former pastoral property recently taken over as the Bulleringa National Park.

The area is reasonably remote with the main access, the Gulf Development Road the only sealed road. This and the secondary access roads and station roads are often impassable during the wet season due to the many river and creek crossings. Off-road vehicle and foot access is generally good in the pastoral leases because of tracks pushed into remote areas by the pastoralists, and because of the cattle-paths along stream banks. The townships of Georgetown and Mount Surprise occur on or near the southern margin of the work area, and Chillagoe is well to the east. Georgetown and Mount Surprise are on the Gulf Development Road and Mount Surprise is on the Cairns-Forsayth railway line. The weekly mail plane calls at Georgetown and at several properties in the area.

1.2 Climate

The area has a semi-arid, monsoonal climate with heavy rains largely restricted to the period November-April. Average annual rainfall at Georgetown township is 831 mm (Bureau of Meteorology, 1971). River and stream flow patterns closely follow rainfall.

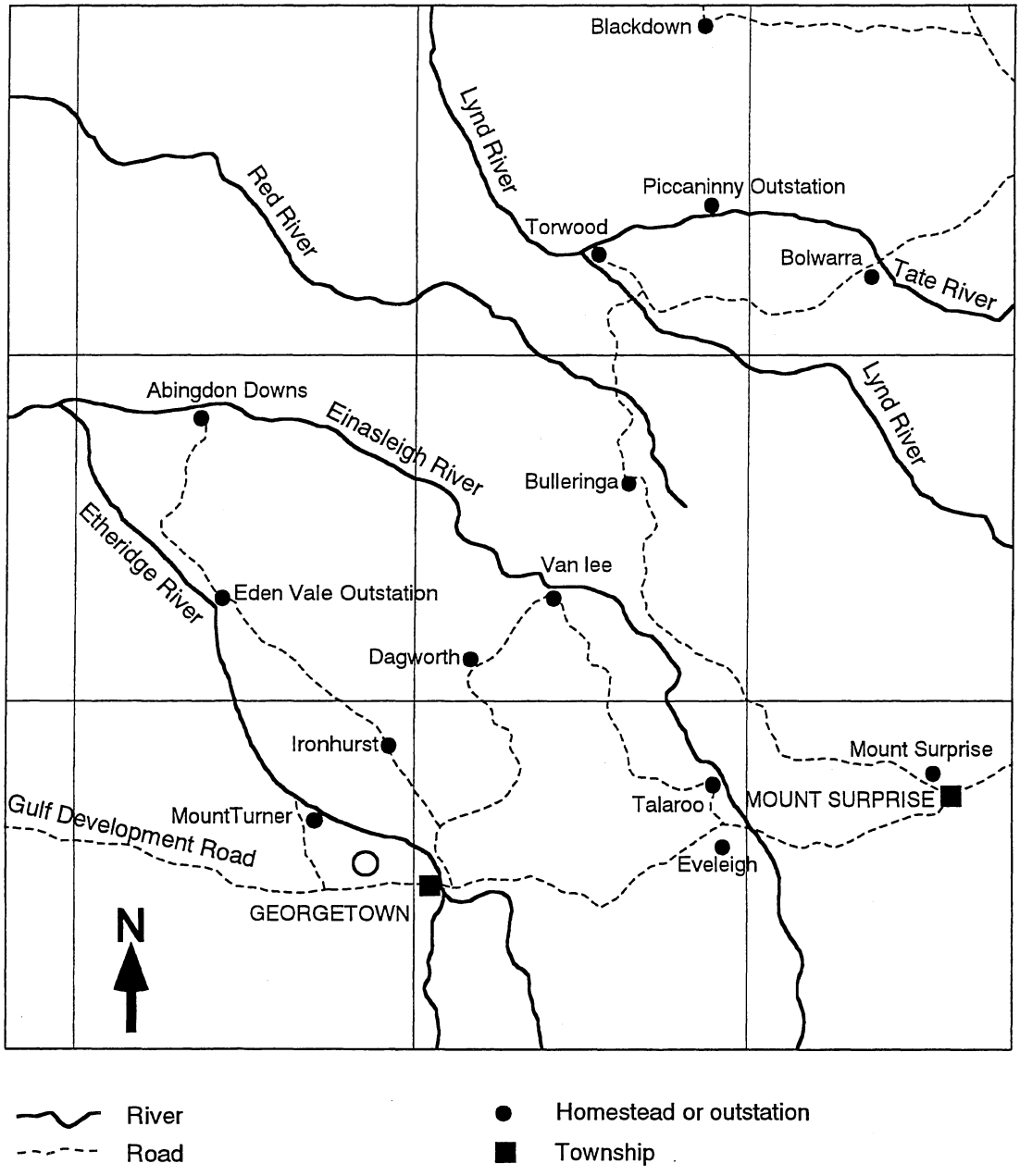

Figure 2(a). Access in the Red River Region survey area.

The average maximum and minimum temperatures at Georgetown for January are 34.4°C and 22.0°C respectively, and for July are 28.1°C and 11.8°C respectively.

1.3 Physiography, Vegetation and Access

Although regolith mapping was carried out over the RED RIVER 1:250 000 during the 1993 field program, no similar mapping has been carried out on the adjacent ATHERTON, EINASLEIGH and GEORGETOWN 1:250 000 sheet areas, parts of which are in the survey area. The physiography of the RED RIVER sheet area is described in Smart and Bain (1977), but the only data which are consistent across the survey area are the 'Land Systems' described in Twidale (1966) and Galloway and others (1970) for the Leichhardt-Gilbert and Mitchell-Normanby areas of north Queensland, respectively. A synthesis of their data is shown in Figure 2(b).

The **Georgetown Uplands** (Smart and Bain, 1977) correspond to four of the 'Land Systems' (see Figure 2(b) key) and are undulating plains with low hills, mesas and narrow incised valleys occurring mostly in the south-eastern half of the GALLOWAY, the western parts of the LYNDBROOK and MUNGANA, and the northern part of the MOUNT SURPRISE, 1:100 000 sheet areas. The uplands are developed mainly on igneous and metamorphic rocks, with a few mesas of younger sandstone. These are erosional areas and the regolith could be expected to have developed in-situ.

The **McBride Basalt Plateau** (White, 1962) covers much of the north part of the MOUNT SURPRISE sheet area and consists of basalt extruded from over 100 vents. The regolith is also in-situ.

The **Bulimba and Holroyd Plains** (Smart and Bain, 1977) consist of rolling hills, low mesas and a few alluvial flats, and cover most of the ABINGDON DOWNS, the north-western half of the GALLOWAY and most of the BLACKDOWN 1:100 000 sheet areas. These are erosional surfaces (in-situ regolith) in the east (Bulimba Plain) grading to lower relief, old land surfaces in the west (Holroyd Plain). The tops of the mesas represent the original surfaces of the plains. Drainage patterns are controlled by jointing in the sandstone and many streams have steep sides and sandy bottoms. These have developed mainly on the Rolling Downs Group and the Bulimba Formation.

Most of the survey area is covered by erosional surfaces, the exceptions being along the western margin in the Holroyd Plain. It is therefore likely that regolith over most of the survey area has developed in-situ and that the stream sediments reflect the geochemical characteristics of their catchment basins.

Most of the area is covered by open to moderately dense eucalyptus woodland, with a variety of box, ironbark and bloodwoods from 6 to 12m high. Melalucas proliferate near watercourses, and small trees and bushes are common in the higher, range areas. Dense stands of lancewood were encountered in the south of the ABINGDON DOWNS sheet area and thick stands of rubber vine infested many creek banks.
Access during the survey was variable over both the Georgetown Uplands and the Bulimba Plain although in the flatter areas, where most pastoral activity occurs, there are many station roads and off-road access was generally very good. In the more rugged areas access was only by tracks pushed in by pastoralists and miners. Much of these areas were sampled by helicopter. Access on the McBride Basalt Plateau was uncomfortable rather than difficult, due to numerous basalt boulders and rubber vine infestations.

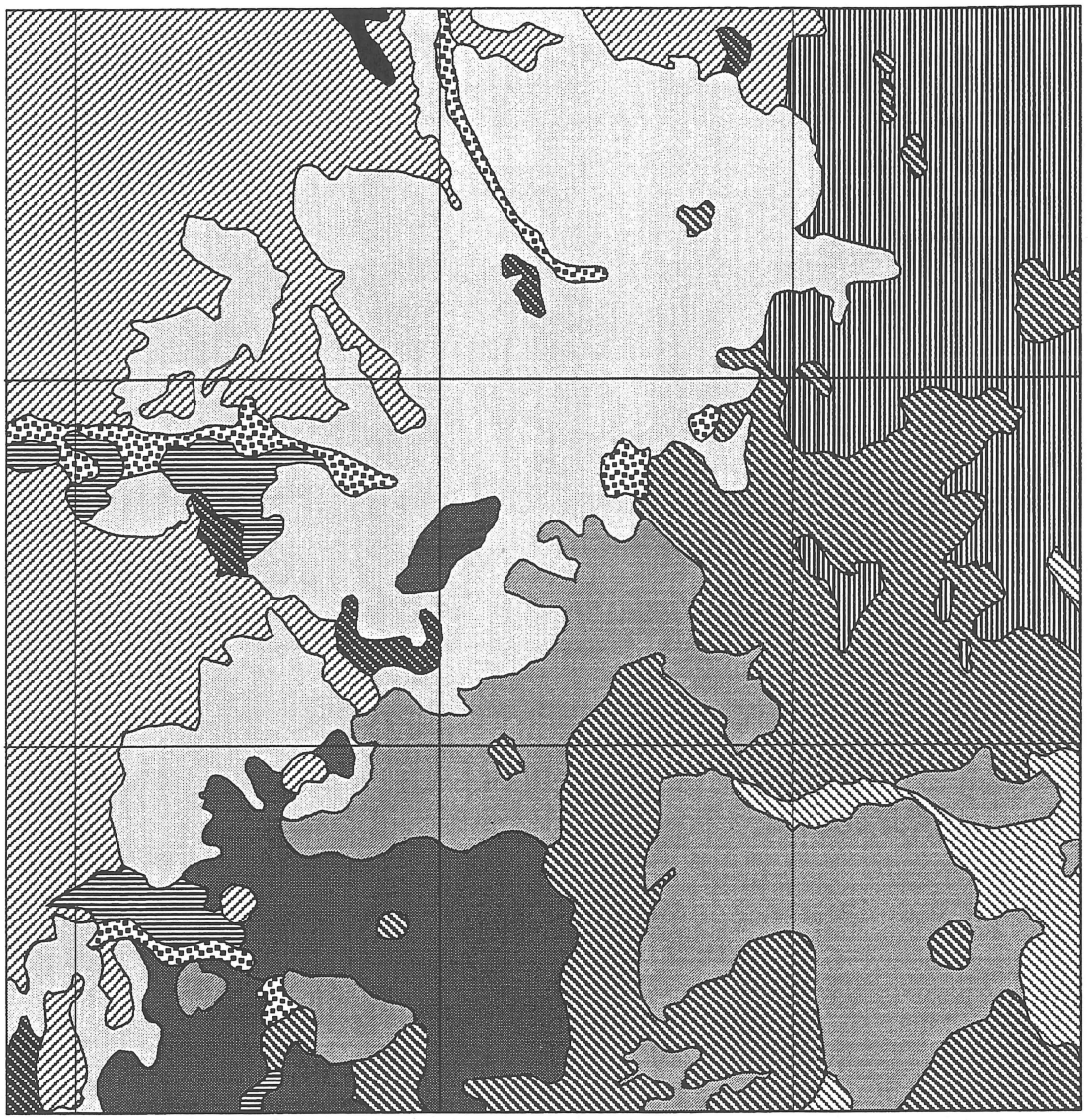

Georgetown Uplands

- Hilly Country on granites. metamorphics and sediments. Skeletal soils and rock outcrops. Ironbark woodland plus grassland, 200-900m elevation, 55-100cm rainfall
- Undulating country, low stony hills on metamorphics and granite. Massive earths and uniform sandy soil. Ironbark and stringybark woodland
- Irregular to gently undulating plains on granites and metamorphics. Red and yellow podzolics and rare earths, 150-750m elevation, 55-85cm rainfall
- Rolling plains on granite and some metamorphics. Skeletal shallow grits, sands and silts, 90-450m elevation, 60-75cm rainfall

McBride Basalt Plateau

- Irregular stony plains on basalt. Krasnozem soils and black earths. Ironwood woodlands and mid-height grasslands (stock rate moderately high), 425-900m elevation, 50-75cm rainfall

Bulimba and Holroyd Plains

- Broken Tablelands on sediments (eg Rolling Downs Group). Lancewood over bare ground or sparse grass, 150-750m elevation, 40-80cm rainfall
- Plains of erosion on sediments. Light texture brown soils to red and yellow earths. Stringybark woodland, 75-230m elevation, 60-85cm rainfall
- Plains of erosion on sediments (eg Rolling Downs group) and some granite. Light texture brown soils to skeletal shallow grits, Georgetown box woodland, 75-300m elevation.
- Outwash plains on terrestrial deposits, mostly unconsolidated sand. Red and yellow earths. Stringybark woodland, 90-150m elevation, 75cm rainfall.
- Narrow alluvial plains, light texture brown soils. Frontage woodland and grassland (stock rate high, 15-75m elevation, 75-85cm rainfall.

Figure 2(b). Physiography of the Red River Region (after Twidale, 1966; Galloway and others, 1970; Smart and Bain, 1977).

Drainage in the area centres on 5 west-flowing river systems (see Figure 2(a)). The largest is the Einasleigh River which flows north through the MOUNT SURPRISE sheet area and then north-west to west before ultimately joining the Gilbert River. The Etheridge River flows north-west through the FOREST HOME and ABINGDON DOWNS sheet areas and joins the Einasleigh west of Abingdon Downs homestead. The Red River rises in the north-east of the GALLOWAY sheet area and flows north-west, joining the Staaten River near the gulf. The Lynd River flows north-west to west through the LYNDBROOK and BLACKDOWN sheet areas, and is a tributary of the Mitchell River. The Tate River flows north-west through the MUNGANA sheet area and then westward to joins the Lynd at Torwood homestead.

GEOLOGY and MINERALISATION

2.1 Geology

The following is a brief account of the principal features of the surficial geology of the survey area in the Georgetown Region. The survey area covers parts of four (4) 1:250 000 geological map sheet areas, namely RED RIVER (Smart and Bain, 1977), ATHERTON (Best, 1962), GEORGETOWN (White, 1962b) and EINASLEIGH (White, 1962a).
From 1972 to 1982 the Bureau of Mineral Resources (now AGSO) and GSQ carried out geological mapping at 1:100 000 scale in the Georgetown area, including the FOREST HOME, GEORGETOWN and parts of the MOUNT SURPRISE sheet areas. A special 1:250 000 scale map of the Georgetown area was produced (Bain and others, 1985). In 1993 the NGMA's North Queensland Party remapped the metamorphic and igneous rocks of the RED RIVER 1:250 000 sheet area (Mackenzie and others, 1996). GSQ has remapped the EINASLEIGH (Withnall and Grimes, 1995) and ATHERTON (Donchak and Bultitude, 1994) 1:250 000 sheet areas.
AGSO and GSQ are in the process of compiling a synthesis volume and accompanying atlas covering the Cape York Peninsula.

AGSO/GSQ references to the geology, surficial geochemistry and mineralisation of the area include:

Best, 1962 (Geology of the Atherton sheet area)
White, 1962a (Geology of the Einasleigh sheet area)
White, 1962b (Geology of the Georgetown sheet area)
Keyser and Wolff, 1964 (Geology and mineralisation - Chillagoe area)
White, 1965 (Geology of Georgetown-Clarke River area)
Branch, 1966 (Volcanics and granites of Georgetown Inlier)
Oversby and others, 1975 (Georgetown, Coen and Yambo Inliers)
Rossiter, 1975 (Orientation geochemical survey)
Wall and Withnall, 1975 (Georgetown Inlier - mineralisation)
Smart and Bain, 1977 (Geology of the Red River sheet area)
Oversby and others, 1978 (Georgetown 1:100 000 sheet)
Rossiter and Scott, 1978 (Geochemistry of Forsayth sheet area)
Sheraton and Labonne, 1978 (Igneous rocks of the Georgetown area)
Withnall, 1978 (Mines, etc, Georgetown 1:100 000 sheet)
Rossiter and Scott, 1979 (Geochemical data for the Gilberton sheet area)
Scott and Rossiter, 1979 (Geochemical data for the Georgetown sheet area)

Withnall and Mackenzie, 1981 (North Head-Forest Home area)
Cruikshank and others, 1983 (Geochemical data for the North Head and Forest Home sheet areas)
Bain and others, 1985 (Geology of the Georgetown area)
Warnick, 1985 (Geology of Mount Surprise-Einasleigh region)
Warnick, 1989 (Geology of Mount Surprise-Einasleigh region)
Withnall, 1989 (Geology of south-eastern Georgetown Inlier)
Bain and others, 1990 (Proterozoic inliers, geology and mineralisation)
Withnall and Grimes, 1991 (Geology of the Einasleigh sheet area)
Champion and Mackenzie, 1994 (North Queensland Igneous Rocks - Atlas)
Donchak and Bultitude, 1994 (Geology of the Atherton sheet area)
Withnall and Grimes, 1995 (Geology of the Einasleigh sheet area)
Mackenzie and others, 1996 (Geology of the Red River sheet area)
Bultitude and others, 1997 (Geology of the Hodgkinson Basin)

The geology described below is condensed from the most recent maps and the draft of the synthesis volume.

The oldest rocks cropping out in the area are the Proterozoic metamorphic, doleritic and granitic infrastructure rocks of the Region (formerly referred to as the Georgetown Inlier). These have been intruded or covered by Palaeozoic granitic and volcanic suprastructure rocks, and this event may have reset the isotopic ages of many older rocks/minerals rendering interpretation difficult. In the south-east extensive flows of Cainozoic basalt cover large areas. To the north-west, in and beyond the survey area, the Proterozoic rocks are overlain by Mesozoic sediments of the Carpentaria Basin. A simplified general geology map is shown in Figure 3.

2.1.1 Proterozoic Rocks

The oldest rocks cropping out in the survey area are the Proterozoic Dargalong and McDevitt Metamorphics, the Einasleigh Metamorphics and Robertson River Subgroup (the Daniel Creek, Lane Creek and Corbett Formations) of the Etheridge Group, the Cobbold Metadolerite, and the granites of the Forsayth Supersuite (the Aurora, Delaney and Forsayth Granites). They are intruded by Palaeozoic granites and are overlain by Palaeozoic and Cainozoic Volcanics, and Mesozoic sediments.

The **Dargalong** and **McDevitt Metamorphics** probably grade into each other and crop out in the north-east of the GALLOWAY 1:100 000 sheet area and along the northern margin of the LYNDBROOK sheet areas. The McDevitt Metamorphics are amphibolite facies and comprise schist and minor amphibolite, and in the east, contain a number of bodies of metadolerite. The Dargalong Metamorphics are amphibolite-granulite(?) facies and comprise gneiss, migmatite and textural 'granulite' with minor schist, quartzite and amphibolite.

The **Einasleigh Metamorphics,** of the **Etheridge Group**, crop out between Talaroo and Eveleigh homesteads along the eastern margin of the GEORGETOWN sheet area, and through to south-west of Mount Surprise township in the MOUNT SURPRISE sheet area. The Einasleigh Metamorphics are amphibolite-granulite(?) facies and comprise gneiss, migmatite and textural 'granulite' with minor schist, quartzite and amphibolite and rare marble. The **Robertson River Subgroup** (Daniel Creek, Lane Creek and Corbett Formations) of the **Etheridge Group**, crops out between south-west of Huonfels homestead

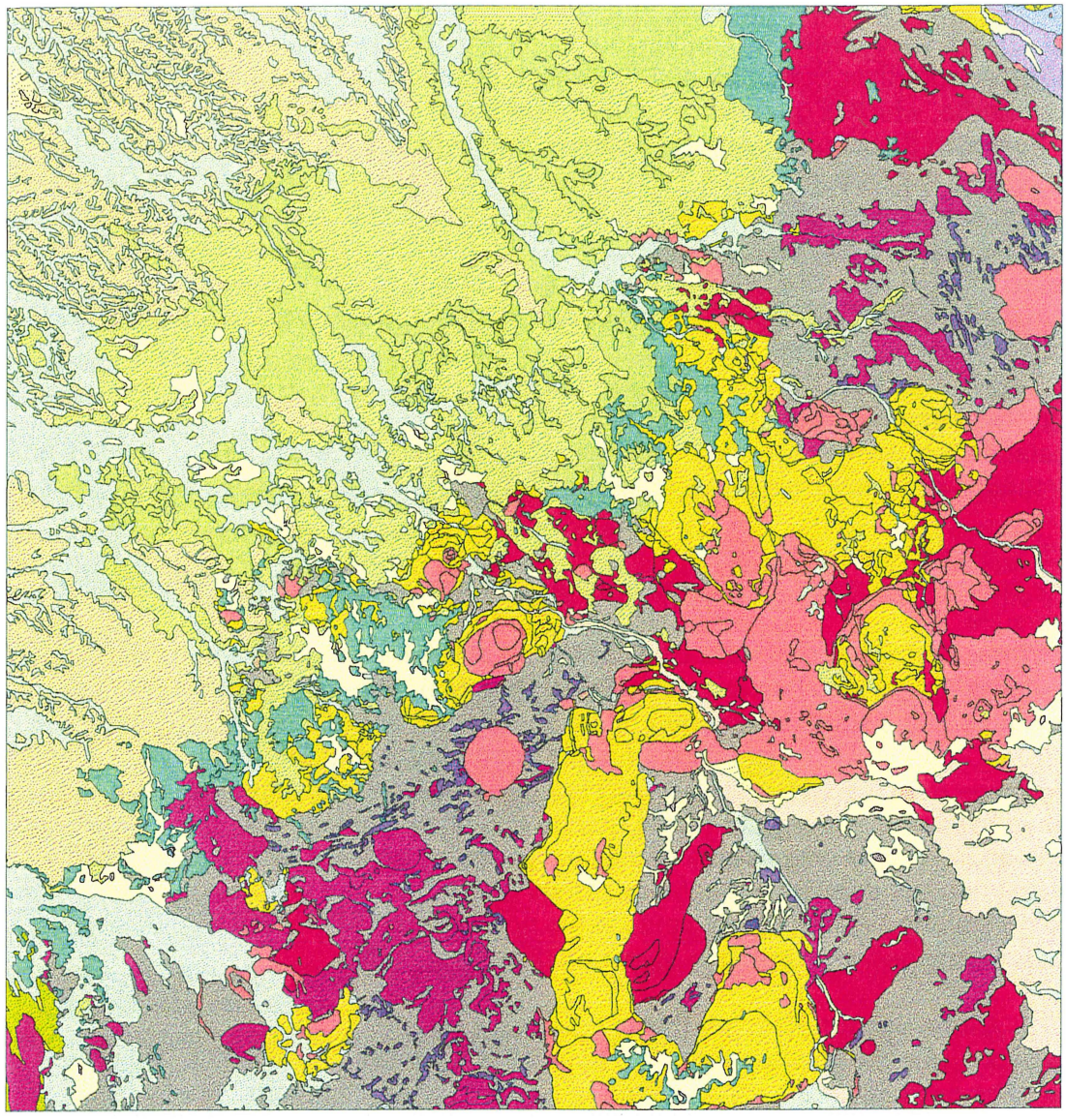

Figure 3. General geology of the Red River Region.

in the FOREST HOME sheet area, and east and north of Van Lee homestead in the GALLOWAY sheet area. All contain mudstone and siltstone grading into mica schist.
The Robertson River Subgroup and Einasleigh Metamorphics are intruded by the **Cobbold Metadolerite**, which is greenschist-amphibolite facies.
The **Forsayth Supersuite** (Aurora, Delaney, Forsayth and Fig Tree Hill Granites) crops out near, and to the north of, Mount Turner west of Georgetown township. The Delaney and Forsayth Granites are pale to bluish or dark grey, medium to coarse grained, porphyritic muscovite-biotite (Delaney), or biotite (Forsayth), granites. Both contain large K-feldspar phenocrysts. The Aurora Granite is a pale grey, fine to medium grained, muscovite-biotite leucogranite. The Fig Tree Hill Granite crops out in the south-west of the MUNGANA sheet area (Bultitude and others, 1997).

2.1.2 Palaeozoic Rocks

Substantial intrusive activity occurred during the Silurian-Devonian period, but this has been overshadowed by intrusive and extrusive activity in the Carboniferous-Permian period.

2.1.2.1 Silurian-Devonian Rocks

In the survey area these include the granites and granodiorites of the White Springs Supersuite.
The **White Springs Supersuite** crops out north of the Einasleigh River in the GALLOWAY sheet area (Cope, Van Lee and Jape Creek Granites), from north-west of Van Lee homestead to the south-east corner of the sheet area, and in the western part of the ATHERTON 1:250 000 sheet area (Nundah Granodiorite and Blackman Gap Complex). They range from medium grained, epidote-muscovite-biotite granite (Van Lee) to medium grained to variably porphyritic, biotite granite and granodiorite (Cope, Jape Creek and unnamed), and pale grey to cream, medium to coarse grained, biotite-muscovite granodiorite (Nundah Granodiorite) to granite (Blackman Gap Complex). Much of the area occupied by the Nundah Granodiorite in the northern part of the MUNGANA sheet area once was mapped as Dargalong Metamorphics (Best, 1962).

2.1.2.2 Carboniferous-Permian Rocks

This period saw the emplacement of a number of extrusive and intrusive units in the survey area. The most important are the Maureen, Silent Creek, Scardons, Warby, Newcastle Range and Galloway Volcanic Groups, and the O'Briens Creek, Kangaroo Creek, Brodies Camp, Yataga and Claret Creek granite supersuites.

The **Maureen Volcanic Group** (Puranga Rhyolite and Ironhurst Formation) crops out on the border between the FOREST HOME and ABINGDON DOWNS sheet areas. The volcanics are bimodal containing rhyolites, andesites, dacites, and minor basalt. Many units are ignimbritic, and, lithologically, the group closely resembles the Namarrong Volcanic Subgroup of the Newcastle Range Volcanic Group.
The **Silent Creek Volcanic Group** (Laragon Volcanics, and Eden Vale and Mount Emu Rhyolites) crop out in the ABINGDON DOWNS sheet area, east of the Eden Vale outstation. They are mostly rhyolitic to rhyodacitic ignimbrites.
The **Scardons Volcanic Group** crops out on the border between the GALLOWAY and LYNDBROOK sheet areas, and continues into the BLACKDOWN sheet area to the north. The volcanics were emplaced in two phases, the older rocks being rhyolitic, andesitic and dacitic ignimbrites cropping out in the north and east (Hammock Creek Rhyolite and Duffers Creek Dacite), and the younger rocks rhyolite to rhyolitic ignimbrite (Red River, Angelsey, Pretty Swamp and Dickson Creek Rhyolites).

The **Warby Volcanic Group** crops out in the western part of the LYNDBROOK sheet area. The rocks are rhyolite, dacite and rhyolitic ignimbrite. Recently the Scardons and Warby Volcanics Groups have been combined into the **Paget Volcanic Group**, with each being reclassified as a subgroup.
The **Newcastle Range Volcanic Group** is the most extensive volcanic complex in the Georgetown Region, and crops out as the Newcastle Range, mostly in the GEORGETOWN sheet area, but with extensions into the GALLOWAY and MOUNT SURPRISE sheet areas. The Namarrong Volcanic Subgroup (Cumbana and Brodies Gap Rhyolites, and Dagworth and Twin Dams Andesites) forms the northern extension of the group and crops out across the border between the GEORGETOWN and GALLOWAY sheet areas at Mount Direction and to the east. The volcanics are bimodal. The Eveleigh Volcanic Subgroup (Shrimp Creek, Mosaic Gully, Beril Peak and Yellow Jacket Rhyolites) forms the eastern extension of the group extending into the western part of the MOUNT SURPRISE sheet area. The rocks are mostly rhyolite and rhyolitic ignimbrite with minor andesite and dacite.
The **Galloway Volcanic Group** (Parallel Creek Rhyolite, and Paulet, Dynan and Camp Oven Dacites) crops out north of Dagworth homestead in the GALLOWAY and eastern margin of the ABINGDON DOWNS sheet areas. The group consists of roughly equal amounts of rhyolitic and dacitic ignimbrites, and is thus unlike all other volcanic groups in the survey area.

The **O'Briens Creek Supersuite** (Corduroy Swamp, Fork Yard, First Bull Run, Elizabeth Creek, Angore, Mount Max and McCord Granites) corresponds to the Elizabeth Creek Granite of earlier workers (Best, 1962; de Keyser and Wolff, 1964; Branch, 1966; de Keyser and Lucas, 1968; Smart and Bain, 1977; Sheraton and Labonne, 1978) and the Herbert River Granite (Best, 1962). The granites crop out in the south-eastern corner of the GALLOWAY, and south-western part of the LYNDBROOK sheet areas and in adjacent areas of the GEORGETOWN and MOUNT SURPRISE sheet areas. The granites area characteristically pale pink to white, alkali-feldspar-rich biotite granites, leucogranites and microgranites. Alteration, especially greisenation, is extensive and most granites contain some Sn-W-Mo mineralisation.
The **Kangaroo Creek Supersuite** (Bull Creek, Copper Bush and Campbell Mountain Granites) crops out north of Dagworth homestead in the GALLOWAY sheet area and often intrude comagmatic rocks of the Galloway Volcanic Group. The most common type is uneven-grained to porphyritic biotite to hornblende-biotite granite.
The **Brodies Camp Supersuite** (Knob Camp Granodiorite and Aylesbury Microgranite) crops out north of, and adjacent to, rocks of the O'Briens Creek Supersuite in the GALLOWAY sheet area. The supersuite is associated with, and also intrudes, the Scardons Volcanic Group. The rocks range from hornblende-biotite granodiorite to biotite granites, microgranites and rhyolite.
The **Yataga Supersuite** (Yatage Granodiorite) crops out south of Dagworth homestead, across the border between the GALLOWAY and GEORGETOWN sheet areas. The rocks grade from hornblende-biotite tonalite to hornblende-biotite granodiorite.
The **Claret Creek Supersuite** (Bonnor Creek Granite) crops out in the LYNDBROOK and MOUNT SURPRISE sheet areas, and comprises grey to cream, fine to medium grained, biotite to biotite-hornblende granite.

2.1.3 Mesozoic Rocks

In the west to north-west the granites and metamorphics are overlain by Mesozoic sediments of the Carpentaria Basin, namely the Gilbert River Formation and the Rolling Downs Group. These units appear to be of little economic interest but areas adjacent (5-10 km) to the known extent of the hard rocks were sampled.

The **Gilbert River Formation** (Coffin Hill and Yappar Members) consists of quartzose sandstones with minor conglomerate, siltstone and shale, ferruginised in outcrop. It unconformably overlays the older rocks.
The **Rolling Downs Group** (Wallumbilla Formation) is a fossil-bearing marine mudstone and siltstone, stratigraphically between the Gilbert River Formation (older) and the Bulimba Formation.

2.1.4 Cainozoic Rocks

The **Bulimba Formation** is a poorly sorted clayey quartzose sandstone and granule conglomerate and also unconformably overlays older rocks.
The **McBride Basalt Group** (Undarra Basalt) is a group of olivine basalts which has extruded over the central and northern parts of the EINASLEIGH 1:250 000 sheet area, forming the McBride Basalt Plateau. It covers much of the eastern part of the MOUNT SURPRISE sheet area with a small exposure stretching across to the western margin of the sheet area. In the GALLOWAY sheet area a small exposure exists on the island between the Einasleigh River and Parallel Creek anabranch.

Analyses of rock units of interest were extracted from AGSO's ROCKCHEM whole rock geochemical database.

2.2 Mineralisation

The MINLOC Database (joint Bureau of Resource Science/AGSO) lists 338 mines, abandoned mines, prospects and mineral occurrences in, or immediately adjacent to, the survey area (Figure 4). Overall these occurrences contain, presumably as major or 'economic' constituents, Ag (191 occurrences), As (1), Au (191), Be (3), Bi (13), Cu (127), Mo (16), Ni (1), Pb(42), Sb (4), Sn (74), U (7), W (12) and Zn (7), plus a number of non-metallic occurrences such as bentonite, fluorite, limestone, mica, topaz and silica. The distribution of Ag, Au, Cu, Pb-Zn, Sn-W and U occurrences are shown in Appendix A. Most occurrences are of historical interest only, or are small and therefore sub-economic to uneconomic. The survey area does cover part of the Etheridge Gold Field.

2.2.1 Gold and Silver

Gold occurrences (Figure A2) are concentrated in the area of the Etheridge Gold Field, and in the MUNGANA sheet area. Ag occurrences (Figure A1) follow a similar pattern.
The Etheridge Gold Field produced some 18,700 kg of gold between 1877 and 1957. The survey area covers a number of mines south of Mount Turner and west of Georgetown township and the Lane Creek Mine near Ironhurst homestead, both in the FOREST HOME sheet area. Quartz reefs contained gold, pyrite, galena, chalcopyrite and sphalerite (Cribb, 1939). About 7,800 tonnes of Cu and 4,200 tonnes of Pb were also won from the goldfield (White, 1962a).
Gold and silver were recovered in the Cardross area (see below).

2.2.2 Copper

Cu occurrences (Figure A3) are mainly concentrated in the north, in the Cardross area (de Keyser and Wolff, 1964), and south of the MUNGANA sheet area, although significant occurrences occur outside these areas. Mines in the Cardross area appear to have been worked between 1898 and about 1921. Total recorded production amounted to about 2,000 tonnes of copper, 68 kg of gold and 2,710 kg of silver. Mineralisation occurs in fissures in 'Dargalong Metamorphics' (now mapped as Nundah Granodiorite?), and the presence of arsenopyrite, galena, sphalerite, wolframite, cassiterite, and bismuth and molybdenum minerals also were recorded.

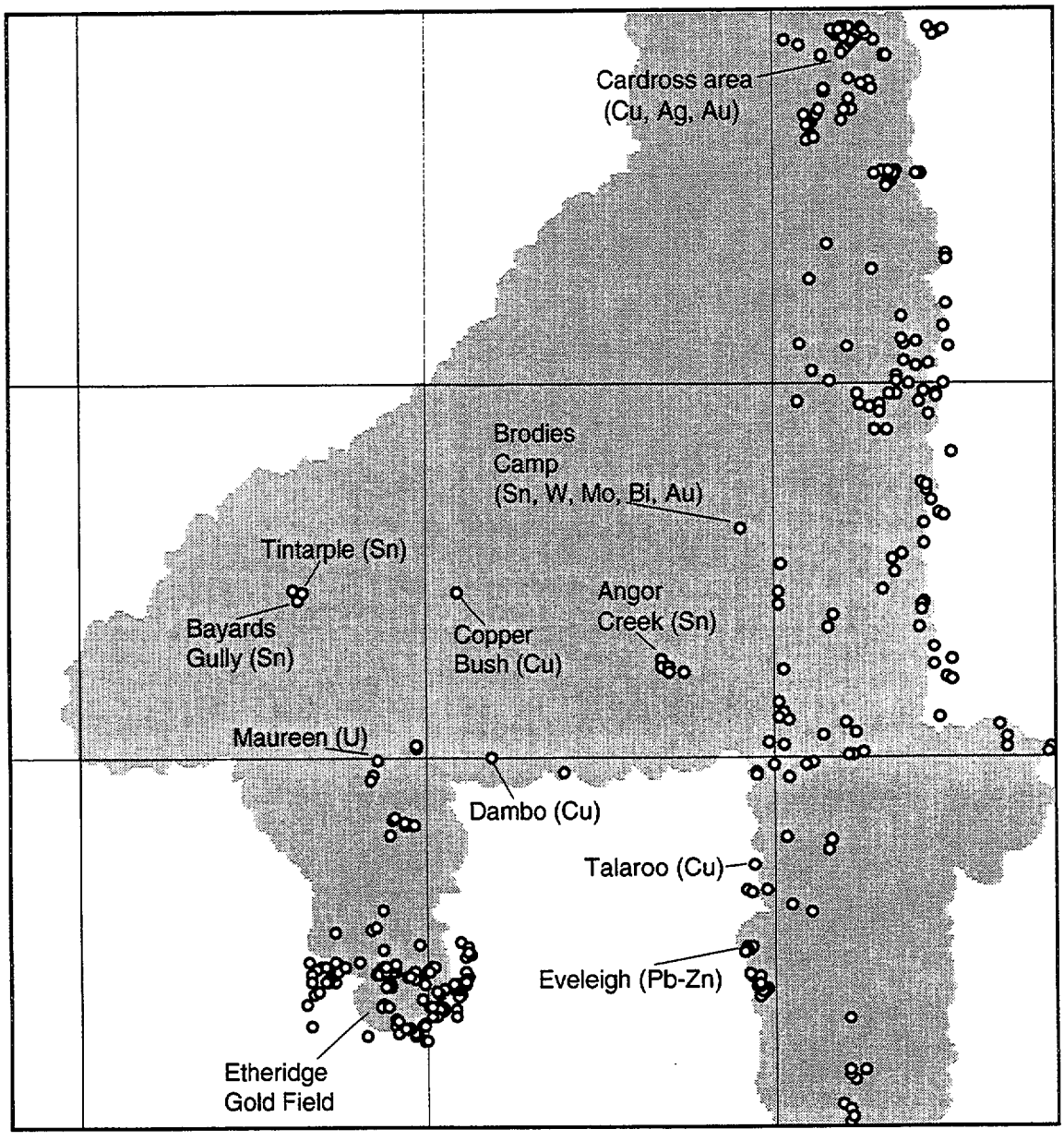

Figure 4. All occurrences (N=388) in, or immediately adjacent to, the RED RIVER Region survey area (after MINLOC, November, 1994).

The Copper Bush Prospect (ML418) about 20 km north-west of Van Lee homestead in the GALLOWAY sheet area, comprises two small patches of malachite in weathered Galloway Volcanics (Sawers, 1965). Samples assayed at up to 8% Cu.
The Dambo Prospect, 5 km south of the Dagworth homestead and also in the GALLOWAY sheet area, is a copper-bearing gossan in hornblende-biotite (Yataga -Withnall, 1978) granodiorite (Smart and Bain, 1977). Mineralisation includes chalcopyrite and bismuthinite.
The Talaroo Copper Mine near Talaroo homestead occurs in Einasleigh Metamorphics on the edge of the survey area in the GEORGETOWN sheet area. The mine produced about 8 tons of Cu (White, 1962a).

2.2.3 Lead and Zinc

Pb-Zn (Figure A4) occurrences are concentrated along the eastern margin of the Etheridge Gold Field, and in the southern MUNGANA-northern LYNDBROOK sheet areas.
The Eveleigh silver-lead mine near Eveleigh homestead is on the edge of the survey area. The ore is contained in fissures in Einasleigh Metamorphics. In a number of lodes galena is associated with Cu and Zn minerals, in one with Sn and in another with Au (Denmead and Ridgway, 1947; Denmead, 1950). Between 1947 and 1953 mining yielded 24.5 tonnes of Pb and 64 kg of Ag (White, 1962a).

2.2.4 Tin and Tungsten

Sn and W occurrences (Figure A5) are concentrated in the eastern part of the survey area, probably near the granites of the O'Briens Creek Supersuite.
At Brodies Camp, in the GALLOWAY sheet area, cassiterite, wolframite and minor molybdenite, bismuthinite and gold are disseminated in a greisen at the contact between Scardons Volcanics and Corduroy Swamp Granite. No production records appear to have been kept but mining is thought to have occurred between 1913 and 1925 (Smart and Bain, 1977).
Also in the GALLOWAY sheet area cassiterite was recovered from alluvium in stream and gullies in and near Angor Creek. Small quantities of lode tin and wolfram were taken from the Angore Granite although deposits are generally too small and too erratic to be economic. Mining began in 1901 and has been sporadic since. Tin-bearing alluvium also occurs in the LYNDBROOK, near Fulford Creek, and MOUNT SURPRISE sheet areas, to the east and south-east of the Angor Creek area. The 'Elizabeth Creek Granite' (now the O'Briens Creek Supersuite) are thought to be the source of the cassiterite (Best, 1962; Smart and Bain, 1977).
Alluvial Sn deposits at Tintarple and Bayards Gully, about 15 km north-east of the Eden Vale outstation in the ABINGDON DOWNS sheet area, are more restricted but richer than the Angor Creek deposits. Also discovered in 1901 they were worked until 1922 by which time total production was about 14 tonnes of cassiterite. The current source appears to be a Sn-bearing placer bed at the base of Gilbert River Formation sediments, although the original source of Sn in the placer is not known (Smart and Bain, 1977).

2.2.5 Uranium

U occurrences (Figure A6) are few and occur in an arc from north-east to west of Georgetown township.
Mineralisation at the Maureen Prospect comprises uraninite, fluorite and molybdenite within the basal sedimentary sequence of the Galloway Volcanics. The mineralisation, however, cuts across bedding and replaces mineral grains and appears to be related to fractures. The source may be hydrothermal fluids from an unexposed body of 'Elizabeth Creek Granite' which is relatively enriched in U and Th (Smart and Bain, 1977). The prospect is 25 km south-east of the Eden Vale outstation in the ABINGDON DOWNS sheet area. A

similar but much smaller deposit occurs about 2.5 km to the south in the FOREST HOME sheet area.

SAMPLING, CHEMICAL ANALYSIS and DATA PROCESSING

3.1 Sampling

The sampling program was regional in concept and was based on an average sample density of one sample per 10-15 km^2. The aim was to cover all of the areas of 'hard' (igneous and metamorphic) rocks in the survey area, and adjacent areas of overlying sedimentary rocks. Major drainage basins were outlined on 1:100 000 topographic maps and sample sites positioned to give basins of the required average size while ensuring good coverage of important rock units, specifically the granitic and metamorphic rocks in the survey area.

For the first 3 weeks of the sampling program sample sites were accessed by 4-wheel drive vehicle with occasional walks into sample sites in more rugged, or otherwise isolated, terrain. Each sampling team was equipped with either a Magellan Nav 1000 Pro or a Pronav GPS100 Global Positioning System (GPS) which was used for navigation and site location. During the sampling program twenty-four hour GPS coverage was available in 2-D mode. In this phase of the program samples near the base camp and near known roads and tracks were collected.

This was followed by a helicopter sampling program of one week duration. The helicopter, a Bell Jet Ranger II from Bob Smith Helicopter Services (Trinity Beach, Qld), was equipped with a Pronav GPS100 for navigation. The helicopter was used to access the more rugged and remote areas in the LYNDBROOK, BLACKDOWN (in both 1992 and 1993), north-western and western GALLOWAY and eastern and western ABINGDON DOWNS sheet areas.

A further one and a half weeks of vehicle operations concluded the 1992 sampling program. The 1993 sampling program will be detailed in the Hann River Region record (Cruikshank and Brugman, 1997).

At each sample site two size fraction samples were collected. The first was 50-70g of -180u (-#80 mesh) fine sediment stored in a plastic vial and is considered to be the 'standard' sieved stream sediment for the Georgetown region (Rossiter, 1975). The second was 5-6 kg of -1 mm coarse sediment doubled bagged in large plastic sample bags and was collected specifically for bulk cyanide leach determination of Au (+-Pd and Pt) (Elliot and Towsey, 1989), and for possible future heavy mineral analysis. Where possible sieving was carried out at the sample site using aluminium bodied sieves fitted with nylon bolting cloth to minimise contamination. Wet samples were placed in plastic trays on return to base camp, dried in the sun and then sieved. The fine sediment was pulverised further using motor driven mortar grinders fitted with agate vessels. Samples were shipped to Canberra in AGSO vehicles for sorting, analysis and storage.

Duplicate samples (labelled as splits A and B) were collected at a number of sites to test the reproducibility of the sampling. These were analysed separately but for many of the statistical tests and mapping exercises the average value of the two splits was used.

A total of 843 sites in the BLACKDOWN, MUNGANA, ABINGDON DOWNS, GALLOWAY, LYNDBROOK, FOREST HOME, GEORGETOWN and MOUNT SURPRISE 1:100 000 sheet areas were sampled, including 15 in duplicate. Sample sites and a mask of the area sampled are shown in Figure 5, and the area covered is approximately 8,500 km^2. Table 1

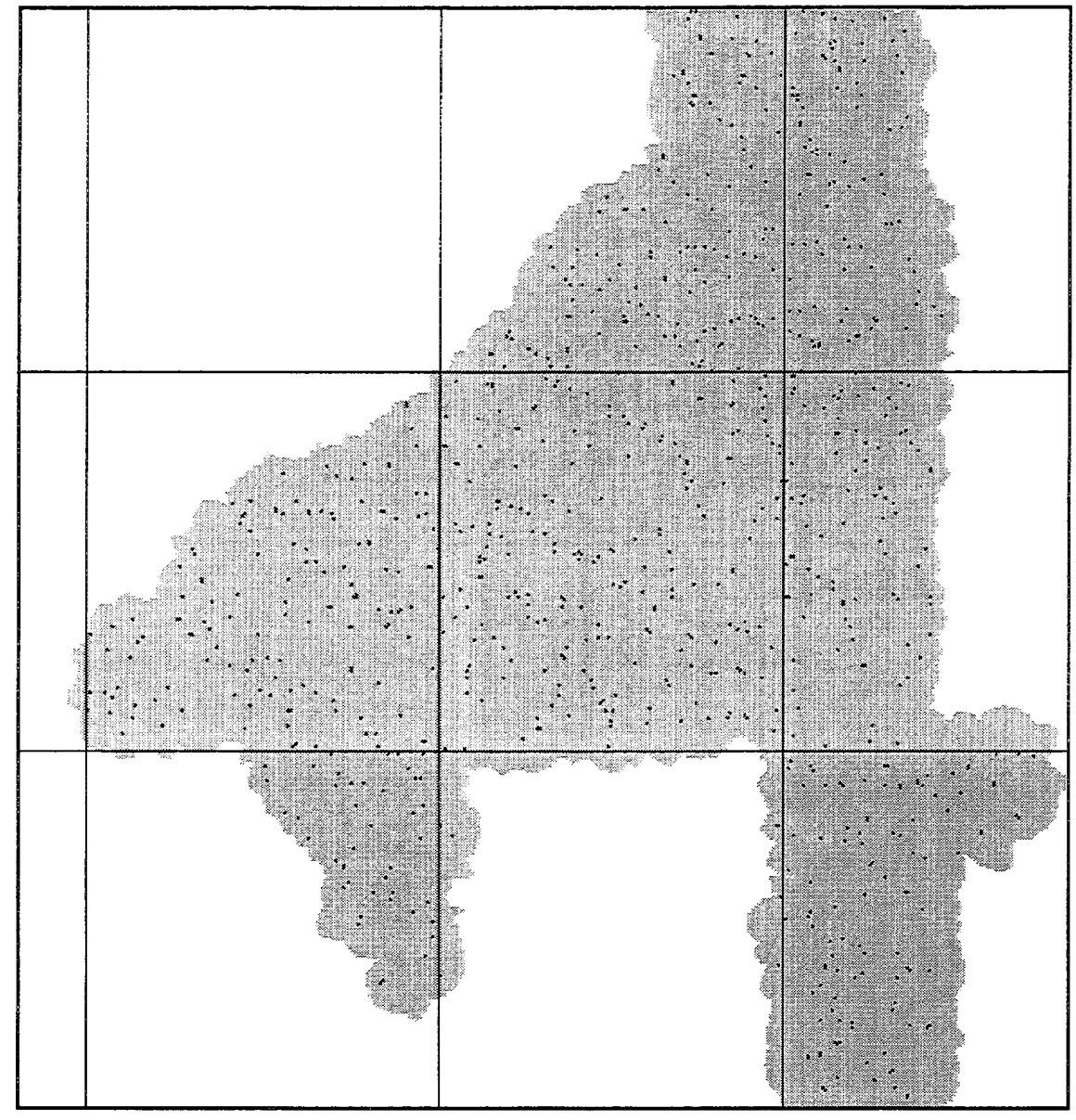

143.0 144.0 17.0 18.0

Red River 7563	Blackdown 7663	Mungana 7763
Abingdon Downs 7562	Galloway 7662	Lyndbrook 7762
Forest Home 7561	Georgetown 7661	Mount Surprise 7761

Figure 5. Sample sites for the Red River Region survey (N=843).

lists the 1:100 000 map sheet areas in which samples were collected, and the range of sample numbers allocated to each sheet. Sample sites were aligned to the drainage shown on the topographic maps listed in Table 1.

Table 1. Map sheet areas sampled.

Sheet Name(Number)	Number of samples	Sample Numbers
Blackdown (7663)*	75	2001-2083 (1992)
	59	2058-2142 (1993)
Mungana (7763)*	27	2604-2708 (1992)
	66	2601-2712 (1993)
Abingdon Downs (7562)*	147	1301-1451
Galloway (7662)*	218	1001-1220
Lyndbrook (7762)*	89	1601-1680
Forest Home (7561)*	47	9301-9347
Georgetown (7561)**	5	9001-9005
Mount Surprise (7761)**	110	9602-9727

Samples are prefixed by 9202 (1992) or by 9302 (1993)
* - map in Series R631, Edition 1-AAS, Australian Geodetic Datum 1966 (Royal Australian Survey Corps).
** - map Edition 1, National Topographic Map Series, Australian Geodetic Datum 1966 (Division of National Mapping).

3.2 Chemical Analysis

The fine sediment was analysed for 31 elements in AGSO's Geochemical Laboratory using X-ray Fluorescence Spectrometry (XRFS). An aliquot of the fine sediment was split off and sent to Analabs in Perth for analysis of 8 elements by Inductively-Coupled Plasma/Mass Spectrometry (ICP-MS).
Since the Bulk Cyanide Leach (BCL) separation for Au determination would effectively consume the entire coarse sample (i.e. render it unsuitable for further analysis) it was decided to split off a 2 kg aliquot of each coarse sample for BCL analysis and to archive the remaining sediment for future study. The 2 kg splits were sent to Australian Laboratory Services (ASL) in Brisbane for analysis. Pt and Pd were included for screening purposes although the BCL method is generally considered as not completely suitable for Pt.

3.2.1 AGSO Analyses

Thirty-one elements (As, Ba, Bi, Ce, Cr, Cu, Fe, Ga, Ge, Hf, La, Mn, Mo, Nb, Nd, Ni, Pb, Rb, Sc, Se, Sn, Sr, Ta, Th, Ti, U, V, W, Y, Zn and Zr) were analysed for by XRFS.

Sample powder was mixed with a binder and pressed into a 40 mm diameter pellet. After air-drying, the pellet was analysed using Philips PW1404 and PW1450 X-ray spectrometers with 72 and 60 position sample changers respectively. Raw count-rates were corrected for inter-element and mass-absorption effects and converted into element concentrations using the methodology of Norrish and Chappell (1977). Analysis was in 3 separate runs determined by the X-ray tube used, the inter-element corrections necessary and the mass absorption correction applied. The instrument runs are listed in Table 2.

Table 2. Analytical runs for XRFS listing tube target, and tube voltage and current. Values in parenthesis are detection limits in ppm.

	1	2	3
Tube target	Mo	Au	Au
Voltage (kV)	90	90*/60	60
Current (mA)	30	30*/40	40
	Th (2)	Sn (2)*	Fe (1000)
	Rb (1)	Nb (2)*	Ti (5)
	Pb (2)	Zr (1)*	Mn (2)
	Y (1)	Mo (2)*	V (2)
	Sr (1)	Ni (1)	Cr (1)
	U (0.5)	Cu (1)	Ba (4)
	Se (1)	Zn (1)	La (2)
	Ga (1)	Hf (2)	Ce (5)
	As (0.5)	Ta (2)	Nd (2)
	Bi (2)		Sc (1)
	W (3)		
	Ge (0.5)		

Two samples from those collected in the 1990 program (and subsequently labelled CY-1 and CY-2) had been used as temporary XRFS secondary standards and were analysed with each batch of the RED RIVER samples. Estimated from these replicate analyses, the analytical precision (1s) for most elements was better than +-8% for concentrations at 10 ppm, better than +-4% between 20 and 100 ppm, and less than +-2% at concentrations greater than 100 ppm. Precision for XRFS Runs 1 and 2 was consistently better by a factor of about 2 than that for Run 3, which involved measurements at long wavelengths (>1.74A) and used an Fe corrected mass absorption coefficient.
Full descriptions of the methodology used are given in Cruikshank and Pyke (1993).

3.2.2 ICP-MS Analyses

Several of the 31 elements listed above, for example Bi, Mo and W, gave few detectable values by XRFS. Analabs offer an ICP-MS method (Code GI201) involving a $HClO_4$/HCl/HF total digestion and detection limits an order of magnitude or more better then XRFS. Aliquots of the fine sediment samples were split off and sent for analysis by this scheme. Several elements not in the original list were added. The elements analysed, with detection limits (ppm) in parenthesis, were Be (0.1), Bi (0.1), Cd (0.1), Mo (0.1), P (20), Sb (0.05), Tl (0.5) and W (0.1).
The sensitivity and ability to analyse for most naturally occurring elements makes the ICP-MS technique highly suitable for environmental geochemical studies.

3.2.3 Bulk Cyanide Leach Analyses

BCL has become a de facto standard for the detection of Au mineralisation. Its advantages include the ability to detect the ultra fine Au common to epithermal deposits, and the large sample weight (1-10 kg) used gives very low detection limits at the ppt level (Elliot and Towsey, 1989). Unfortunately methodology for both sampling and analysis varies greatly starting with the coarseness of the material collected, through the use of static or dynamic leaching, and ending with the analytical method used to determine Au in the cyanide solution. All coarse samples collected during the life of the North Queensland Project were

of the same size fraction, that is -1 mm, and the same laboratory and analytical methodology was used for each survey.
After examining technical details of commercially available methodology Australian Laboratory Services (ALS) in Brisbane was chosen and the 2 kg aliquots were analysed by their method PM216. Although the extraction of Pt is reputed to be as low as 20% by BCL, both Pt and Pd were included in the analyses for screening purposes.

All analytical data, along with location data, were collated into a flat ASCII data files in MS-DOS format for data analysis. Copies of the data file (GT92SGD) are available from:

AGSO Sales Centre
GPO Box 378
CANBERRA ACT 2601
AUSTRALIA
Phone: (06) 2499519
Fax: (06) 2576466

3.3 Data Analysis

The large quantities of data resulting from a regional geochemical survey can be reduced to more manageable proportions by the application of univariate and multivariate statistical methods to describe the behaviour of the elements and their inter-element relationships. Similarly, the spatial distribution of an element, or elements, can be shown by either using a digitised representation of each sample's drainage basin coloured (or greyscaled, patterned, etc) according to the concentration of the element in the sample (Bonham-Carter and others, 1987; Cruikshank, 1990), or as images prepared from data systematically gridded from the essentially random data (sample) points of the survey (Eggo and others, 1990,1995; Cruikshank, 1994; Cruikshank and Butrovski, 1994). The former honours the spatial integrity of the data but is time consuming to implement, while the later is quick and sufficiently spatially honest to adequately show regional geochemical distribution patterns. Basic univariate and multivariate statistics for the dataset were estimated using proprietary software on an IBM-compatible micro-computer. More detailed univariate and multivariate analyses of the data, including multiple and stepwise multiple regression and principal component factor analysis, were made using STATVIEW II (Abacus Concepts, Berkeley, California) and DATA DESK PROFESSIONAL (Odesta Corporation, Northbrook, Illinois) running on an Apple Macintosh II computer. DATA DESK PROFESSIONAL also allowed a more visual/intuitive approach to data analysis. These programs also produced tables and graphs (histograms, scattergrams, etc) which were cut and pasted into CANVAS 3.5 (Deneba Software, Miami, Florida) for sizing, annotation and printing. Line maps and diagrams were also produced on CANVAS.
Locations on the Australian Map Grid (AMG) were converted to Latitude/ Longitude using a propriety program so that plots could be related exactly to the boundaries of the map sheet area, and across the boundaries of AMG zones (Zones 54 and 55). XYZ data for each element (X=Longitude, Y=Latitude, Z=Element value) were gridded using GRID from SURFER V4 (Golden Software, Golden, Colorado) on an IBM-compatible computer. Six equal area panels bounded by longitudes 142.90°, 143.65° and 144.40°, and latitudes 17.00°, 17.5°, 18.00° and 18.50° (each 301 columns by 201 rows, or 60,501 grid points) were gridded since GRID could produce only 65536 grid points per grid file. The grid files for the 6 panels were seamlessly combined to give a working grid file with parameters as shown in Table 3.

Table 3. Parameters of EBAGOOLA sheet area grid files.

Longitude	minimum	142.90°
	maximum	144.40°
Latitude	minimum	17.00°
	maximum	18.50°
Grid spacing		0.0025°
No. of columns		601
No. of rows		601
Interpolation method		Kriging
Search radius		0.050°
Nearest neighbours		10

A location approximating to the geometric centre (centroid) of each sample basin was used in preference to the sample site as this more accurately represents the spatial relationship between drainage basins, and reduces the possibility of averaging effects on data points which may be close together although actually representing widely spaced drainage basins. This latter effect is a significant problem when gridding data from low density sampling programs (Eggo and others, 1990,1995). A buffer zone, equivalent to 0.05° of latitude, along the southern margins of the WALSH and BELLEVUE 1:100 000 sheet areas, which lie immediately to the north of the RED RIVER Region, were included in the raw element data to be gridded to enhance continuity with future images for the HANN RIVER Region. No buffer was added for images of statistically derived parameters since these were estimated from data for the sheet area only. Grid files were converted to 8-bit (0-255) 'image' files by 'slicing' (classification) into 9 ranges based on preset proportions of the number of non-zero values (Table 4). All grid points more than the distance equivalent to 0.050° (about 5.5 km) from any sample point have been assigned a value of zero and are coloured white. The conversion programs also added border and location marks, usually decimals of degrees of latitude and longitude.

Table 4. Percentage ranges for 'sliced' images and corresponding pseudo colours and greyscales.

	Percentage of values	Range	Approximate pseudo colour	Greyscale
1	100.0-99.9	0.1	Black	Black
2	99.9-99.0	0.9	Red	Darkest grey
3	99.0-98.0	1.0	Orange	
4	98.0-95.0	3.0	Yellow	
5	95.0-90.0	5.0	Yellow-green	8 steps
6	90.0-80.0	10.0	Green	of grey
7	80.0-60.0	20.0	Green-blue	
8	60.0-30.0	30.0	Light blue	
9	30.0- 0.0	30.0	Dark blue	Lightest grey

Image files were translated into Macintosh format and loaded into IMAGE (National Institute of Health, USA) using the pseudo colour or greyscale palettes listed in Table 4.

Additional image processing, including production of RGB composite images, was carried out using PHOTOSHOP V2.0 (Adobe Systems Inc.). The pseudo colour or greyscale

images were stored as PICT files and imported into CANVAS for annotation and addition of the concentration key. Colour and greyscale images were reproduced on a Canon Postscript colour photocopier/printer.

Although colour images are more visually appealing and permit rapid identification of areas belonging to each concentration range (Cruikshank, 1994), low volume colour printing is relatively expensive and in this record greyscale images have been used for reasons of economy. Colour images for most elements (raw data) and for many statistically derived parameters are included in a separate colour atlas covering the RED RIVER Region (Cruikshank, 1995).

STATISTICAL ANALYSIS

Element values below the detection limit of the analytical method used (Not Detected or ND values) appear in the datafile as the negative of the detection limit value. For the following statistical calculations a value of half the detection limit has been substituted. For example, Sn by XRFS has a theoretical detection limit of 2 ppm under the analytical conditions used, and ND values appear as -2 in the datafile and are treated as 1 (ppm) in the calculations. An element symbol suffixed with an asterisk (*) indicates that analysis was by ICP-MS at Analabs, Perth. Similarly, a cross-hatch (#) indicates BCL/GFAAS by ALS, Brisbane. No suffix indicates analysis in AGSO's laboratory.

4.1 Duplicate Samples

Duplicate samples were collected at a number of sample sites to test the overall reproducibility of the sampling and analytical procedures. Data for 15 pairs of duplicate samples were compared using the 'paired t-test' (Koch and Link, 1970) which computes a confidence interval for the population mean of the differences between paired observations, in this case the duplicate samples. A confidence interval is used because experimental error (sampling + analytical) would normally preclude obtaining the same results for the duplicate samples. If the confidence interval includes zero, or the calculated t-statistic is inside the range +-T, then the conclusion is that the duplicate samples are not statistically different. No significant difference was found at the 2% confidence level and only Ga, Nb and Zr differed at the 10% confidence level. The sampling, and analysis, was held to be statistically reproducible at the confidence levels tested. An average value for each element in each 'duplicate' sample has been used for all following data analysis and imagery.

4.2 Summary Univariate Statistics

Summary univariate statistics are shown in Table 5. These include the minimum, maximum, median, arithmetic (raw data) mean, standard deviation, skewness, coefficient of variation, geometric (log-transformed) mean, geometric deviation, skewness, and arithmetic mean, standard deviation and skewness of a trimmed sample population from which the top and bottom 15% of values for the total dataset were deleted. The trimmed data and geometric statistics are considered (Ellis and Steele, 1982; Eggo and others, 1990,1995) to be more robust, that is less subject to the effects of outliers, than the raw data statistics, and therefore better define the background character of the data. Data for four elements (Bi, Mo, Se and Ta) contained a large number (>80%) of ND values and no statistical parameters other than minimum, maximum and median were recorded.

Table 5. Basic statistical parameters for RED RIVER Region data (N=843). Values are in parts per million (ppm), except for Au#, Pd# and Pt# which are in parts per billion (ppb). Trimmed statistics have top and bottom 15% of values deleted (N=590).

				Raw data			
	Min.	Max.	Med.	Mean	S.D.	Skew	C.o.V.%
Element							
As	-0.5	117.0	2.0	4.32	9.23	6.10	214
Au#	-0.01	25.5	0.07	0.30	1.34	12.0	447
Ba	40	1911	466	485.6	250.4	0.59	51.6
Be*	0.17	15.8	1.5	1.80	1.39	3.99	77.3
Bi	-2	12	-2				
Bi*	-0.10	14.6	0.35	0.54	0.85	10.5	158
Cd*	-0.10	0.87	0.10	0.12	0.09	2.39	78
Ce	14	2571	77	118.9	159.7	8.35	134
Cr	3	319	50	57.4	40.4	2.19	70.3
Cu	-1	53	8	9.89	7.86	1.66	79.5
Fe	5000	147000	18000	22260	13750	2.35	61.8
Ga	-1	28	10	10.1	5.12	0.37	50.9
Ge	1	5.5	2.5	2.55	0.73	0.39	28.7
Hf	2	135	14	17.3	12.8	13.47	73.8
La	5	1325	37	59.1	83.4	8.45	141
Mn	28	5343	327	440.6	425.3	3.58	96.5
Mo	-2	13	-2				
Mo*	-0.10	5.91	0.70	0.76	0.50	2.08	65.3
Nb	4	209	18	20.0	12.3	5.92	61.4
Nd	4	1125	31	49.3	70.8	8.64	143
Ni	-1	107	7	9.86	9.33	3.06	94.6
P*	-20	3902	213	297.8	282.3	4.44	94.8
Pb	6	179	25	27.6	15.2	4.07	55.3
Pd#	-0.01	1.19	0.06	0.10	0.11	3.51	106
Pt#	-0.01	0.38	0.04	0.04	0.03	2.59	75
Rb	4	616	66	90.0	88.2	2.45	97.9
Sb*	-0.05	298	0.45	1.09	10.8	25.71	988
Sc	1	42	8	8.86	4.89	1.72	55.2
Se	-1	1	-1				
Sn	-2	4462	8	33.6	165.0	23.2	492
Sr	6	579	51	71.4	71.9	2.43	101
Ta	-2	8	-2				
Th	2	691	22	40.1	52.1	4.85	130
Ti	1017	99999	5438	8830	10750	4.30	122
Tl*	-0.5	3.39	0.57	0.66	0.49	1.66	74.8
U	-0.5	56	4.5	6.22	5.82	3.16	93.5
V	6	571	57	67.3	47.2	2.72	70.1
W	-3	48	5	6.33	5.07	2.47	80.2
W*	-0.10	59.1	1.13	2.06	3.82	8.29	185
Y	7	583	49	67.1	60.8	3.06	90.7
Zn	4	295	33	35.9	23.6	2.54	65.6
Zr	121	5844	607	785.1	629.8	2.97	80.2

- signifies element analysed by Bulk Cyanide Leach method (Australian Laboratory Services, Brisbane)

* - signifies element analysed by ICP-MS (Analabs, Perth)

All other elements analysed by AGSO (formerly BMR) laboratories in Canberra

	Log-transformed data			Trimmed data		
	Mean	G.D.	Skew	Mean	S.D.	Skew
Element						
As	1.98	3.26	0.17	2.35	1.24	0.61
Au#	0.08	3.62	0.89	0.09	0.05	1.26
Ba	416.1	1.80	-0.55	469.2	164.6	0.02
Be*	1.48	1.86	0.11	1.57	0.53	0.38
Bi						
Bi*	0.39	2.02	0.94	0.38	0.14	0.92
Cd*	0.09	1.92	0.57	0.10	0.05	0.55
Ce	84.7	2.11	0.68	87.1	35.9	0.74
Cr	45.7	2.05	-0.65	51.2	15.9	0.29
Cu	7.29	2.26	-0.29	8.32	3.83	0.53
Fe	19090	1.73	0.19	19807	6316	0.60
Ga	8.41	1.98	-1.45	9.82	3.06	0.02
Ge	2.44	1.35	-0.46	2.53	0.41	0.09
Hf	14.5	1.75	0.49	14.7	4.40	0.64
La	40.9	2.18	0.63	42.3	18.4	0.79
Mn	301.3	2.49	-0.27	358.4	173.4	0.46
Mo						
Mo*	0.59	2.28	-1.24	0.72	0.26	0.20
Nb	17.9	1.58	0.38	18.1	4.19	0.36
Nd	33.7	2.22	0.54	35.4	15.4	0.72
Ni	6.74	2.49	-0.26	8.02	4.24	0.57
P*	224.0	2.09	0.18	238.3	102.2	0.74
Pb	24.8	1.57	0.22	25.5	6.02	0.14
Pd#	0.06	2.71	-0.29	0.07	0.04	0.83
Pt#	0.03	2.58	-0.61	0.03	0.02	-0.28
Rb	59.3	2.62	-0.27	71.8	36.4	0.45
Sb*	0.48	2.22	0.61	0.49	0.15	0.71
Sc	7.73	1.69	-0.10	8.10	2.40	0.47
Se						
Sn	9.82	4.02	0.50	12.0	9.43	1.26
Sr	47.3	2.51	0.02	54.5	27.8	0.50
Ta						
Th	25.7	2.43	0.49	27.3	14.4	1.06
Ti	6190	2.13	0.84	6163	2579	1.07
Tl*	0.52	1.99	0.31	0.55	0.27	0.20
U	4.60	2.19	-0.24	4.94	1.84	0.58
V	54.3	1.97	-0.35	60.0	21.4	0.45
W	4.79	2.16	-0.14	5.40	2.23	0.01
W*	1.06	3.17	-0.16	1.30	0.74	0.69
Y	51.4	2.00	0.45	52.7	20.2	0.64
Zn	29.3	1.95	-0.39	32.9	11.9	0.19
Zr	630.4	1.89	0.45	648.5	240.7	0.71

The number of sample populations and their distribution types for each element were assessed from histograms, and raw data and log-transformed data probability plots (Sinclair, 1974, 1991) generated by DATA DESK IV and STATVIEW II (Appendix B). Most populations had one or more outliers which did not fit the assessed distributions, but which were of insufficient numbers to constitute a separate population. With the exceptions of Ga and Mo* the element populations appear to follow log-normal distributions and so log-transformed values were used in the factor analysis.

4.3 Summary Multivariate Statistics

4.3.1 Correlations

The statistical correlation between pairs of elements often highlights significant geochemical associations but must be treated with some caution. A high correlation 'does not prove cause and effect' (Eggo and others, 1990,1995) but, if an underlying geochemical rationale can be elucidated, may quantify the relationship. The size of the RED RIVER dataset (N=843) reduces the possibility of chance correlations sometimes found in small datasets. The Pearson product-moment correlation method assumes normally distributed sample populations and as many elements (see Table 5) appear to follow the log-normal distribution, matrices of coefficients calculated from both raw data and log-transformed data are shown in Table C1 in Appendix C. Spearman Rank Correlation is a non-parametric method which makes no assumptions about the distributions the data follow. A matrix of correlation coefficients from this method is shown in Table C2, also in Appendix C. All data were included in the calculations but coefficients for Bi, Mo, and Se may be considered as suspect but informative.

For a population of 843 samples any Pearson correlation coefficient greater than 0.13 or less than -0.13 is statistically significant. However, to separate highly correlated associations from the less correlated and potentially chance associations, only coefficients of 0.5 and higher or -0.50 and less (for which variation in element X cause 25% or more of the variation in element Y) have been considered. Several highly correlated groupings are discernible from all three sets of coefficients. These are:-

- Ce - La - Nd - P* - Th - U - W - Y
- Cr - Cu - Fe - Mn - Ni - Sc - Ti - V - Zn
- Be* - Ga - Rb - Tl*
- Hf - Zr
- Ba - Sr

4.3.2 Factor Analysis

In order to quantify the obvious interdependence of many of the variables the data were subjected to Principal Component Factor Analysis. Factor analysis determines whether multi-variate data occupy the same number of dimensions as the number of variables, or are contained in a smaller number of dimensions implying a lesser number of independent variables (Koch and Link, 1971). The procedure operates from a matrix of Pearson product-moment correlation coefficients and therefore is bound by the same assumptions and limitations of that technique, principally the assumption that data are normally distributed, and the limitation of the adverse effects of outliers. For these reasons log-transformed data were used and scattergrams of apparently highly correlated element pairs were viewed to reduce the incidence of outlier effects. The procedure was carried out, using STATVIEW II, on log-transformed data for the 38 elements for which full parameters are listed in Table 5. The analysis produced 8 factors each with Eigenvalues greater than 1 and which between them 'explained' at least 75% of the variability in the data (STATVIEW II manual, Feldman and others, 1990).

The factor loadings indicate the correlation between the variables and the factors. In this exercise the pattern matrix contains 304 values from 38 variables and 8 factors and many loadings, although statistically significant, are below an arbitrary level of 'practical significance'. This is the minimum amount of a variable's variance which reasonably is to be accounted for by the factor, a general level being +-0.30 (Dillon and Goldstein, 1984). Alternatively, only the loading with the largest absolute value for each variable is considered. In this exercise a composite approach has been used with the largest absolute value for each element labelled as a major contributors to a factor, while other practically significant loadings will be labelled as minor contributors. Table 6(a) lists the more significant factor loadings and the proportion of variation in the dataset due to each factor, and Table 6(b) the primary intercorrelations between factors. The communalities represent the proportion of the variance of the variable that can be predicted by the factors extracted, that is high communalities (>0.6) are desirable since low communalities are generally given by elements which have significant numbers of 'not detected' values, or which are not strongly correlated with any other element (Eggo and others, 1990,1995).

Factor 1 comprises a strong association between Ce, Nd, La, Th, Y, U, P* and Nb, with minor contributions from Mn, Ba, Pb, W, Hf, Zr, Ti, Rb and Sr, and accounts for 30.8% of the total variability in the data analysed. The communalities of the prime elements are all high (>0.8) indicating that most of the variance due to these elements is accounted for by the factor extracted.
There is strong statistical and spatial (see next section) correlation between the Rare Earth Elements (REE) Ce, La and Nd, and Th, and between these and Y, U and P*. This is consistent with the presence of resistant heavy minerals, such as the light rare earth/thorium phosphate mineral monazite ([LREE,Th]PO_4)and the yttrium/heavy rare earth phosphate xenotime ([Y,HREE]PO_4), in the sediment (Price and Ferguson, 1980; Cruikshank, 1994).

Factor 2 comprises V, Fe, Ni, Sc, Cu, Cr, Ti, Zn and Mn, with minor contributions from Sr, Ga, As and Pd#, and a negative contribution from Zr. This factor accounts for 18.2% of the total variability and all prime elements have high communalities.
The primary association seems to centre on Fe and is probably partly due to products from the weathering of Fe-rich minerals (e.g. ferro-magnesium and Fe-sulphide minerals), and partly due to secondary scavenging by hydrated Fe (and Mn) oxides (Cruikshank, 1994).

Factor 3 comprises Rb, Tl*, Be*, Ga, Ba, Pb and Sr, with minor contributions from Zn, Mn, W*, Mo*, U and Th, and a negative contribution from Cr. This factor accounts for 10.3% of the total variability. All prime elements have high communality values (>0.65).
This factor appears to be related to the weathering of granitic rocks, particularly to the weathering of K-rich minerals such as K-feldspar ($KAlSi_3O_8$), biotite ($K(Mg,Fe^{2+})_3(AlSi_3)O_{10}(OH,F)_2$) and muscovite, ($KAl_2(AlSi_3O_{10})(OH,F)_2$)(Cruikshank, 1994) and shows strong intercorrelation with Factor 1 (see Table 6(b)).

Factor 4 comprises Bi*, Sn, Hf, W, Zr and W*, with minor contributions from Nb, Y and U, and negative contributions from Sr and Ba. This factor accounts for 6.4% of the total variability, but Bi* (0.67), Sn (0.64) and W (0.62) have moderate only communality values. The inclusion of Sn, Hf, Zr and W/W* suggests resistant heavy minerals such as cassiterite (SnO_2), zircon ($(Zr,Hf)SiO_4$) and wolframite ($(Fe,Mn)WO_4$), common from the weathering of granites.

Table 6(a). Rotated factor loadings, eigenvalues and communalities for RED RIVER Region log-transformed data (N=843).

	Communalities	F1	F2	F3	F4	F5	F6	F7	F8
As	0.608		0.320			0.526		0.378	
Au#	0.500					0.565			
Ba	0.855	0.424		0.663	-0.329				
Be*	0.780			0.810					
Bi*	0.666				0.721				
Cd*	0.698						0.799		
Ce	0.951	0.927							
Cr	0.826		0.746	-0.480					
Cu	0.840		0.825						
Fe	0.931		0.894						
Ga	0.811		0.351	0.799					
Ge	0.665					-0.355	0.452		0.372
Hf	0.814	0.393			0.640				-0.363
La	0.936	0.914							
Mn	0.864	0.425	0.598	0.462					
Mo*	0.645			0.359				0.522	
Nb	0.818	0.547			0.477			-0.342	
Nd	0.946	0.924							
Ni	0.899		0.885						
P*	0.811	0.652						0.334	
Pb	0.649	0.421		0.617					
Pd#	0.720		0.305			0.305			0.716
Pt#	0.617					0.767			
Rb	0.906	0.350		0.881					
Sb*	0.705							0.793	
Sc	0.866		0.869						
Sn	0.642				0.687				
Sr	0.754		0.301	0.451	0.534	-0.406			
Th	0.920	0.876							
Ti	0.885	0.359	0.676					-0.438	
Tl*	0.801			0.819					
U	0.866	0.787		0.304	0.326				
V	0.948		0.910						
W	0.621	0.412			0.615				
W*	0.753			0.462	0.538			0.453	
Y	0.878	0.807			0.399				
Zn	0.857		0.613	0.597					
Zr	0.840	0.360	-0.319		0.606				-0.367
Eigenvalues		11.72	6.93	3.92	2.42	1.74	1.25	1.13	1.00
Proportion of original variance (%)		30.8	18.2	10.3	6.4	4.6	3.3	3.0	2.6
Cumulative (%)		30.8	49.0	59.3	65.7	70.3	73.6	76.6	79.2

Table6(b). Primary intercorrelations for Factors above.

	F1	F2	F3	F4	F5	F6	F7	F8
F1								
F2	0.335							
F3	0.528	0.306						
F4	0.210	-0.188	0.177					
F5	0.199	0.134	0.040	-0.133				
F6	0.073	0.201	0.126	0.084	-0.109			
F7	0.035	-0.152	0.138	0.059	0.159	-0.094		
F8	0.041	0.207	0.055	-0.183	0.133	-0.004	0.029	

Factor 5 comprises Pt#, Au# and As, with a minor contribution from Pd#, and a negative contribution from Ge. This factor accounts for 4.6% of the total variability although communality values for Pt# (0.62), Au# (0.50) and As (0.61) are all moderate to low indicating that some of the variability of these elements is not accounted for by the factor. The factor is obviously associated with precious metal mineralisation.

Factor 6 comprises Cd* and Ge and accounts for 3.3% of the total variability. The association is not known.

Factor 7 comprises Sb* and Mo*, with minor contributions from W*, As and P*, and negative contributions from Ti and Nb. The factor accounts for 3.0% of the total variability. The factor possibly represents a sulphide mineral association (Sb*, Mo*, W* and As).

Factor 8 comprises Pd#, with minor contributions from Ge and Au# (compare with Factor 5), and negative contributions from Zr and Hf. This factor accounts for 2.6% of the total variability.

INTERPRETATION

The following interpretation uses the factor groupings discussed in the previous section and relates high values with underlying geology, or to possible regolith or mineralisation causes.

5.1 Factor 1

Factor 1 comprises Ce, Nd, La, Th, Y, U, P* and Nb, with minor contributions from Mn, Ba, Pb, W, Hf, Zr, Ti, Rb and Sr, and is considered to be due to the concentration of resistant accessory minerals from weathered granitic and metamorphic rocks, with a minor contribution from elements released during the weathering of K-minerals, mainly from granites. The relative abundances of the prime elements in the factor are shown in box plots in Figure 6. Figure 7 shows image maps for the distribution of Ce, Th, Y, U, P* and scores for Factor 1 (F1) in the RED RIVER Region.

The light REE's (LREE's), Ce, La and Nd, show almost identical spatial distribution patterns with coherent highs over areas underlain by the Dargalong and McDevitt Metamorphics, Nundah Granodiorite and Fig Tree Hill Granite. Th, U and Y show patchy highs in this area,

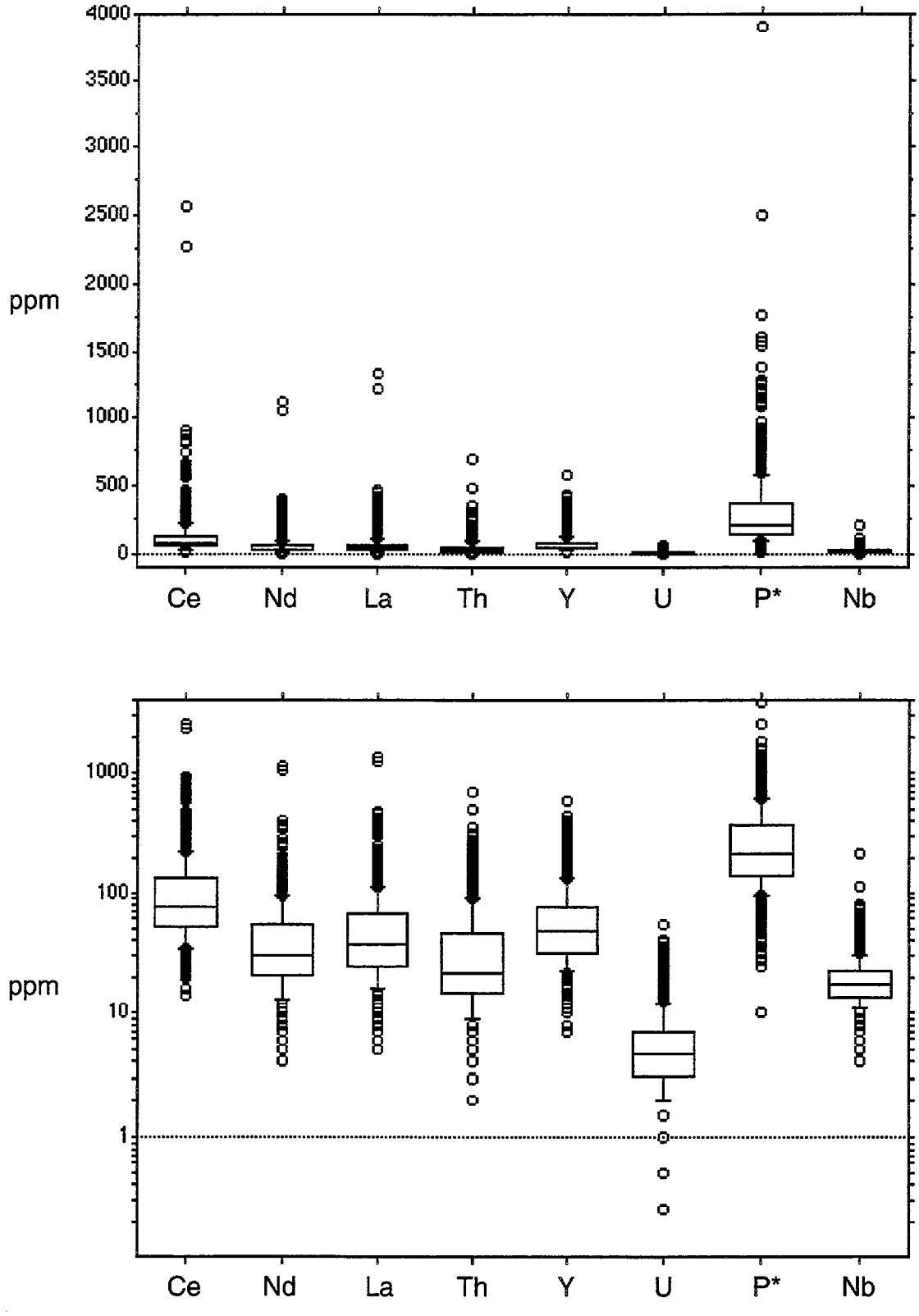

Figure 6. Relative abundances of prime elements in Factor 1.

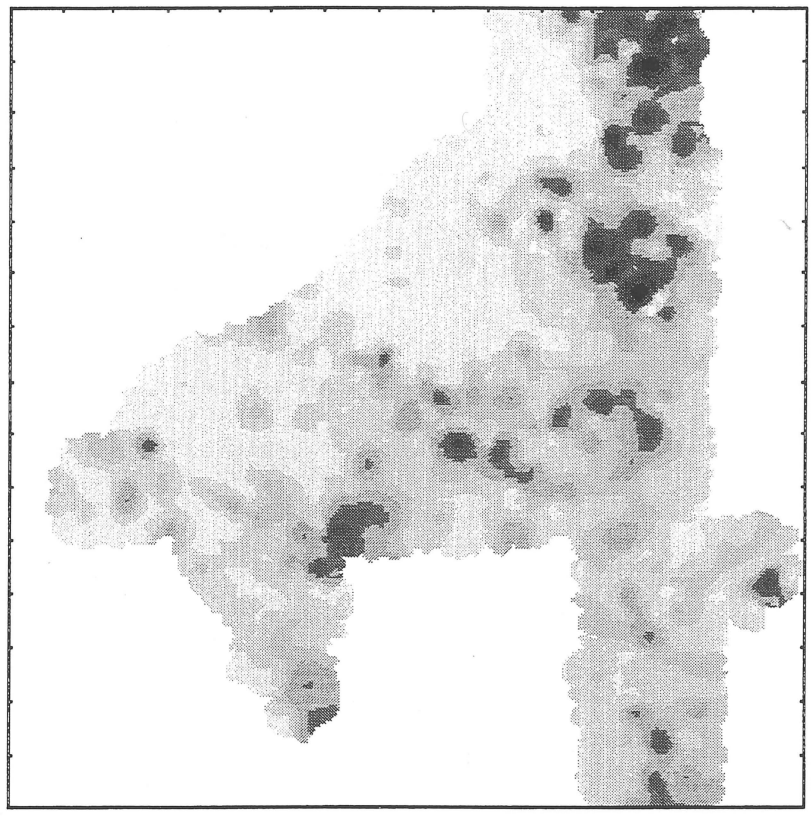

Ce

Th

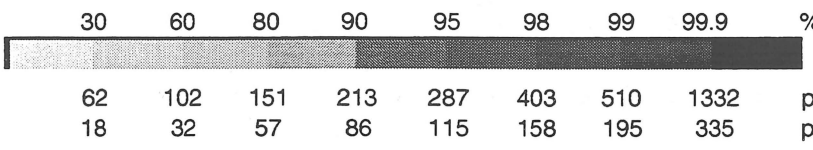

Figure 7. Image maps for Ce, Th, Y, U, P* and F1 scores in the Red River Region.

Y

U

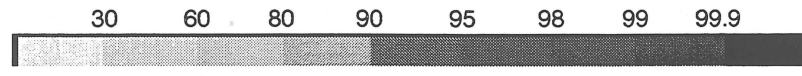

30	60	80	90	95	98	99	99.9	%
37	59	90	130	167	211	243	346	ppm Y
3.7	5.6	8.3	11.8	15.5	20.1	23.9	33.0	ppm U

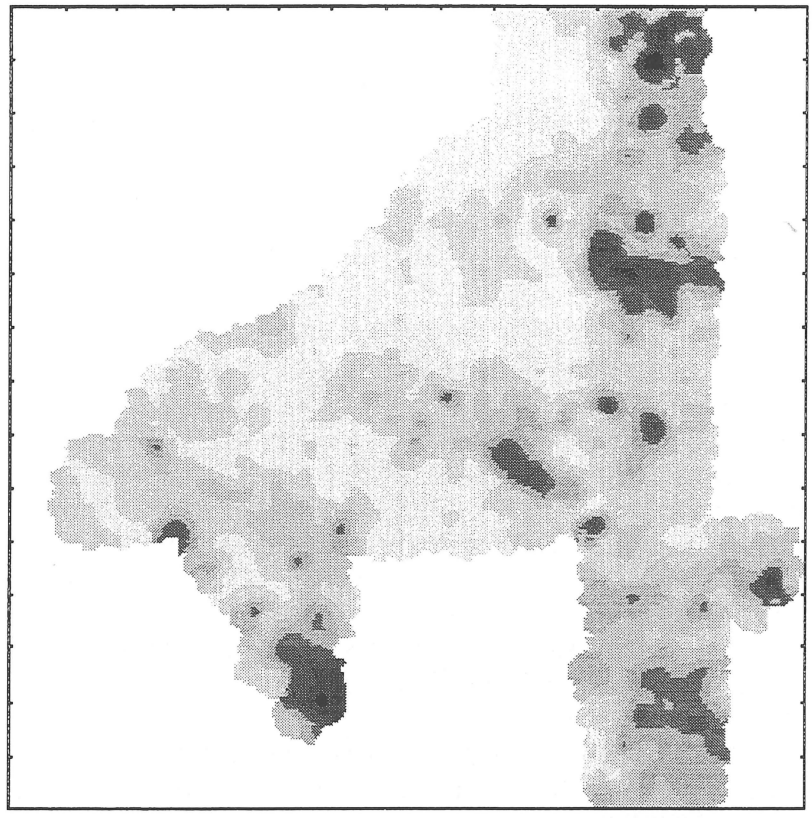

P*

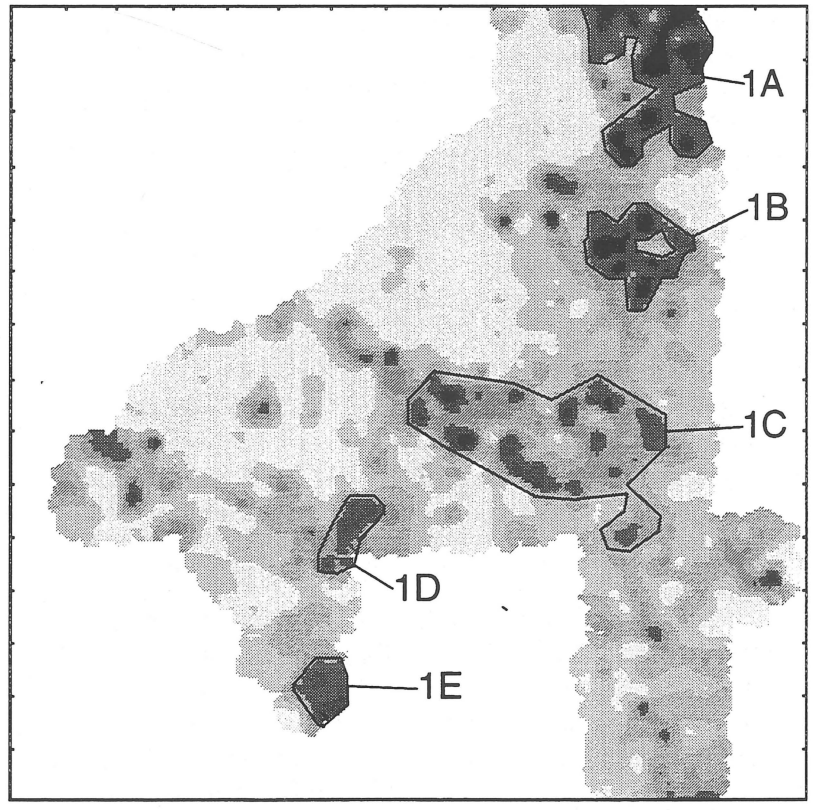

F1

30	60	80	90	95	98	99	99.9	%
162	281	433	562	706	928	1167	2011	ppm P*
-0.45	0.11	0.63	1.11	1.48	1.93	2.25	2.95	F1 scores

and also over the O'Briens Creek granites. P* shows a similar distribution but also has a high in the Mount Turner area.

Clusters of high factor scores occur over 5 areas (Areas **1A-E** in Figure 7) of the region. These are as follows:

Area **1A** (see Figure 7) is east of Blackdown homestead and north of the Tate River in the north of the MUNGANA sheet area. The area is drained largely by the Nundah and Brown/ Williamstown Creek systems and consists of undulating plains with low stony hills underlain by Nundah Granodiorite and Dargalong Metamorphics. The area is erosional and regolith has most likely been developed in-situ. The area shows strong highs for Ce, Nd and La, and moderate highs for Th, Y, U and P*. The north of the area is mineralised with many small Cu mines (Keyser and Wolff, 1964). The area also shows an extensive As, Bi*, Cu and Sb* high. The Nundah Granodiorite is not overly endowed with the elements comprising this factor so highs may be due to either the Dargalong Metamorphics, or to a series of rhyolite dykes which, incidentally, trend in the same north-easterly direction as the high.

Area **1B** lies across the border of the MUNGANA and LYNDBROOK sheet areas, south-west of Bolwarra homestead. It is drained by the Pinnacle Creek system and smaller tributaries of the Lynd River. The area is similar in form to area **1A** and is underlain by McDevitt Metamorphics interspersed with Fig Tree Hill Granite. The Fig Tree Hill Granite is a high U (>15 ppm) and moderate Th (20-30 ppm) granite (Champion and Mackenzie, 1994; ROCKCHEM). The area shows strong highs for Ce, La, Nd, U and P*, and moderate highs for Th and Y. One sample contained very high concentrations of Ce, Fe, La, Mn, Nb, Nd, Sc, Ta, Ti and V.

Area **1C** is an east-west trending group of scattered highs on the GALLOWAY and LYNDBROOK sheet areas, drained by the Parallel, Martin and Dickson Creek systems. The area is gently undulating to hilly country and overlays granites of the O'Briens Creek Supersuite (mostly in the east) and granites of the White Springs Supersuite (mostly in the west), plus patches of Scardons Volcanics and Lane Creek Formation. Strong highs for Th, Y, U, Rb and W occur in the eastern part of area **1C** and extend to the south-east (over Corduroy Swamp, Angore and Elizabeth Creek Granites), with moderate highs for Ce, La, Nd and P*, mostly to the west (Jape Creek Granodiorite). A large Nb high occurs in the south-east, just outside the area designated as area **1C**.

Area **1D** lies in the south west corner of the GALLOWAY sheet area and is drained by the headwaters of Galloway Creek and by tributaries of Fiery Creek. The area is to the north-west to south-west of, and close to, Dagworth homestead. The area is irregular to gently undulating plains over the Robertson River subgroup of the Etheridge Formation interspersed with Cobbold Metadolerite. The area shows highs for Ce, La and Nd, with moderate highs for Th and U. It is also the centre of a strong Cu high (see Figure 11), and is on the edge of a strong Mn, Nb and Ti high immediately to the east.

Area **1E** is south-east of Mount Turner in the FOREST HOME sheet area. The area comprises rolling plains over Forsayth (and Delaney) Granite. The area shows strong highs for P*, Ba and Pb, and moderate highs for Ce, La, Nd and Th. It also shows a

strong Au# high (see Figure 24). The area contains a number of abandoned gold mines of the Etheridge Goldfield.

The REE's, Ce, La and Nd, have extremely strong statistical correlations ($r > 0.98$ for raw data, log-transformed data, and Spearman's rank correlation), and show virtually identical image distribution maps. The strong statistical relationships between the REE's, and relationships between selected F1 elements are shown as scatterplots in Figure 8. In the EBAGOOLA stream sediment survey (Cruikshank, 1994) the strong statistical and spatial correlation extended to Th, and to a lesser degree to P*, and was deemed to be consistent with the presence of these elements (plus U) in the resistant mineral monazite (Price and Ferguson, 1980) concentrated in the bed lode of streams draining rocks containing the mineral. Similarly, the correspondence between Y and P* (plus U) in other areas was deemed to be due to presence of xenotime weathered from rocks containing higher proportions of this resistant phosphate mineral. In the RED RIVER Region the relationship between REE's and Th is not as tight, with Th showing a slightly stronger association with Y than in the EBAGOOLA area. Also, the relationship of REE, Th and Y with P* does not appear to be as strong, although it must be noted that in all samples where high concentrations of these elements occur, there appears to be a significant excess of P over the amount notionally required to form phosphate minerals such as monazite and xenotime, estimated from the P*, REE, Th, Y and U values for the individual samples. This suggests that P* may be present in significant quantities of other minerals such as apatite ($Ca_5[PO_4]_3[OH,F,Cl]$ - which also can contain small amounts of REE, Th, Y and U), and that the REE, Th and Y (plus U) may also be found in the non-phosphate, epidote mineral allanite ($[Ca,Mn,Ce,La,Y,Th]_2[Fe^{2+},Fe^{3+},Ti][Al,Fe^{3+}]_2\ O.OH[Si_2O_7][SiO_4]$), both of which have been recorded as accessory minerals in granites in the area (Sheraton and Labonne, 1978). Other than monazite as an accessory in 'greisenised varieties of the 'Elizabeth Creek Granite' (Sheraton and Labonne, 1978), monazite and xenotime are not generally acknowledged as present at significant levels in the granites, although this is not to say they are completely absent. Indeed, some stream sediments contain up to an estimated 1% of the heavy minerals by weight. The minor contributions from Hf and Zr, and Ti are probably due to the concentration of small amounts (cf Factor 4) of the resistant minerals zircon and sphene ($CaTi[SiO_4](O,OH,F)$) in the same heavy mineral 'traps' as the monazite and xenotime. Both are recorded as accessory minerals in the granites (Sheraton and Labonne, 1978).

The major difference between monazite and xenotime on the one hand, and allanite is in the stability of the minerals in the secondary environment. Both monazite and xenotime are moderately resistant to weathering and would tend to accumulate in the bed lode, most likely without significant loss of U. Allanite is less stable in the secondary environment and weathers to hydrated Fe- and Al-oxides, and silica, with a weathered crust rich in ThO_2 but depleted in REE relative to the original mineral (Deer and others, 1962). Under prevailing surficial conditions (ie oxidising) U is likely to be highly mobile (Levinson, 1974).

The distribution of U (Figure 7) follows that of the REE, Th and Y. Many high values are concentrated in the north in areas **1A** and **1B**, possibly in accumulations of monazite and xenotime, or of weathering products of allanite, from the metamorphics. In the south high values occur mostly over granites of the O'Briens Creek Supersuite (eg Angore and Elizabeth Creek Granites), which is relatively high in U (ROCKCHEM database - average of 11 ppm and maximum of 26 ppm compared with 4.8 ppm granite average, Krauskopf, 1967). Common rock forming minerals can contain 2 to 8 ppm U, and monazite, xenotime and zircon up to 20,000 ppm, 35,000 ppm and 10,000 ppm U respectively (Price and Ferguson, 1980). However, it is not the U which is concentrated in these, and other,

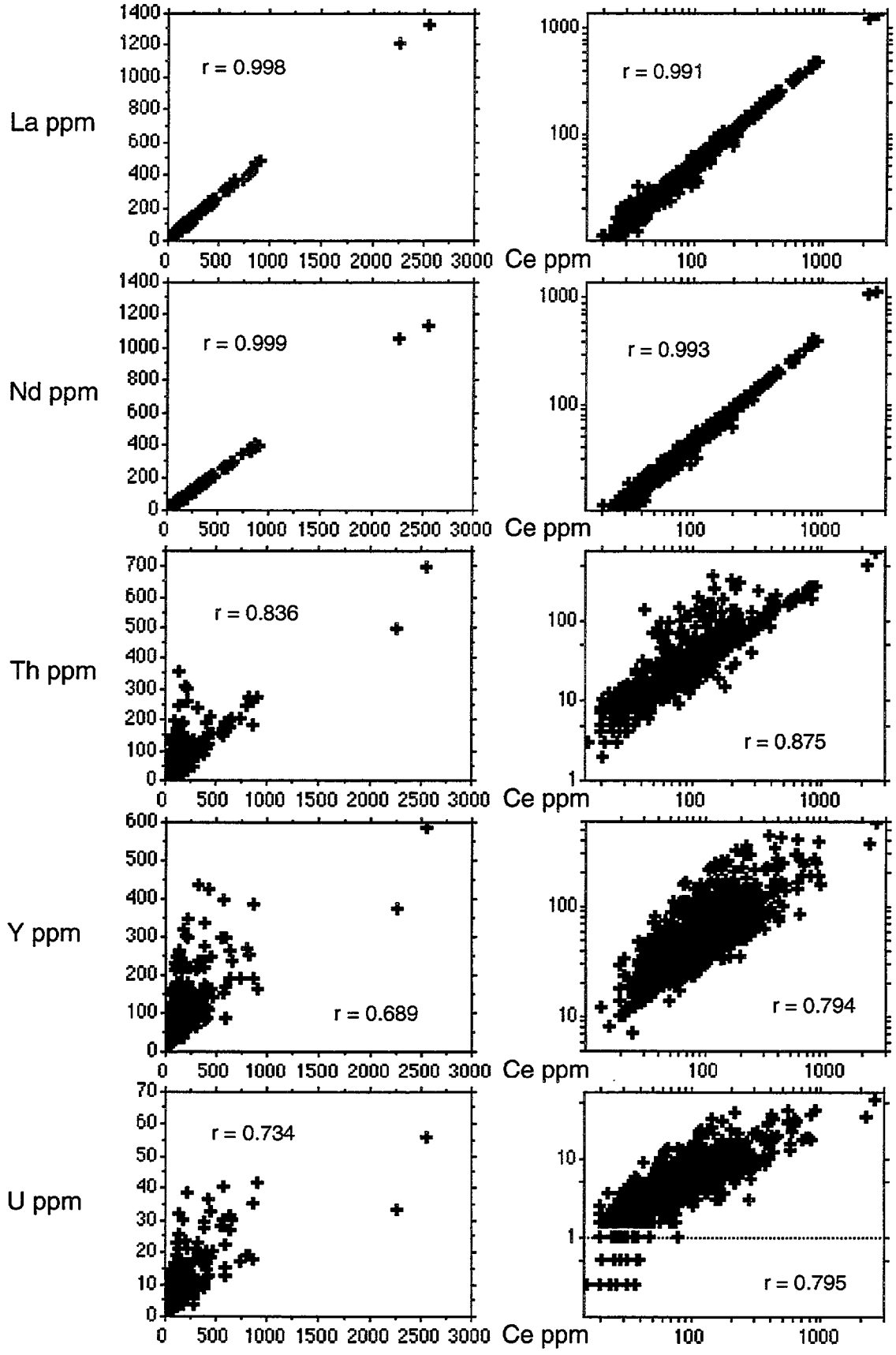

Figure 8. Raw data and log-transformed scatterplots of selected pairs of Factor 1 elements (**r** is the Pearson correlation coefficient).

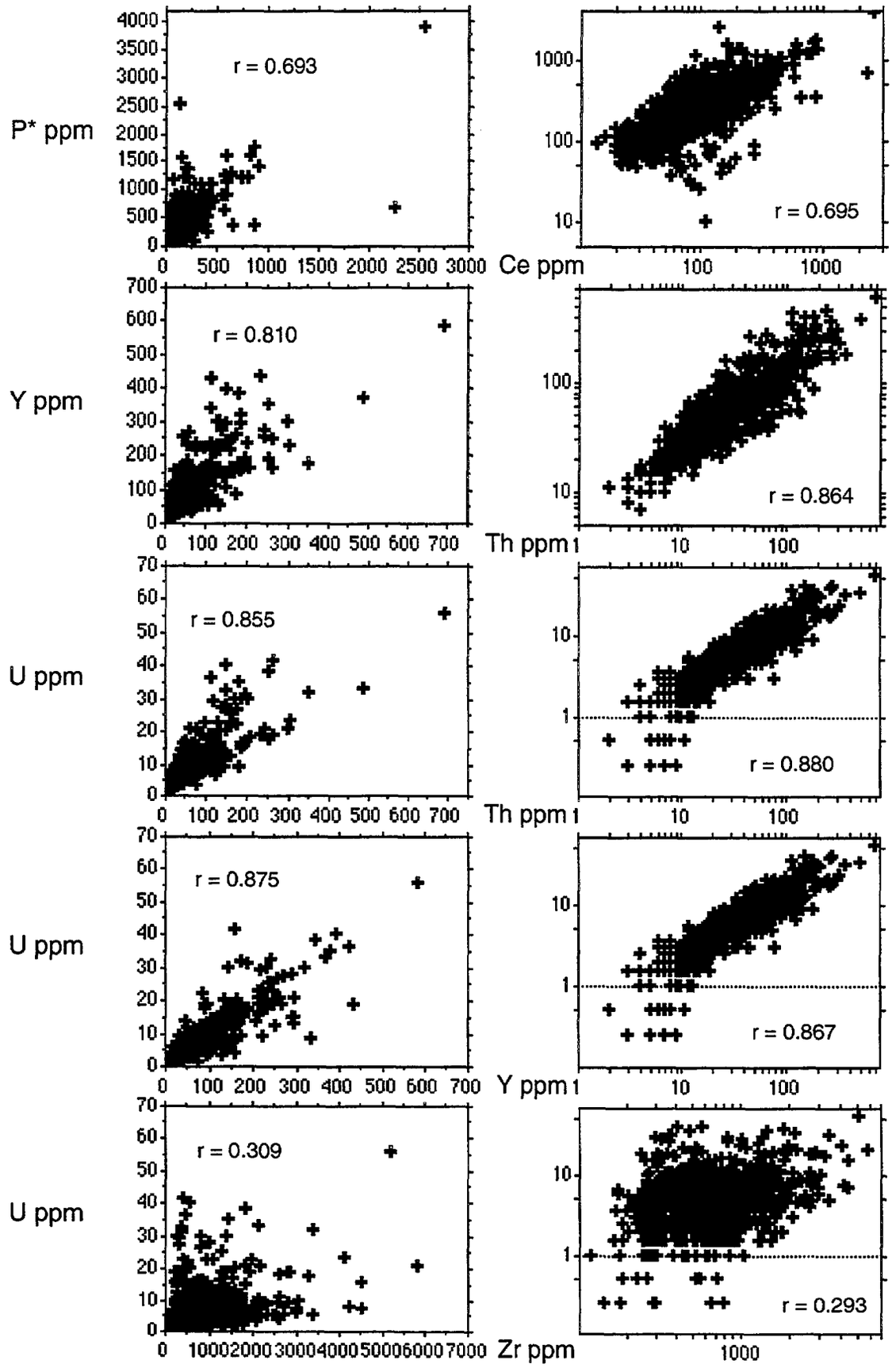

resistant minerals, which is of economic interest but the more mobile U species which can be adsorbed onto clays and hydrated Fe and Mn oxides. The problem then is to define the later in the presence of the former. The most satisfactory method to determine mobile U species is to leach the samples and to determine U in the leachates. This is not often practical, especially on a regional scale.

In the absence of these data Price and Ferguson (1980) substituted a form of lithochemical compensation by examining the ratios of U to elements which are an essential component of each of the resistant minerals, for example Hf for zircon, Ce and Th for monazite and Dy for xenotime. The author used a similar approach for the EBAGOOLA survey (Cruikshank, 1994) using instead (Ce+La+Nd+Th) for monazite, Y for xenotime and Zr for zircon. Price and Ferguson (1980) also used estimates of residual U contents derived from correction of the total U value for U in the common rock forming minerals, the resistant minerals listed above and in other entities including organic phases. Lithochemical correction from predicted values from linear regressions of U against the values of the associated elements, and against principal component factor scores were also attempted. Unfortunately, U has a relatively short dispersion train (<1 km) downstream from mineralisation in northern Australia (Foy and Gingrich, 1977; Hoatson and Cruikshank, 1985; Cruikshank and others, 1993). For a sampling density of 1 per 10-15 km^2 most basins have stream lengths of 3 km or more, so that U from mineralisation can be easily lost in a background of U from other sources.

The most promising approach appears to be regression of log-transformed data against factor scores, with deletion of highly anomalous residuals to produce a regression equation more adequately representing the background population (Eggo and others, 1990,1995; Cruikshank, 1994). STATVIEW II was used for simple regression of log(U) against F1 and the U residuals (U_{res}) estimated. All samples (29 in number) with U_{res} greater than mean plus 2 standard deviations (equal to 7.72 ppm U_{res}) were eliminated from a recalculation of the regression. The final simple regression equation was:

$$\log(U_p) = 0.255*F1 + 0.649$$

where U_p is the U value predicted from the F1 score. U_p, in ppm, was subtracted from the total (measured) U value giving U_{res}. An image map of U_{res} is shown in Figure 9(a). High residuals occur over 2 areas of O'Briens Creek Supersuite granites (mostly Angore and Elizabeth Creek Granites) in the south, and over Fig Tree Hill Granite (+- Dargalong and McDevitt Metamorphics in the north. Although U is a major component of Factor 1 it also is a minor contributor to Factor 3, thought to represent K-rich minerals, and Factor 4, thought to be associated with resistant minerals such as cassiterite and zircon. The regression concept was extended to a step-wise multiple regression of log(U) against all factor scores since none of the factors extracted appears to be related directly to U mineralisation. Factors 5 and 6 were eliminated from the regression. The regression was recalculated after elimination of 16 samples with residuals greater than 5.65 ppm, giving the following equation:

$$\log(U_p) = 0.259*F1 + 0.038*F2 + 0.104*F3 + 0.113*F4 - 0.021*F7 + 0.056*F8 + 0.659$$

An image map is shown in Figure 9(b). The high residuals over the O'Briens Creek Supersuite granites have been all but eliminated, no doubt due to the influence of Factors 3 and 4 which show highs in this area. The residual U highs over the two areas (Areas **1Y** and **1Z** in Figure 9) over the Fig Tree Hill Granite (+-Dargalong and McDevitt

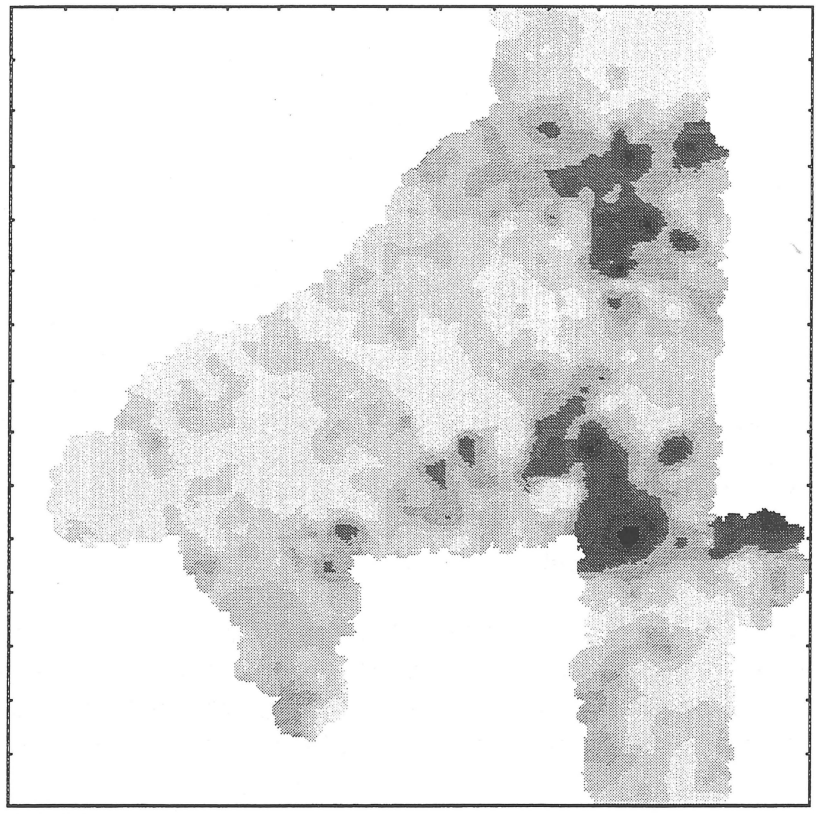

U_{res}

(a) Simple regression of log(U) v's F1.

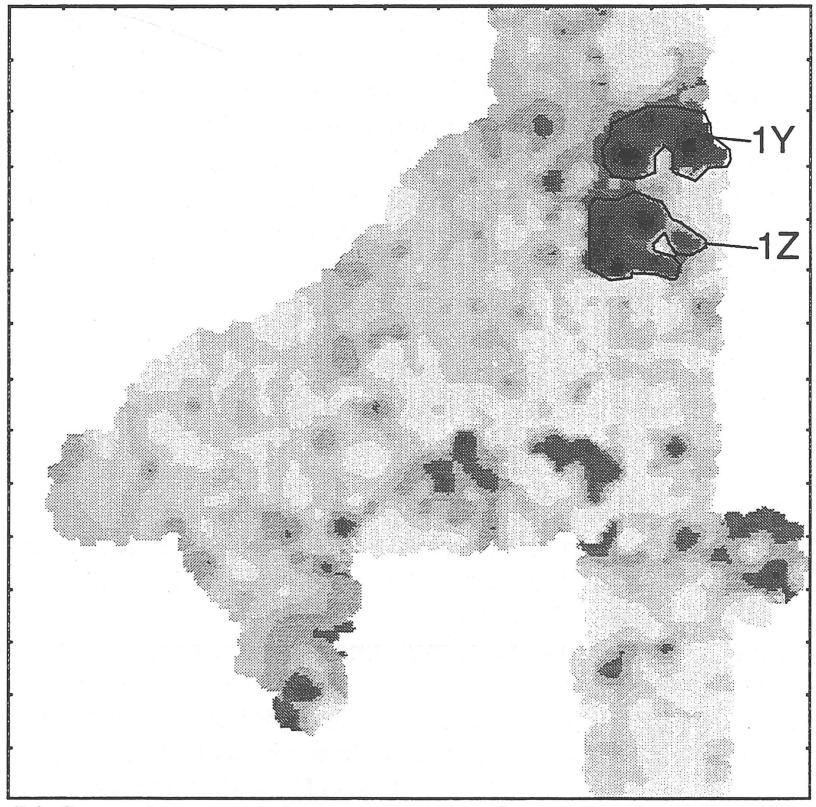

U_{res}

(b) Stepwise multiple regression of log(U) v's all factors (F5 and F6 eliminated).

30	60	80	90	95	98	99	99.9	%
-0.45	0.79	2.16	3.77	6.56	10.2	12.4	21.0	U_{res} (Simple)
-0.32	0.39	0.96	1.60	2.66	4.98	6.80	11.5	U_{res} (Stepwise)

Figure 9. Simple and stepwise regression of log(U) against factor scores.

Metamorphics), and displaced slightly from it in the directions of the prevailing drainage, are correspondingly more extensive and more intense. The northern area (**1Y**) sits astride a drainage ridge and is drained by the northward-flowing Brown/Williamstown Creek system, and the Big Black Gin Creek system, a tributary of the Tate River. Big Black Gin Creek also drains the McCord Granite outside the survey area to the east. The southern area (**1Z**) is drained by the Pinnacle Creek system. The Fig tree Hill Granite is a high U (16 ppm [ROCKCHEM] cf 4.8 ppm granite average [Krauskopf, 1967]) and moderately high Th (29 ppm cf 17 ppm) granite (Th/U low at 1.8). The McCord Granite is also high U (15 ppm). The Dargalong and McDevitt Metamorphics are low to moderate in U (maximum U values of 8 ppm and 11 ppm respectively) so that the residual (or mobile) U may reasonably be expected to have originated with the granites. Residual values derived from the step-wise regression have been used in subsequent calculations, etc using U residuals, for example in the calculation of the Uranium Index (Section 5.9.2.6).

P* shows moderate to strong highs in area **1A** and **1B**, subdued highs in area **1C**, very little in area **1D**, and a very strong high in area **1E**, south-east of Mount Turner. Area **1E** is over Forsayth and Delaney Granites (+- Daniel Creek Formation). The Forsayth Granite has relatively high P contents (ROCKCHEM). P is a basic constituent of apatite, monazite and xenotime.

The distribution of Nb is less coherent with respect to Factor 1 scores and comprises one or two high values in, or a group of moderate values in or adjacent to, a nominated area. Area **1B** contains a single sample which has the highest Nb content recorded for the survey (209 ppm) plus several moderate values (65 and 32 ppm) in or adjacent to the south border of the area. The high value occurs near contact between McDevitt Metamorphics and O'Briens Creek granites. Groups of moderate to high values occur to the south-east of area **1C,** over granites of the O'Briens Creek Supersuite, and to the east of area **1D,** over Yataga Granodiorite and adjacent Lane Creek Formation. Nb is mostly likely to occur in zircon or Ti-minerals such as ilmenite ($FeTiO_3$) and sphene, although the spatial and statistical relationship between Nb and Ti is stronger than that between Nb and Zr. As stated above, zircon and sphene have been recorded as accessory minerals in the 'Elizabeth Creek' and 'Forsayth' Granites of Sheraton and Labonne (1978).

5.2 Factor 2

Factor 2 comprises V, Fe, Ni, Sc, Cu, Cr, Ti, Zn and Mn, with minor contributions from Sr, Ga, As and Pd#, and a negative contribution from Zr. The relative abundances of the prime elements of the factor are shown in Figure 10. Figure 11 shows image maps for the distribution of Fe, Ni, Cu, Ti, Zn and F2 scores.
The factor relates to the geochemistry of Fe, including the entry of Cr, Cu, Ni, Sc V, etc into Fe-rich, mafic minerals such as pyroxenes, amphiboles and biotite in basalts, diorites and their metamorphic products, and the co-precipitation with, or adsorbtion onto, hydrated Fe-oxides in the secondary environment of these and other elements such as Zn (Wedepohl, 1972). Scatterplots showing the relationships between Fe and elements in the factor are shown in Figure 12.

The image maps for V, Fe, Sc, Ti and Mn differ only in the emphasis given to one area or another with highs occurring over Einasleigh and McDevitt Metamorphics, and the Lane Creek Formation (+- Cobbold Metadolerite). Ni, and to a lesser extent Cr, give highs over the Undarra Basalt and Einasleigh Metamorphics, and patchy highs over the Lane Creek Formation (+- Cobbold Metadolerite) and McDevitt Metamorphics. Cr also shows strong

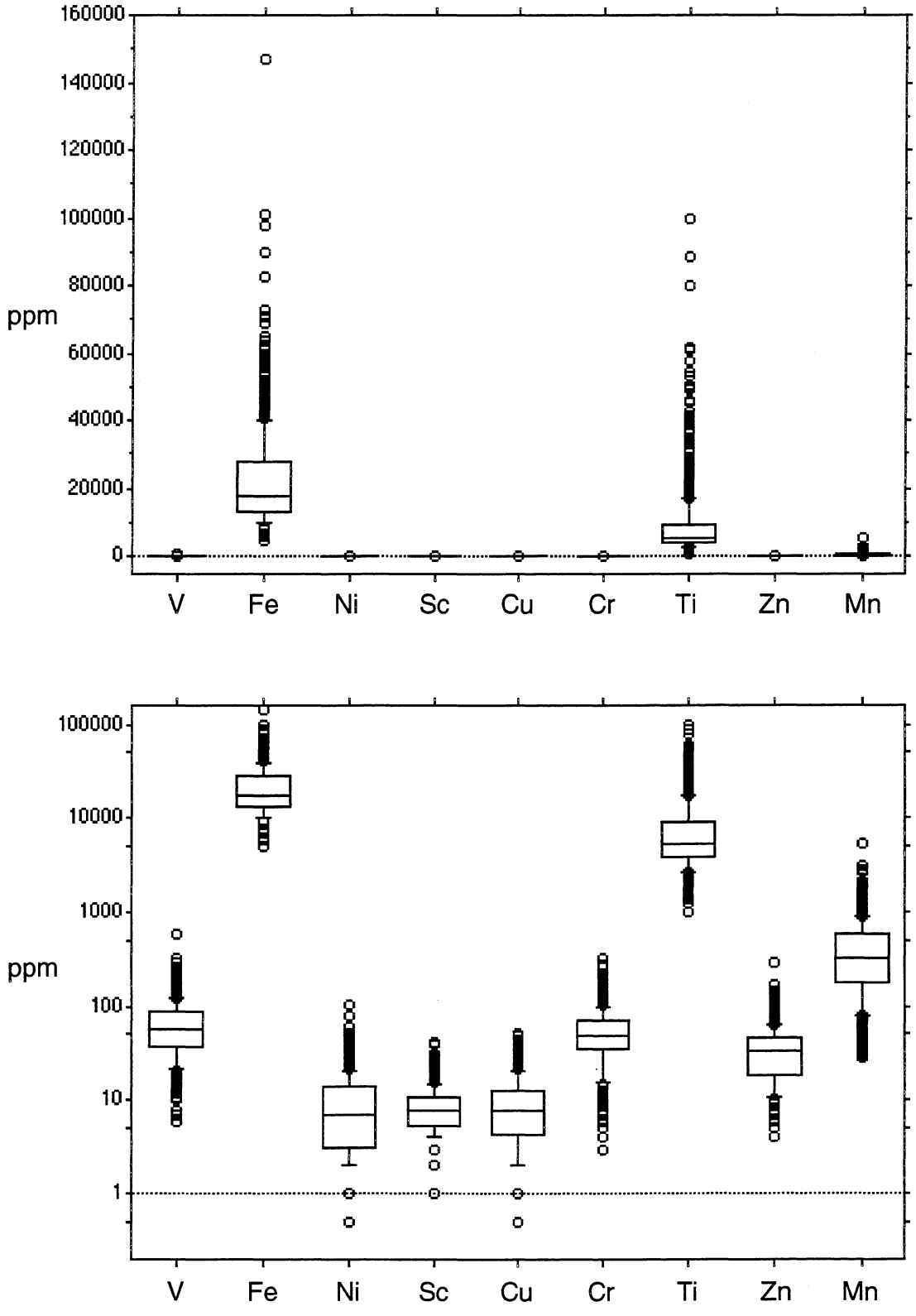

Figure 10. Relative abundances of prime elements in Factor 2.

Figure 11. Image maps for Fe, Ni, Cu, Ti, Zn and F2 scores in the Red River Region.

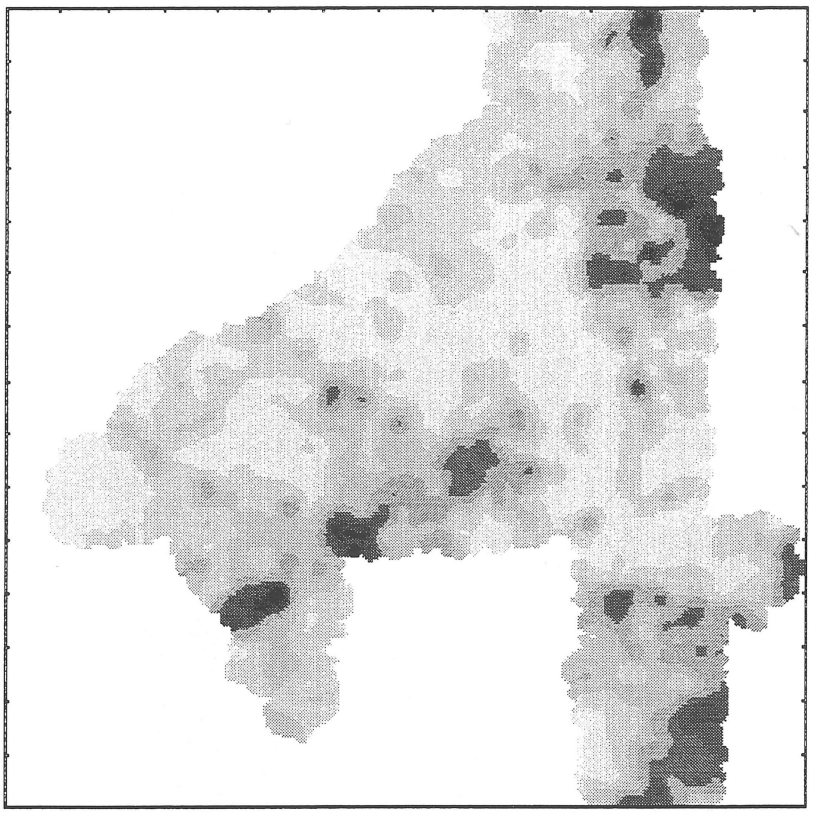

Cu

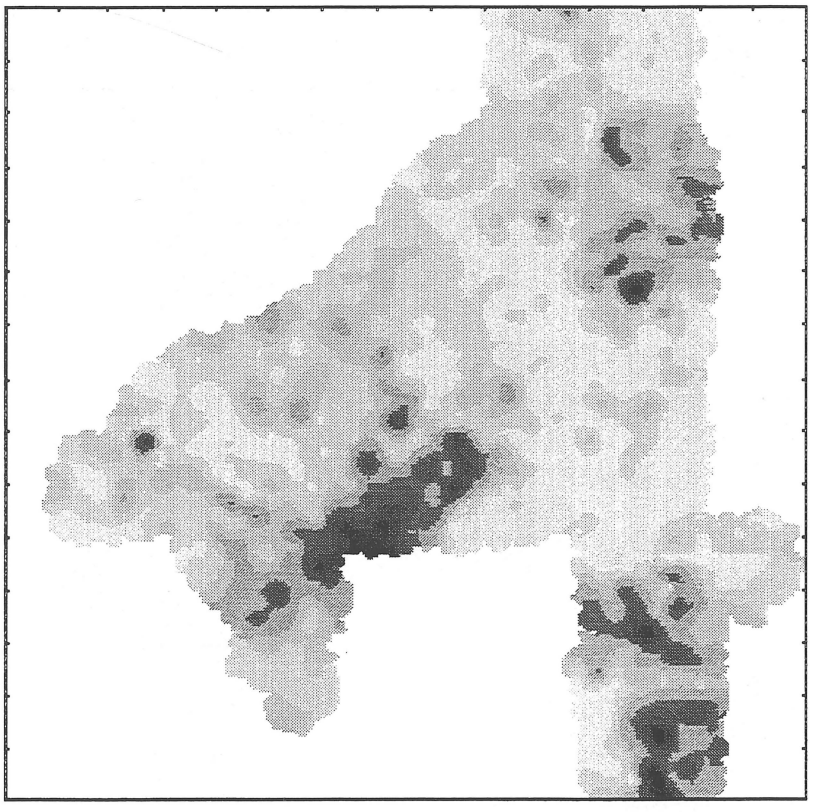

Ti

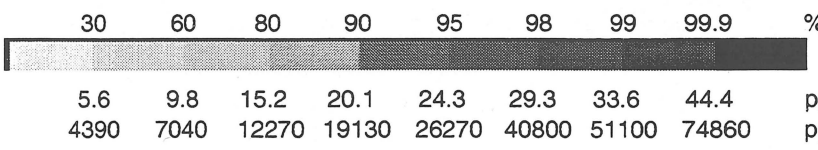

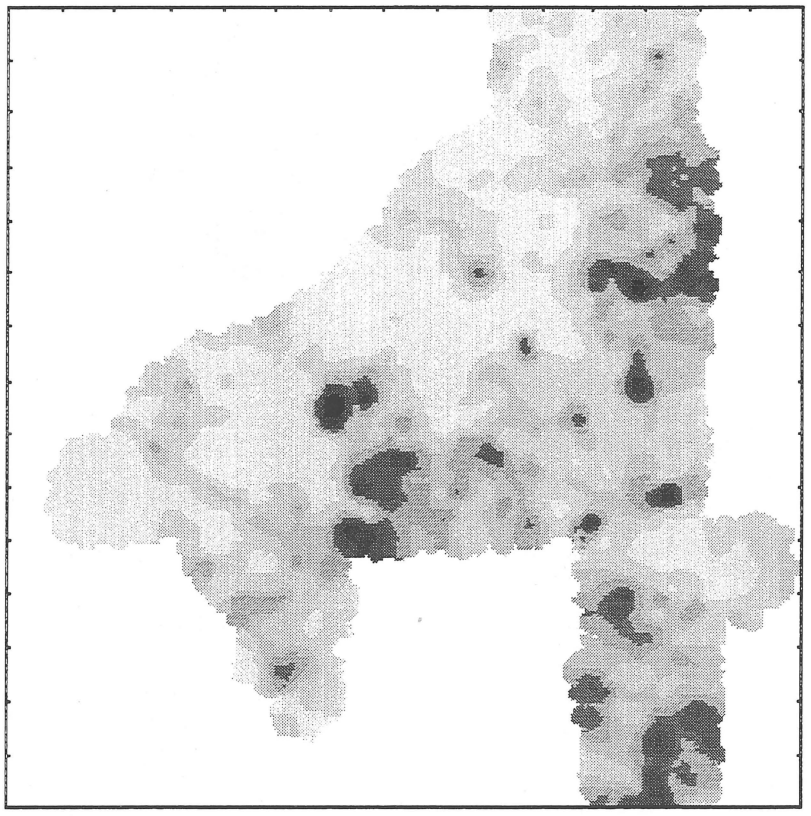

Zn

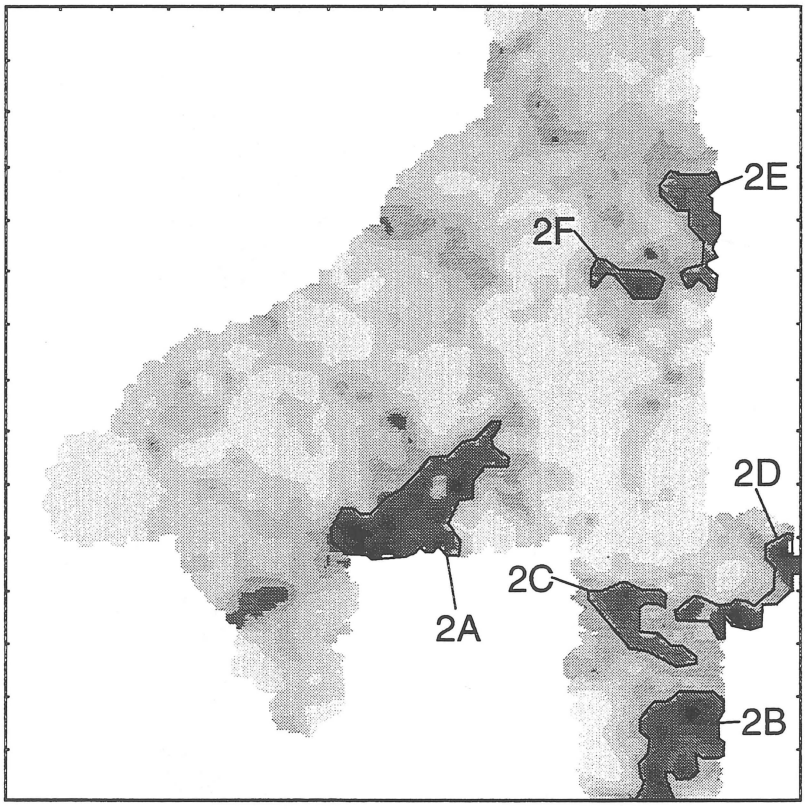

F2

30	60	80	90	95	98	99	99.9	%
24	39	52	63	71	83	94	163	ppm Zn
-0.44	0.26	0.83	1.21	1.49	1.82	2.03	2.63	F2 scores

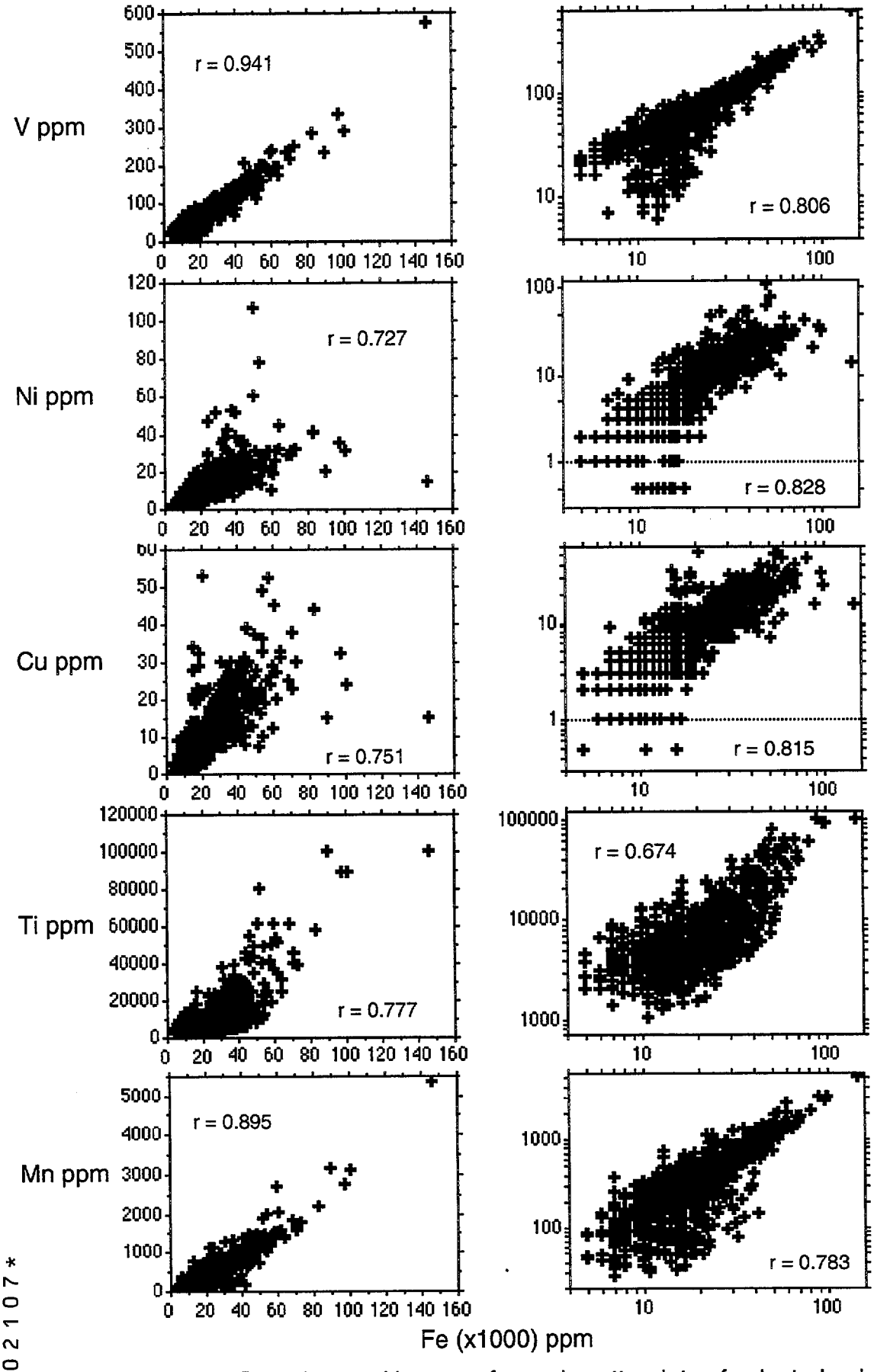

Figure 12. Raw data and log-transformed scatterplots of selected pairs of Factor 2 elements (r is the Pearson correlation coefficient).

highs over the Mesozoic sedimentary rocks to the north-west. Cu and Zn shows patchy highs over the metamorphics units and Lane Creek Formation, and Nundah Granodiorite, but, Cu in particular, lows over most/many felsic intrusive and extrusive rocks. Zn also shows highs in areas which may represent Zn mineralisation.

Factor 2 scores have a distribution similar to that of V or Fe, with concentrations of highs occurring at:-

Area **2A** (see Figure 11) runs from south west of Dagworth homestead to east of Van Lee homestead in the GALLOWAY sheet area. The area is drained by the Spring, Dagworth and Cattle Creek systems. Topography is irregular to gently undulating plains with some hilly country, overlying Yataga Granodiorite, Lane Creek Formation and Cobbold Dolerite. Strong highs for V, Fe, Sc, Ti and Zn and moderate highs for Ni, Cu, Cr, Zn and Zr, are present although those for Ni, Cu, Zn and Zr tend to be patchy or confined to parts of the area. The area contains the Dambo Cu Prospect (Smart and Bain, 1977) south of Dagworth homestead and corresponding to the Cu high.

Area **2B** is drained by the Telegraph and Ellendale Creek systems in the southern part of the MOUNT SURPRISE sheet area. Form is as for area **2A**, but the area is underlain by Einasleigh Metamorphics and Puppy Camp Granodiorite. The area shows strong highs for V, Fe, Ni, Sc, Ti, Zn and Mn, with moderate highs for Cu and Ga.

Area **2C** is drained by Junction Creek and its tributaries and covers an area from west of Mount Surprise township to north-east of Eveleigh homestead, also in the MOUNT SURPRISE sheet area. The area shows strong highs for Fe, Ni, Ti and Mn with moderate to patchy highs for V, Sc, Cr and Zn. The form of the area is also similar to that of area **2A**. The area is underlain by Einasleigh Metamorphics.

Area **2D** is in two parts, north-east and immediately south-west of Mount Surprise township, in the MOUNT SURPRISE sheet area. The area shows strong highs for Ni and Cr, and moderate highs for Fe and Cu. The area is irregular stony plains over Undarra Basalt of the McBride Basalt Group, and is drained by Elizabeth and Black Spring Creeks.

Area **2E** lies between the Lynd and Tate Rivers, near Bolwarra homestead in the MUNGANA and LYNDBROOK sheet areas. The area is undulating country with stony hills over Fig Tree Hill Granite and McDevitt Metamorphics, including metadolerite. Strong highs for V, Cu and Zn and moderate highs for Fe, Sc, Ti and Mn are evident.

Area **2F** lies astride of the MUNGANA/LYNDBROOK border, south-west of Bolwarra homestead. The area is drained by Pinnacle Creek and tributaries of the Lynd River. It is similar in form to area **2E** and is over Fig Tree Hill Granite and McDevitt Metamorphics, including metadolerite. The area shows strong highs for V, Fe, Sc, Ti, Zn and Mn, and a moderate high for Cu.

The highest concentrations of Fe occur over the Einasleigh and McDevitt Metamorphics, and the Lane Creek Formation of the Robertson River Group of the Etheridge Formation. This is consistent with the generally higher Fe contents of the metasedimentary and

metamorphic rocks, at least in comparison with the granites and acid volcanics in the area. Table 7 lists the approximate averages for total Fe by rock type in the survey area.

Table 7. Averages for total-Fe (as Fe_2O_3) by rock type, in the survey area (from ROCKCHEM).

Rhyolites	2.1%
Granites	2.2%
Metamorphics	5.5%
Andesites	8.1%
Metasediments	8.5%
Basalt	11.2%
Metadolerite	12.3%

Ni shows wide-spread highs over the Undarra Basalt (Area **2D** in Figure 11) and Einasleigh Metamorphics (+- Cobbold Metadolerite - Areas **2B** and **2C**), mostly in the MOUNT SURPRISE sheet area. Lesser, and more scattered, highs occur over the Lane Creek Formation (Robertson River Subgroup of the Etheridge Formation - Area **2A**) and McDevitt Metamorphics (Areas **2E** and **2F**). Large areas of lows occur over some units, in particular granites of the O'Briens Creek Supersuite and Scardons Volcanics. This is consistent with whole rock geochemistry of the units since the McBride Basalt (average 184 ppm Ni in the rock), Cobbold Metadolerite (117 ppm), Lane Creek Formation (71 ppm), Einasleigh Metamorphics (61 ppm),and McDevitt Metamorphics (29ppm) are among the most Ni-rich units in the region. This compares with 1 ppm for both the O'Briens Creek Supersuite granites and Scardons Volcanics (ROCKCHEM).

Cr values for rocks in the survey area show similar trends to Ni values ($r = 0.92$). As with Ni, Cr in stream sediments also shows highs over the Undarra Basalt (McBride Basalt Group - average 267 ppm Cr in the rock), Einasleigh Metamorphics (196 ppm) and Lane Creek Formation (206 ppm) , and lows over the O'Briens Creek Supersuite granites and Scardons Volcanics, but the strongest and most extensive highs occur over the Mesozoic sedimentary rocks in the BLACKDOWN sheet area. No analyses are available for the basin sedimentary rocks.

Cu shows a strong high at the western end of Area **2A**, over the Lane Creek Formation, and an area which includes the Dambo Cu Prospect. Other highs occur in Areas **2B** over Einasleigh Metamorphics, and Areas **2E** and **2F** over McDevitt Metamorphics. Other Cu specific highs occur in an area noted for numerous abandoned Cu mines over Nundah Granodiorite and Dargalong Metamorphics in the north of the MUNGANA sheet area in the Cardross area (Keyser and Wolff, 1964), and at the south-western end of the Lane Creek Formation near Mount Turner.
Simple regression of log(Cu) against F2 scores, after elimination of 31 samples giving residuals greater than 11.25 ppm, gave predicted Cu according to the equation:

$$\log(Cu_p) = 0.284*F2 + 0.849$$

with an image map of the residuals ($Cu - Cu_p$) shown in Figure 13(a). A step-wise multiple regression (32 samples greater than 7.88 ppm eliminated) gave the equation:

$$\log(Cup) = 0.060*F1 + 0.288*F2 + 0.060*F3 - 0.043*F4 + 0.073*F5 + 0.016*F7 + 0.050*F8 + 0.852$$

and an image map of residuals as shown in Figure 13(b). The strongest residual Cu highs occur in the northern and southern parts of the MUNGANA sheet area, in areas containing numerous abandoned Cu mines and Cu mineral occurrences (compare Figures 13 and A3 [in Appendix A]). The northern-most of these, at Cardross, will be discussed further in relation to an As high over the area (see Section 5.5). The high near the Dambo Prospect has been eliminated indicating that it was due to lithochemical factors and not did highlight the mineralisation as such. Like U, Cu also has a very restricted (<1 km) dispersion train in tropical areas (Hoatson and Cruikshank, 1985) such that small scale mineralisation may not be detected in basins of the size used in this survey.

Zinc is an element which, although relatively mobile in the secondary environment under normal conditions, is particularly prone to concentration by coprecipitation with, or adsorbtion onto, hydrated Fe and Mn oxide precipitates (Nichol and others, 1967; Jenne, 1968). Consequently, false anomalies due to scavenging sometimes appear in geochemical surveys, anomalies which have little or no direct relationship to either bedrock geochemistry or to mineralisation. Therefore moderate to high Zn values in samples relatively low in Fe and/or Mn may be of greater interest than higher Zn values in samples with high Fe and/or Mn contents. Interactive scatterplots (from DATA DESK) depicting Zn/Fe, Zn/Mn and location are shown in Figure 14, interactive in that points highlighted in one plot are automatically highlighted in all others. A number of areas of interest are defined by high, or by clusters of high and moderate, Zn/low Fe-Mn values.
Factor 2, Zn's prime factor, obviously represents the Zn/Fe/Mn relationship and simple regression of log(Zn) against F2 scores, (22 samples with residuals greater than 42.42 ppm eliminated after first pass) gave the equation:

$$\log(Zn_p) = 0.185*F2 + 1.452$$

and the image map of residuals shown in Figure 15(a). However, Zn had almost equal factor loadings in F2 and F3 so the process was extended to step-wise multiple regression (18 samples greater than 25.53 ppm eliminated) which eliminated no factors and gave:

$$\log(Zn_p) = 0.0.079*F1 + 0.179*F2 + 0.165*F3 + 0.011*F4 + 0.050*F5 + 0.019*F6 - 0.022*F7 - 0.027*F8 + 1.460$$

and the image map in Figure 15(b). Both sets of residuals highlight the areas of interest defined in Figure 14. Area **2X** is on the border of the ABINGDON DOWNS and GALLOWAY sheet areas and also corresponds to part of a residual Pb high. The area is drained by Bull and Kangaroo Creeks and is underlain by rocks of the Galloway Volcanic Group, the Kangaroo Creek Supersuite and Campbell Mountain Granite. This area does not contain recorded Zn or Pb mineralisation. Area **2Y** is in the LYNDBROOK sheet area and is drained by Rocky Creek. The area is underlain by Scardons Volcanics, and also shows highs for residual Cu and Pb which do not correspond to recorded Cu, Pb or Zn occurrences. Area **2Z** is drained by Big Western Creek and is underlain by rocks of the Warby Volcanic Group, also shows a residual Pb high which does not correspond to recorded mineral occurrences.

5.3 Factor 3

Factor 3 comprises Rb, Tl*, Be*, Ga, Ba, Pb and Sr, with minor contributions from Zn, Mn, W*, Mo*, U and Th, and a negative contribution from Cr. The factor is considered to be due to the weathering of K-rich minerals, probably from granites, since all of the principal factor

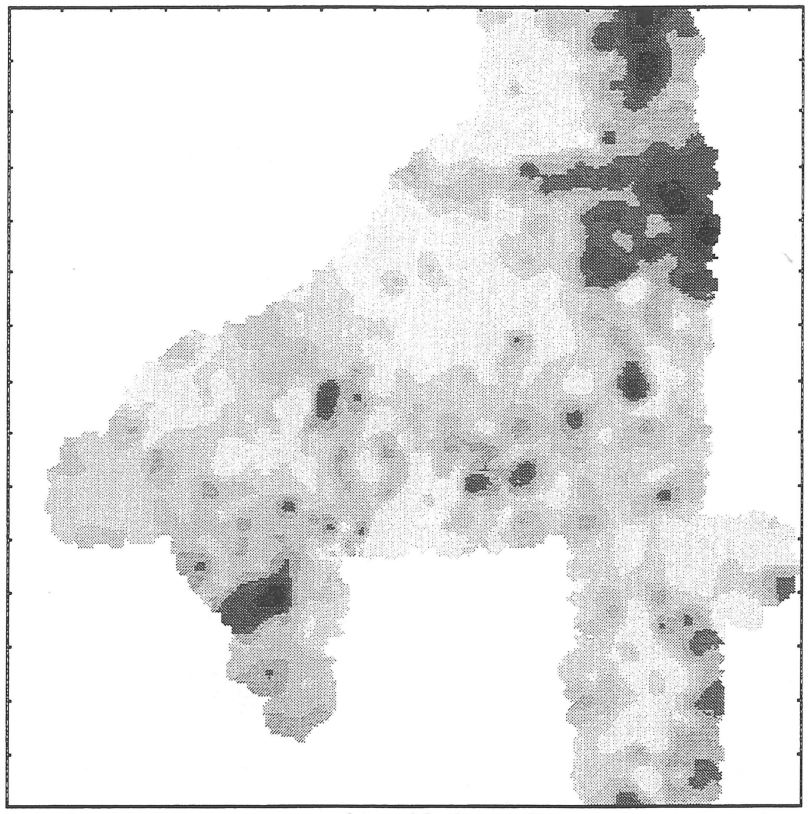

Cu_{res}

(a) Simple Regression of log(Cu) v's F2

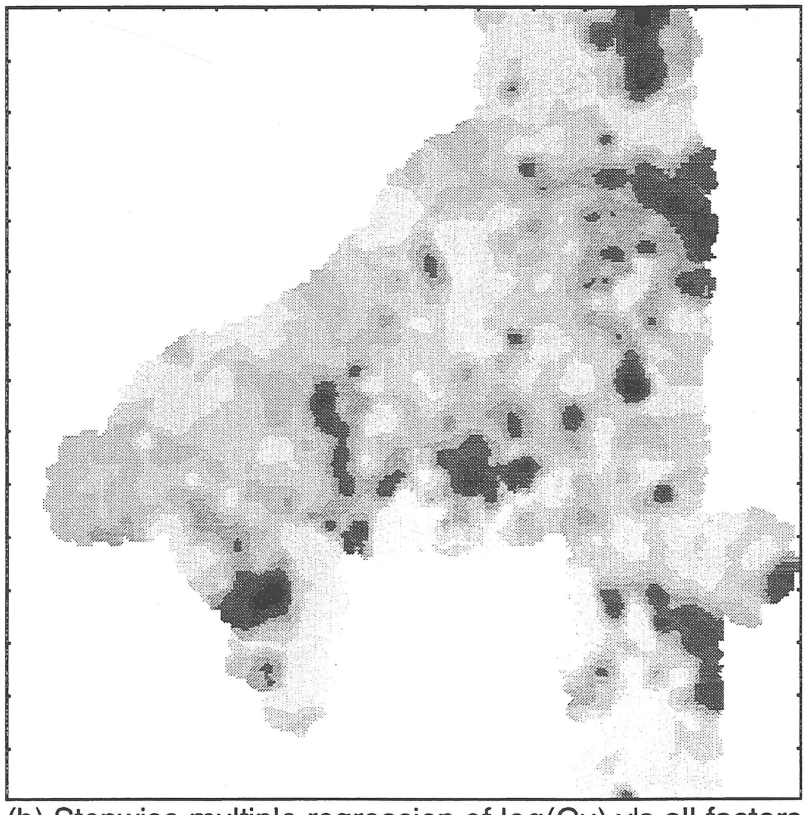

Cu_{res}

(b) Stepwise multiple regression of log(Cu) v's all factors (F6 eliminated).

30	60	80	90	95	98	99	99.9	%	
-0.79	1.11	3.49	6.46	9.35	13.5	17.4	30.9		Cu_{res} (Simple)
-0.54	0.74	2.14	3.90	6.27	9.48	12.1	25.4		Cu_{res} (Stepwise)

Figure 13. Simple and stepwise regression of log(Cu) against factor scores.

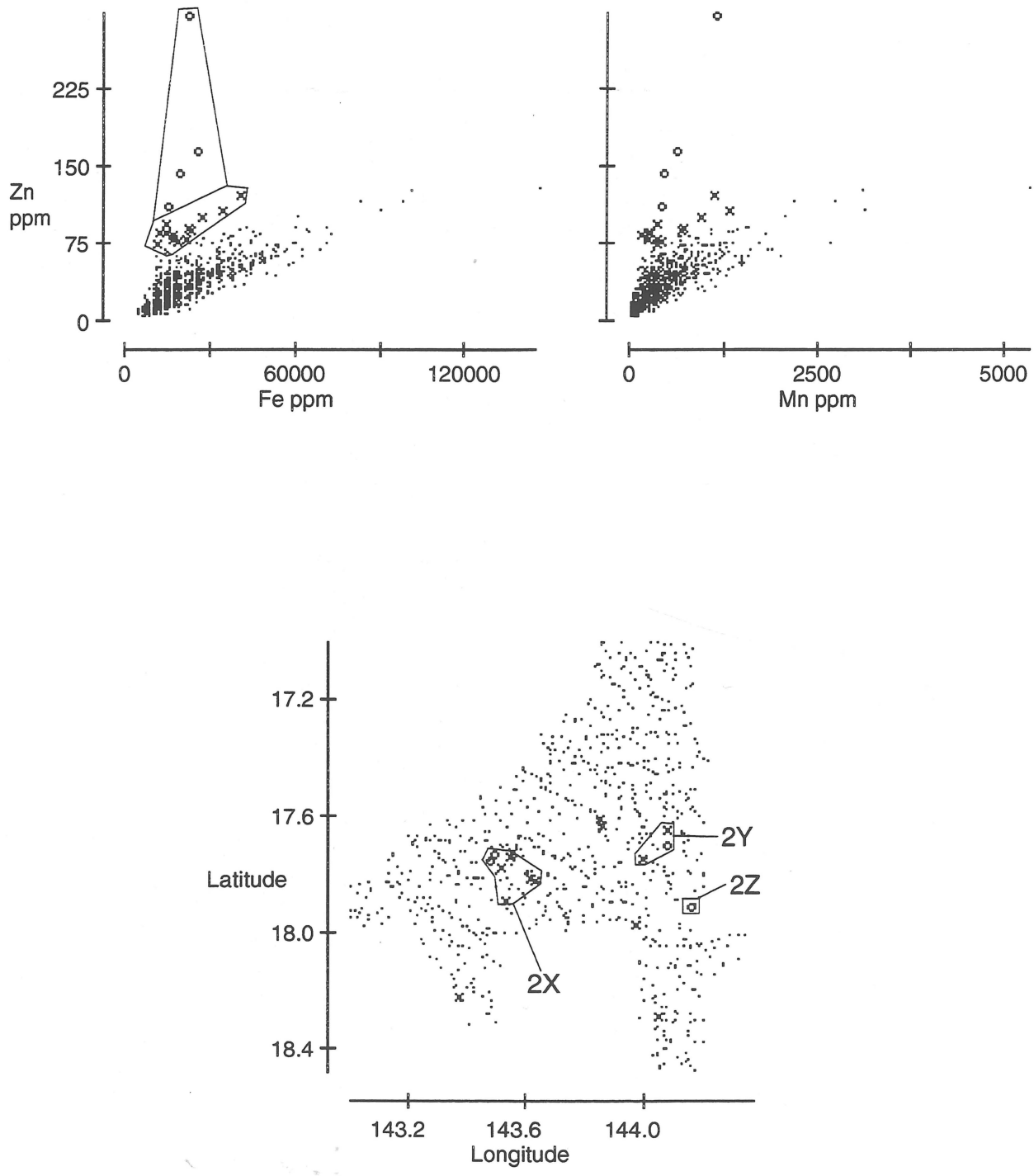

Figure 14. Interactive plots of Zn/Fe and Zn/Mn with location, defining three areas of interest.

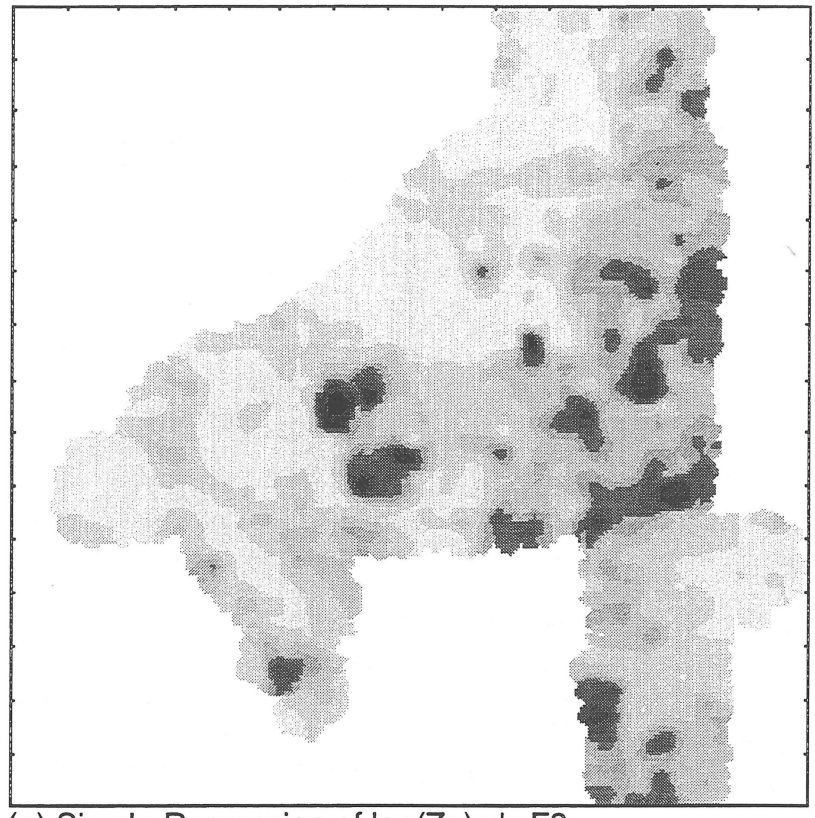

Zn_{res}

(a) Simple Regression of log(Zn) v's F2

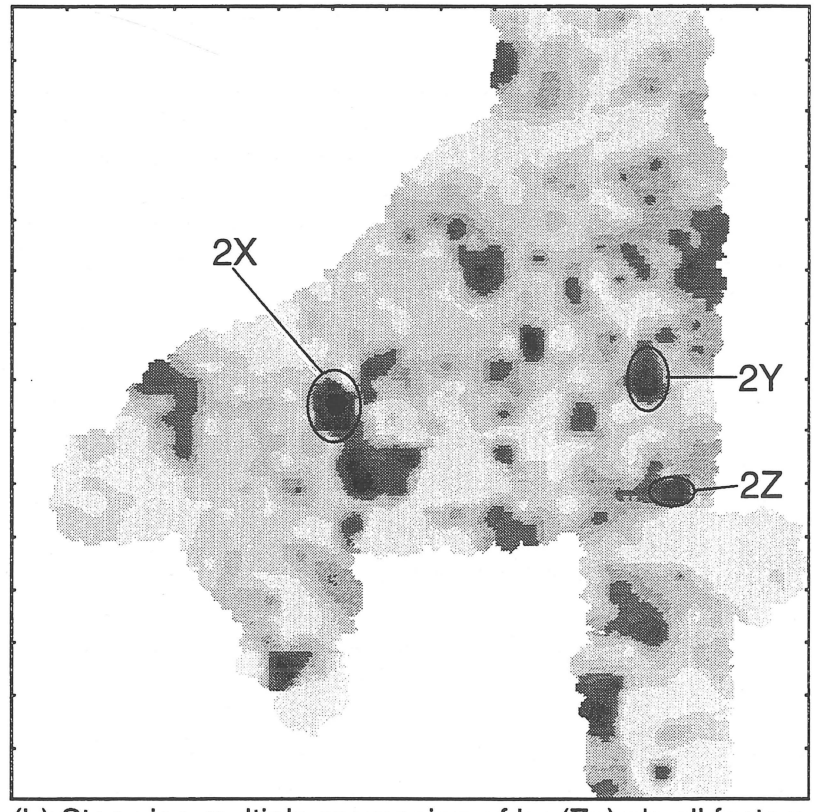

Zn_{res}

(b) Stepwise multiple regression of log(Zn) v's all factors (none elimminated).

30	60	80	90	95	98	99	99.9	%	
-4.46	6.45	15.8	23.9	31.2	41.8	51.7	135		Zn_{res} (Simple)
-2.47	1.56	6.57	11.0	16.3	24.1	31.5	100		Zn_{res} (Stepwise)

Figure 15. Simple and stepwise regression of log(Zn) against factor scores.

elements are known to concentrate in the common K/Al minerals such as K-feldspar, biotite and muscovite (Cruikshank, 1994). The relative abundances of the principal factor elements are shown in Figure 16, and image maps for Rb, Ba, Pb and F3 are shown in Figure 17.

Factor 3 elements tend to concentrate over granites and felsic volcanics, and are generally low over the sedimentary rocks to the west. The relationships between the principal factor elements are shown in scatterplots in Figure 18. Rb, Tl* and Be* show similar distribution patterns with large highs over the granites of the O'Briens Creek Supersuite, and consistently low values over the Einasleigh Metamorphics. Ga is also high over the Elizabeth Creek Granite of the O'Briens Creek Supersuite, and is patchy over the Einasleigh Metamorphics and Mosaic Gully Rhyolite. Ba is patchy over Scardons Volcanics, Puppy Camp and Mount Webster Granodiorites (+- Einasleigh Metamorphics) and the Aurora, Delaney and Forsayth Granites (+- Daniel Creek Formation) near Mount Turner. Pb shows patchy highs over the Elizabeth Creek Granite, Scardons and Warby Volcanics and the Aurora, Delaney and Forsayth Granites (+- Daniel Creek Formation) near Mount Turner, plus several anomalies which may represent Pb-Zn mineralisation. Sr shows a large high over Puppy Camp and Mount Webster Granodiorites and adjacent Einasleigh Metamorphics, and over the Jape Creek Granite and unnamed granite of the White Springs Supersuite.

Factor 3 scores show and number of highs in the survey area, these being:-

Area **3A** (see Figure 17) occurs in the south-west corner of the LYNDBROOK sheet area, and adjacent parts of the GALLOWAY and MOUNT SURPRISE sheet areas. The area is hilly country drained by tributaries of Fulford and Elizabeth Creeks. The area is underlain by Elizabeth Creek and Bonnor Creek Granites, and Warby Volcanics. The area shows strong highs for Rb, Be*, Ga (all mostly in west), Tl* and Pb, with moderate highs for Ba (mostly in east, very low in west), Zn, W*, Mo*, U and Th (both mostly in west).

Area **3B** centres on Brodies Camp (abandoned tin mining area) in the GALLOWAY sheet area. The area is hilly country drained by Dickson Creek and overlays the Corduroy Swamp and Angore Granites of the O'Briens Creek Supersuite. The area shows highs for Rb, Tl*, Ga, W* and Th, with moderate highs for Be*, Pb and U. Brodies Camp was mined, or contained, Sn, W, Mo, Bi and Au (MINLOC).

Area **3C** lies to the north-east of Area **3B** in the LYNDBROOK sheet area. The area is also hilly, and is drained by the Dickson and Rocky Creek systems. The area is over Scardons Volcanics. Strong Ba, Pb and Zn highs occur with moderate Tl* and Mo* highs. Rb, Be*, Ga, Sr, Mn, W*, U and Th are all low.

Area **3D** lies to the north-east of Area **3C**, also in the LYNDBROOK sheet area. The area is also hilly, overlaying Scardons Volcanics and is drained by tributaries of Fulford Creek. The area shows a strong Mo* high, with moderate highs for Be*, Ga and Ba.

Area **3E** occurs in hills drained by the Einasleigh River in the MOUNT SURPRISE sheet area. The area is underlain by the Mosaic Creek Rhyolite and shows strong highs for Tl*, Be*, Ga and Pb, with a moderate high for Rb.

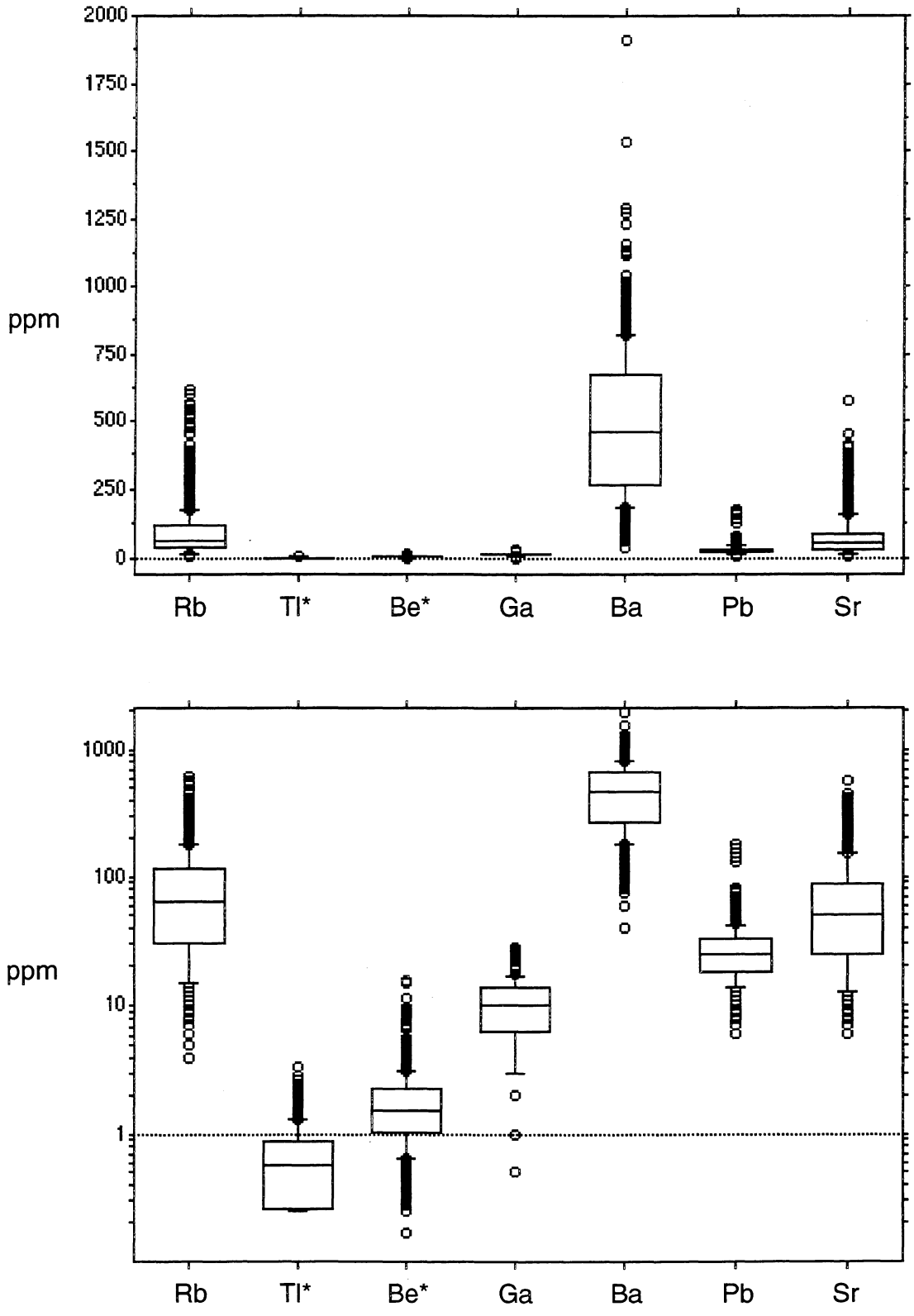

Figure 16. Relative abundances of prime elements in Factor 3.

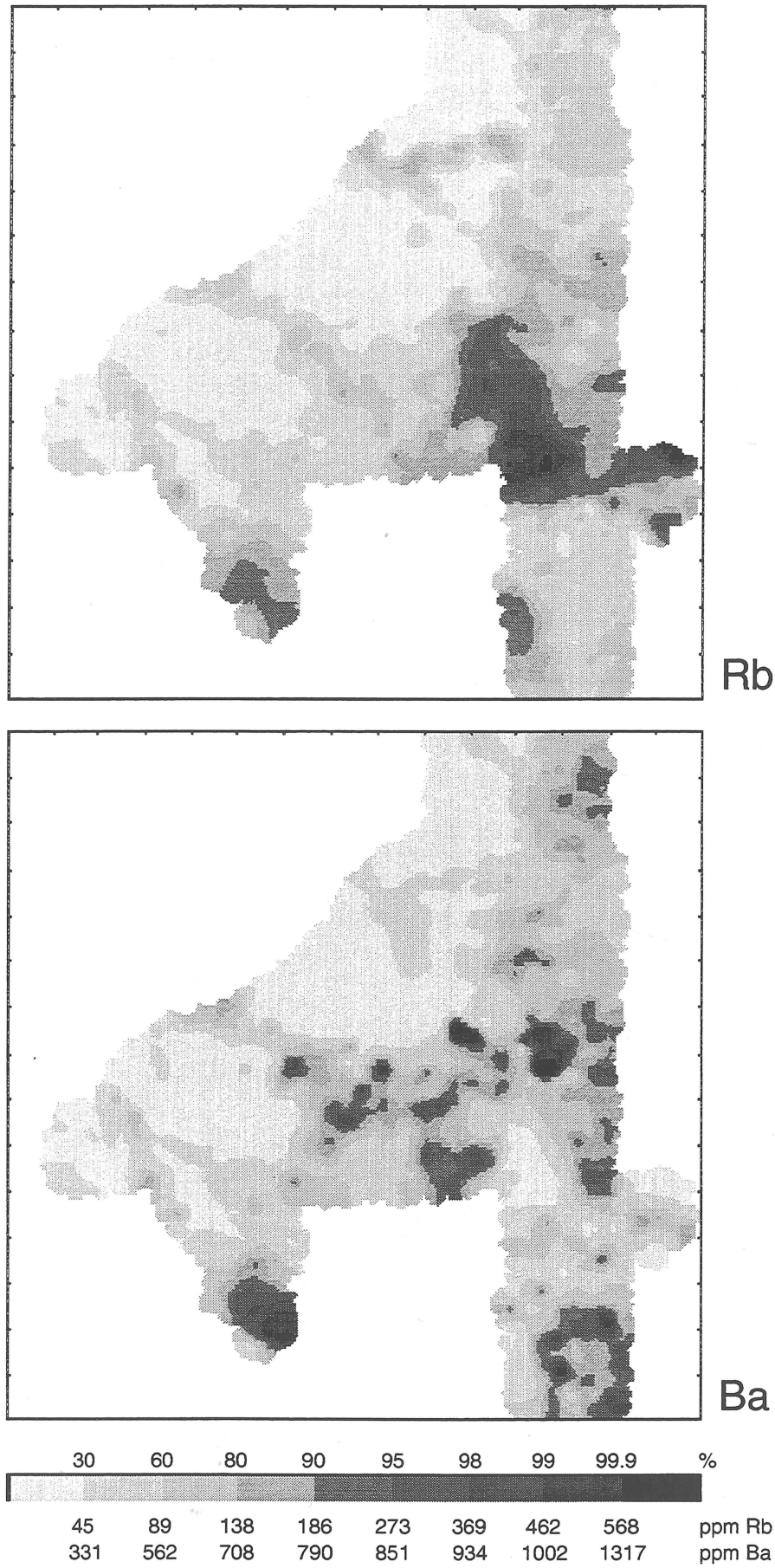

Figure 17. Image maps for Rb, Ba, Pb and F3 scores in the Red River Region.

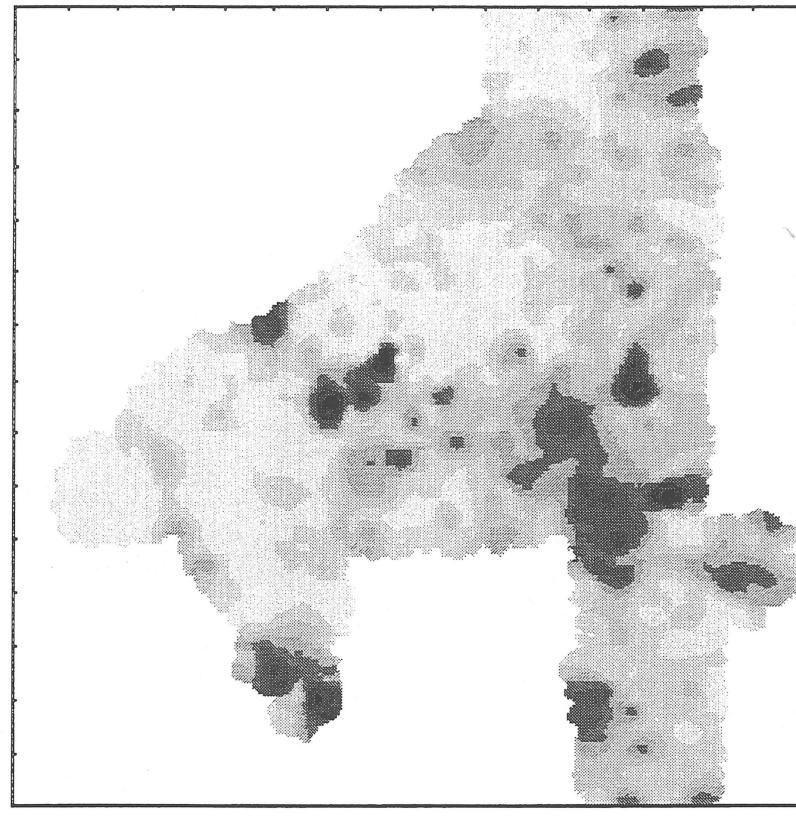

Pb

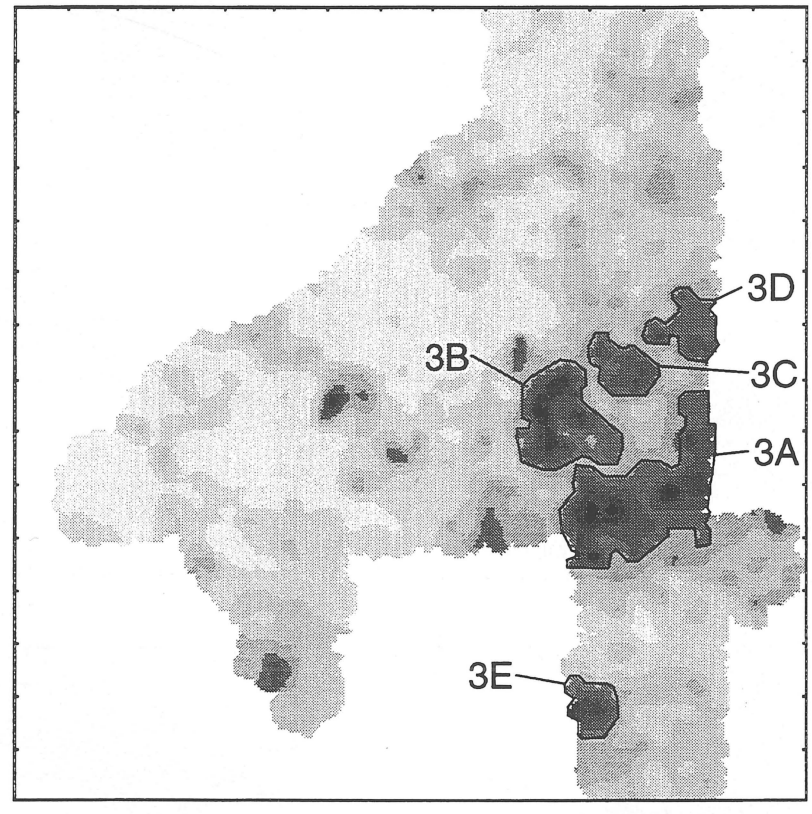

F3

30	60	80	90	95	98	99	99.9	%
21	29	35	42	49	58	68	119	ppm Pb
-0.44	0.31	0.82	1.27	1.58	1.87	2.03	2.40	F3 scores

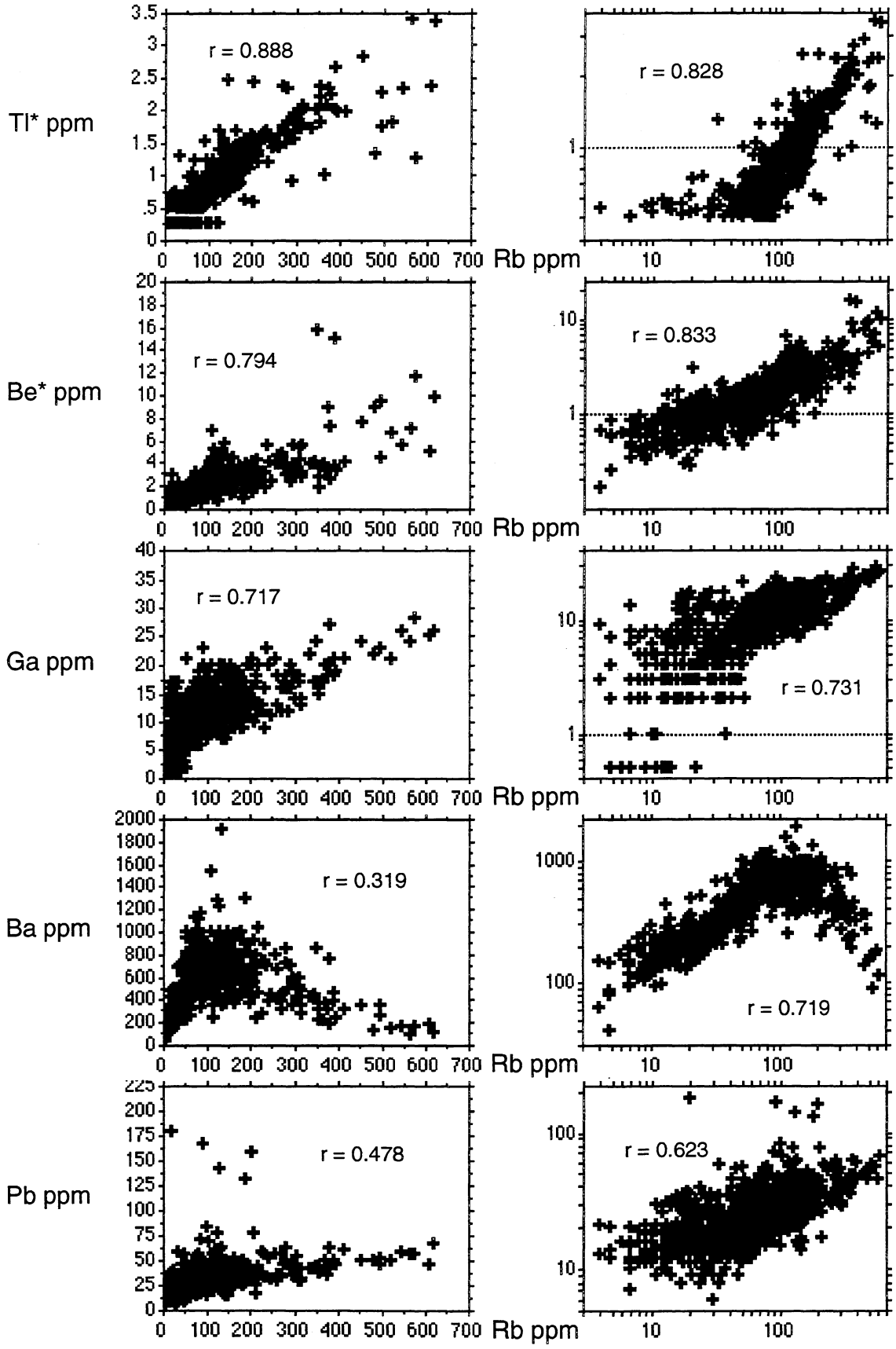

Figure 18. Raw data and log-transformed scatterplots of selected pairs of Factor 3 elements (**r** is the Pearson correlation coefficient).

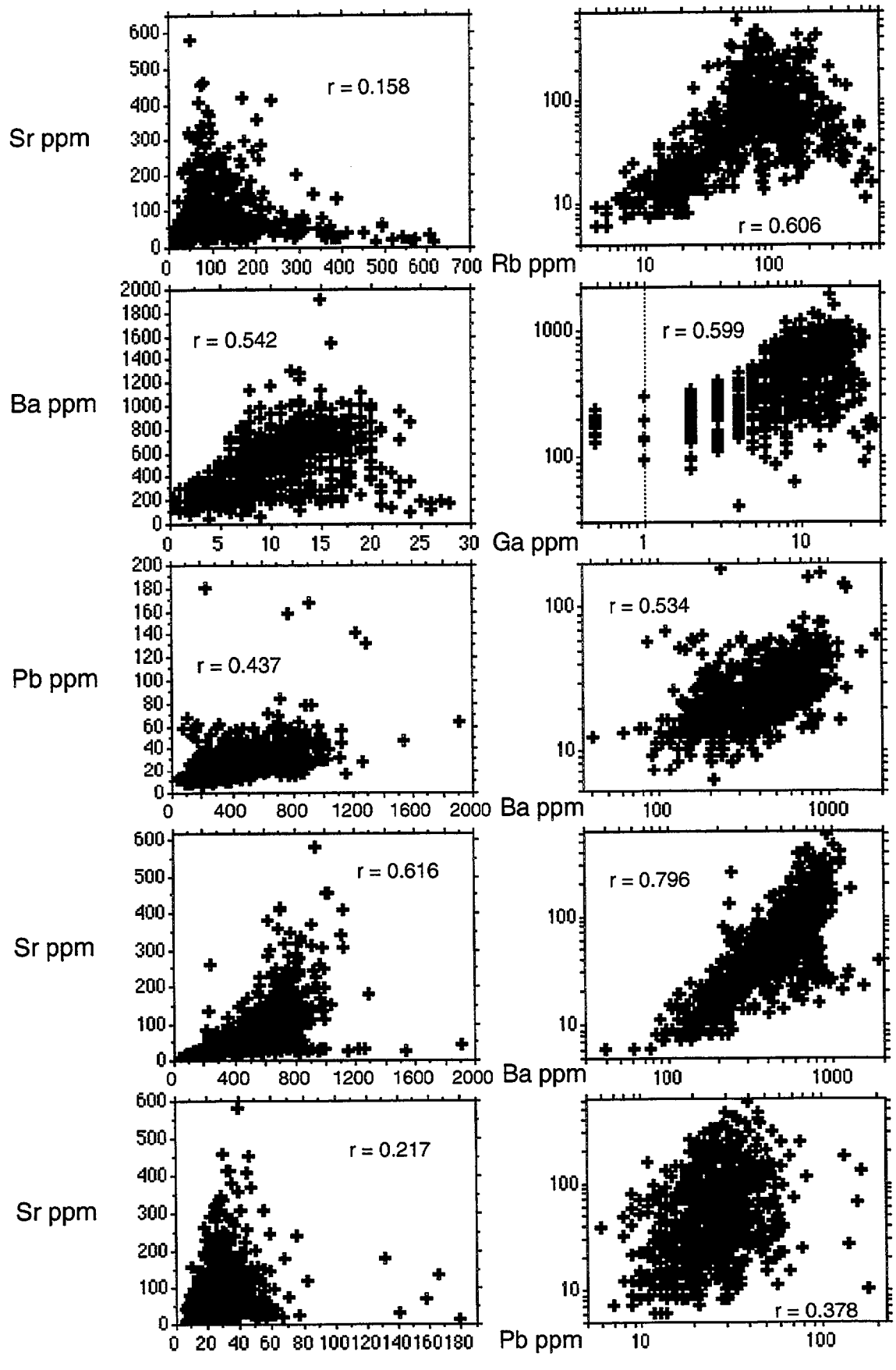

As stated above, and shown in the scatterplots in Figure 18, Rb, Tl*, Be* and Ga have similar distribution patterns and largely concentrate over the granites of the O'Briens Creek Supersuite. In contrast, Ba and Sr show similar low value distributions to the elements above, but their highs tend to be adjacent to, rather than corresponding with, highs for Rb, etc. Scatterplots of Rb against Ba and Sr are shown in Figure 18, and show unusual 'hooked' shapes seemingly representing positive correlation between Rb and Ba, and Rb and Sr, up to about 130 ppm Rb in each case, and negative correlations for Rb greater than 130 ppm. For the 661 samples with Rb less than 130 ppm, the coefficient of correlation between log(Rb) and log(Ba) is 0.895, but for the 182 samples with Rb greater than or equal to 130 ppm it is -0.719. The high Rb samples cluster over granites of the O'Briens Creek Supersuite (Figures 17 and 19), which have the highest average Rb contents and the highest Rb value of the whole rock analyses listed in ROCKCHEM. For the 58 samples of 'Elizabeth Creek Granite' (now O'Briens Creek Supersuite granites) retrieved from ROCKCHEM, there is strong positive correlation between K_2O and Rb, and between Ba and Sr, and negative correlation between K_2O and Rb on the one hand and Ba and Sr on the other (Figure 20). In the stream sediment sample population the strong positive statistical and spatial correlation between Rb and Ba, and between Rb and Sr, for low values of Rb (i.e. <130 ppm), due to samples away from the O'Briens Creek granites, appears to be sufficient to include Ba and Sr in Factor 3 although the Ba and Sr highs do not coincide with those of the other principal factor elements.

The only element of direct economic interest in this factor is Pb. In the EBAGOOLA survey Pb highs appeared to be due to the weathering of K-rich minerals (Cruikshank, 1994). In the Red River Region there appears to be more likelihood of Pb mineralisation (see Zn in Factor 2) as a number of high Pb values correspond to high Zn values and, more importantly, are spatially separated from high Rb or Ba values. The Rb values are probably the most reliable indicator of K_2O content in the bedrock and the samples with high Pb and low Rb (circles in Figure 21) relate well with the high Zn, low Fe/Mn values shown in Figure 14.
Simple regression between log(Pb) and F3 scores, after elimination of 18 samples greater than 27.46 ppm, gave the equation:

$$\log(Pb_p) = 0.116*F3 + 1.384$$

The image map of residual Pb is shown in Figure 22(a). As no factor appeared to be directly related to Pb mineralisation, a stepwise multiple regression of log(Pb) against scores for all factor eliminated Factors 2, 5 and 6 and, after elimination of 17 samples greater than 24.24 ppm, gave the equation:

$$\log(Pb_p) = 0.082*F1 + 0.112*F3 + 0.052*F4 + 0.018*F7 - 0.015*F8 + 1.385$$

The distribution of residuals is shown in the image map in Figure 22(b) and highlights areas **2X**, **2Y** and **2Z** as for Zn in Figure 15. These areas may represent potential Pb-Zn mineralisation.

5.4 Factor 4

Factor 4 comprises Bi*, Sn, Hf, W, Zr and W*, with minor contributions from Nb, Y and U, and negative contributions from Sr and Ba. The principal elements of the factor suggest that it represents the resistant heavy minerals cassiterite (Sn), zircon (Zr and Hf) and

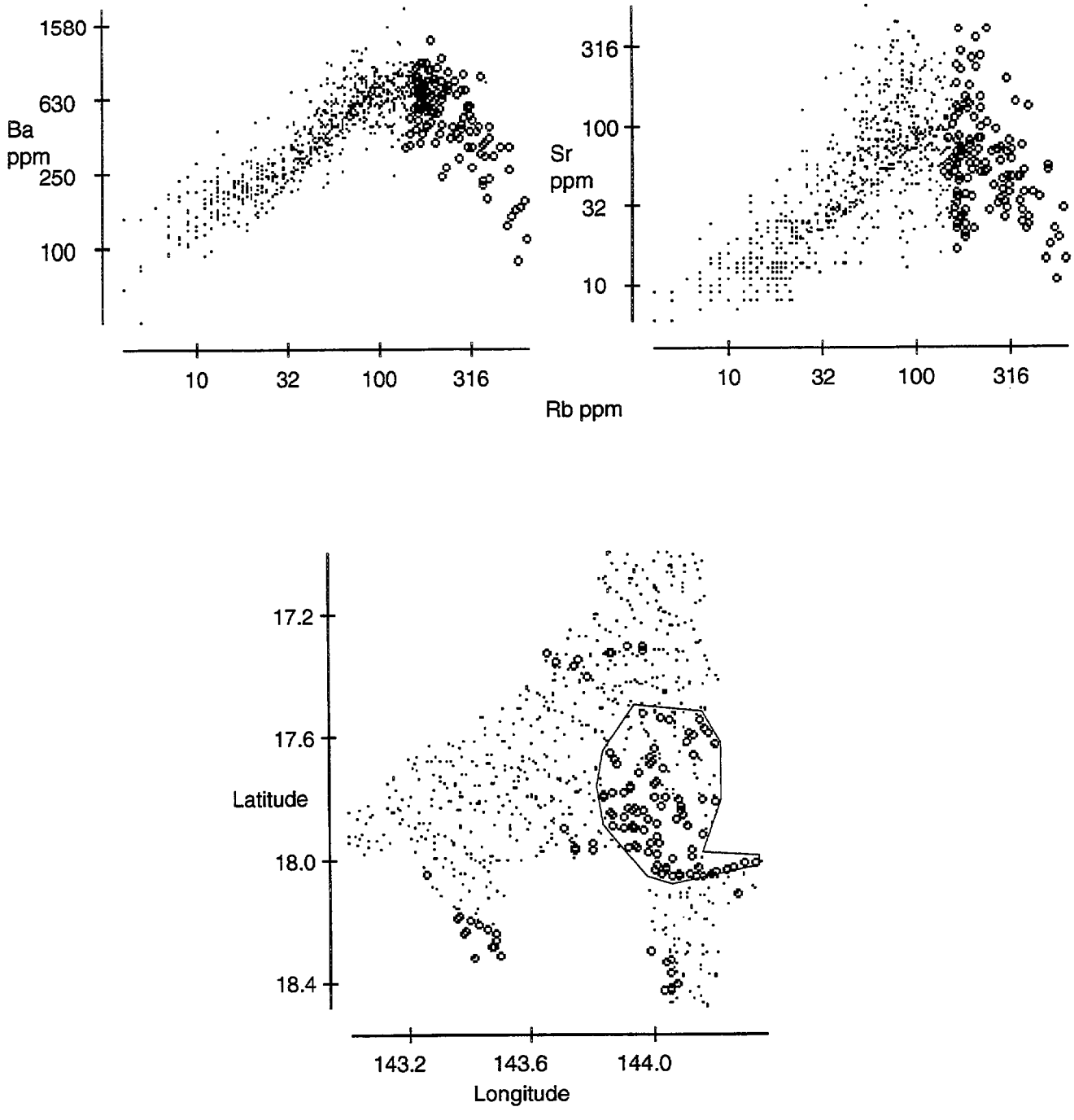

Figure 19. Interactive plots of Ba/Rb and Sr/Rb with location, showing concentrations of samples over O'Briens Creek granites.

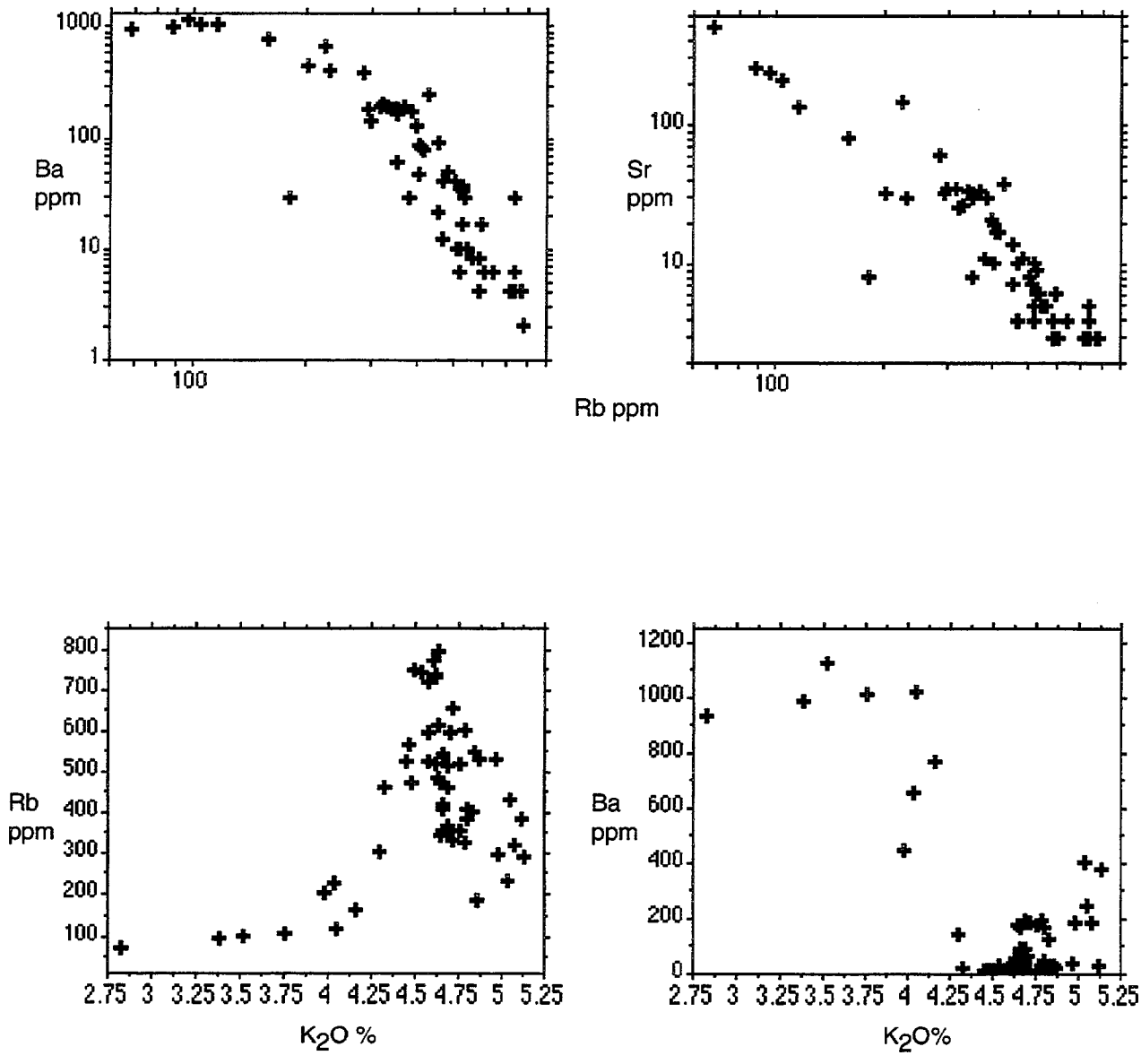

Figure 20. Scatterplots showing relationships between Ba/Rb, Sr/Rb, Rb/K_2O and Ba/K_2O in granites of the O'Briens Creek Supersuite.

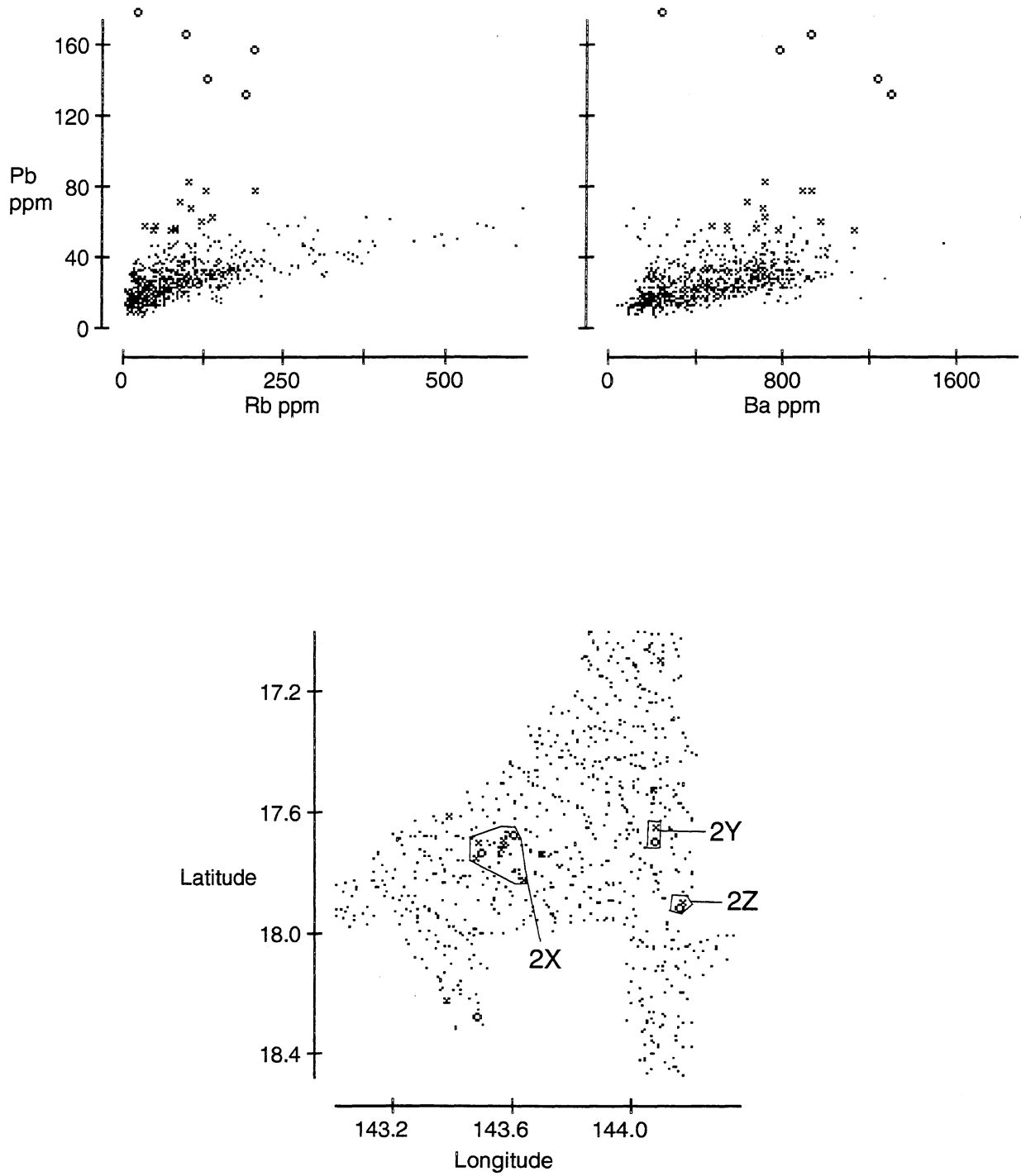

Figure 21. Interactive plots of Pb/Rb and Pb/Ba with location.

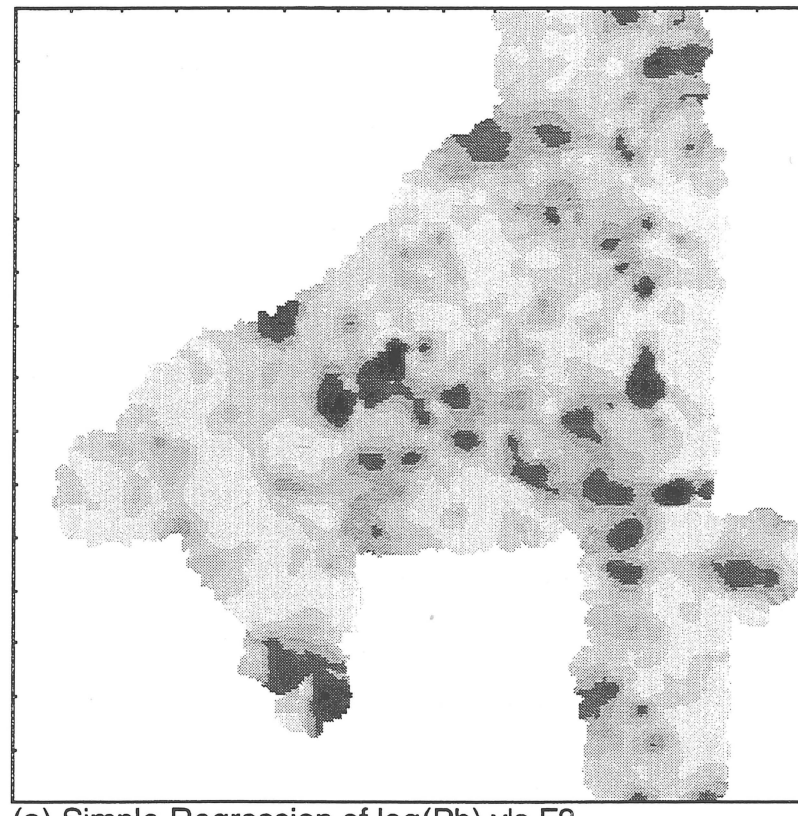

Pb_{res}

(a) Simple Regression of log(Pb) v's F3

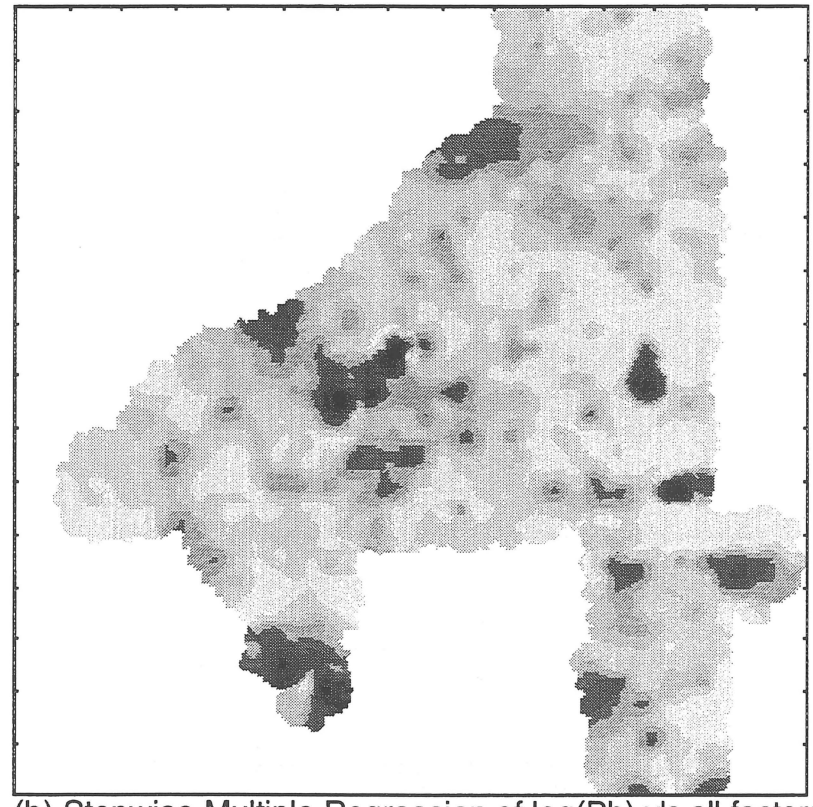

Pb_{res}

(b) Stepwise Multiple Regression of log(Pb) v's all factors (F2, F5 and F6 eliminated)

30	60	80	90	95	98	99	99.9	%
-2.23	2.36	7.98	12.3	16.5	25.3	37.3	83.7	Pb_{res} (Simple)
-1.66	1.70	5.22	9.31	14.2	26.0	36.6	82.7	Pb_{res} (Stepwise)

Figure 22. Simple and stepwise regression of log(Pb) against factor scores.

wolframite (W/W*) in the stream sediment bed lode. Figure 23 shows image maps for Sn, Zr, W and F4 scores. The image maps for Zr and Hf are essentially identical.

The factor scores seem more in sympathy with Bi*, W and W* than with Sn, Hf and Zr, although there is a general similarity between the distribution patterns of low values for the elements. Bi*, W and W* show coherent highs over and adjacent to the granites of the O'Briens Creek Supersuite, over the Nundah Granodiorite at Cardross (similar to area **1A)** and over the Mesozoic sediments (mostly Bulimba Formation) near the Tate River. Highs for Sn, Hf and Zr tend to be patchy and often do not correspond to factor highs. The highs generally follow granites and acid volcanics, but a number of highs occur in, or over, the Mesozoic sedimentary rocks to the west of the igneous rocks. Areas over metamorphics and associated sedimentary units, for example the McDevitt and Einasleigh Metamorphics, and the Lane Creek Formation, are consistently low in Factor 4 elements.

Factor scores show a number of highs, as follows:

Area **4A** (Figure 23) is hilly country in the south-west corner of the LYNDBROOK sheet area. The area is drained by tributaries of Elizabeth and Fulford Creeks and overlays granites of the O'Briens Creek Supersuite (mostly Elizabeth Creek Granite). The area shows highs for W, W*, Nb, Y and U plus a strong, single sample high for Bi* (14.6 ppm).

Area **4B** is in hilly country north-west of area **4A**, in the GALLOWAY sheet area. The area is underlain by granites of the O'Briens Creek Supersuite (Corduroy Swamp and Angore Granites) and by Scardons Volcanics and is drained by Angore and Dickson Creeks. The area is high in Bi*, W, W*, Hf, Zr, Y and U, and moderate in Sn and Nb.

Area **4C** is also hilly country underlain by granites of the O'Briens Creek Supersuite, in the LYNDBROOK/MOUNT SURPRISE sheet areas. The area is drained by Black Spring Creek. Strong highs for W, Nb, Y and U and moderate highs for Sn and W* are evident.

Area **4D** occurs in broken tableland overlying rocks of the Bulimba Formation (+- Rolling Downs Group) and, in the south, McDevitt Metamorphics and Three Horse Lagoon Granite. The area is drained by Sugarbag and Massie Creek in the BLACKDOWN sheet area. The area is essentially a large medium-level Bi* high with moderate Sn, Hf, Zr and W* presence. A single Sn occurrence north of the Tate River over Bulimba Formation has been recorded (Mackenzie and others, 1996).

Area **4E** is in hilly country surrounded by undulating plain, on the border between the GALLOWAY and GEORGETOWN sheet areas. The area is underlain by Yatage Granodiorite and is drained by Dagworth Creek. The area shows strong Hf and Zr highs.

The Sn average for the 843 samples from the survey area is 33.6 ppm (Geometric mean 9.8 ppm, and trimmed mean 12.0 ppm), compared with 16.5 ppm (3.1 ppm/3.2 ppm)for the Hann River Region (Cruikshank and Brugman, 1997) immediately to the north, and 5.0 ppm (2.1 ppm/2.0 ppm) for the EBAGOOLA sheet area (Cruikshank, 1994). The region no doubt qualifies as a 'Tin' province.
A number of Sn occurrences are recorded in the Angore area of the GALLOWAY sheet area over Corduroy Swamp, Angore and Jape Creek Granites (Mackenzie and others,

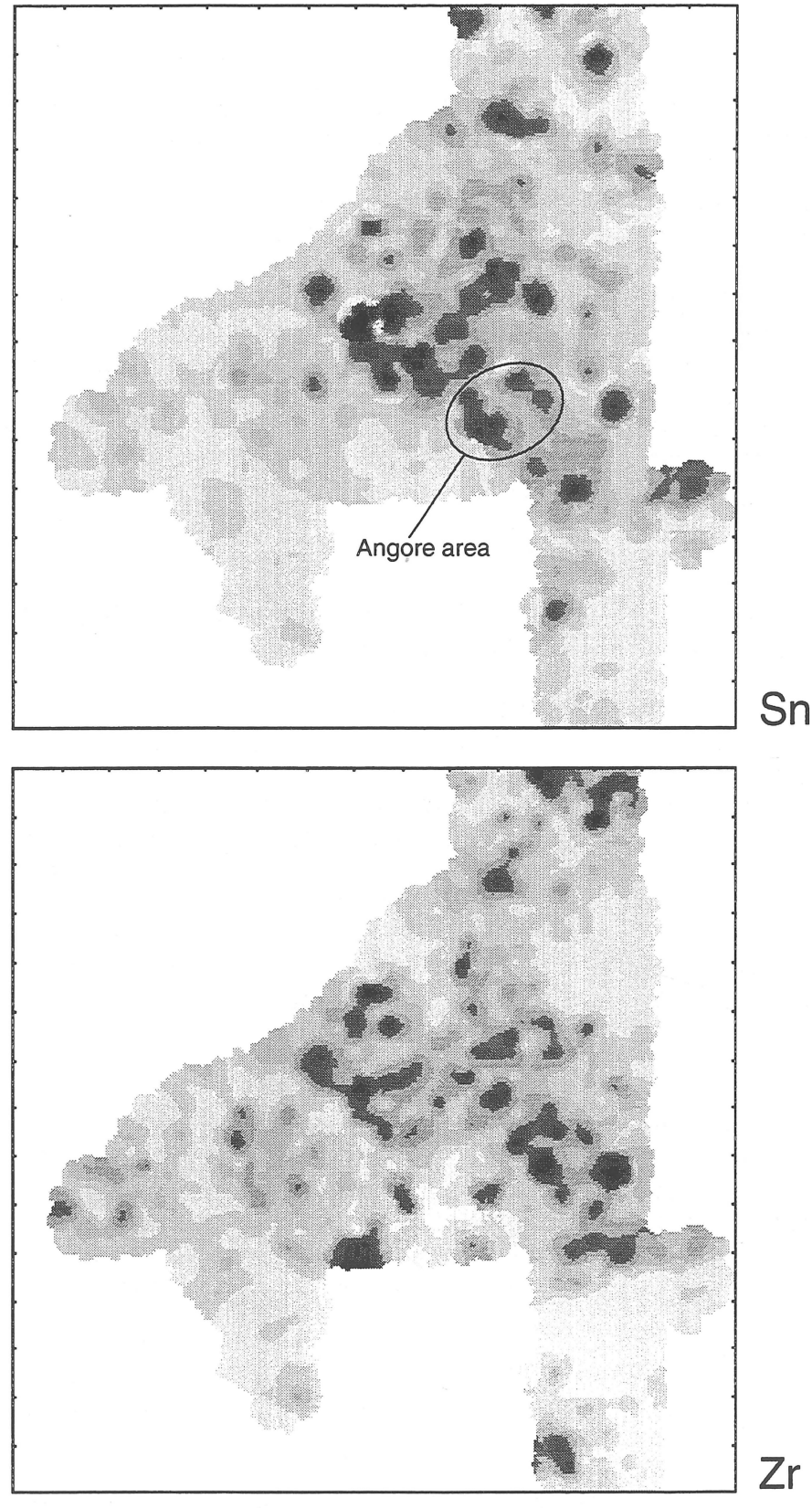

Figure 23. Image maps Sn, Zr, W and F4 scores in the Red River Region.

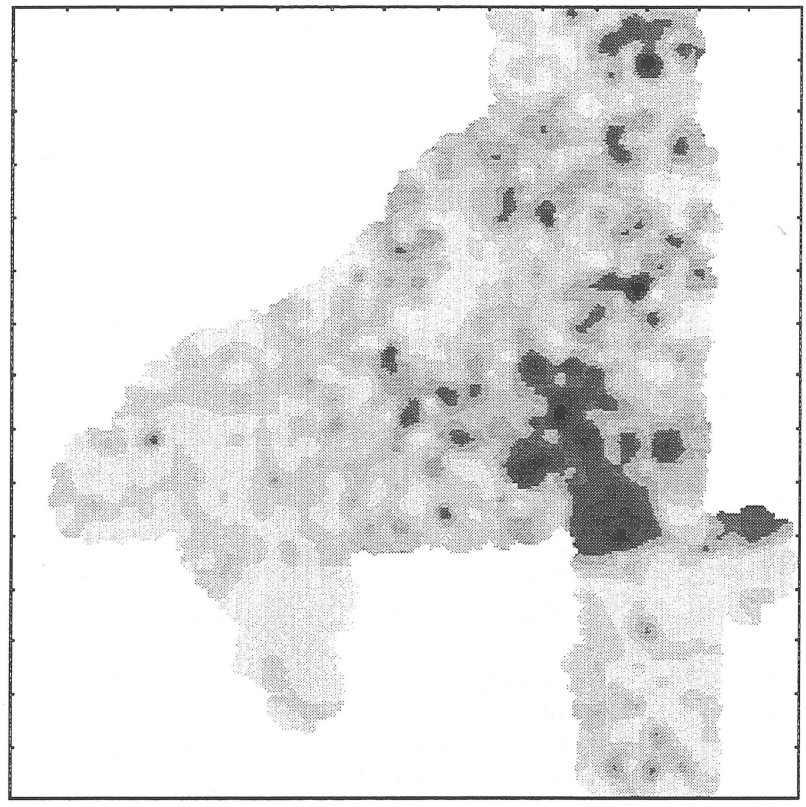

W

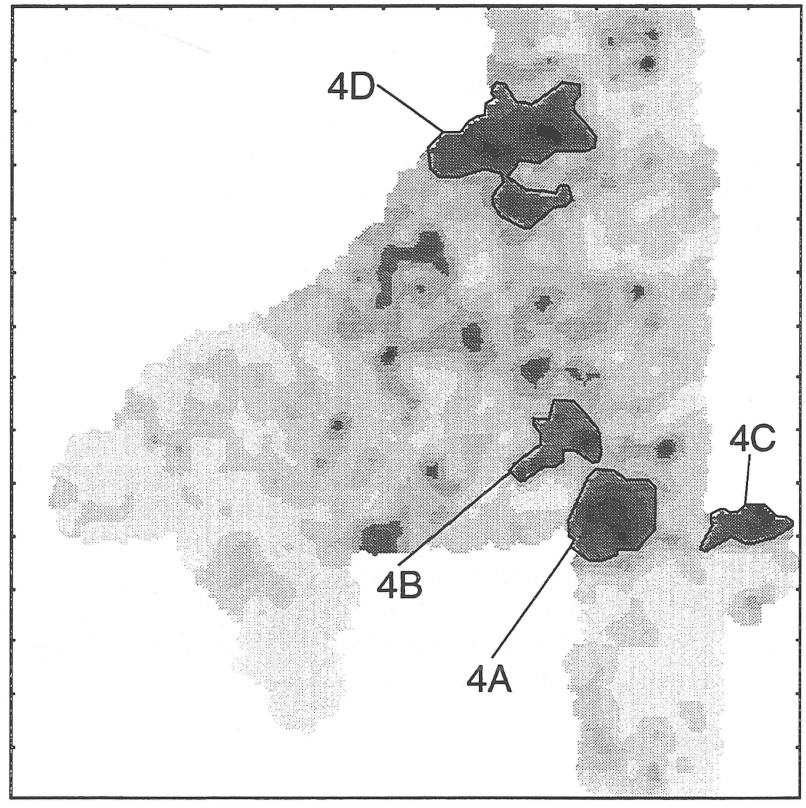

F4

30 60 80 90 95 98 99 99.9 %

4.0 6.1 8.3 10.9 14.0 18.1 21.0 30.1 ppm W

-0.55 0.14 0.67 1.14 1.65 2.12 2.34 2.90 F4 scores

1996) (see Figure 23). The granites of the O'Briens Creek Supersuite (the Elizabeth Creek Granite of Sheraton and Labonne, 1978), which includes the Corduroy Swamp and Angore Granites, are high Sn granites with an average Sn value of 12ppm (cf granite Sn average of 3 ppm, Krauskopf, 1967) and a maximum value of 77 ppm (ROCKCHEM). This area has been worked for alluvial Sn since about 1901, and later for lode Sn (and W) from the 'Elizabeth Creek Granite' (Smart and Bain, 1977). Workings over the Jape Creek Granite were all of alluvial deposits so it is likely that the Sn was weathered from the 'Elizabeth Creek Granite'. Like most Sn occurrence in the survey area, the deposits were too small or too erratic to be worked profitably at moderate to large scale. Other Sn occurrences are recorded over Scardons Volcanics to the north and Van Lee Granite (White Springs Supersuite) to the west in the GALLOWAY sheet area (Mackenzie and others, 1996), and along the eastern margin of the survey area (Figure A5 - Appendix A) including the Cardross area in the north of the MUNGANA sheet area. Sn deposits in the survey area are either very small bedrock lodes generally too small to be worked profitably, or small alluvial deposits with grade and tonnage characteristics that favour exploration only in times of high Sn prices.
However, many of the stream sediment highs in the area, including the highest, occur over Mesozoic sedimentary rocks adjacent and to the west of, or interfingered with, the granites and volcanics. It should be noted that the sediment in many of the streams draining these Mesozoic rocks is mostly coarse material because of the predominantly coarse quartzose nature of the source rocks. The pattern of many Sn highs occurring over Mesozoic sediments also occurred in the EBAGOOLA sheet area (Cruikshank, 1994) and in the Hann River Region (Cruikshank and Brugman, 1997). As noted above, an Sn occurrence has been recorded in Area **4D**, over rocks of the Bulimba Formation (Mackenzie and others, 1996). This is about 15 km north-east of the nearest exposed granite, the Three Horse Lagoon Granite. Also small amounts of alluvial Sn was recovered at Tintarple and Bayards Gully east of the Eden Vale outstation in the ABINGDON DOWNS sheet area. The Sn had been shed from placer beds at the base of nearby sandstones of the Gilbert River Formation but the ultimate source of the Sn was not known (Smart and Bain, 1977).

The Angore and Brodies Camp areas also contain a number of W occurrences (Mackenzie and others, 1996), as does the Cardross area in the north of the MUNGANA sheet area. These are high-lighted in a large W high which covers the combined areas **4A** and **4B** over the Angore area, and a smaller, patchy high over the Cardross area. The magnitude of the W highs is very much less than that of the Sn highs (14 ppm at the 95% range for W compared with 122 ppm for Sn).

Bi* shows a strong high in the Cardross area in the north of the MUNGANA sheet area. This corresponds to highs for As (see Figure 24 and Section 5.5) and Sb (Figure 28). Other Bi* highs occur in the Angore area over granites of the O'Briens Creek Supersuite, and in Area **4D**. The later contains an Au high (see below).

5.5 Factor 5

Factor 5 includes Pt#, Au# and As with a minor contribution from Pd# and a negative contribution from Ge. This factor obviously represents a precious metal association, As being frequently associated with Au# mineralisation in the region. Image maps for Au#, Pt#, As and F5 scores area shown in Figure 24. Although Pd# resides in another factor (F8), it is the sole principal element in that factor and has an obvious relationship with the elements in this factor. The image map for Pd# is shown in Figure 29.

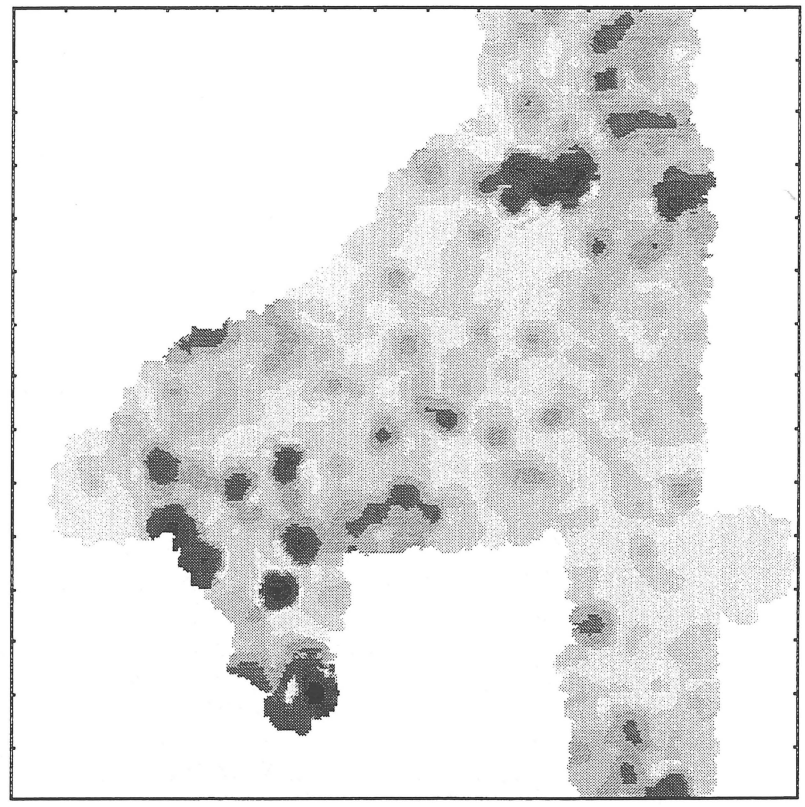

Au#

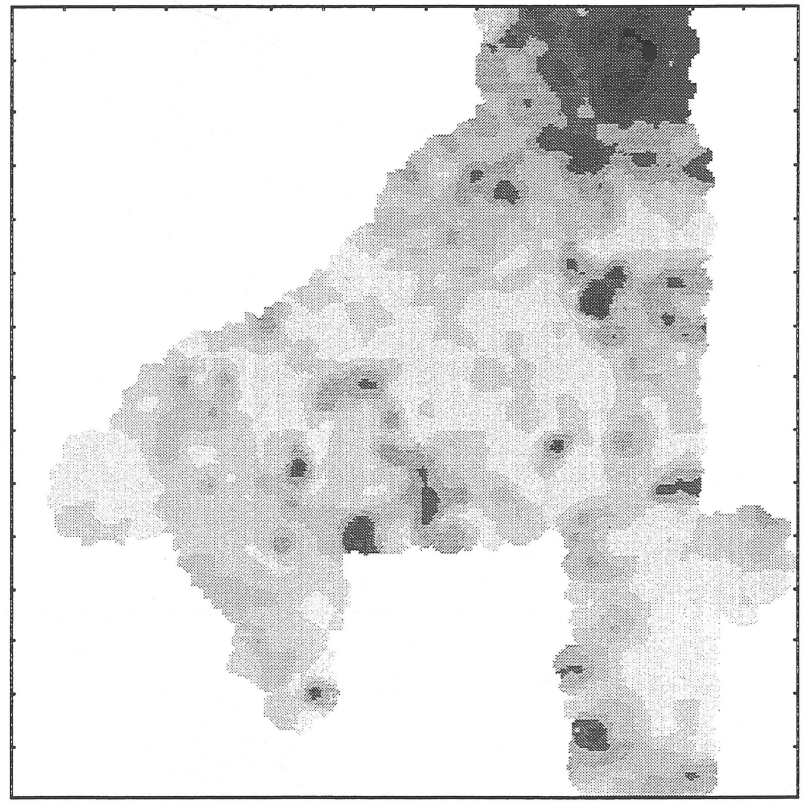

As

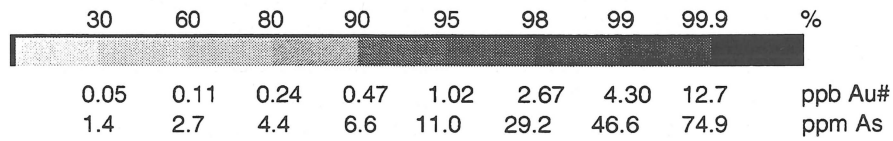

Figure 24. Image maps of Au#, As, Pt# and F5 scores in the Red River Region.

Pt#

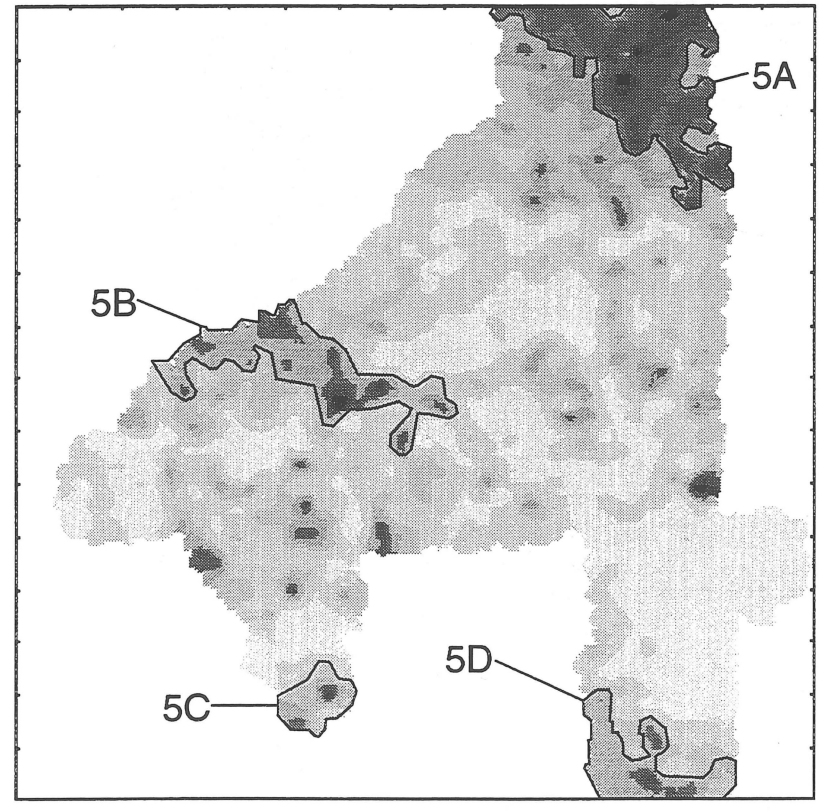

F5

65				80	95	98	99.9	% Pt#
30	60	80	90	95	98	99	99.9	% F5
0.04				0.05	0.08	0.10	0.17	ppb Pt#
-0.41	0.25	0.74	1.07	1.37	1.64	1.81	2.08	F5 scores

Factor scores show a very large high in the north of the MUNGANA sheet area plus a number of small, scattered highs.
Areas of interest are as follows:

Area **5A** is the large factor high near Cardross comprising undulating country with low stony hills underlain mostly by Nundah Granodiorite, Dargalong Metamorphics and, in the west, sedimentary rocks of the Gilbert River Formation and the Rolling Downs Group. The area is drained by the Cardross, Nundah and Williamstown/Brown Creek systems. The area shows a large As high with a moderate Au# presence, plus highs for Sb* (Factor 7 in Figure 27), Bi* (in Factor 4), Cu (Factor 2 in Figures 11 and 13) and Factor 1 elements (Area **1A** in Figure 7). The area contains a number of Ag, Au and Cu occurrences (Figures A1-3, Appendix A).

Area **5B** is a number of scattered highs in the north-eastern part of the ABINGDON DOWNS sheet area and the north-western part of the GALLOWAY sheet area following the course of the Einasleigh River. The area is broken tableland and rolling plains underlain by Galloway Volcanics in the east, and sedimentary rocks, mostly of the Bulimba Formation, in the west. The area shows Pt# highs.

Area **5C** near Mount Turner in the FOREST HOME sheet area. This includes parts of the Etheridge Gold Field and shows a large number of Ag and Au occurrences. The area is gently undulating to rolling plains with hilly country near Mount Turner and is drained by tributaries of the Etheridge River. The area is underlain by Forsayth, Aurora and Delaney Granites and the Lane Creek Formation. The area shows Au# and Pd# highs.

Area **5D** in the southern part of the MOUNT SURPRISE sheet area. The area is gently undulating plains flanked by hilly country and is drained by tributaries of the Einasleigh River. It is underlain by Puppy Camp Granodiorite and Einasleigh Metamorphics. The area shows highs for Pd#, Pt# and minor Au#. Several Ag and Au occurrences have been noted in the general area.

The most economically important of the elements is Au# which shows highs in area **5C** near Mount Turner and in the area to the north (the Etheridge Gold Field), in area **5D** and in area **5A** and to its south. Gold anomalies are frequently hard to reproduce in successive surveys because sediments are reworked each year during and after the annual 'wet' (Fletcher, 1990). High flow rates, caused by above average rainfall, can mobilise larger and heavier/denser sediment grains, including gold, bringing them into the active bed lode. Conversely, low flow rates may mobilise only the less dense sediment and effectively bury anomalies. Therefore BCL Au values greater than 0.5 ppb are generally held to be of 'interest', that is indicating Au may be somewhere in the system, whereas values less than 0.5 ppb are not taken as proof positive that it is not. Grid values greater than 0.5 ppb are shown in Figure 25, overlain by Au occurrences (Figure A2, Appendix A). The most interesting high is near the Piccaninny Outstation in the BLACKDOWN sheet area (area **5X** Figure 25). The high occurs on both sides of the Tate River (Figure 26) and initial thoughts were of contamination from the Tate River bed lode when the river is in full flood during the wet season (the Tate is not noted for Au-bearing alluvials). However, this would appear not to be the case as several samples from sites well removed from the river are also anomalous, and tributaries of the Tate River upstream of area **5X** show little or no enrichment in, or contamination by, gold. There is no known Au mineralisation immediately upstream from the anomaly. The area is underlain by McDevitt Metamorphics, Three Horse

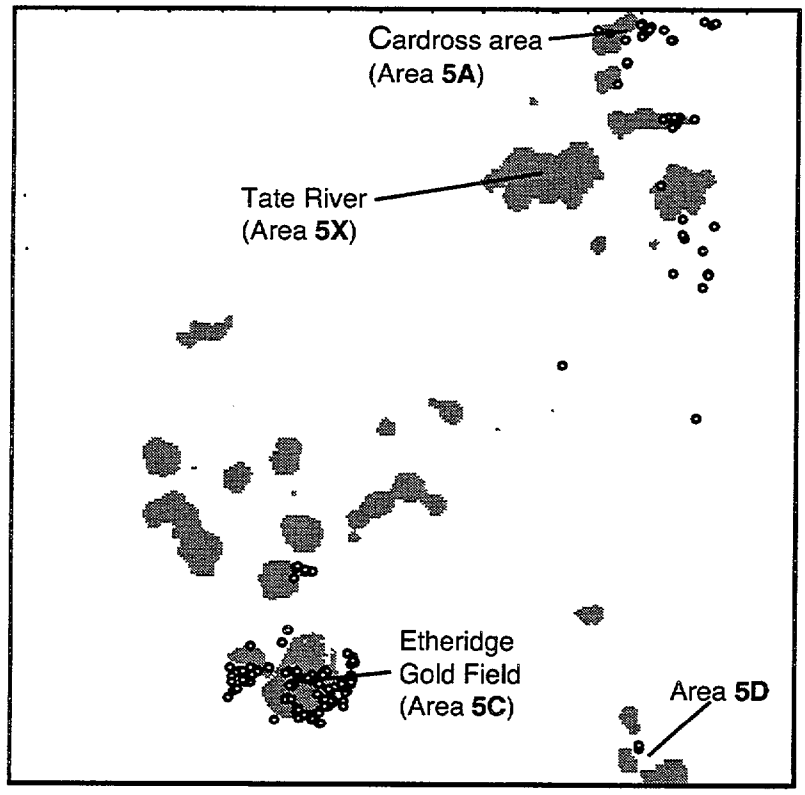

Figure 25. Shaded area shows Au greater than 0.5ppb, overlain by Au occurrences (see Figure B2 - Appendix B).

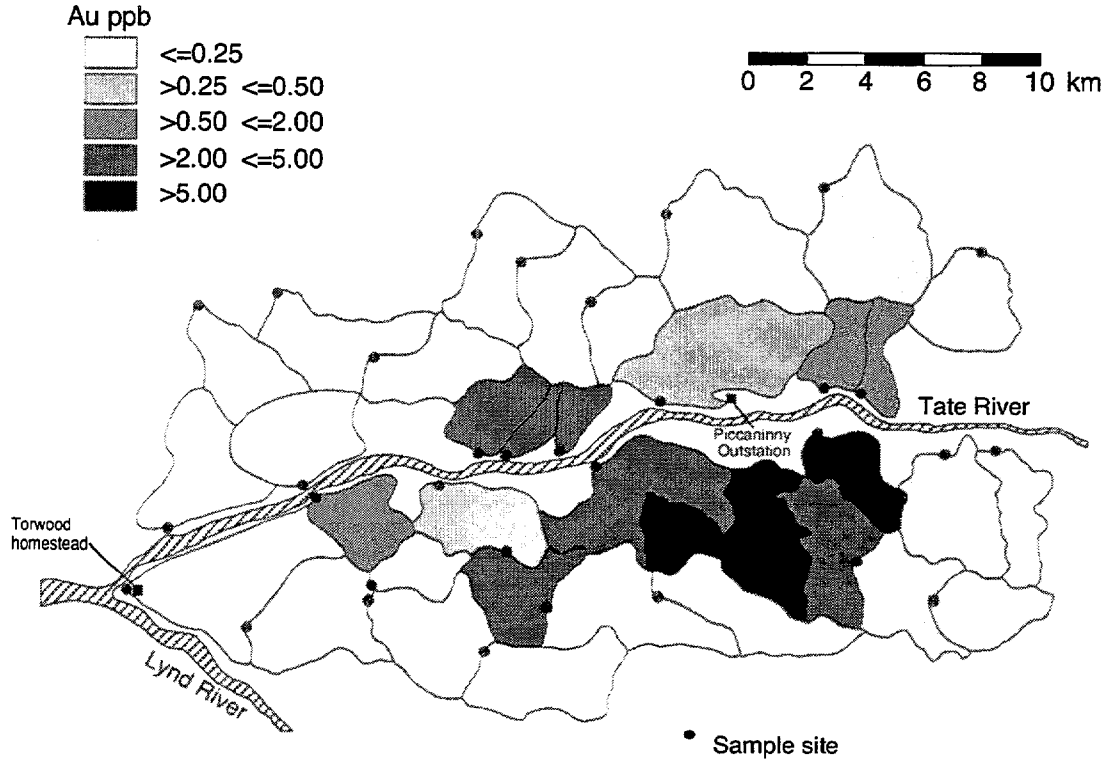

Figure 26. Gold values in Area 5X near the Tate River.

Lagoon Granite and Reamba Volcanics. These were originally mapped as Dargalong Metamorphics, Forsayth Granite and Scardons Volcanics and little is known of their geochemical characteristics.

As stated in the Methods section, extraction of Pt by Bulk Cyanide Leach is reputed to be as low as 20%, and results were included for screening purposes only. Consequently, the values recorded are very low (0.38 ppb maximum) and not too far above the detection limit (0.05 ppb). Area **5B** contains a number Pt# highs in an area between the northern side of the Einasleigh River and the Etheridge River. The area is largely underlain by sedimentary rocks but in the east, where the highest value(s) occurs, it is underlain by granites of the White Springs Supersuite and Galloway Volcanics. The origins of the highs are probably alluvial.

Pd# shows highs in the western part of area **5B**, and in areas **5C** and **5D**. There is also an area of highs (area **8X** in Figure 29) near Bolwarra homestead in the MUNGANA sheet area, with a train of moderate values trending west approximating the course of the Tate River. Area **8X** is over McDevitt and Dargalong Metamorphics, and Fig Tree Hill Granite.

Arsenic is a good indicator/pathfinder for a number of styles of mineralisation (Boyle and Jonasson, 1973). Area **5A** contains a large As high plus a number of 'interesting' Au# values (see Figure 25). The most significant aspect is the coincidence of highs for As, Sb* and Bi*, all elements from Group VA of the periodic table. These have strong chalcophile character and, collectively, may be good indicators of sulphide mineralisation. The area, then known as Cardross, was a Cu mining area in the early part of this century when about 90 kg of Au, 2700 kg of Ag and 2000 tonnes of Cu were won in the field (Keyser and Wolff, 1964). The ores were said to contain 'pyrite, chalcopyrite, much arsenopyrite, and magnetite, in various proportions', with Au values reaching one ounce per ton of ore. Wolframite, cassiterite and traces of Bi and Mo minerals were also recorded, but 'galena and sphalerite were found only in a few (of the 60 or so) mines'. In these reports the mineralisation was stated as being in 'very irregular composite fissure systems' in Dargalong Metamorphics (Keyser and Wolff, 1964: and as mapped by Best, 1962) but much of the area has been remapped as Nundah Granodiorite. The association Ag-As-Au-Bi-Cu-Mo-Sn-W (+-Pb-Zn) may be found in vein/stockwork mineralisation in granites and associated sediments (Boyle and Jonasson, 1973).

5.6 Factor 6

Factor 6 has Cd* and Ge as its' principal elements. The patterns in the F6 scores are essentially those of Cd*, some of which also corresponds to the distribution of Ge. Figure 27 shows image maps for Cd* and F6 scores. The geochemical association between Cd and Ge is not obvious.
Areas of note are as follows:

Area **6A** (Figure 27) is in the southern part of the MOUNT SURPRISE sheet area and is gently undulating plains surrounded by hilly country. The area is underlain by Puppy Camp Granodiorite, Mosaic Gully Rhyolite and Einasleigh Metamorphics, and is drained by tributaries of the Einasleigh River including Telegraph, Jardine, Ellendale and Little Stockman Creeks. The area is high in Cd* and, to a lesser extent, in Ge. This roughly corresponds to area **2B** (which contains a Zn high).

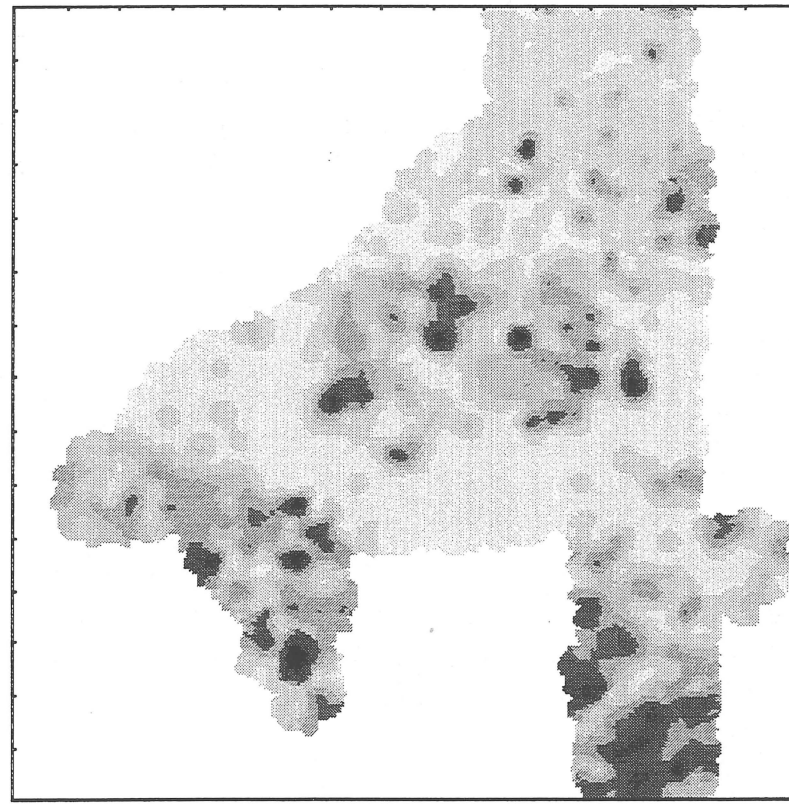

Cd*

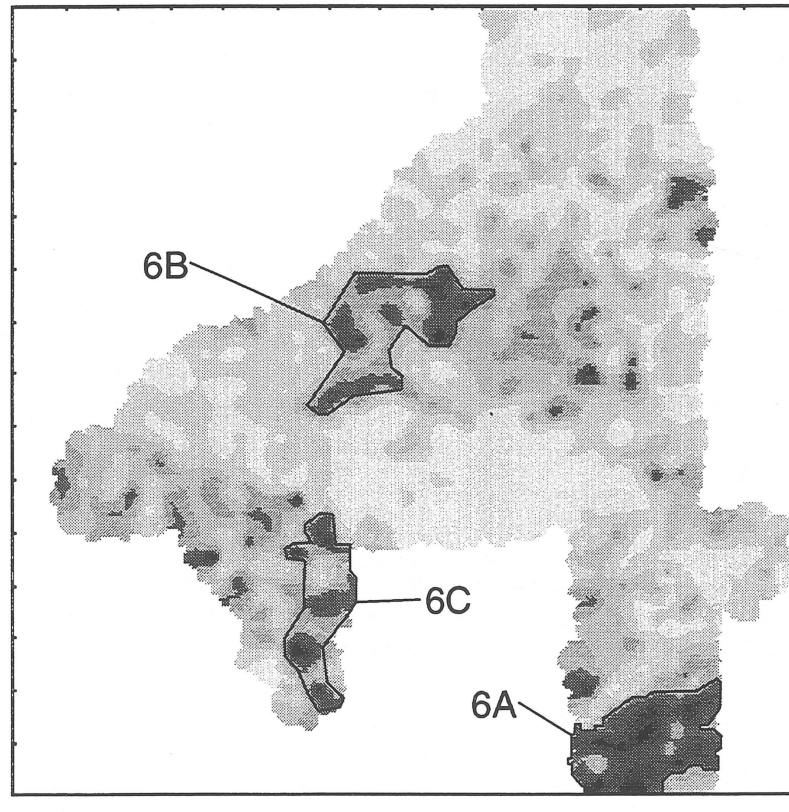

F6

30	60	80	90	95	98	99	99.9	%
0.07	0.12	0.17	0.22	0.26	0.34	0.38	0.53	ppm Cd*
-0.47	0.22	0.82	1.20	1.55	1.90	2.07	2.33	F6 scores

Figure 27. Image maps for Cd* and F6 scores in the Red River Region.

Area **6B** is a number of scattered highs in broken tableland in the northern part of the GALLOWAY sheet area. The area is drained by tributaries of Red River and is underlain by sedimentary rocks. The area shows a number of highs for Cd*, but little for Ge. It also contains a high which corresponds to the residual Zn high in area **2X** (Figure 15).

Area **6C** also contains a number of scattered highs and is in the FOREST HOME sheet area north of Mount Turner. The area comprises gently undulating to rolling plains with hilly country at Mount Turner. The area is underlain by Forsayth, Aurora and Delaney Granites, Lane Creek Formation and Maureen Volcanic Group. The area contains patchy highs for Cd* and a larger, more coherent high for Ge.

Cd* also shows a high corresponding to the residual Zn high in area **2Y**.

5.7 Factor 7

This factor has Sb* and Mo* as its' principal elements with W*, As and P* as minor contributors and Ti and Nb as negative contributors. Again the geochemical associations are not obvious other than the chalcophile character of Sb and As, and to a lesser extent, Mo. Image maps for Sb* and Mo* are shown in Figure 28.

Two samples from the Angore/Pudding Creek system near the Angore Tin Field in the GALLOWAY sheet area gave very high analyses for Sb (298 and 96.2 ppm). These are shown as area **7X** in Figure 28. The origin of these extremely high values (the next highest is 4.98 ppm) is not clear as the samples show little else that is unusual. Elimination of these samples from factor analysis produced only marginal changes related to position in the factor list rather than change in the compositions of factors.

The patterns inherent in the image map of F7 scores are essentially those of Sb*, but with far less emphasis on the two very high samples described above. Neither F7 or Sb* image maps show any obvious similarity to that of Mo*. Sb* shows a large high in the Cardross area (cf area **1A** in Figure 7) in the northern part of the MUNGAGA sheet area. This corresponds to As and Bi* highs detailed above, and to Factor 1 elements in area 1A, for example P*. In contrast, Mo* is very low in this area.

5.8 Factor 8

Factor 8 comprises Pd# with minor contributions from Ge and Au#, and negative contributions from Zr and Hf. The image map for Pd# is shown in Figure 29. This factor would appear to be insignificant and the distribution of Pd# has been discussed in relation to Factor 5 above.

5.9 Mineral Potential

The assessment of the economic potential of an area can be facilitated by plotting the spatial distributions of elements of economic interest and of pathfinder elements, both of which may have been derived directly or indirectly from mineralisation. It is therefore advantageous to minimise the effects due to lithochemical and/or secondary processes by estimating 'residuals' for elements of direct economic interest with suffer significant lithochemical overprinting (eg Cu, Pb, U and Zn), and to high-light coincident concentrations of groups of elements associated with various styles of mineralisation.

Sb*

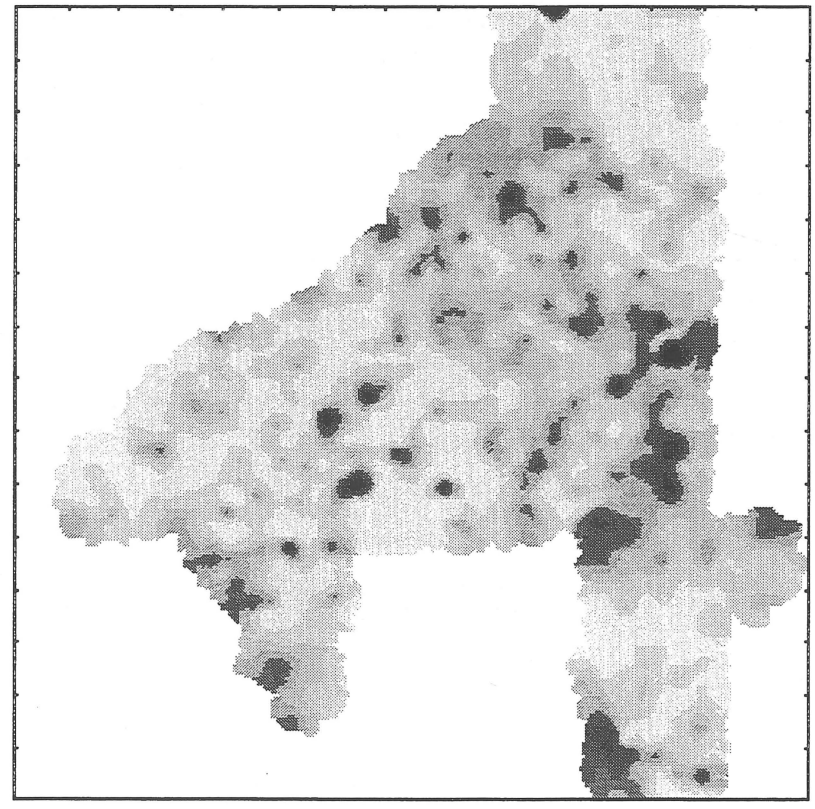

Mo*

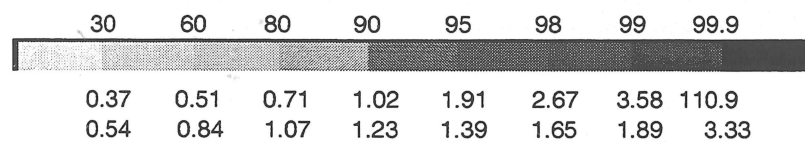

Figure 28. Image maps for Sb* and Mo* in the Red River Region.

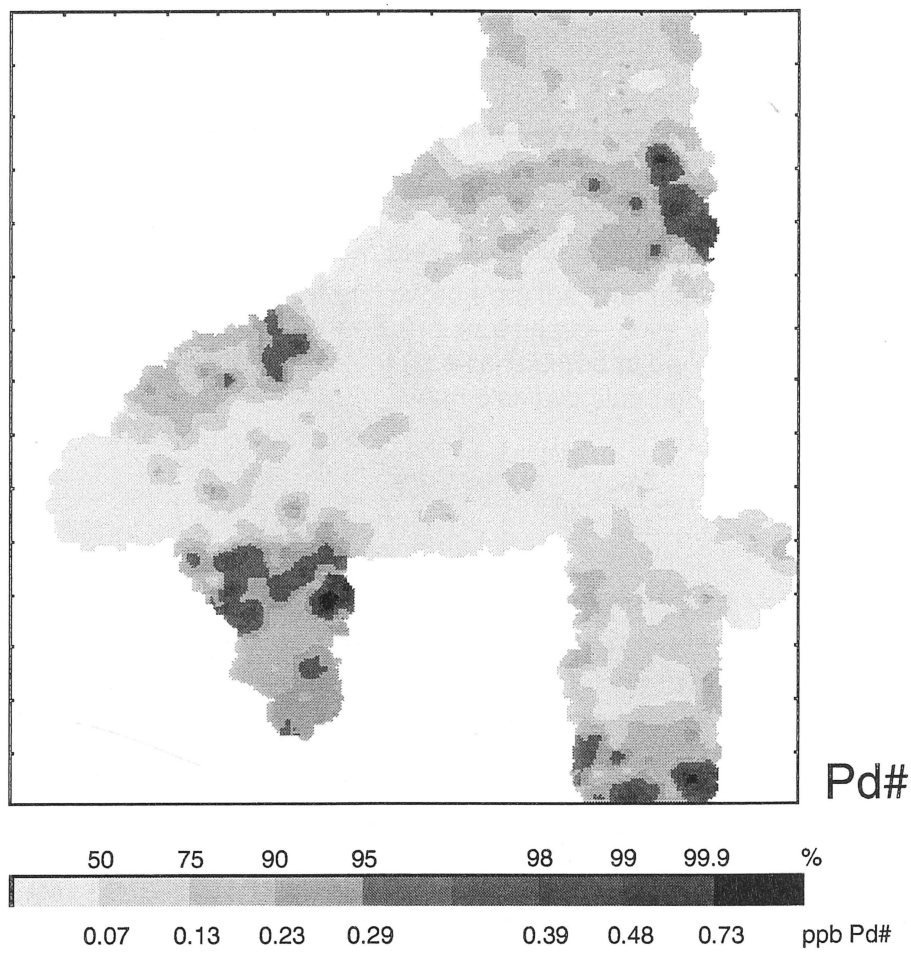

Figure 29. Image map for Pd# in the Red River Region.

5.9.1 Element Residuals

Residuals were estimated for Cu (Figure 13), Pb (Figure 22), U (Figure 9) and Zn (Figure 15) by regression of the element against factor scores in which the elements have significant lithochemical contributions (or conversely against factors in which the element has no obvious mineralisation association). The spatial distributions, and coincidences, of the upper 2% of grid values for each of Cu_{res} (Red), Pb_{res} (Green) and Zn_{res} (Blue) are shown in Figure 30 where the patterns for the elements were combined as an RGB image and superimposed on a greyscale representation of the area sampled. Cu_{res}, Pb_{res} and Zn_{res} highs coincide at Areas **2X**, **2Y** and **2Z** (see Figure 15), these being areas of interest with regard to possible Pb-Zn-Cu mineralisation. Area **2X** is near the Copper Bush (Cu) Prospect.

U_{res} shows highs (see Figure 9) over and displaced from the Fig Tree Hill Granite, and downstream from the McCord Granite to the east of the survey area. These are high U granites with low to moderate Th/U ratios.

5.9.2 Additive Indices

A powerful method of defining potential targets is that of additive indices (Chaffee, 1983; Eggo and others, 1990,1995; Cruikshank, 1994) in which values for economic and

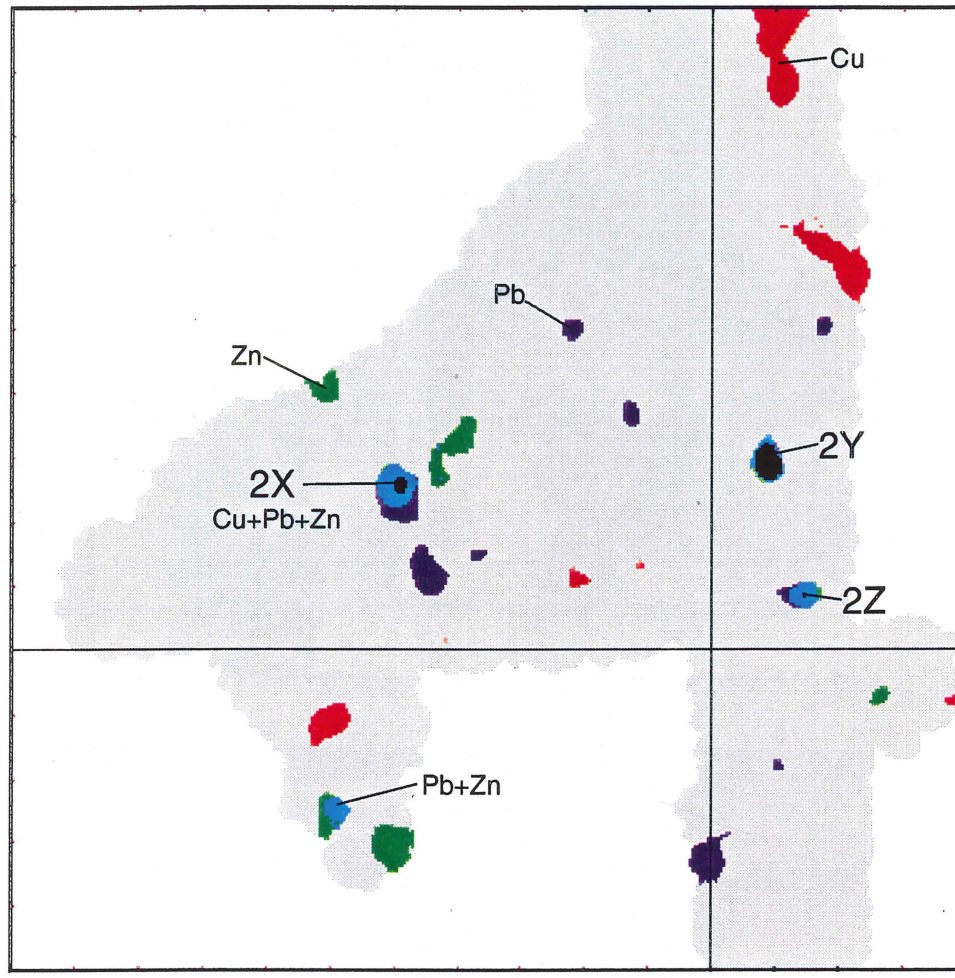

Figure 30. Areas covered by upper 2% of grid values for residuals of Cu (Red), Pb (Green) and Zn (Blue) in the Red River Region. Coincidence of 2 or more of the elements produce the colours shown.

pathfinder elements characteristic of particular types of mineralisation are summed with the highest totals defining the most likely target areas. To compensate for the large variations in the ranges of absolute element values that the components of a particular characteristic group may contain, a standardised value (SV) is estimated as follows:

$$SV_i = (X_i - X)/SD$$

where X_i is the value of an element in sample i, and X and SD are the mean and standard deviation respectively for that element estimated from the total population. The standardised value is therefore in 'SD' or standard deviation units with a mean of zero, and high values, for example greater than 2, may be considered to be 'highly' anomalous in traditional terms as these are greater than 'mean plus two standard deviations'. Index values for each sample were calculated as follows:

$$Index_i = \sum_{e=1}^{e=n} SV_{e,i}$$

Residual values for U, Cu, Zn and Pb have been used in place of the total or as measured values. Index values for a number of mineralisation types were calculated for each sample, gridded and are presented as images. The choice of elements to be included in an index is essentially arbitrary but should be based on common element/mineralisation associations and any available knowledge of mineralisation in the general area. The mineralisation types and the elements used to calculate the indexes are:

5.9.2.1 Gold Index (AUI) - As + Au# + Sb*

Gold mineralisation in the Etheridge Goldfield contained chalcopyrite, galena and sphalerite, as well as arsenopyrite (Cribb, 1939; Wall and Withnall, 1975). Since Cu, Pb and Zn also occur in mineralisation in their own right these have not been included in the equation. Figure 31(a) shows the image map for AUI. The map high-lights the Cardross area (As, Sb* and minor Au#), the Tate River area (Au# - area **5X** in Figure 25), and the Mount Turner area (Au# - the Etheridge Gold Field). Other highs are annotated with the elements responsible.

5.9.2.2 Base Metal Index (BMI) - Ba + Cu_{res} + Pb_{res} + Zn_{res}

The BMI element association is from Levinson (1974), and represents simple Cu-Pb-Zn or Pb-Zn mineralisation. Figure 31(b) shows the image map of the BMI. Potential Pb-Zn mineralisation in areas **2X** (Pb, Zn, Cu and Ba), **2Y** (Pb, Zn, Ba and Cu) and **2Z** (Pb, Zn and Cu) is high-lighted, as are the Mount Turner and Cardross areas. Highs are annotated with the elements which caused them. One Pb-Zn high is in the vicinity of the Eveleigh Ag-Pb mine near the Eveleigh homestead in the GEORGETOWN sheet area.

5.9.2.3 Heavy Mineral Index (HMI) - Ce + La + Nd + P* + Th + Y

The heavy mineral index, HMI, is for the Rare Earth-bearing phosphate minerals monazite and xenotime and the image map is shown in Figure 32(a). Highs are annotated with the elements responsible. The strongest highs are in the MUNGANA and northern LYNDBROOK sheet areas, and appear to be due to monazite-rich (i.e. Ce, La and Nd or

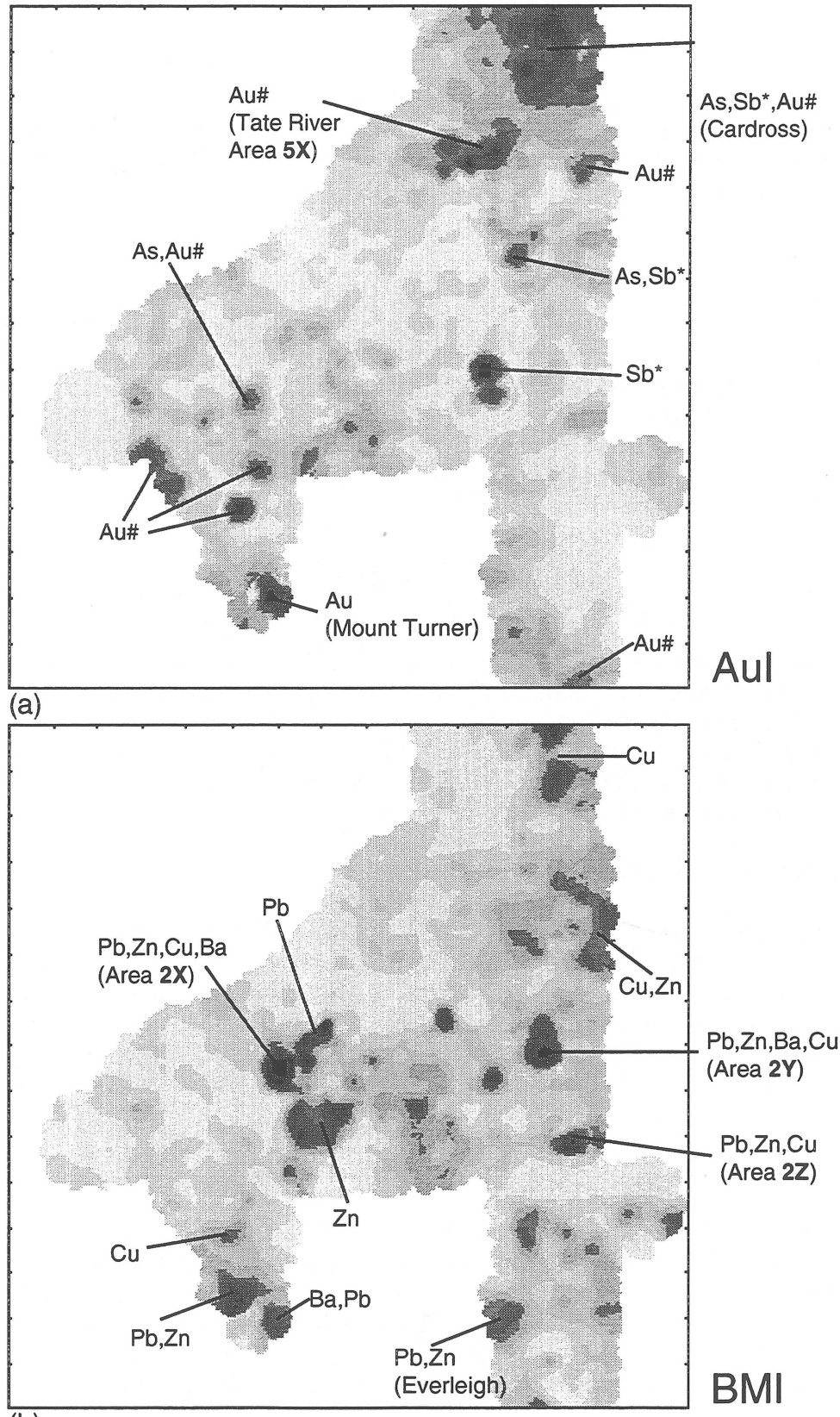

Figure 31. Image maps for Gold Index (AuI) and Base Metal Index (BMI) for the Red River Region.

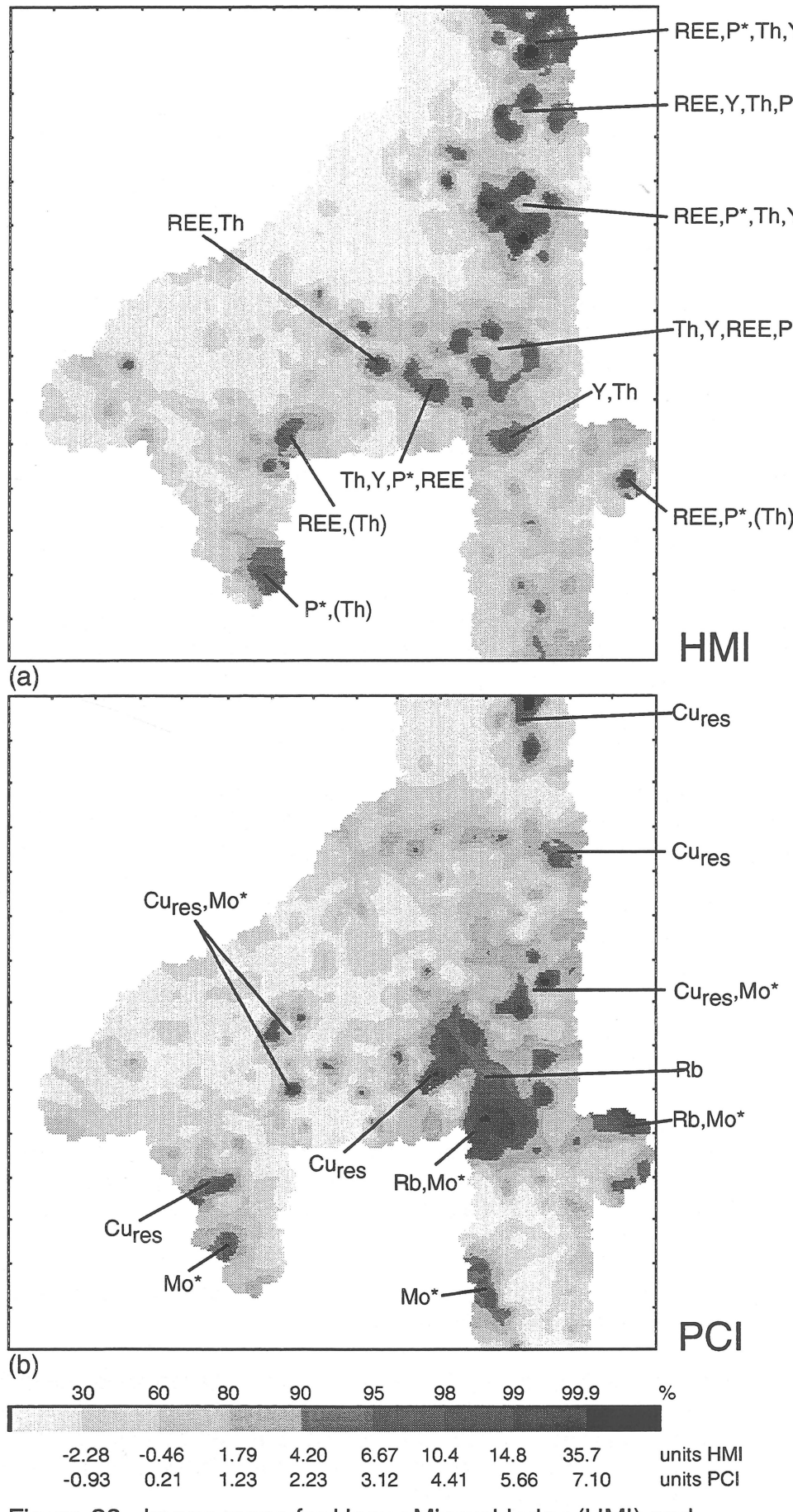

Figure 32. Image maps for Heavy Mineral Index (HMI) and Porphyry Copper Index (PCI) in the Red River Region.

Light Rare Earth Element-rich) sediments. The sample with the highest concentrations of LREE in the northern part of the MUNGANA sheet area would contain about 0.7% monazite by weight, and about 0.1% xenotime based on Ce, La, Nd and Th contents for monazite and Y content for xenotime. The is more than sufficient P* to allow for both minerals.

5.9.2.4 Porphyry Copper Index (PCI) - Cu_{res} + Mo* + Rb

Porphyry copper deposits at Moonmera in central coastal Queensland (Dummett, 1978), and at Coalstoun in southeast Queensland (Ashley and others, 1978) also contain Mo. Rb enrichment in the mineralised zone was also noted at Moonmera, and Rb was included in PCI. The image map for PCI is shown in Figure 32(b). Highs and the element associations responsible are annotated on the image map. The most interesting are those highs away from the Elizabeth Creek Granite, due to that body's high Rb contents. Several small anomalies to the west and the east are high in both Cu_{res} and Mo* and may be prospective.

5.9.2.5 Platinum Index (PTI) - Cr + Ni + Pd# + Pt# + V

PTI defines areas likely to contain mafic/ultramafic rocks which may have potential for platinum group elements. The image map is shown in Figure 33(a), annotated with the elements responsible for highs. Most highs occur over the Undarra Basalt or over metamorphic rocks.

5.9.2.6 Uranium Index (UI) - As + Bi* + Mo* + U_{res}

Uranium deposits in the Georgetown Region to the south of the survey area generally contain As, Bi and Mo (Rossiter and Scott, 1978). The Maureen Prospect in the ABINGDON DOWNS sheet area is a U-fluorite-Mo deposit. Figure 33(b) shows the distribution of UI scores. U, as represented by U_{res}, appears to be overwhelmed by As, Bi* and Mo* (see annotations for highs) suggesting that the image map of U_{res} is possibly a better indication of potential U mineralisation.

CONCLUSIONS

Colour (and greyscale) image maps of the survey area effectively represent the spatial distributions of the elements, and of a number of derived statistical parameters, and were invaluable in the interpretation of the regional stream sediment geochemistry of the survey area. Colour image maps (as in the associated atlas) have greater impact than the greyscale versions but are more costly to reproduce.

Variations in the data are accounted for by the extraction of 8 factors, the first 3 of which account for most of the variation. These are:

- Factor 1 (Ce, Nd, La, Th, Y, U, P* and Nb) is believed to be due to the presence in the stream sediment of the resistant phosphate minerals monazite (LREE and Th) and xenotime (Y), although the epidote mineral allanite, or its' weathering products, may also be present in some areas. These minerals can contain significant concentrations of U.

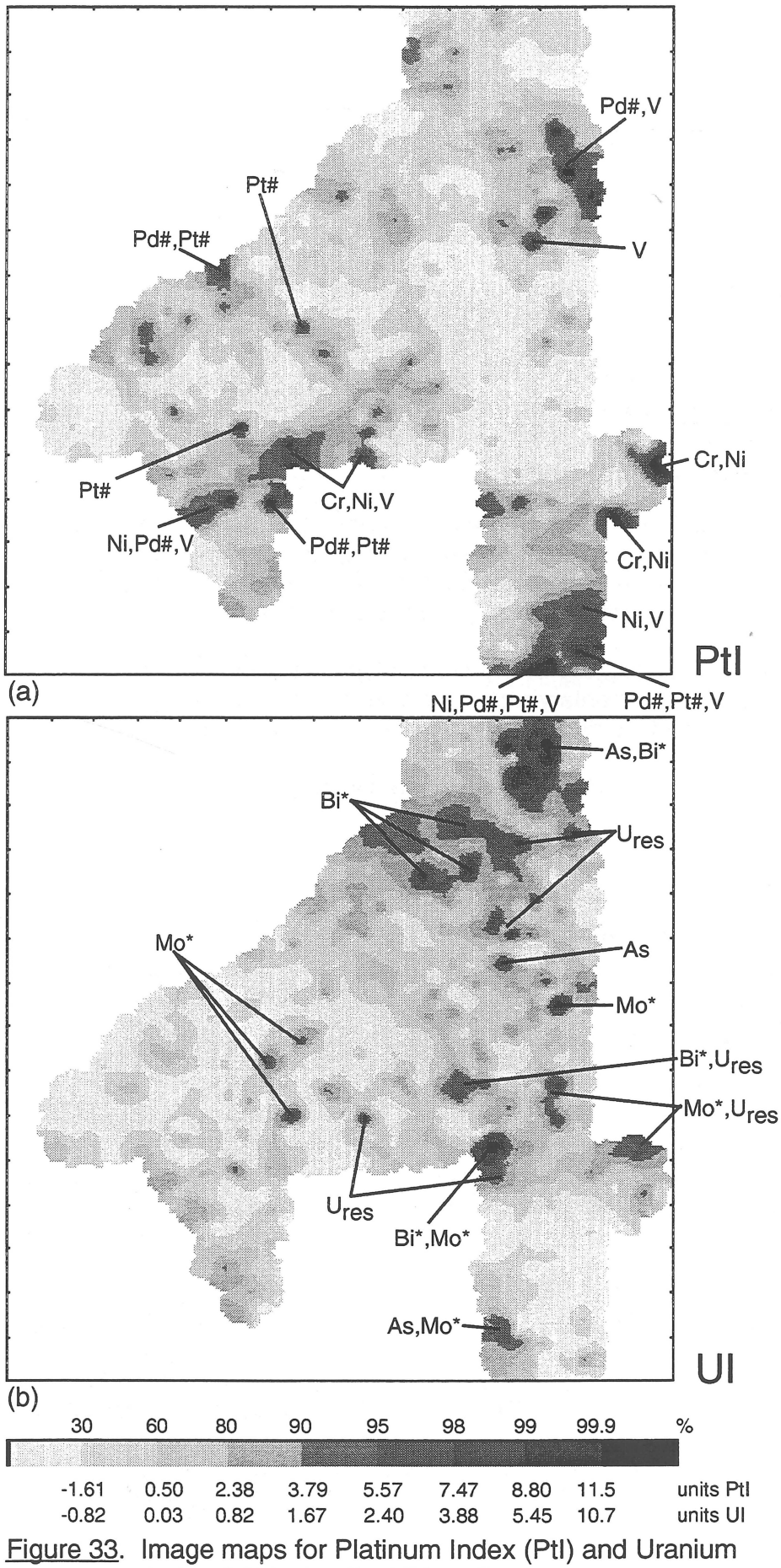

Figure 33. Image maps for Platinum Index (PtI) and Uranium Index (UI) in the Red River Region.

- Factor 2 (V, Fe, Ni, Sc, Cu, Cr, Ti, Zn and Mn) is thought to reflect the geochemistry of Fe-rich minerals in bedrock, and scavenging by hydrated Fe (and Mn) oxides in the the secondary environment.
- Factor 3 (Rb, Tl*, Be*, Ga, Ba, Pb and Sr) is believed to be due to the weathering of K-rich minerals.

The data indicates that the greatest potential is for gold, base metals and tin, although Rare Earth-bearing minerals and uranium could be of interest.

Apart from delineating known gold mineralisation in the Etheridge Gold Field and in the Cardross area, the data showed an extensive Au anomaly on both banks of the Tate River near the Piccaninny Outstation. The anomaly overlies granite, felsic volcanics and metamorphics.

A number of Pb-Zn (+-Cu) anomalies are of potential interest, the largest being near the Copper Bush Prospect. These are enhanced as element residuals, that is measured values 'corrected' for lithochemical effects from the bedrock. An RGB image map shows coincidence of Cu_{res}, Pb_{res} and Zn_{res} at these anomalies.

Sn is widespread, occurring over granites of the O'Briens Creek Supersuite, and, more prevalently, over sedimentary rocks to the west of the granites and metamorphics. Sn in, or from, Mesozoic sediments seems to be a feature of the region.

U_{res} highlights two high-U granites in an area which may have some (limited) potential for mineralisation.

ACKNOWLEDGMENTS

The author wishes to thank J.G. Pyke, J. Pye, L. Roberts, J. Astin, C. Agnew, R Bates, D. Butrovski and A. Tate for their invaluable assistance in carrying out the sampling program, J.G. Pyke, W. Pappas and L. Webber for analysing the samples in AGSO's Geochemical Laboratory, P.C. Brugman for assistance in the preparation of the manuscript, and J.H.C. Bain and C.F. Pain for their critical reviews of the manuscript.

REFERENCES

ASHLEY, P.M., BILLINGTON, W.G., GRAHAM, R.L., and NEALE, R.C., 1978. Geology of the Coalstoun porphyry copper prospect, southeast Queensland, Australia. Economic Geology, v73, p945-965.

BAIN, J.H.C., WITHNALL, I.W., OVERSBY, B.S. and MACKENZIE, D.E., 1985. Geology of the Georgetown Region, Queensland, 1:250 000 Scale map. Australian Bureau of Mineral Resources, Canberra, ACT.

BAIN, J.H.C., WITHNALL, I.W., OVERSBY, B.S., and MACKENZIE, D.E., 1990. North Queensland Proterozoic inliers and Palaeozoic provinces - regional geology and mineral deposits. In Hughes, F.E., (Editor), Geology of the Mineral Deposits of Australia and Papua New Guinea. The Australasian Institute of Mining and Metallurgy, Melbourne, p963-978.

BEST, J.G., 1962. Atherton 1:250 000 geological series - explanatory notes. Bureau of Mineral Resources, Canberra.

BONHAM-CARTER, G.F., ROGERS, P.J., and ELLWOOD, D.J., 1987. Catchment basin analysis applied to surficial geochemical data, Cobequid Highlands, Nova Scotia. Journal of Geochemical Exploration, v29, p259-278.

BOYLE, R.W., and JONASSON, I.R., 1973. The geochemistry of arsenic and its use as an indicator element in geochemical prospecting. Journal of Geochemical Exploration, v2, p251-296.

BRANCH, C.D., 1966. Volcanic cauldrons, ring complexes, and associated granites of the Georgetown Inlier, Queensland. Bureau of Mineral Resources, Canberra, Bulletin 76.

BULTITUDE, R.J., GARRAD, P.D., and ROBERTS, C.W., 1997. Hodgkinson Basin Geology, 1:500 000 Scale Map, Second Edition. Department of Minerals and Energy, Queensland.

BUREAU of METEOROLOGY, 1971. Bureau of Meteorology (1971) climatic survey - region 16. Bureau of Meteorology, Australia.

CHAFFEE, M.A., 1983. SCORESUM - a technique for displaying and evaluating multi-element geochemical information, with examples of its use in regional mineral assessment programs. In: PARSLOW, G.R., (Editor), Geochemical Exploration, 1982. Journal of Geochemical Exploration, v19, p361-381.

CHAMPION, D.C., and MACKENZIE, D.E., 1994. Metallogenic Atlas Series #2 - North Queensland igneous rocks. Australian Geological Survey Organisation, Canberra.

CRIBB, H.G.S., 1939. Mining in the Georgetown district, Etheridge Goldfield. Queensland Government Mining Journal, Brisbane. v40(475), p402-407.

CRUIKSHANK, B., 1990. Stream-sediment geochemistry of the original Kakadu Conservation Zone, BMR Research Newsletter, No. 12 (April, 1990), Bureau of Mineral Resources, Canberra.

CRUIKSHANK, B.I., 1994. Stream sediment geochemistry of the Ebagoola 1:250 000 sheet area, Cape York Peninsula, north Queensland. Australian Geological Survey Organisation, Canberra. Record 1994/8 (unpublished).

CRUIKSHANK, B.I., 1995. Stream Sediment Geochemical Atlas Series #2, Red River Region, north Queensland. Australian Geological Survey Organisation, Canberra.

CRUIKSHANK, B.I., and BRUGMAN, P.C., 1995. Stream Sediment Geochemical Atlas Series #3, Hann River Region, north Queensland. Australian Geological Survey Organisation, Canberra.

CRUIKSHANK, B.I., and BRUGMAN, P.C., 1997. Stream sediment geochemistry of the Hann River Region, Cape York Peninsula, north Queensland. Australian Geological Survey Organisation, Canberra. Record 1996/22 (Unpublished).

CRUIKSHANK, B.I., and BUTROVSKI, D., 1994. Stream Sediment Geochemical Atlas, Ebagoola sheet area, north Queensland. Australian Geological Survey Organisation, Canberra.

CRUIKSHANK, B.I., HALDANE, J.A., and PYKE, J.G., 1983. Stream-sediment geochemical data - North Head and Forest Home 1:100 000 sheet area. Bureau of Mineral Resources, Australia. Record 1983/26 (unpublished), BMR Microform MF198.

CRUIKSHANK, B.I., HOATSON, D.M., and PYKE, J.G., 1993. A stream-sediment geochemical orientation survey of the Davenport Province, Northern Territory. AGSO Journal of Australian Geology and Geophysics, 14, 77-95.

CRUIKSHANK, B.I., and PYKE, J.G., 1993. Analytical methods used in Minerals and Land Use Program's geochemical laboratory. Australian Geological Survey Organisation, Canberra, Record 1993/26 (unpublished).

DEER, W.A., HOWIE, R.A., and ZUSSMAN, J., 1962. Rock-forming minerals, Volume 1, Ortho- and Ring Silicates. John Wiley and Sons, Inc., New York.

DENMEAD, A.K., 1950. Eveleigh Silver-Lead Field. Queensland Government Mining Journal, v51(581), p168-171.

DENMEAD, A.K., and RIDGWAY, J.E., 1947. Eveleigh silver-lead discovery, Einasleigh. Queensland Government Mining Journal, v48, p362-365.

DILLON, W.R., and GOLDSTEIN, M., 1984. Multivariate analysis, methods and applications. John Wiley and sons, New York.

DONCHAK, P.J.T., and BULTITUDE, R.J., 1994. Geology of the Atherton 1:250 000 Sheet Area. Department of Minerals and Energy, Queensland, Record 1994/5 (unpublished).

DUMMETT, H.T., 1978. Geology of the Moonmera porphyry deposit, Queensland, Australia. Economic Geology v73, p922-944.

EGGO, Alfred J., HARDING, Tony, and BAIN, John, 1990. Advanced interpretation techniques applied to regional stream sediment geochemical data from the Georgetown region, SE54-12, Northeast Queensland. CRAE Report No. 16614 (unpublished).

EGGO, Alfred J., HARDING, Tony, and BAIN, John, 1995. Removal of background processes controlling trace element variability in -80# stream sediment geochemical data, Georgetown Region, Northeast Queensland, Australia. In Extended Abstracts, 17th IGES, Exploring the Tropics, 15-19 May, 1995, Townsville, Australia.

ELLIOTT, S.M., and TOWSEY, C.A., 1989. Regional drainage geochemical gold exploration techniques used in Queensland, Australia. NQ Gold '89 Conference, Townsville.

ELLIS, P.J., and STEELE, T.W., 1982. Five robust indicators of central value. Geostandards Newsletter, v6(2), p207-216.

FELDMAN, D.S., GAGNON, J., HOFMANN, R., and SIMPSON, J., 1990. Statview II, the solutions for data analysis and presentation graphics (manual for computer program). Abacus Concepts, Berkeley.

FLETCHER, W.K., 1990. Dispersion and behaviour of gold in stream sediments. Ministry of Energy, Mines and Petroleum Resources, Province of British Columbia, Geological Survey Branch, Open File 1990-28 (unpublished).

FOY, M.F., and GINGRICH, J.E., 1977. A stream-sediment orientation programme for uranium in the Alligator River Province, Northern Territory, Australia. Journal of Geochemical Exploration, v8, p357-364.

GALLOWAY, R.W., GUNN, R.H., and STORY, R., 1970. Lands of the Mitchell-Normanby area, Queensland. Commonwealth Scientific and Industrial Research Organisation, Australia, Land Research Series, No 26.

HOATSON, D.M., and CRUIKSHANK, B.I., 1985. A stream sediment geochemical orientation survey of the Davenport Province, Northern Territory. Bureau of Mineral Resources, Canberra, Record 1985/44 (unpublished).

JENNE, E.A., 1968. Controls on Mn, Fe, Co, Ni, Cu and Zn concentrations in soils and water: the significant role of hydrous Mn and Fe oxides. Advances in Chemistry series, No. 73, Trace Inorganics in Water. The American Chemical Society.

KEYSER, F. de, and WOLFF, K.W., 1964. The geology and mineral resources of the Chillagoe area. Geological Survey of Queensland, Brisbane, Publication No. 317.

KEYSER, F. de, and LUCAS, K.G., 1968. Geology of the Hodgkinson and Laura Basins, north Queensland. Bureau of Mineral Resources, Canberra, Bulletin No 84.

KOCH, G.S., and LINK, R., 1970. Statistical analysis of geological data. John Wiley and sons, New York.

KOCH, G.S., and LINK, R., 1971. Statistical analysis of geological data, volume II. John Wiley and sons, New York.

KRAUSKOPF, K.B., 1967. Introduction to geochemistry. McGraw-Hill Book Company, New York, p639.

LEVINSON, A.A., 1974. Introduction to exploration geochemistry. Applied Publishing Ltd., Calgary.

MACKENZIE, D.E., WELLMAN, P., BAIN, J.H.C., TRAIL, D.S., von GNIELINSKI, F.E., DOHRENWEND, J.C., and PAIN, C.F., 1996. Red River Geology, (1:250 000 scale map). Australian Geological Survey Organisation, Canberra.

NICHOL, Ian, HORSNAIL, R.F., and WEBB, J.S., 1967. Geochemical patterns in stream sediment related to precipitation of manganese oxides. Transactions of the Institute of Mining and Metallurgy, Section B, v76, pB113-B115.

NORRISH, K., and CHAPPELL, B.W., 1977. X-ray fluorescence spectrometry. In ZUSSMAN, J., (Editor), Physical methods in determinitive Mineralogy, 2nd Edition. Academic Press, London. p201-272.

OVERSBY, B.S., PALFREYMAN, W.D., BLACK, L.P., COOPER, J.A., and BAIN, J.H.C., 1975. Georgetown, Yambo, and Coen Inliers - regional geology. In KNIGHT, C.L. (Editor), Economic Geology of Australia and Papua New Guinea. Australasian Institute of Mining and Metallurgy, Monograph No. 5, v1, 511-516.

PRICE, V., and FERGUSON, R.B., 1980. Stream sediment surveys for uranium. Journal of Geochemical Exploration, v13, p285-304.

ROSSITER, A.G., 1975. An orientation geochemical survey in the Georgetown area, north Queensland, Bureau of Mineral Resources, Canberra, Record 1975/164 (unpublished).

ROSSITER, A.G., and SCOTT, P.A., 1978. Stream-sediment geochemistry of the Forsayth 1:100 000 sheet area, north Queensland. Bureau of Mineral Resources, Canberra, Record 1978/17 (unpublished).

ROSSITER, A.G., and SCOTT, P.A., 1979. Stream-sediment geochemical data - Gilberton 1:100 000 sheet area. Bureau of Mineral Resources, Australia. Record 1979/68 (unpublished). BMR Microform MF109.

SAWERS, J.D., 1965. 'Copper Bush' copper prospect, Abingdon Station, Georgetown. Memorandum to the District Geologist, Charters Towers. GSQ File/Copper-Etheridge 13.8.65.

SCOTT, P.A., and ROSSITER, A.G., 1979. Stream-sediment geochemical data - Georgetown 1:100 000 sheet area. Bureau of Mineral Resources, Australia. Record 1979/118 (unpublished). BMR Microform MF118.

SHERATON, J.W., and LABONNE, B., 1978. Petrology and geochemistry of acid igneous rocks of northeast Queensland. Bureau of Mineral Resources, Canberra, Bulletin 169.

SINCLAIR, A.J., 1974. Selection of threshold values in geochemical data using probability graphs. Journal of Geochemical Exploration, v3, p129-149.

SINCLAIR, A.J., 1991. A fundamental approach to threshold estimation in exploration geochemistry; probability plots revisited. Journal of Geochemical Exploration, v41, p1-22.

SMART, J., and BAIN, J.H.C., 1977. Red River 1:250 000 geological series - explanatory notes. Bureau of Mineral Resources, Canberra.

TWIDALE, C.R., 1966. Geomorphology of the Leichhardt-Gilbert area, north-west Queensland. Commonwealth Scientific and Industrial Research Organisation, Australia. Land Research Series, No. 16.

WALL, L.N., and WITHNALL, I.W., 1975. Georgetown Inlier - mineralisation. In KNIGHT, C.L. (Editor), Economic geology of Australia and Papua New Guinea. Australasian Institute of Mining and Metallurgy, Monograph No. 5, v1, p516-518.

WARNICK, J.V., 1985. Pre-carboniferous geology of the Mount Surprise Einasleigh Region, northe Queensland. Geological Survey of Queensland, Brisbane, Record 1985/60 (unpublished).

WARNICK, J.V., 1989. Pre-Carboniferous geology of the Mount Surprise Einasleigh Region, northe Queensland. Quensland Department of Mines, Brisbane, Report 2.

WEDEPOHL, K.H., 1972. Zinc. In K.H. Wedepohl (Editor), Handbook of Geochemistry, vII-3, Springer-Verlag, Berlin.

WHITE, D.A., 1962a. Einasleigh 1:250 000 geological series - explanatory notes. Bureau of Mineral Resources, Canberra.

WHITE, D.A., 1962b. Georgetown 1:250 000 geological series - explanatory notes. Bureau of Mineral Resources, Canberra.

WHITE, D.A., 1965. The geology of the Georgetown/Clarke River area, Queensland. Bureau of Mineral Resources, Canberra, Bulletin No. 71.

WITHNALL, I.W., 1989. Precambrian and Palaeozoic geology of the southeastern Goergetown Inlier, north Queensland. Quensland Department of Mines, Brisbane, Report 2.

WITHNALL, I.W. and GRIMES, K.G., 1991. Explanatory notes on the Einasleigh 1:250 000 geological sheet. Department of Resource Industries, Queensland, Record 1991/15 (unpublished).

WITHNALL, I.W. and GRIMES, K.G., 1995. Queensland, 1:250 000 geological series explanatory notes to accompany Einasleigh 1:250 000 geological map, sheet SE 55-9. Geological Survey of Queensland, Brisbane.

Appendix A

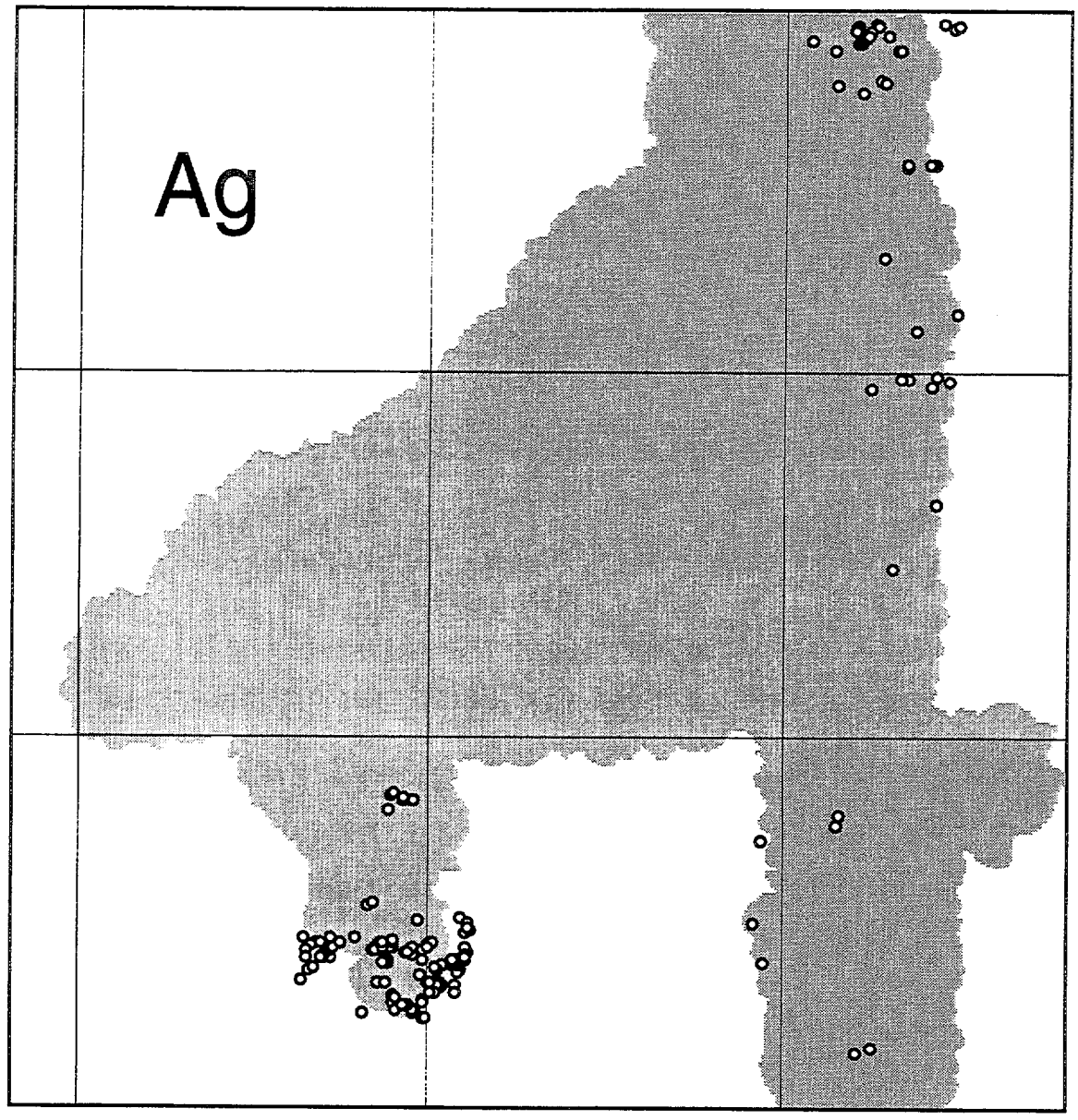

Figure A1. Ag occurrences (N=191) in, or immediately adjacent to, the RED RIVER Region survey area (after MINLOC, November, 1994).

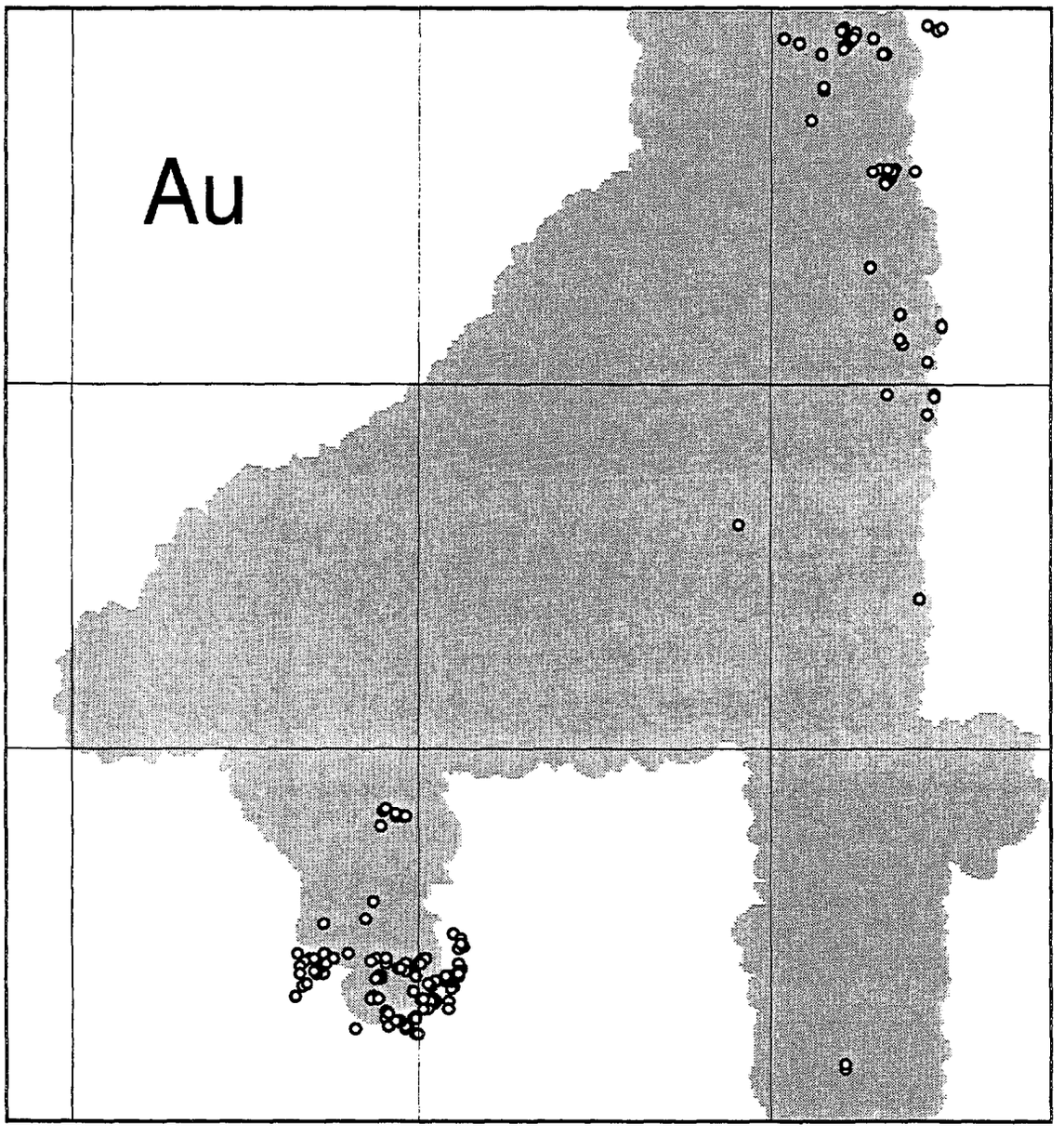

Figure A2. Au occurrences (N=191) in, or immediately adjacent to, the RED RIVER Region survey area (after MINLOC, November, 1994).

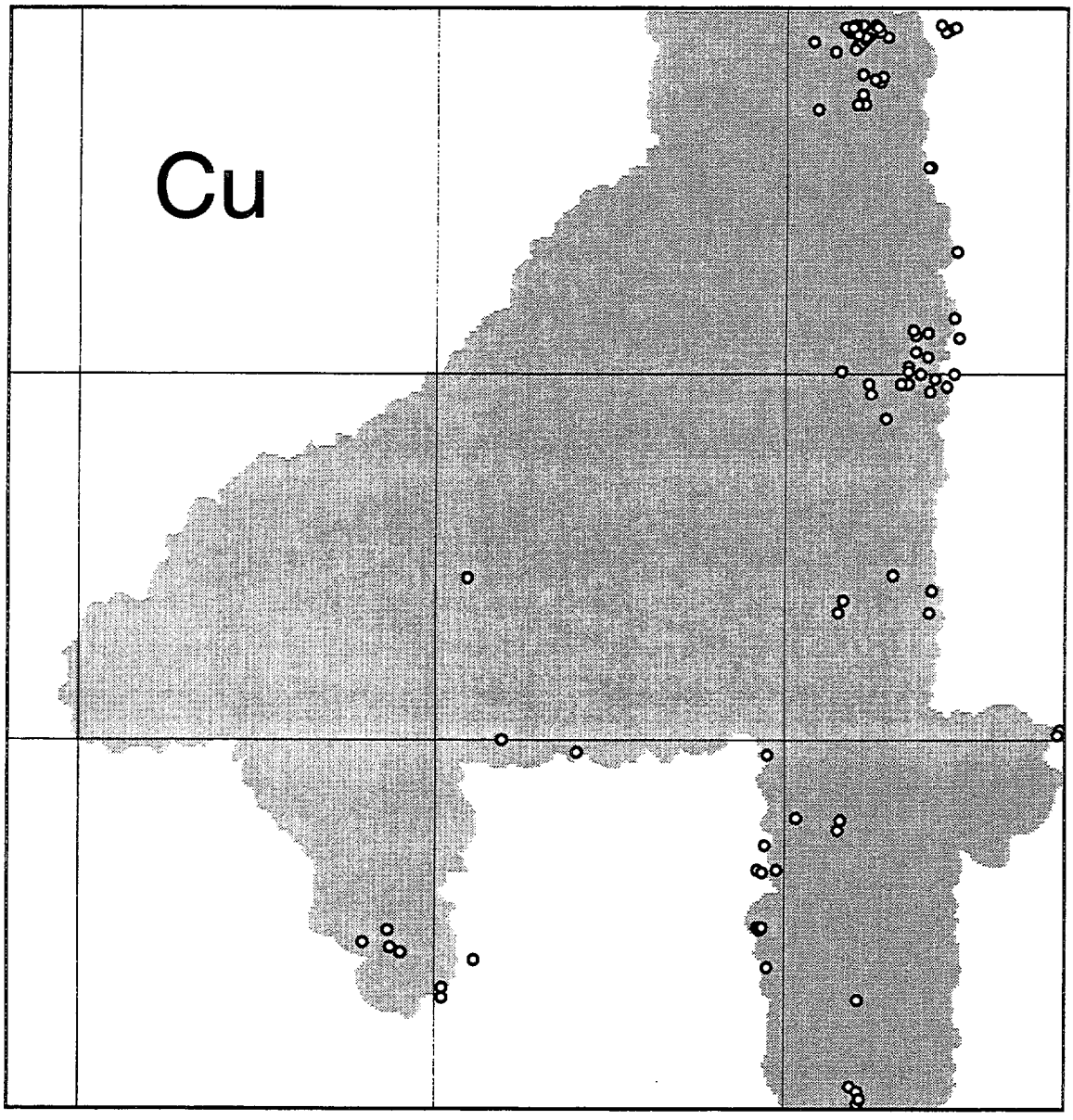

Figure A3. Cu occurrences (N=127) in, or immediately adjacent to, the RED RIVER Region survey area (after MINLOC, November, 1994).

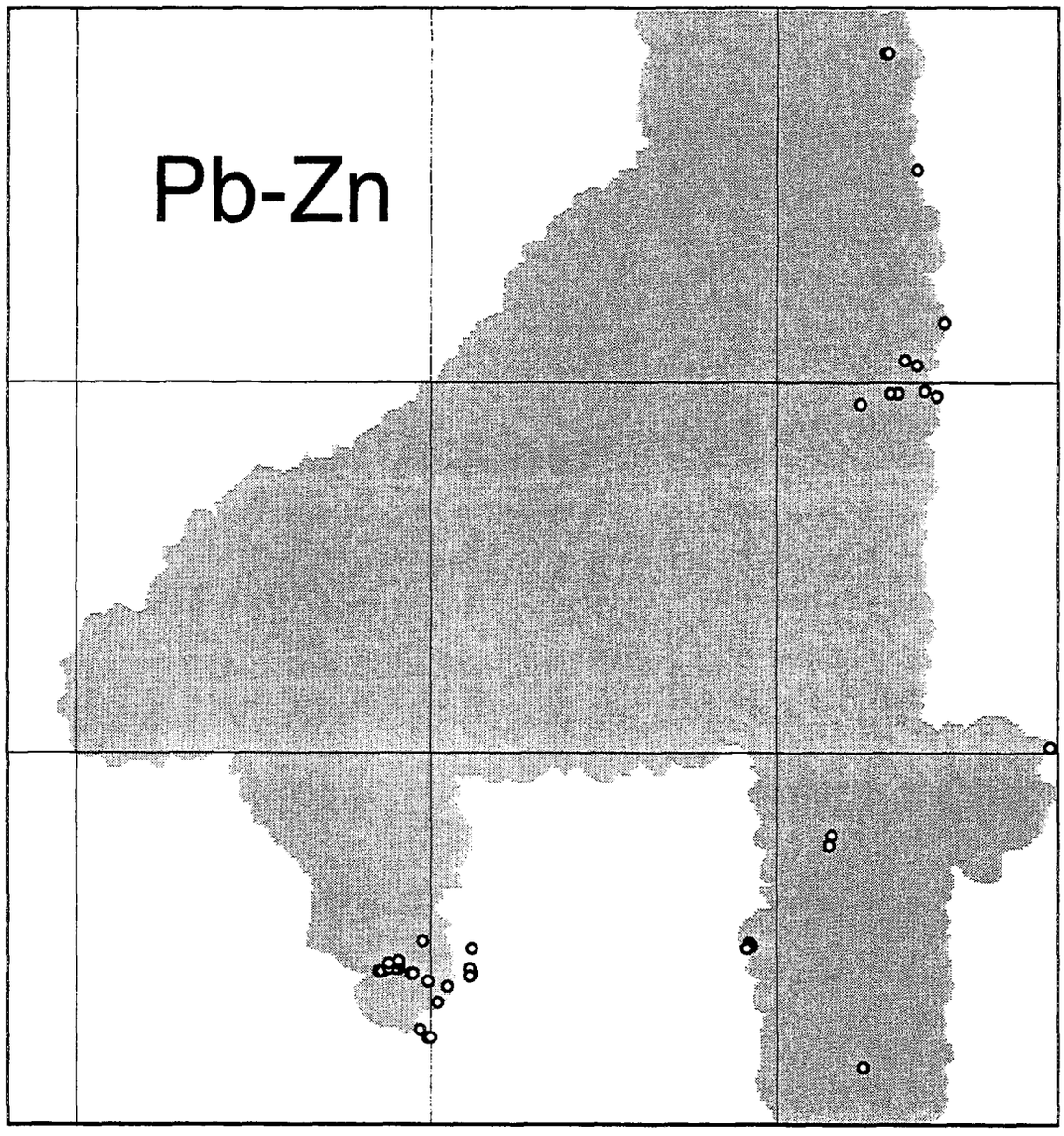

Figure A4. Pb-Zn occurrences (N=45) in, or immediately adjacent to, the RED RIVER Region survey area (after MINLOC, November, 1994).

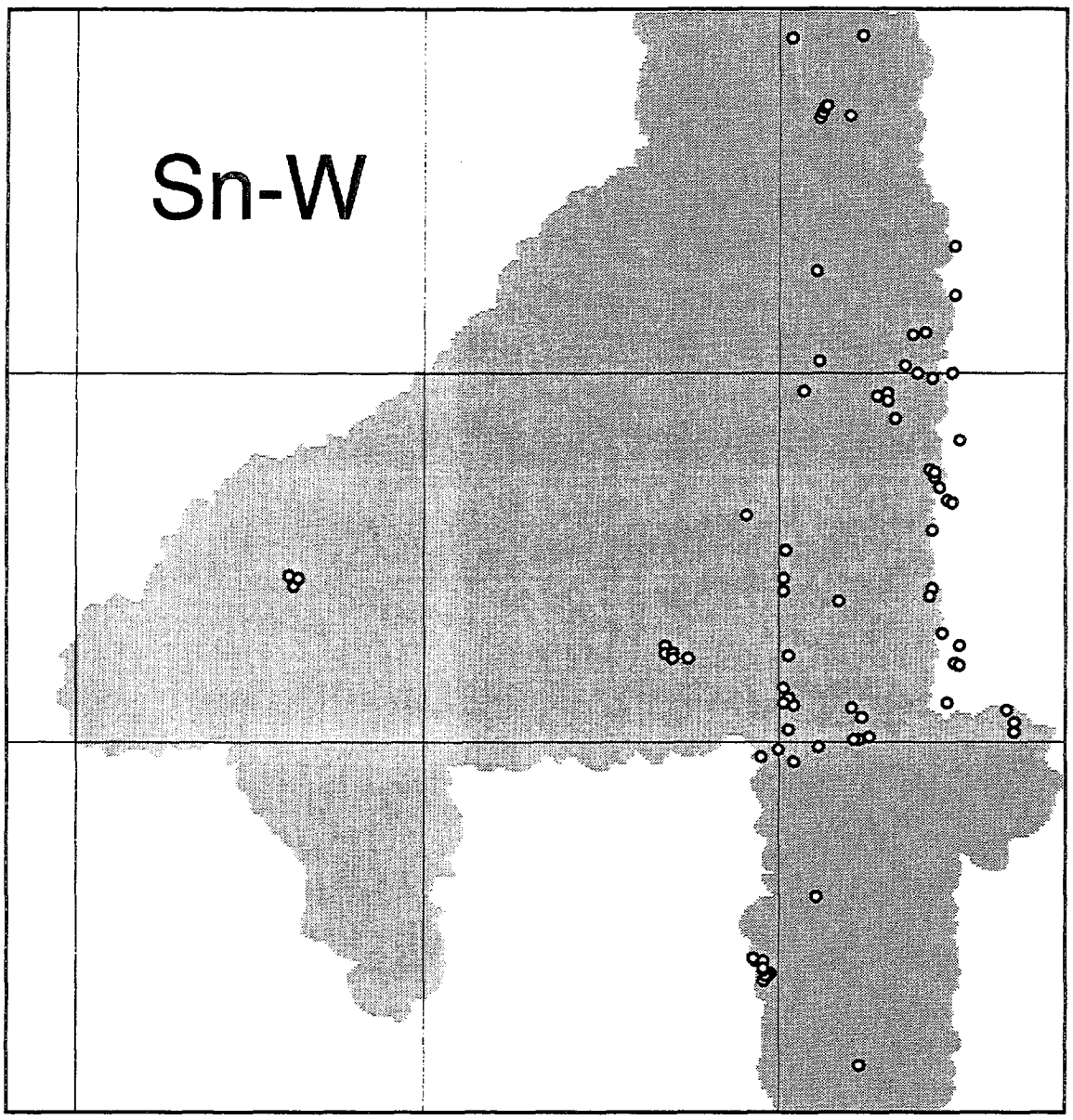

Figure A5. Sn-W occurrences (N=81) in, or immediately adjacent to, the RED RIVER Region survey area (after MINLOC, November, 1994).

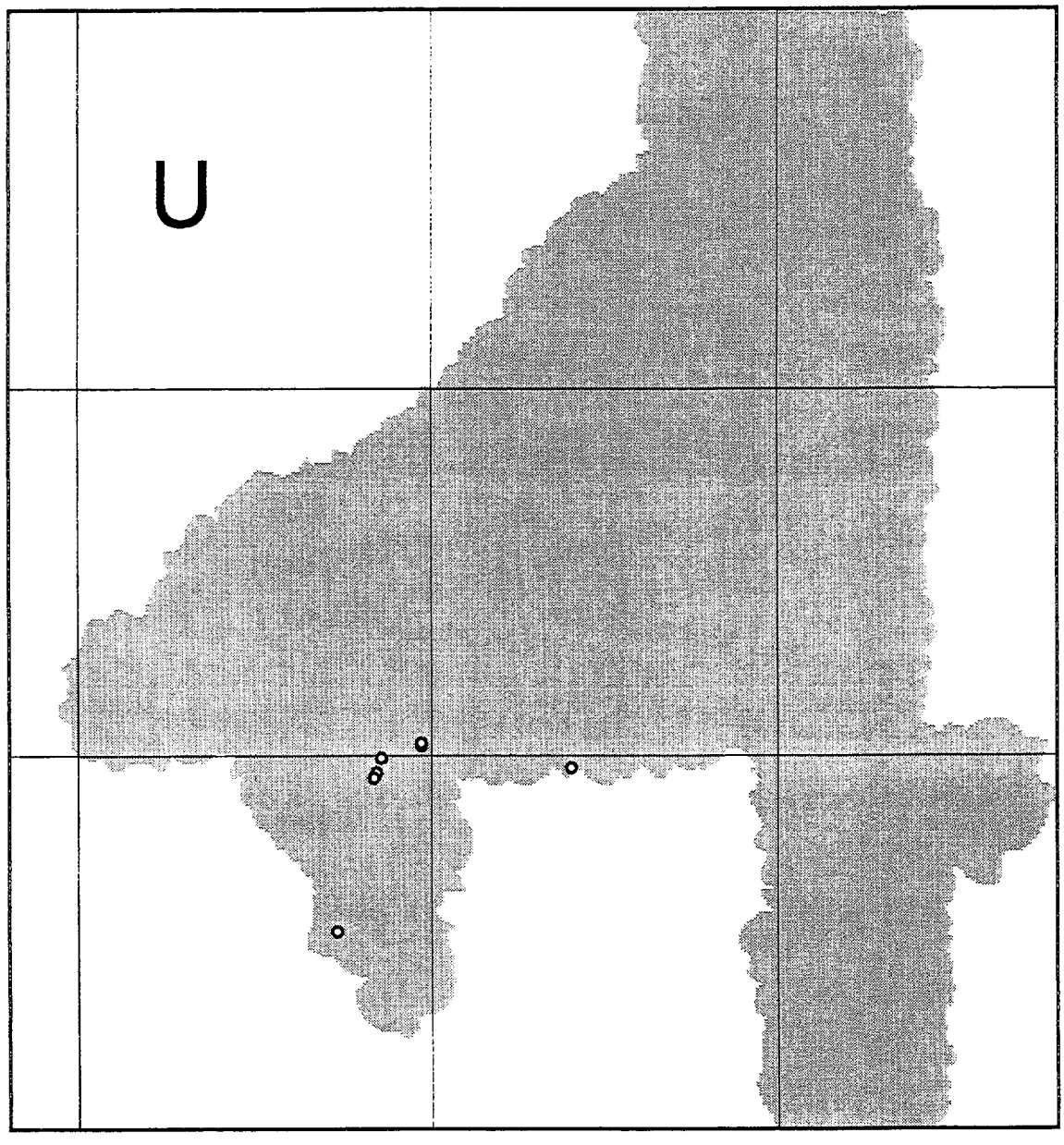

Figure A6. U occurrences (N=7) in, or immediately adjacent to, the RED RIVER Region survey area (after MINLOC, November, 1994).

Appendix B

Silver

Mean:	Std. Dev.:	Std. Error:	Variance:	Coef. Var.:	Count:
.723	.587	.02	.345	81.21	843
Minimum:	**Maximum:**	**Range:**	**Sum:**	**Sum of Sqr.:**	**# Missing:**
.05	8.53	8.48	609.65	731.322	0
# < 10th %:	**10th %:**	**25th %:**	**50th %:**	**75th %:**	**90th %:**
84	.268	.393	.59	.9	1.282
# > 90th %:	**Mode:**	**Geo. Mean:**	**Har. Mean:**	**Kurtosis:**	**Skewness:**
84	.6	.58	.456	45.326	4.786

Detection limit is 0.1 ppm - a value of 0.05 ppm has been substituted in calculations and table.

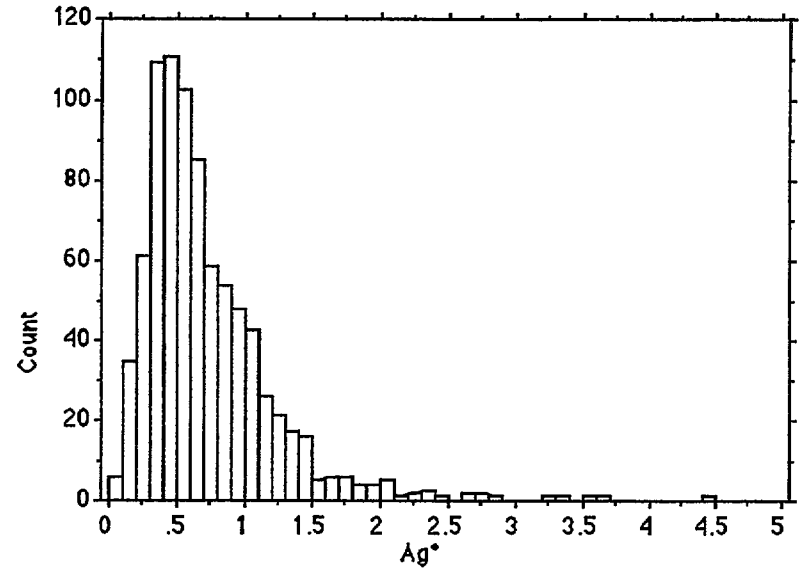

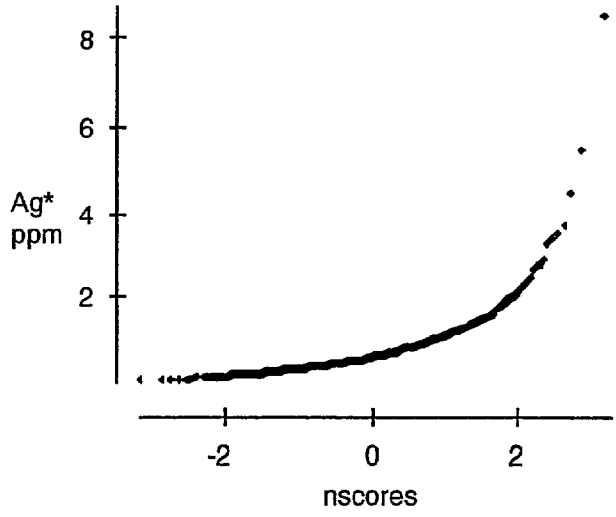

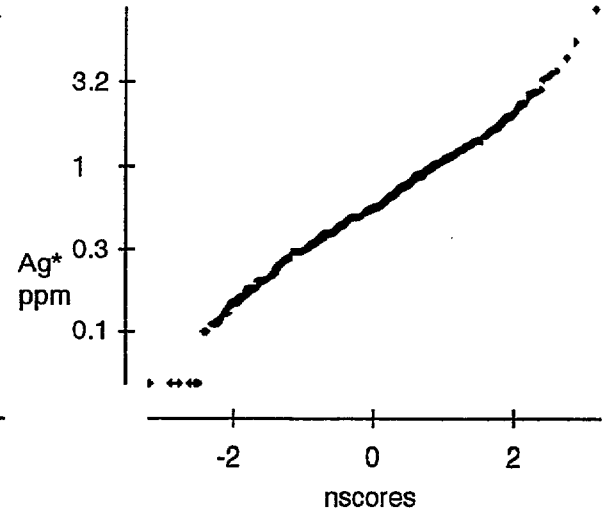

Ag*

Arsenic

Mean:	Std. Dev.:	Std. Error:	Variance:	Coef. Var.:	Count:
4.32	9.229	.318	85.179	213.641	843
Minimum:	**Maximum:**	**Range:**	**Sum:**	**Sum of Sqr.:**	**# Missing:**
.25	117	116.75	3641.75	87453.062	0
# < 10th %:	**10th %:**	**25th %:**	**50th %:**	**75th %:**	**90th %:**
0	.25	1	2	4	7.5
# > 90th %:	**Mode:**	**Geo. Mean:**	**Har. Mean:**	**Kurtosis:**	**Skewness:**
79	1	1.976	1.031	47.149	6.103

Detection limit is 0.5 ppm - a value of 0.25 ppm has been substituted in calculations and table.

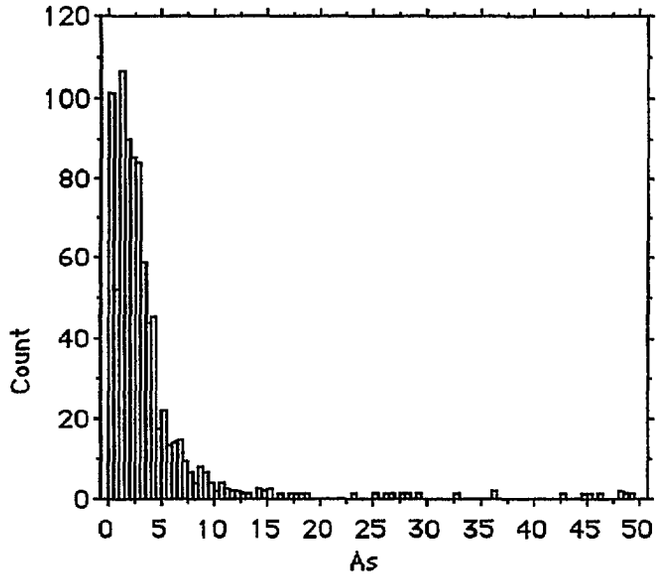

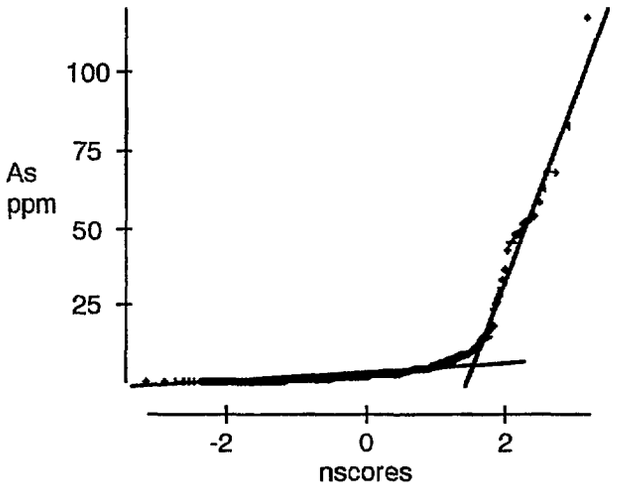

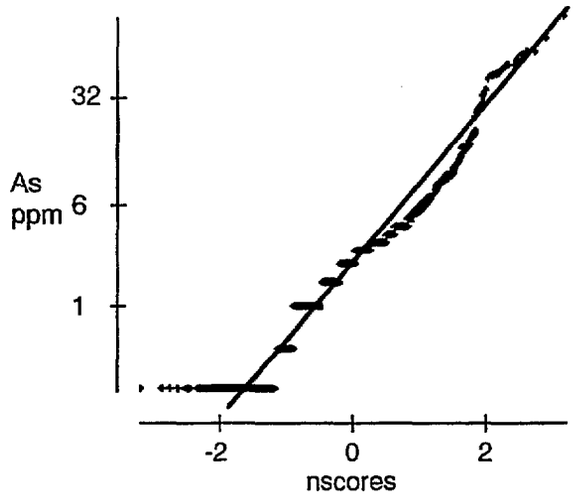

As

Gold

Mean:	Std. Dev.:	Std. Error:	Variance:	Coef. Var.:	Count:
.299	1.341	.046	1.798	448.244	840
Minimum:	**Maximum:**	**Range:**	**Sum:**	**Sum of Sqr.:**	**# Missing:**
.005	25.5	25.495	251.28	1583.677	0
# < 10th %:	**10th %:**	**25th %:**	**50th %:**	**75th %:**	**90th %:**
51	.02	.04	.07	.15	.4
# > 90th %:	**Mode:**	**Geo. Mean:**	**Har. Mean:**	**Kurtosis:**	**Skewness:**
82	.03	.079	.041	182.463	12.017

Detection limit is 0.01 ppb - a value of 0.005 ppb has been substituted in calculations and table.

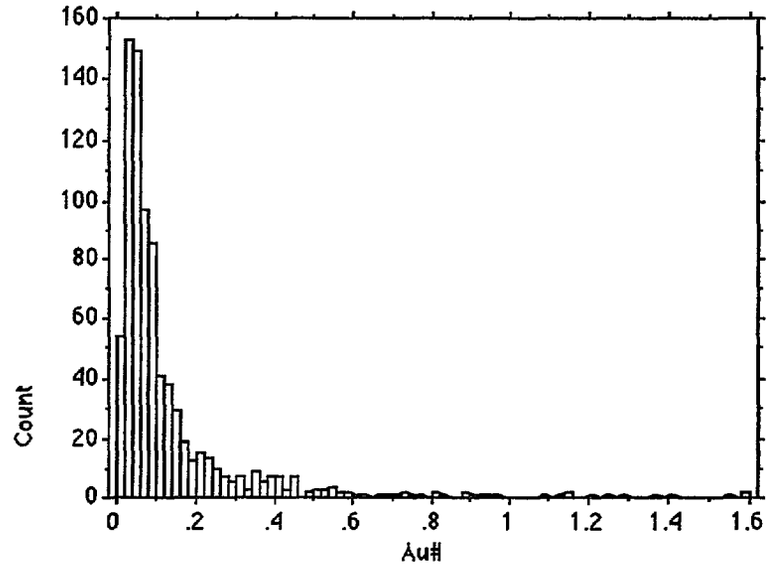

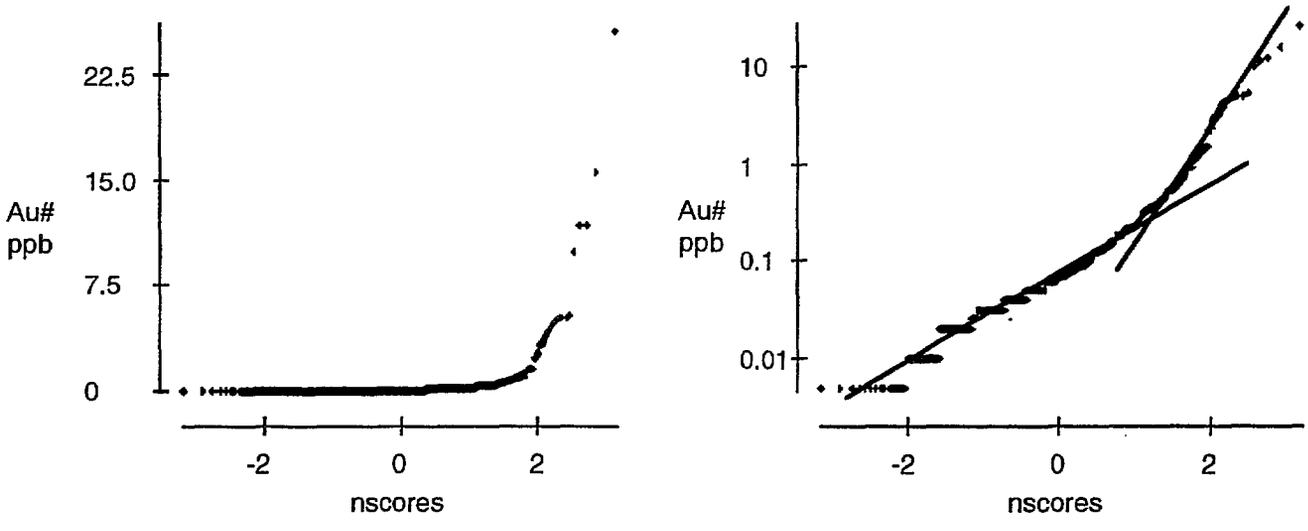

Au#

Barium

Mean:	Std. Dev.:	Std. Error:	Variance:	Coef. Var.:	Count:
485.55	250.364	8.623	62682.096	51.563	843
Minimum:	**Maximum:**	**Range:**	**Sum:**	**Sum of Sqr.:**	**# Missing:**
40	1911	1871	409319	251523335	0
# < 10th %:	**10th %:**	**25th %:**	**50th %:**	**75th %:**	**90th %:**
84	183.8	260.25	466	675.75	820.6
# > 90th %:	**Mode:**	**Geo. Mean:**	**Har. Mean:**	**Kurtosis:**	**Skewness:**
84	232	416.099	344.04	.679	.594

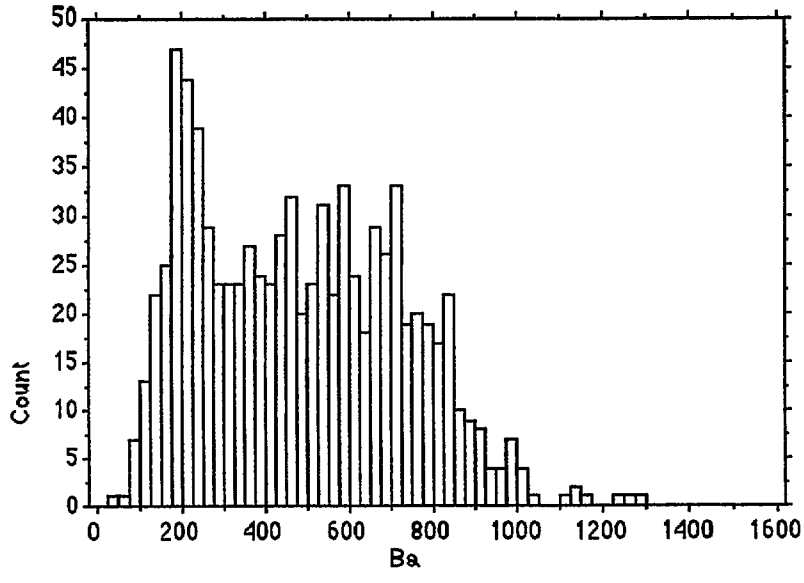

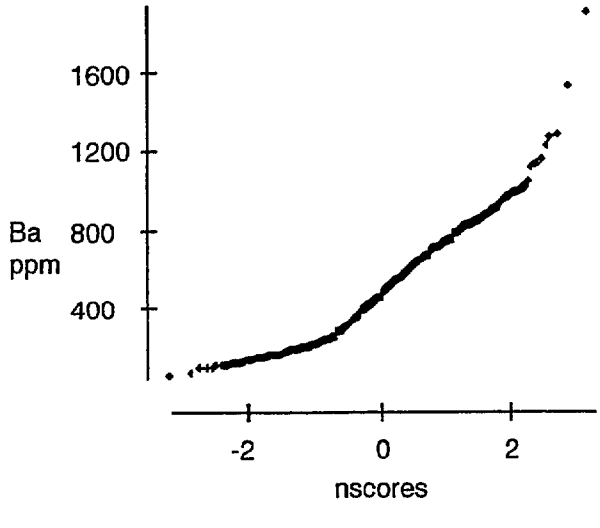

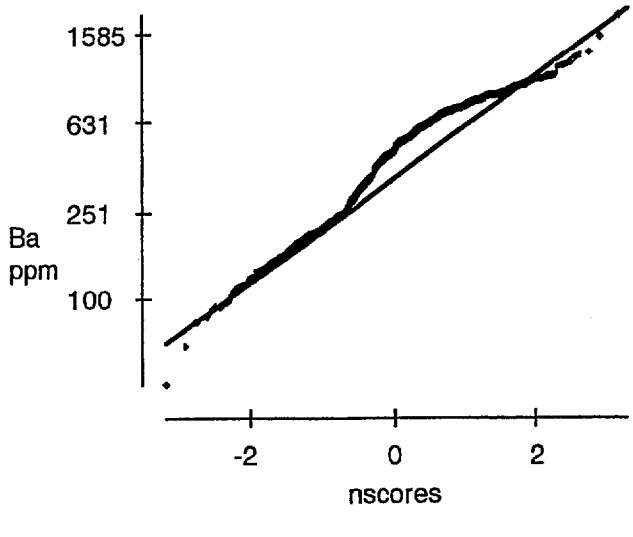

Ba

Beryllium

Mean:	Std. Dev.:	Std. Error:	Variance:	Coef. Var.:	Count:
1.804	1.391	.048	1.935	77.081	843
Minimum:	Maximum:	Range:	Sum:	Sum of Sqr.:	# Missing:
.17	15.8	15.63	1521.16	4373.814	0
# < 10th %:	10th %:	25th %:	50th %:	75th %:	90th %:
80	.65	.97	1.5	2.263	3.144
# > 90th %:	Mode:	Geo. Mean:	Har. Mean:	Kurtosis:	Skewness:
84	.8	1.477	1.221	27.89	3.985

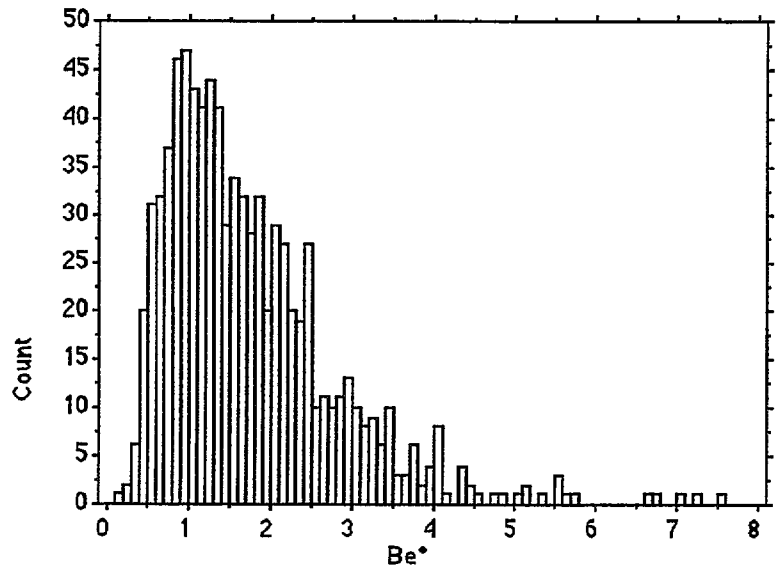

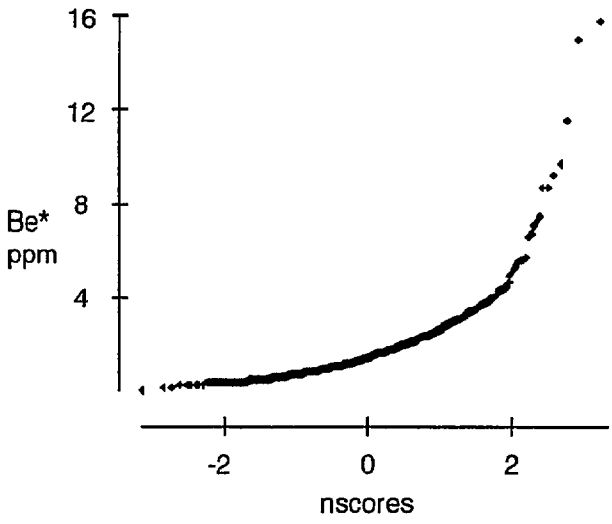

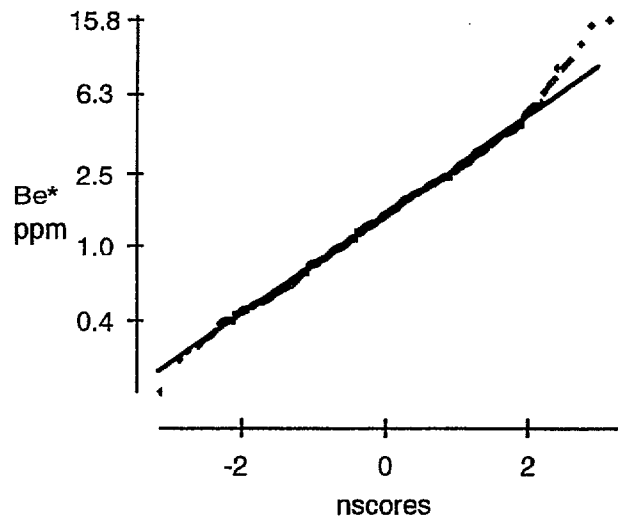

Be*

Bismuth

Mean:	Std. Dev.:	Std. Error:	Variance:	Coef. Var.:	Count:
.538	.852	.029	.727	158.364	843
Minimum:	Maximum:	Range:	Sum:	Sum of Sqr.:	# Missing:
.05	14.6	14.55	453.76	856.06	0
# < 10th %:	10th %:	25th %:	50th %:	75th %:	90th %:
76	.18	.24	.35	.567	1.026
# > 90th %:	Mode:	Geo. Mean:	Har. Mean:	Kurtosis:	Skewness:
84	.3	.386	.314	145.564	10.515

Detection limit is 0.10 ppm - a value of 0.05 ppm has been substituted in calculations and table.

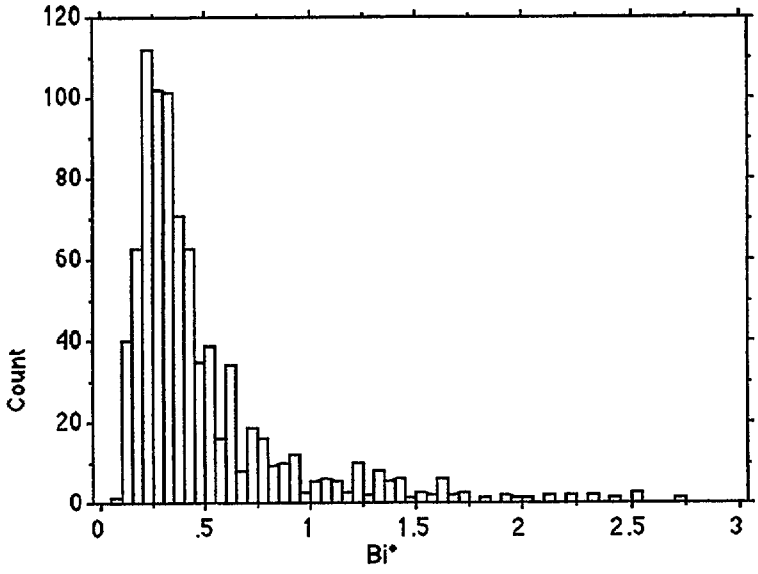

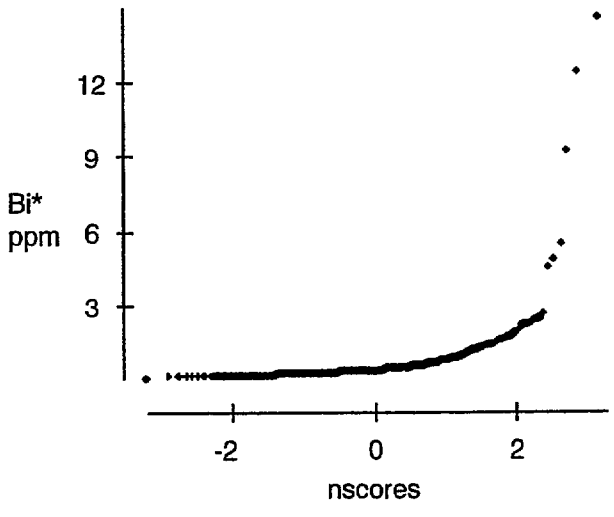

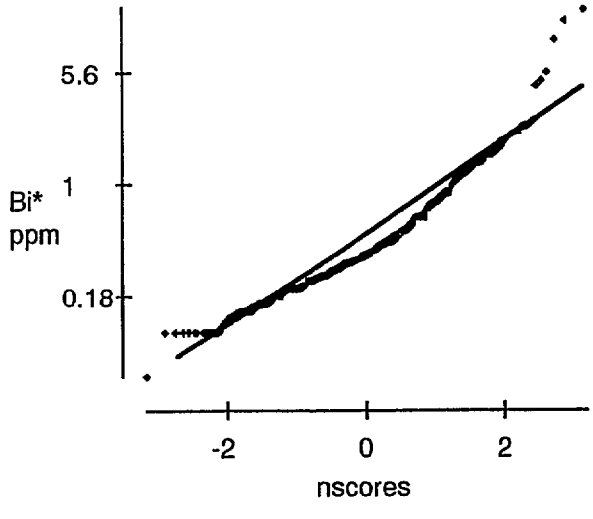

Bi*

Cadmium

Mean:	Std. Dev.:	Std. Error:	Variance:	Coef. Var.:	Count:
.118	.093	.003	.009	78.786	843
Minimum:	**Maximum:**	**Range:**	**Sum:**	**Sum of Sqr.:**	**# Missing:**
.05	.87	.82	99.89	19.175	0
# < 10th %:	**10th %:**	**25th %:**	**50th %:**	**75th %:**	**90th %:**
0	.05	.05	.1	.16	.23
# > 90th %:	**Mode:**	**Geo. Mean:**	**Har. Mean:**	**Kurtosis:**	**Skewness:**
81	.05	.094	.078	9.129	2.385

Detection limit is 0.10 ppm - a value of 0.05 ppm has been substituted in calculations and table.

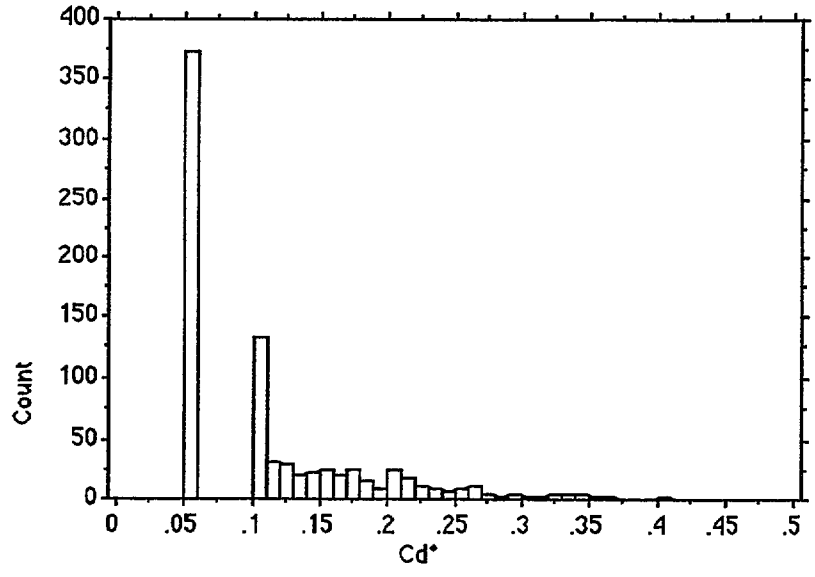

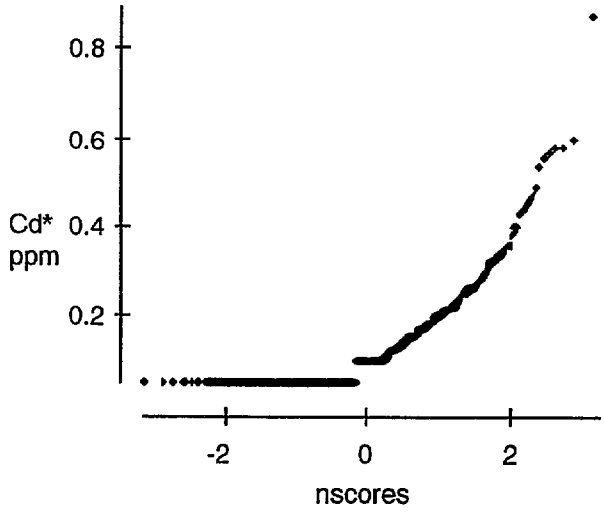

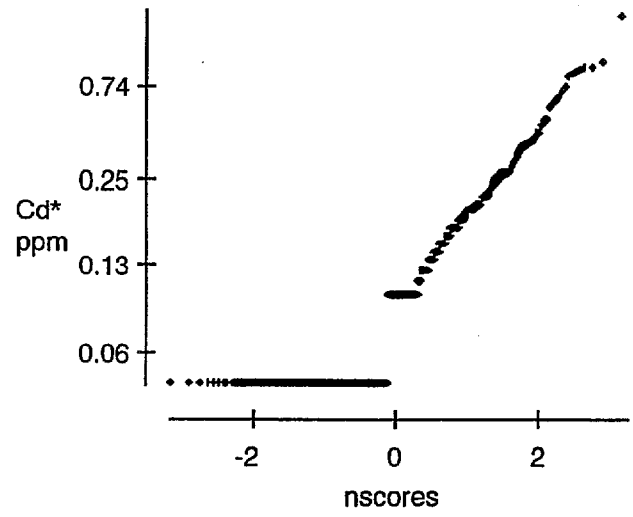

Cd*

Cerium

Mean:	Std. Dev.:	Std. Error:	Variance:	Coef. Var.:	Count:
118.944	159.694	5.5	25502.107	134.259	843
Minimum:	**Maximum:**	**Range:**	**Sum:**	**Sum of Sqr.:**	**# Missing:**
14	2571	2557	100270	33399314	0
# < 10th %:	**10th %:**	**25th %:**	**50th %:**	**75th %:**	**90th %:**
84	34.8	51	77	133	222.4
# > 90th %:	**Mode:**	**Geo. Mean:**	**Har. Mean:**	**Kurtosis:**	**Skewness:**
84	39	84.706	66.622	106.509	8.349

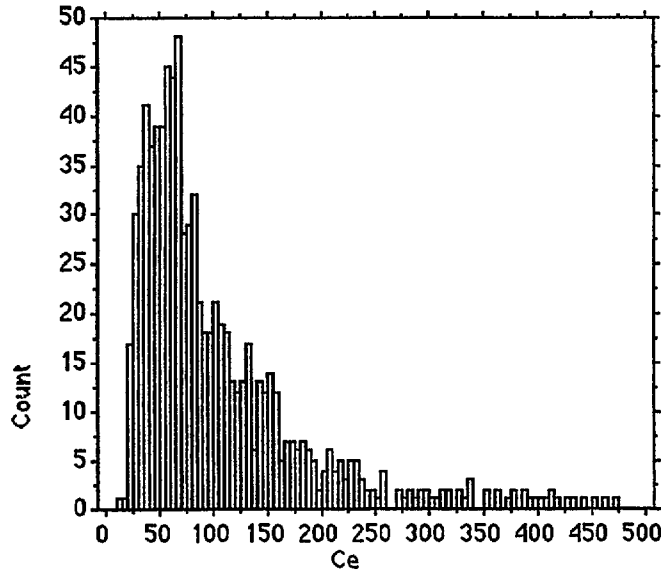

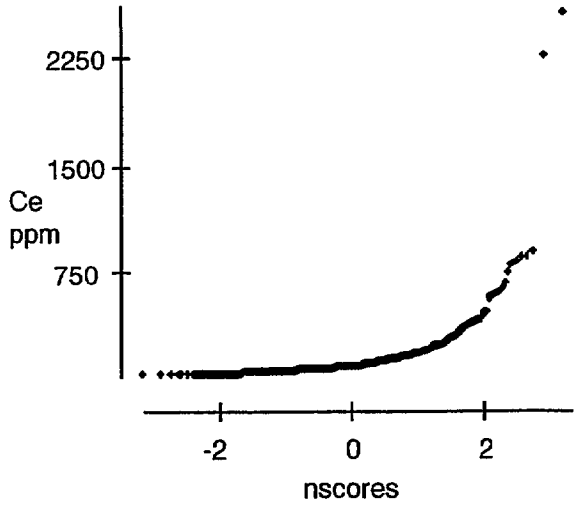

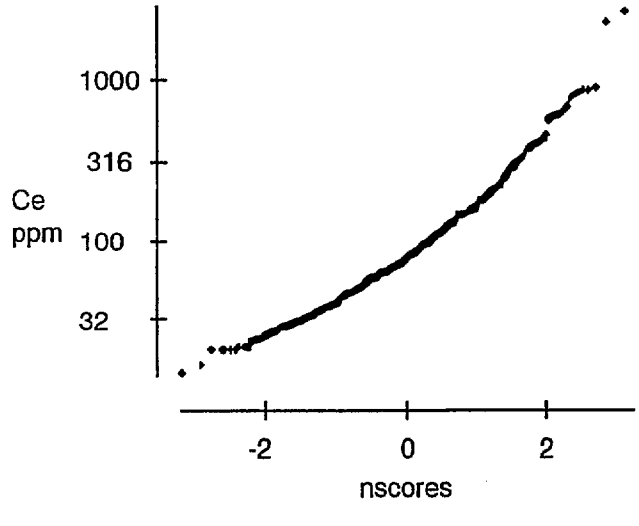

Ce

Chromium

Mean:	Std. Dev.:	Std. Error:	Variance:	Coef. Var.:	Count:
57.441	40.36	1.39	1628.94	70.263	843
Minimum:	**Maximum:**	**Range:**	**Sum:**	**Sum of Sqr.:**	**# Missing:**
3	319	316	48423	4153047	0
# < 10th %:	**10th %:**	**25th %:**	**50th %:**	**75th %:**	**90th %:**
81	16	33	50	70	99
# > 90th %:	**Mode:**	**Geo. Mean:**	**Har. Mean:**	**Kurtosis:**	**Skewness:**
82	43	45.734	33.724	7.621	2.194

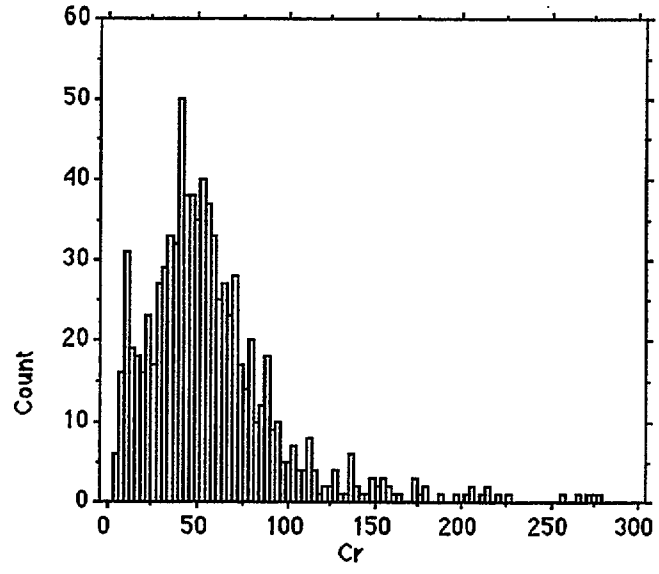

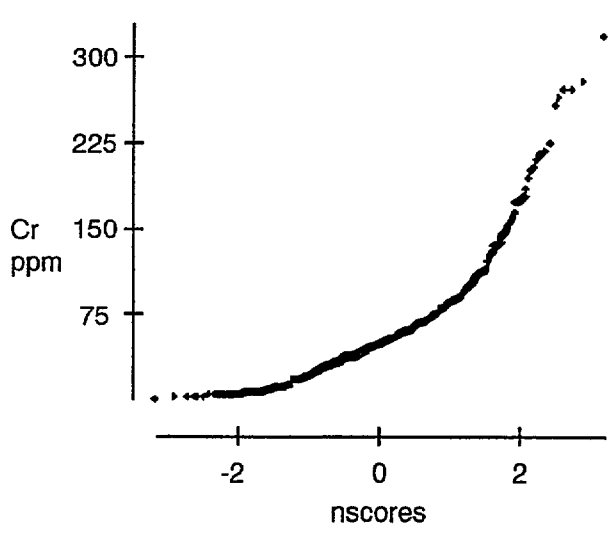

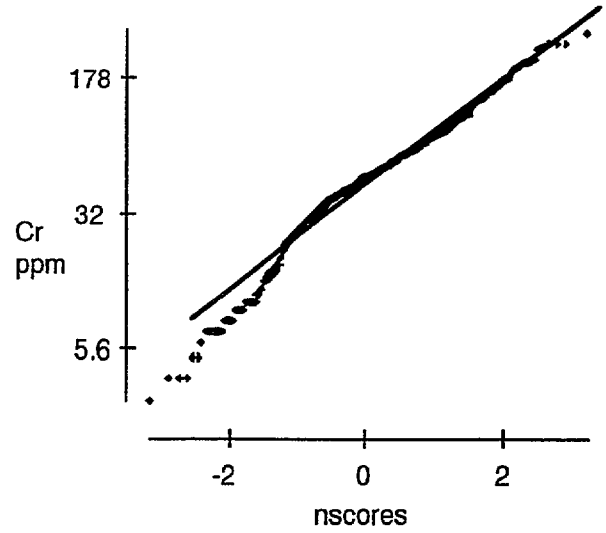

Cr

Copper

Mean:	Std. Dev.:	Std. Error:	Variance:	Coef. Var.:	Count:
9.887	7.86	.271	61.773	79.496	843
Minimum:	**Maximum:**	**Range:**	**Sum:**	**Sum of Sqr.:**	**# Missing:**
.5	53	52.5	8334.5	134413.75	0
# < 10th %:	**10th %:**	**25th %:**	**50th %:**	**75th %:**	**90th %:**
23	2	4	8	13	21
# > 90th %:	**Mode:**	**Geo. Mean:**	**Har. Mean:**	**Kurtosis:**	**Skewness:**
80	5	7.292	5.109	3.709	1.658

Detection limit is 1 ppm - a value of 0.5 ppm has been substituted in calculations and table.

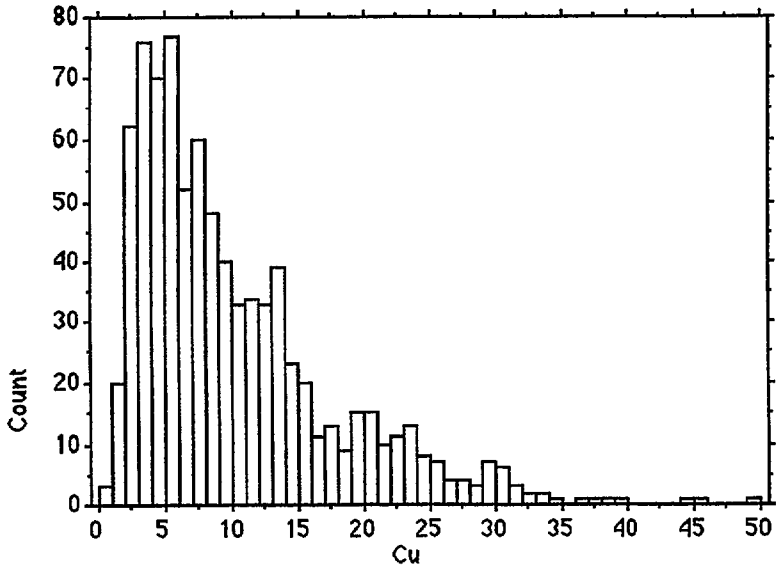

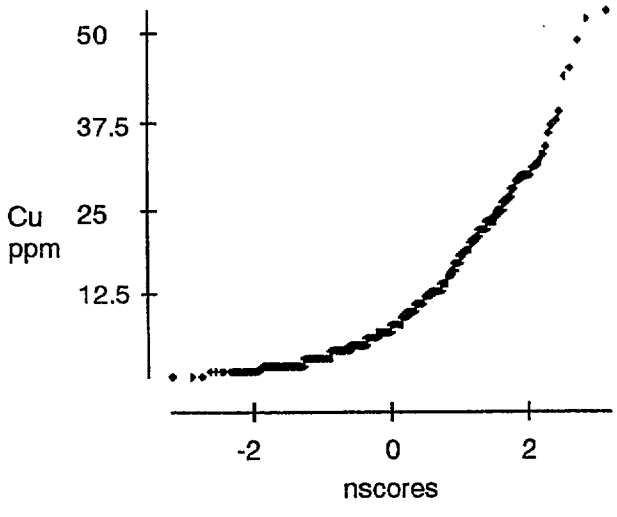

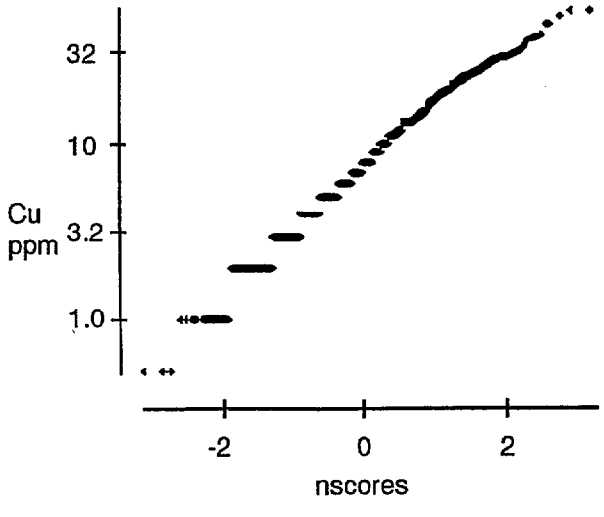

Cu

Iron

Mean:	Std. Dev.:	Std. Error:	Variance:	Coef. Var.:	Count:
22259.786	13748.682	473.53	1.89E8	61.765	843
Minimum:	**Maximum:**	**Range:**	**Sum:**	**Sum of Sqr.:**	**# Missing:**
5000	147000	142000	18765000	5.769E11	0
# < 10th %:	**10th %:**	**25th %:**	**50th %:**	**75th %:**	**90th %:**
80	10000	13000	18000	28000	40000
# > 90th %:	**Mode:**	**Geo. Mean:**	**Har. Mean:**	**Kurtosis:**	**Skewness:**
77	•	19086.604	16531.389	11.275	2.352

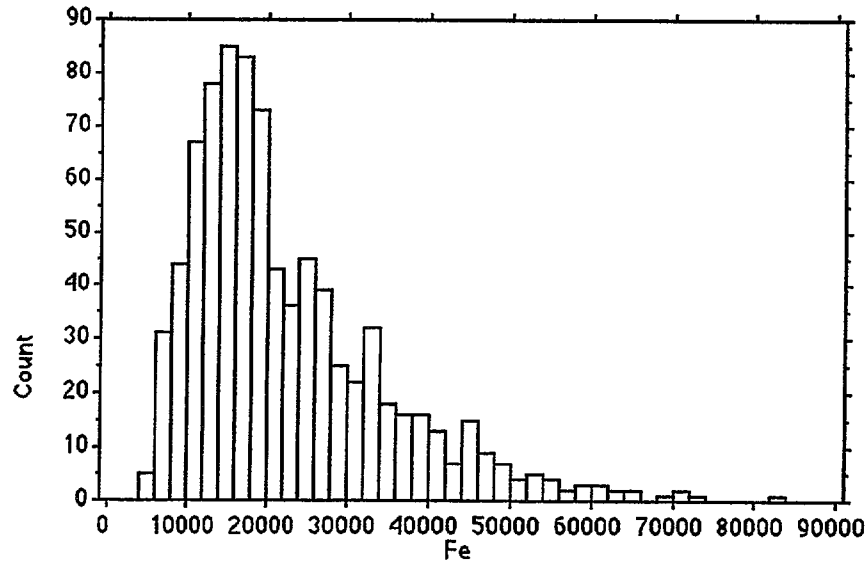

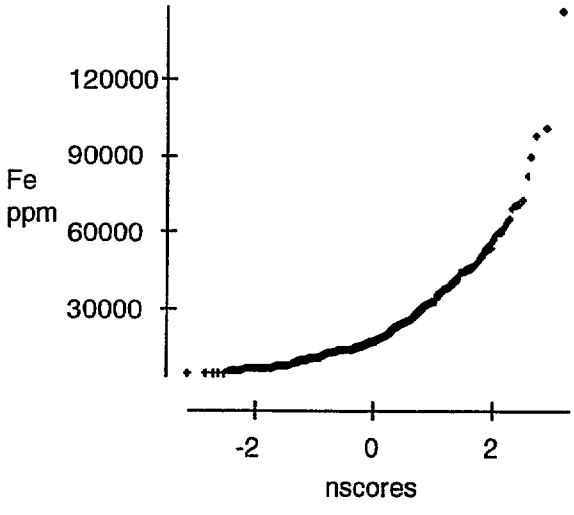

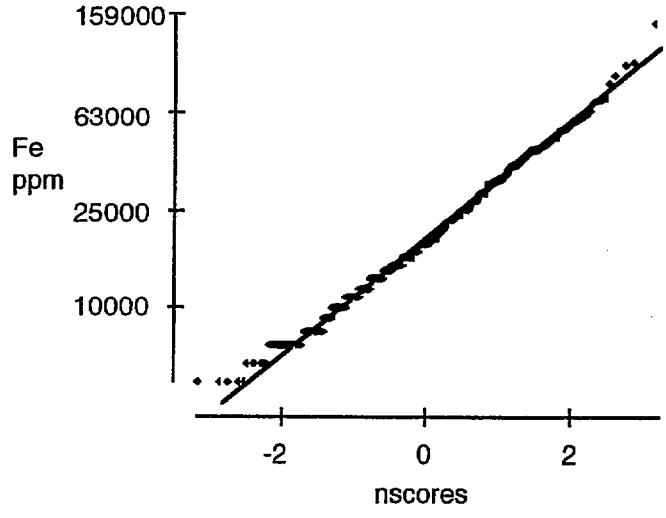

Fe

Gallium

Mean:	Std. Dev.:	Std. Error:	Variance:	Coef. Var.:	Count:
10.047	5.117	.176	26.184	50.929	843
Minimum:	**Maximum:**	**Range:**	**Sum:**	**Sum of Sqr.:**	**# Missing:**
.5	28	27.5	8470	107149	0
# < 10th %:	**10th %:**	**25th %:**	**50th %:**	**75th %:**	**90th %:**
45	3	6	10	13.75	17
# > 90th %:	**Mode:**	**Geo. Mean:**	**Har. Mean:**	**Kurtosis:**	**Skewness:**
62	9	8.408	5.964	-.19	.373

Detection limit is 1 ppm - a value of 0.5 ppm has been substituted in calculations and table.

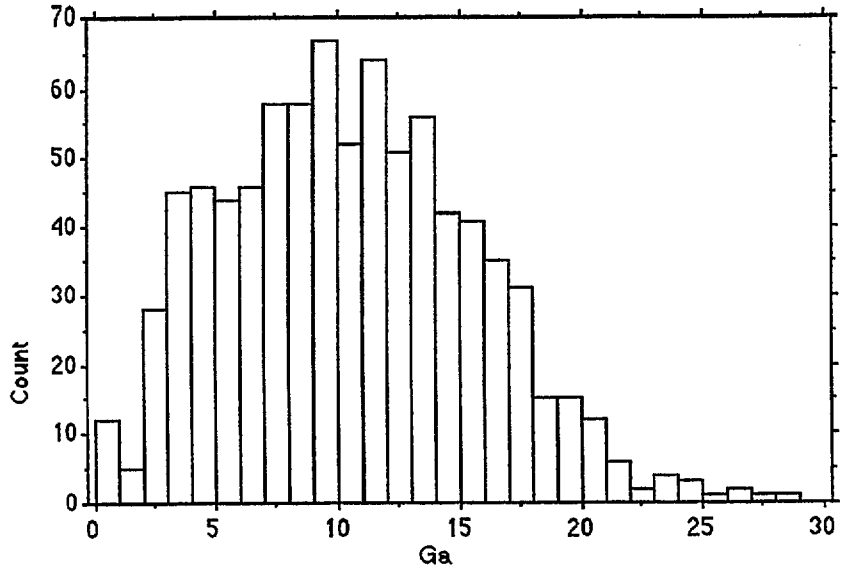

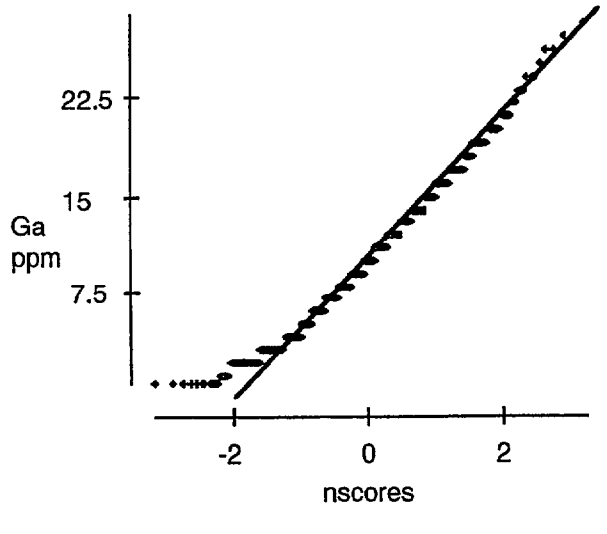

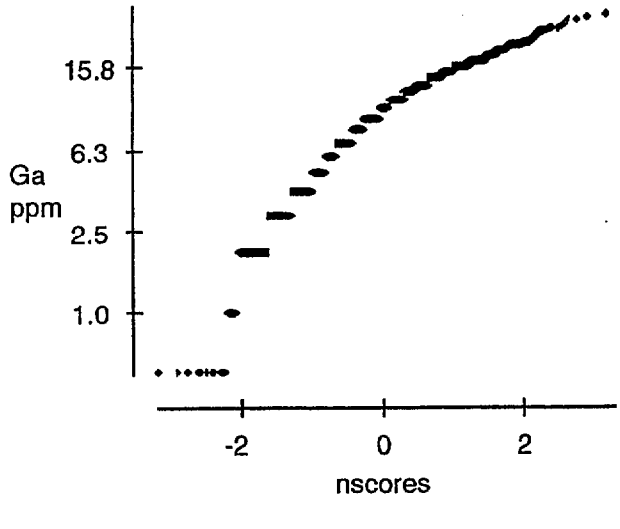

Ga

Germanium

Mean:	Std. Dev.:	Std. Error:	Variance:	Coef. Var.:	Count:
2.552	.731	.025	.535	28.667	843
Minimum:	Maximum:	Range:	Sum:	Sum of Sqr.:	# Missing:
1	5.5	4.5	2151	5939	0
# < 10th %:	10th %:	25th %:	50th %:	75th %:	90th %:
14	1.5	2	2.5	3	3.5
# > 90th %:	Mode:	Geo. Mean:	Har. Mean:	Kurtosis:	Skewness:
40	2.5	2.444	2.331	.272	.386

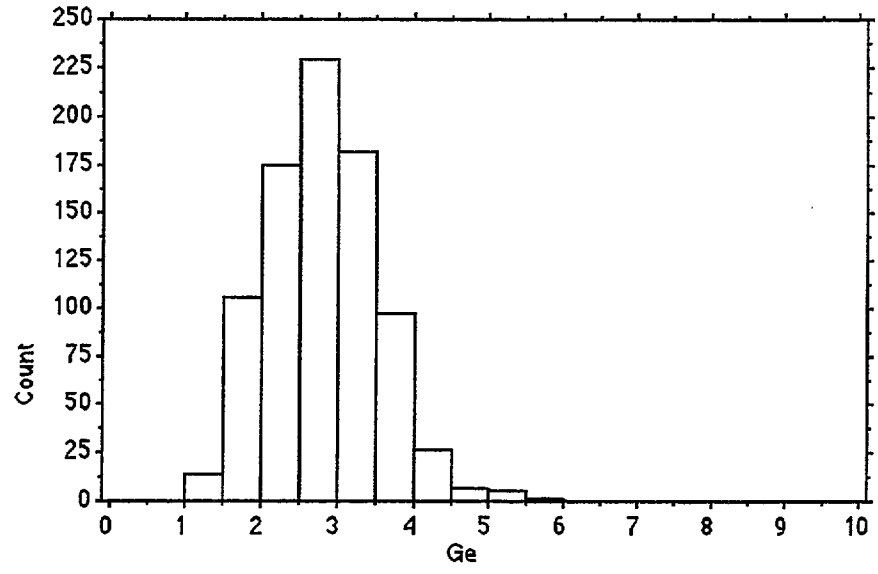

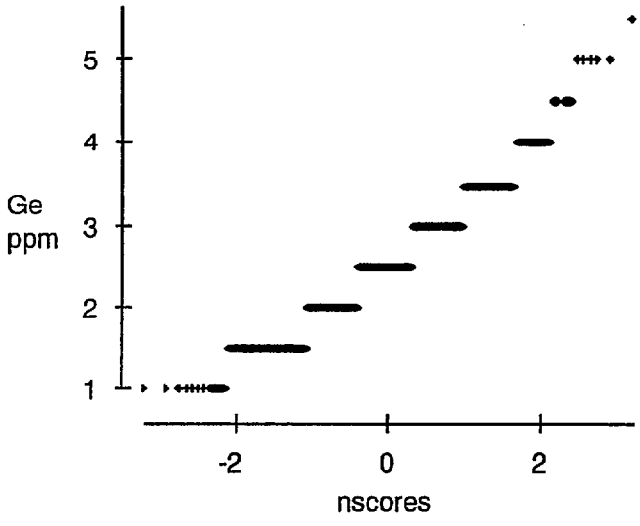

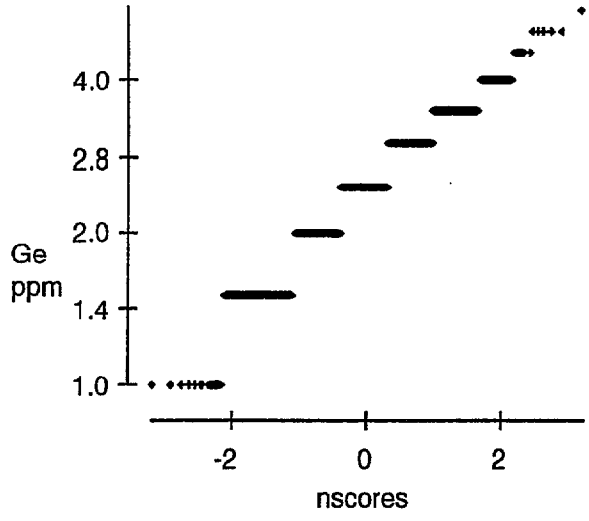

Ge

Hafnium

Mean:	Std. Dev.:	Std. Error:	Variance:	Coef. Var.:	Count:
17.305	12.77	.44	163.065	73.792	843
Minimum:	**Maximum:**	**Range:**	**Sum:**	**Sum of Sqr.:**	**# Missing:**
2	135	133	14588	389744	0
# < 10th %:	**10th %:**	**25th %:**	**50th %:**	**75th %:**	**90th %:**
51	7	10	14	20	30
# > 90th %:	**Mode:**	**Geo. Mean:**	**Har. Mean:**	**Kurtosis:**	**Skewness:**
75	10	14.535	12.563	19.048	3.472

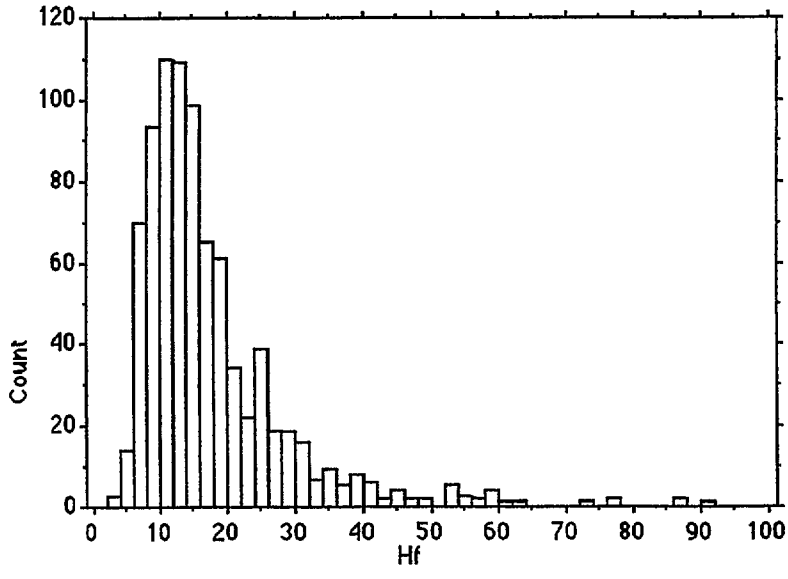

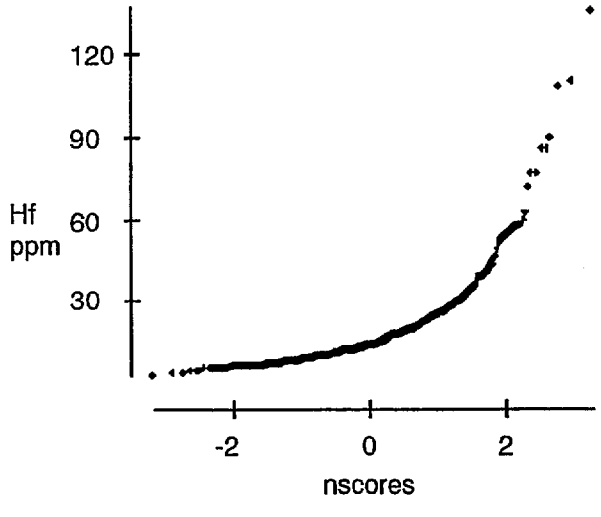

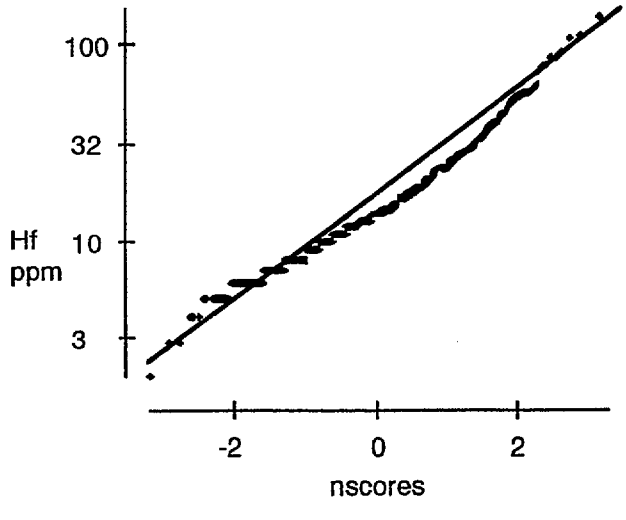

Hf

Lanthanum

Mean:	Std. Dev.:	Std. Error:	Variance:	Coef. Var.:	Count:
59.084	83.38	2.872	6952.298	141.121	843
Minimum:	**Maximum:**	**Range:**	**Sum:**	**Sum of Sqr.:**	**# Missing:**
5	1325	1320	49808	8796702	0
# < 10th %:	**10th %:**	**25th %:**	**50th %:**	**75th %:**	**90th %:**
76	16	24	37	67	112
# > 90th %:	**Mode:**	**Geo. Mean:**	**Har. Mean:**	**Kurtosis:**	**Skewness:**
81	25	40.891	31.396	108.019	8.446

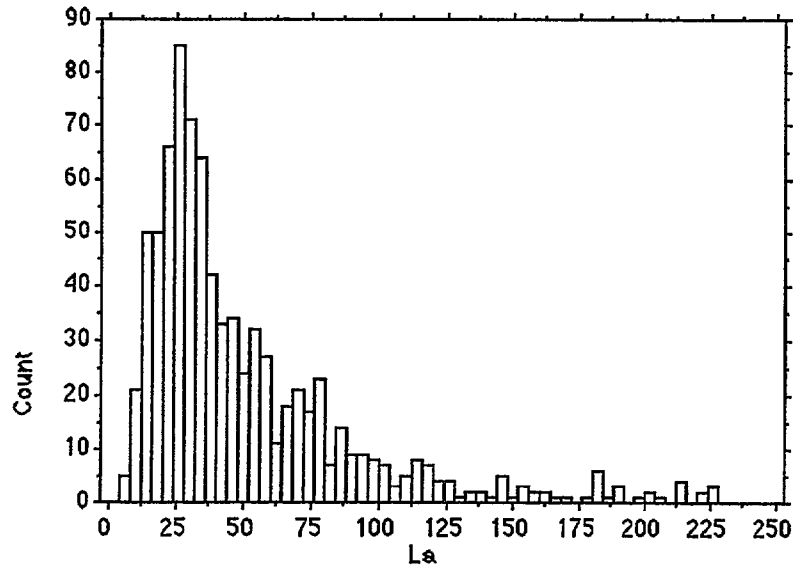

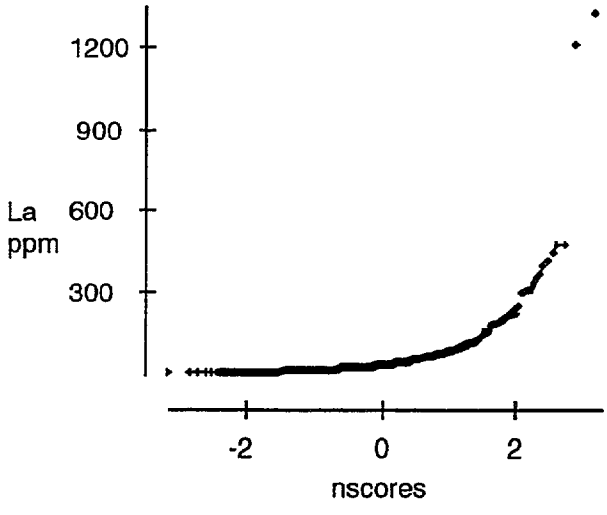

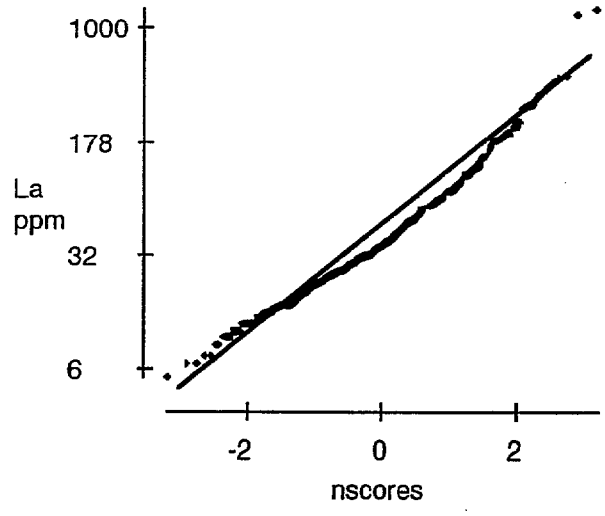

La

Manganese

Mean:	Std. Dev.:	Std. Error:	Variance:	Coef. Var.:	Count:
440.554	425.288	14.648	180869.592	96.535	843
Minimum:	**Maximum:**	**Range:**	**Sum:**	**Sum of Sqr.:**	**# Missing:**
28	5343	5315	371387	315908215	0
# < 10th %:	**10th %:**	**25th %:**	**50th %:**	**75th %:**	**90th %:**
82	81	166	327	589.25	908.2
# > 90th %:	**Mode:**	**Geo. Mean:**	**Har. Mean:**	**Kurtosis:**	**Skewness:**
84	•	301.332	195.386	26.29	3.576

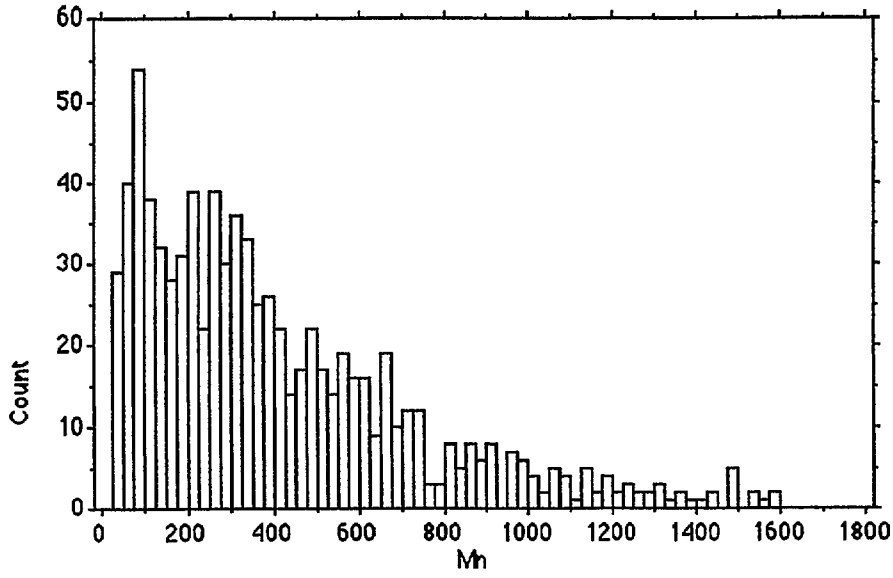

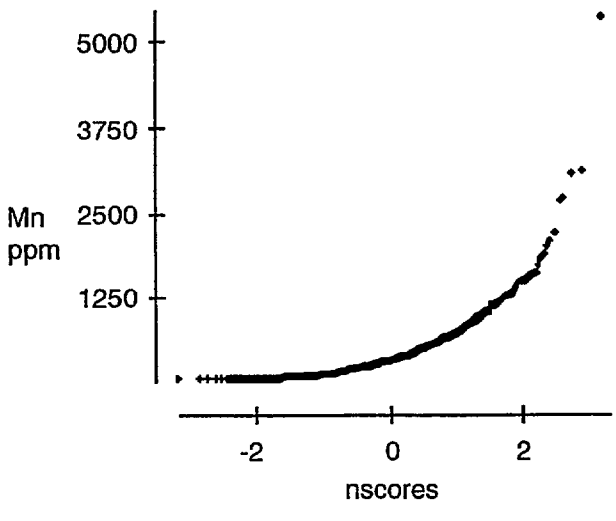

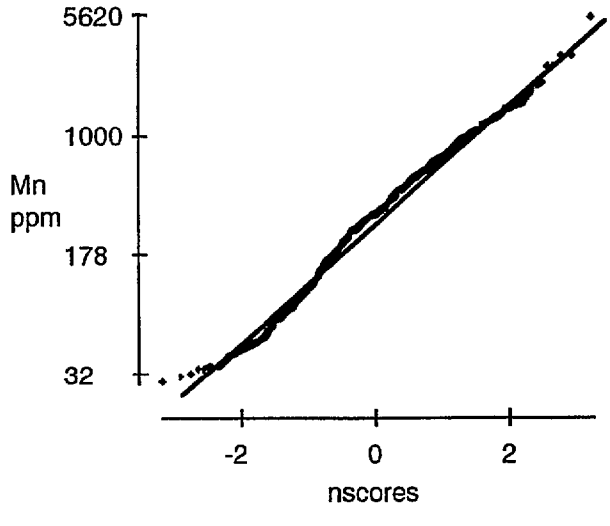

Mn

Molybdenum

Mean:	Std. Dev.:	Std. Error:	Variance:	Coef. Var.:	Count:
.764	.496	.017	.246	64.953	843
Minimum:	**Maximum:**	**Range:**	**Sum:**	**Sum of Sqr.:**	**# Missing:**
.05	5.91	5.86	643.88	699.03	0
# < 10th %:	**10th %:**	**25th %:**	**50th %:**	**75th %:**	**90th %:**
84	.208	.42	.7	1.05	1.35
# > 90th %:	**Mode:**	**Geo. Mean:**	**Har. Mean:**	**Kurtosis:**	**Skewness:**
80	.05	.591	.368	14.46	2.075

Detection limit is 0.10 ppm - a value of 0.05 ppm has been substituted in calculations and table.

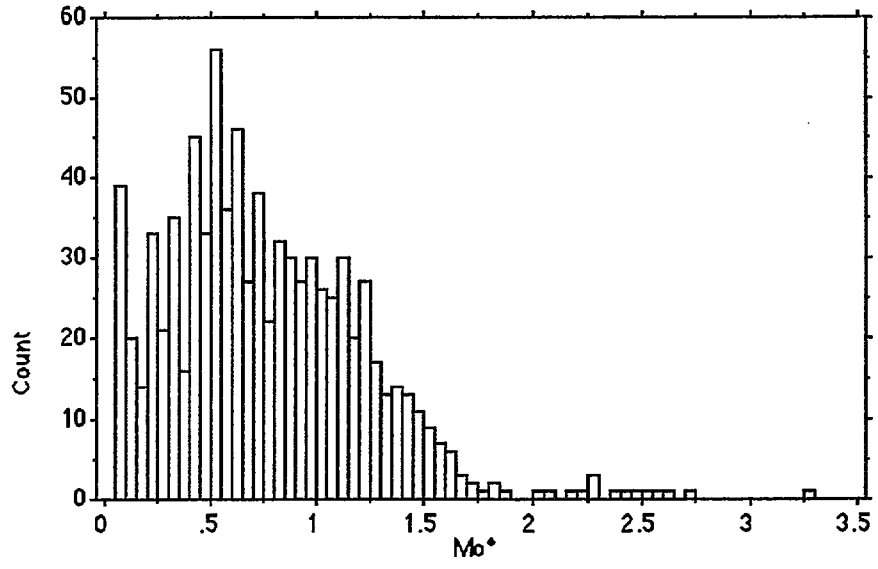

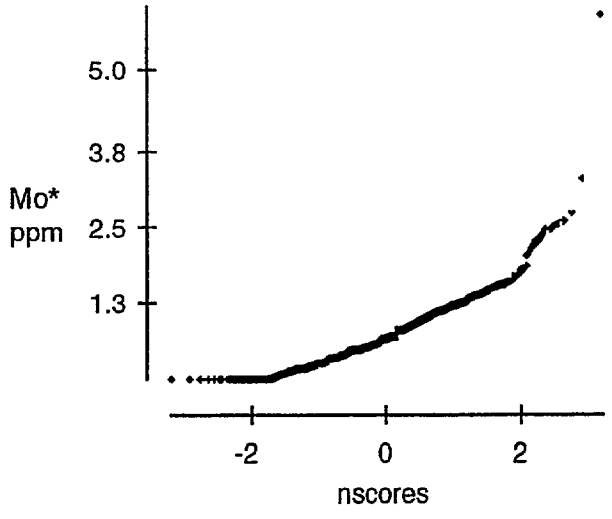

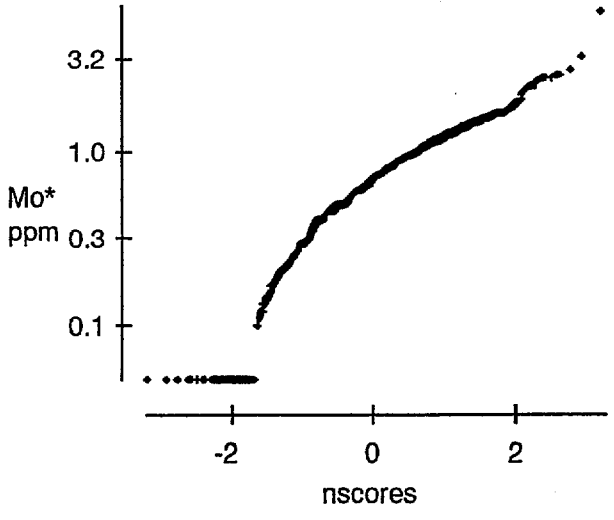

Mo*

Niobium

Mean:	Std. Dev.:	Std. Error:	Variance:	Coef. Var.:	Count:
20.039	12.312	.424	151.582	61.439	843
Minimum:	**Maximum:**	**Range:**	**Sum:**	**Sum of Sqr.:**	**# Missing:**
4	209	205	16893	466153	0
# < 10th %:	**10th %:**	**25th %:**	**50th %:**	**75th %:**	**90th %:**
79	11	13	18	23	31
# > 90th %:	**Mode:**	**Geo. Mean:**	**Har. Mean:**	**Kurtosis:**	**Skewness:**
76	•	17.878	16.165	71.327	5.924

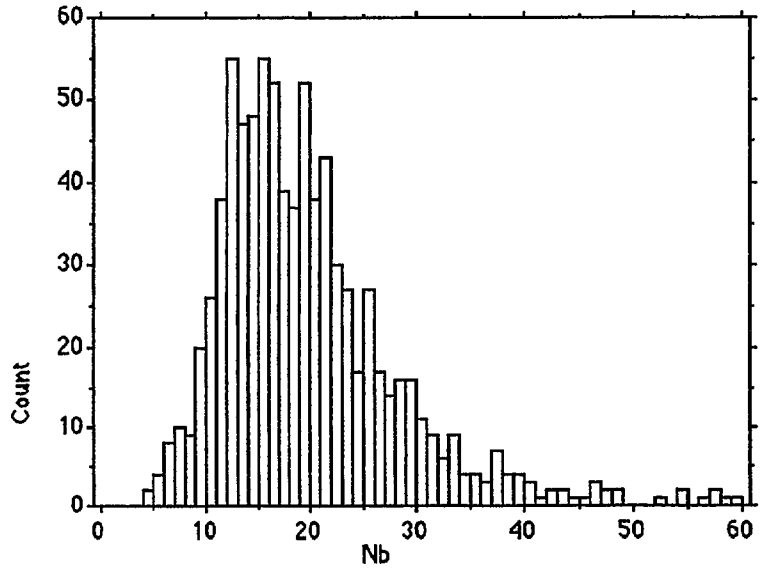

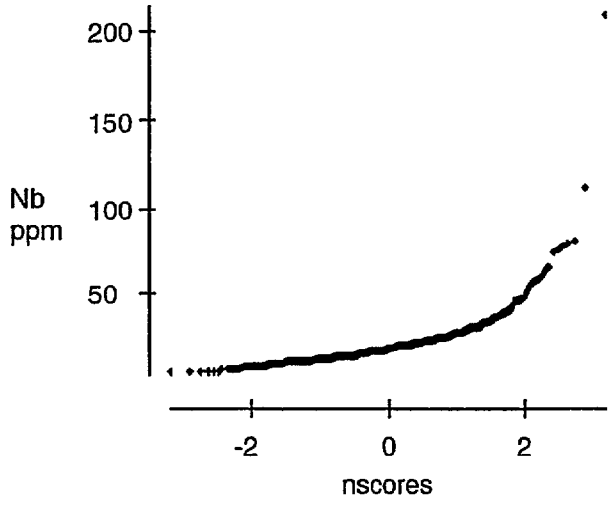

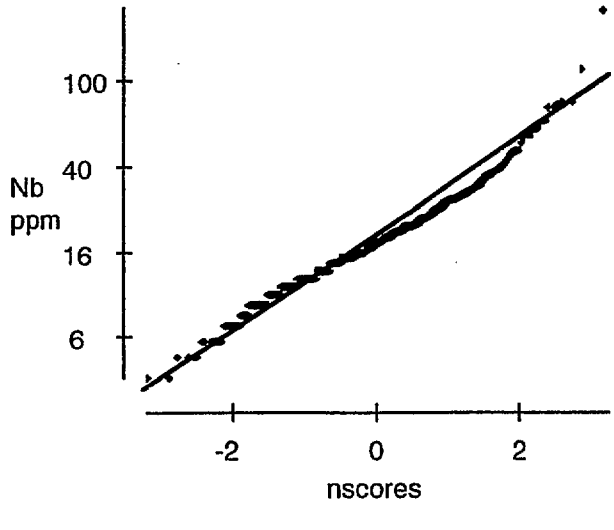

Nb

Neodymium

Mean:	Std. Dev.:	Std. Error:	Variance:	Coef. Var.:	Count:
49.336	70.761	2.437	5007.171	143.428	843
Minimum:	**Maximum:**	**Range:**	**Sum:**	**Sum of Sqr.:**	**# Missing:**
4	1125	1121	41590	6267910	0
# < 10th %:	**10th %:**	**25th %:**	**50th %:**	**75th %:**	**90th %:**
81	13	20	31	56	94.2
# > 90th %:	**Mode:**	**Geo. Mean:**	**Har. Mean:**	**Kurtosis:**	**Skewness:**
84	20	33.738	25.421	112.148	8.642

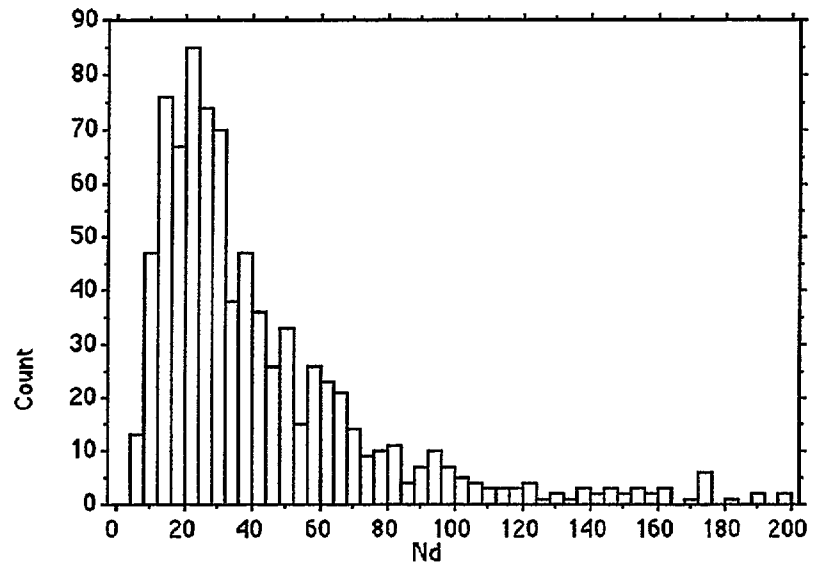

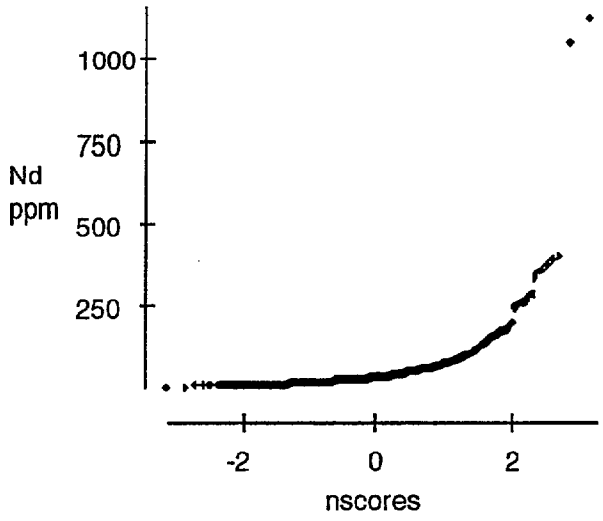

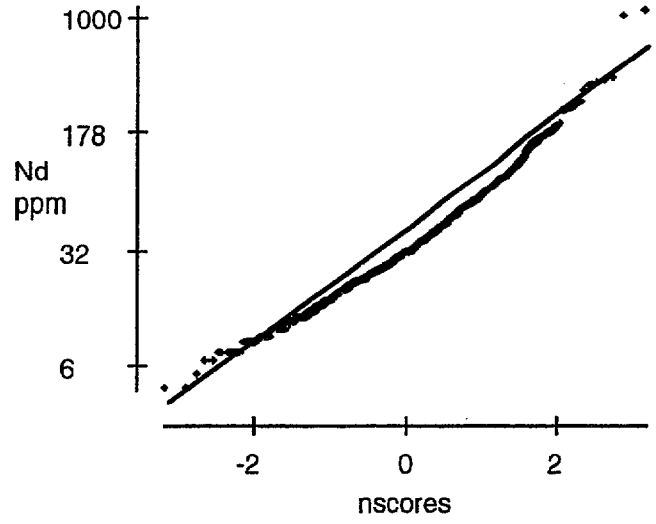

Nd

Nickel

Mean:	Std. Dev.:	Std. Error:	Variance:	Coef. Var.:	Count:
9.857	9.331	.321	87.068	94.664	843
Minimum:	**Maximum:**	**Range:**	**Sum:**	**Sum of Sqr.:**	**# Missing:**
.5	107	106.5	8309.5	155218.75	0
# < 10th %:	**10th %:**	**25th %:**	**50th %:**	**75th %:**	**90th %:**
35	2	3	7	14	21
# > 90th %:	**Mode:**	**Geo. Mean:**	**Har. Mean:**	**Kurtosis:**	**Skewness:**
75	3	6.739	4.334	19.182	3.06

Detection limit is 1 ppm - a value of 0.5 ppm has been substituted in calculations and table.

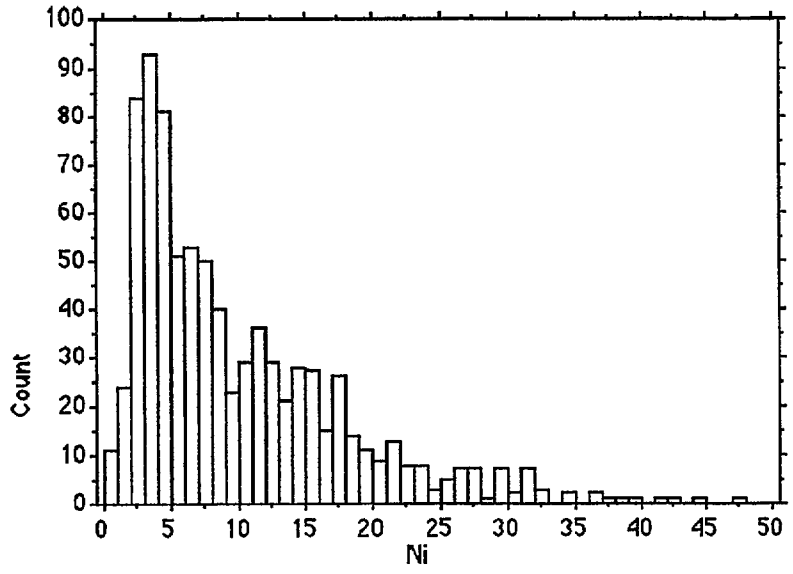

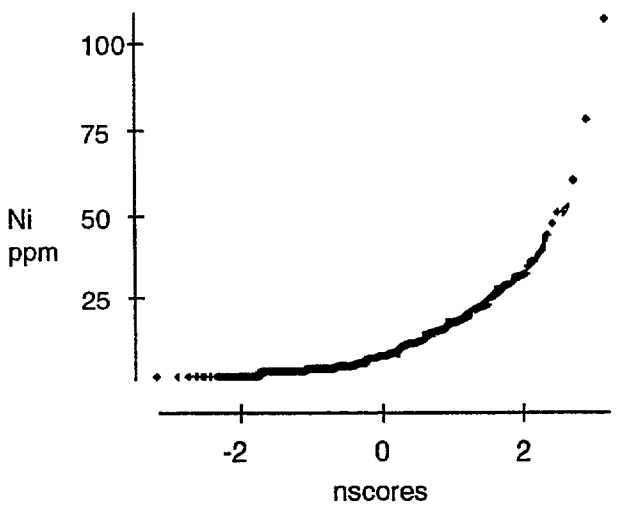

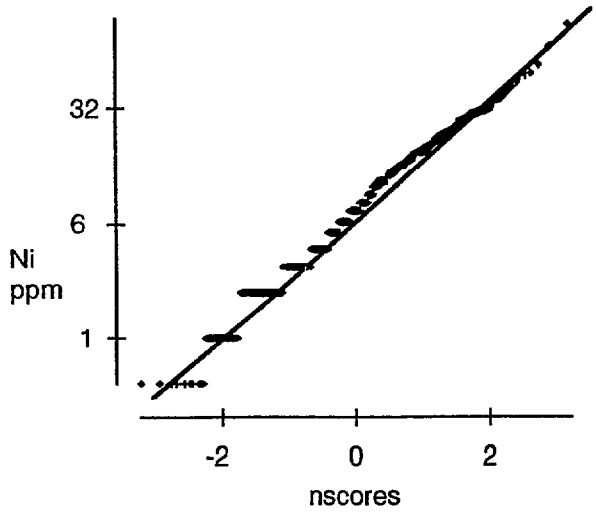

Ni

Phosphorus

Mean:	Std. Dev.:	Std. Error:	Variance:	Coef. Var.:	Count:
297.841	282.279	9.722	79681.215	94.775	843
Minimum:	**Maximum:**	**Range:**	**Sum:**	**Sum of Sqr.:**	**# Missing:**
10	3902	3892	251080	141873512	0
# < 10th %:	**10th %:**	**25th %:**	**50th %:**	**75th %:**	**90th %:**
83	96	134	213	370.5	591.2
# > 90th %:	**Mode:**	**Geo. Mean:**	**Har. Mean:**	**Kurtosis:**	**Skewness:**
84	97	223.95	171.753	38.362	4.435

Detection limit is 20 ppm - a value of 10 ppm has been substituted in calculations and table.

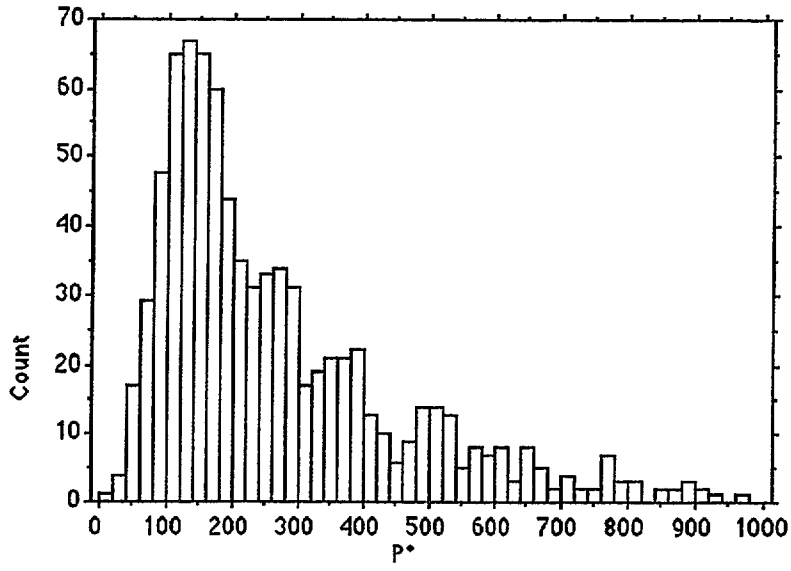

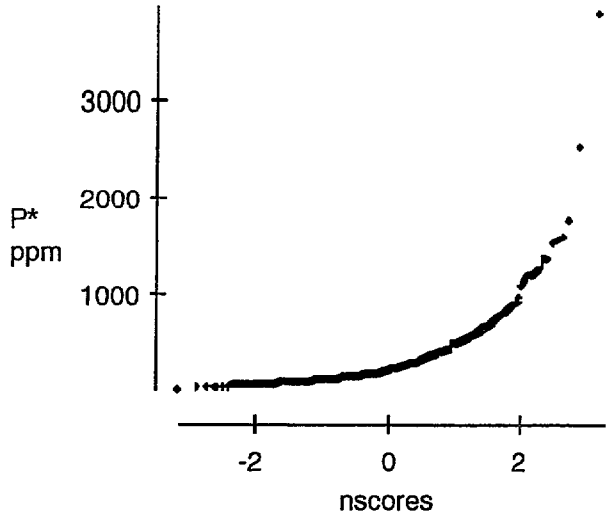

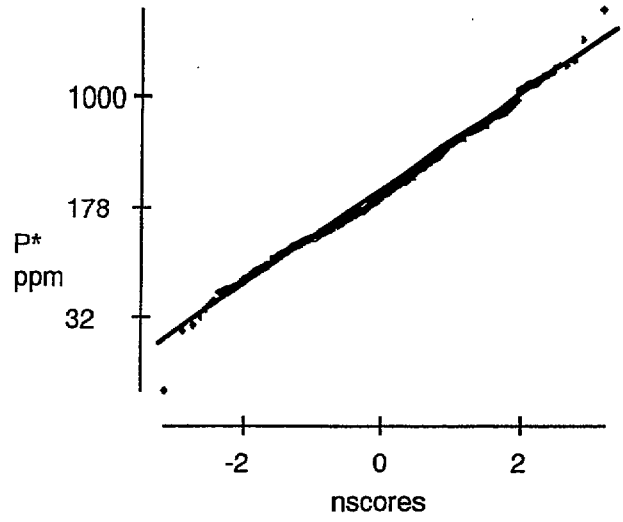

P*

Lead

Mean:	Std. Dev.:	Std. Error:	Variance:	Coef. Var.:	Count:
27.547	15.248	.525	232.488	55.351	843
Minimum:	**Maximum:**	**Range:**	**Sum:**	**Sum of Sqr.:**	**# Missing:**
6	179	173	23222	835448	0
# < 10th %:	**10th %:**	**25th %:**	**50th %:**	**75th %:**	**90th %:**
75	14	18	25	33	42.2
# > 90th %:	**Mode:**	**Geo. Mean:**	**Har. Mean:**	**Kurtosis:**	**Skewness:**
84	•	24.754	22.419	30.817	4.069

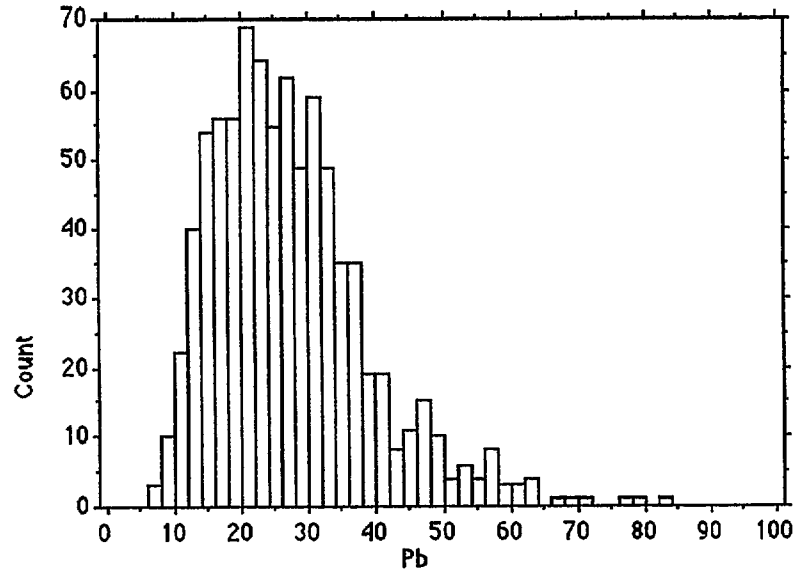

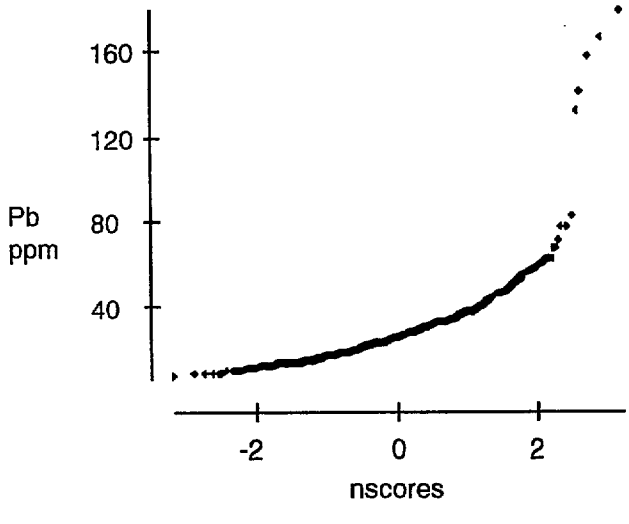

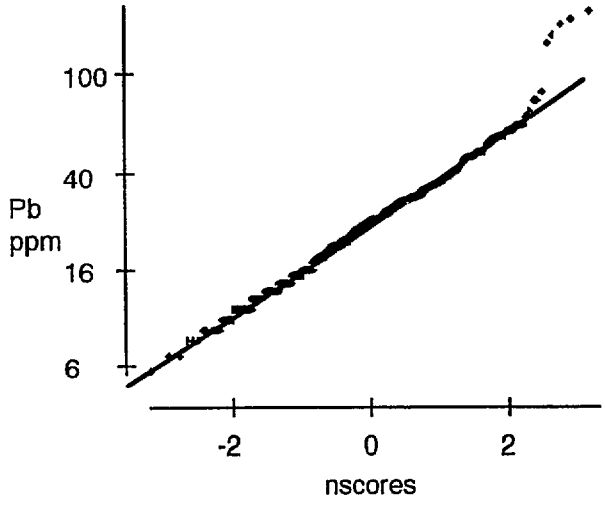

Pb

Palladium

Mean:	Std. Dev.:	Std. Error:	Variance:	Coef. Var.:	Count:
.096	.106	.004	.011	109.981	840
Minimum:	**Maximum:**	**Range:**	**Sum:**	**Sum of Sqr.:**	**# Missing:**
.005	1.19	1.185	81.02	17.256	0
# < 10th %:	**10th %:**	**25th %:**	**50th %:**	**75th %:**	**90th %:**
71	.02	.03	.06	.12	.22
# > 90th %:	**Mode:**	**Geo. Mean:**	**Har. Mean:**	**Kurtosis:**	**Skewness:**
83	.04	.061	.036	21.482	3.509

Detection limit is 0.01 ppb - a value of 0.005 ppb has been substituted in calculations and table.

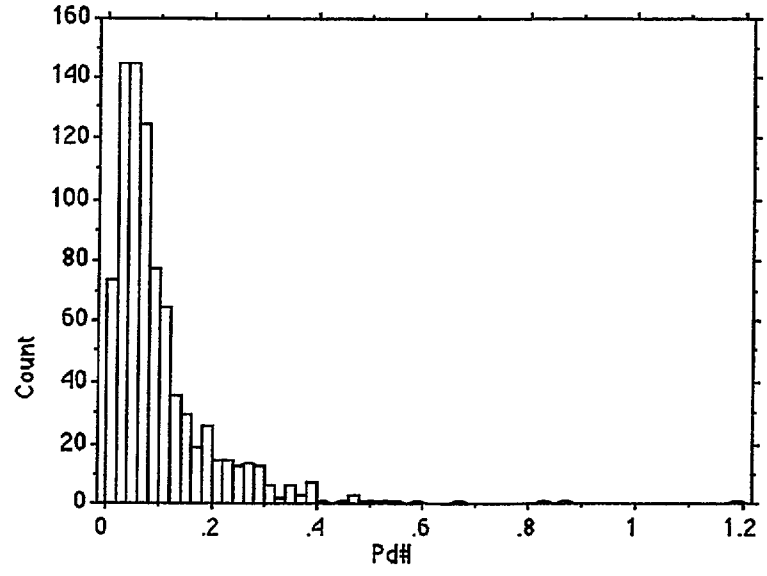

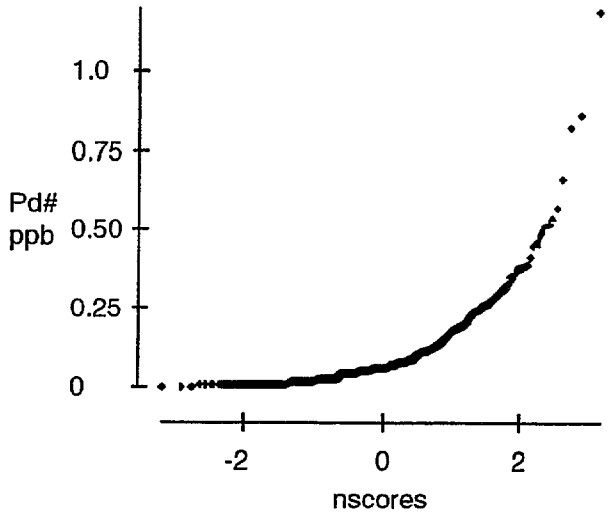

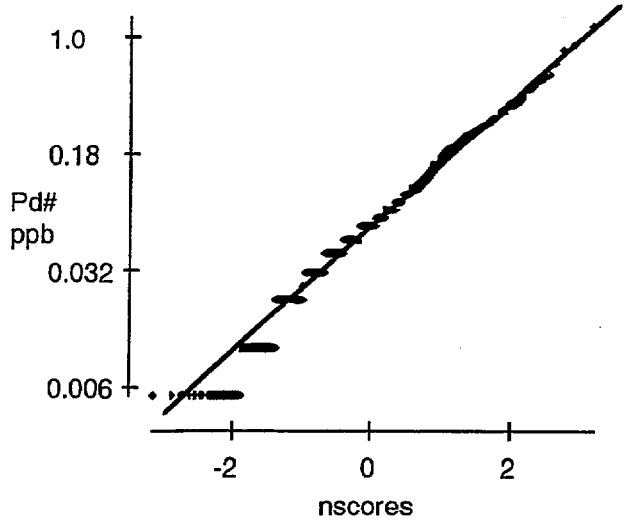

Pd#

Platinum

Mean:	Std. Dev.:	Std. Error:	Variance:	Coef. Var.:	Count:
.038	.03	.001	.001	78.62	840
Minimum:	Maximum:	Range:	Sum:	Sum of Sqr.:	# Missing:
.005	.38	.375	31.975	1.969	0
# < 10th %:	10th %:	25th %:	50th %:	75th %:	90th %:
0	.005	.01	.04	.05	.07
# > 90th %:	Mode:	Geo. Mean:	Har. Mean:	Kurtosis:	Skewness:
73	.05	.027	.016	20.859	2.593

Detection limit is 0.01 ppb - a value of 0.005 ppb has been substituted in calculations and table.

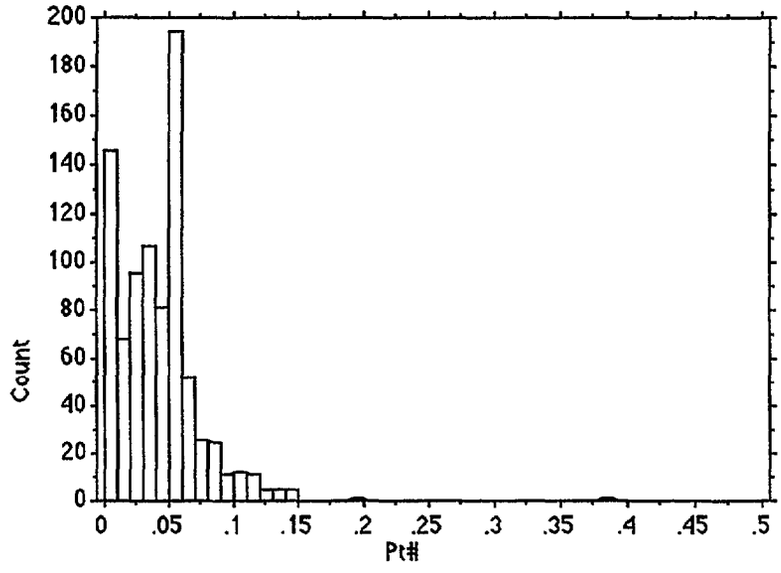

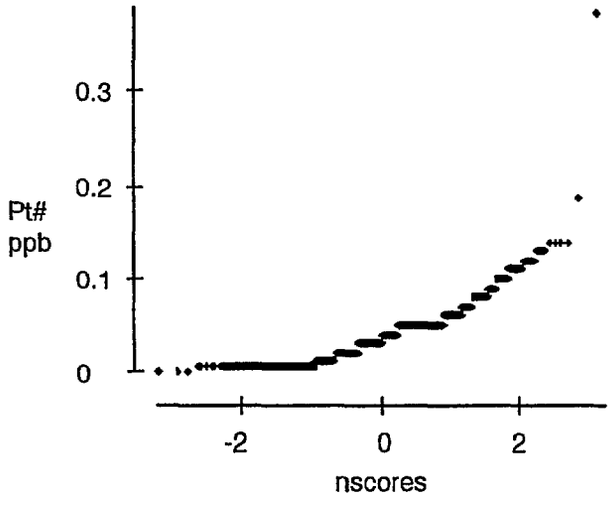

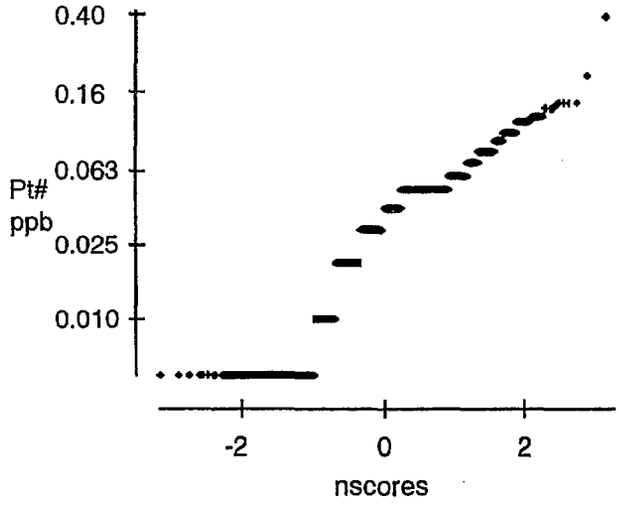

Pt#

Rubidium

Mean:	Std. Dev.:	Std. Error:	Variance:	Coef. Var.:	Count:
90.026	88.164	3.037	7772.866	97.931	843
Minimum:	**Maximum:**	**Range:**	**Sum:**	**Sum of Sqr.:**	**# Missing:**
4	616	612	75892	13377014	0
# < 10th %:	**10th %:**	**25th %:**	**50th %:**	**75th %:**	**90th %:**
81	15	30	66	117.75	178
# > 90th %:	**Mode:**	**Geo. Mean:**	**Har. Mean:**	**Kurtosis:**	**Skewness:**
83	18	59.267	36.527	8.227	2.452

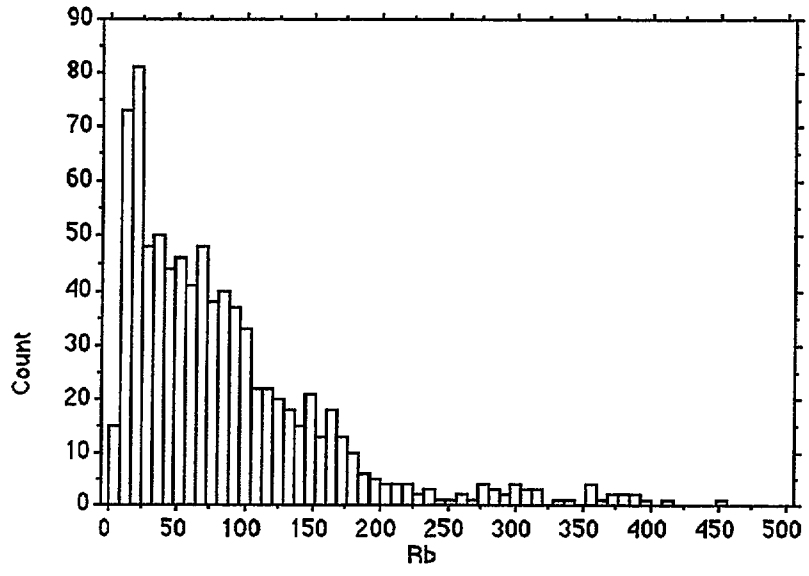

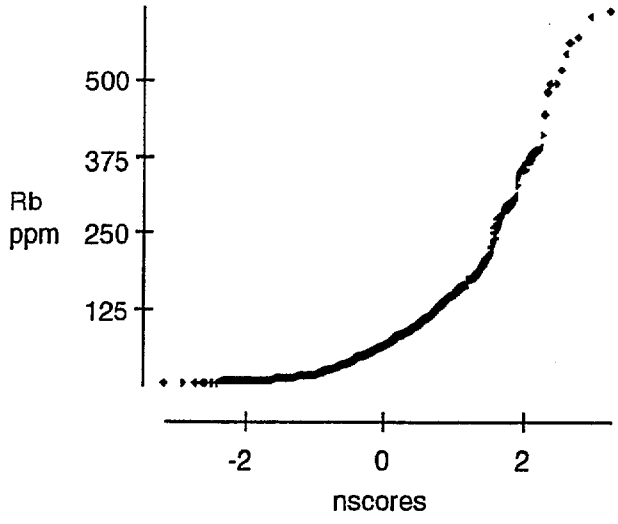

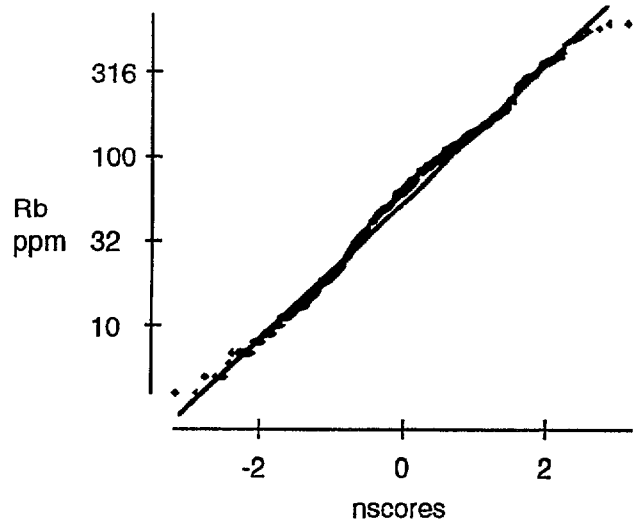

Rb

Antimony

Mean:	Std. Dev.:	Std. Error:	Variance:	Coef. Var.:	Count:
1.087	10.771	.371	116.014	990.782	843
Minimum:	**Maximum:**	**Range:**	**Sum:**	**Sum of Sqr.:**	**# Missing:**
.025	298	297.975	916.44	98679.705	0
# < 10th %:	**10th %:**	**25th %:**	**50th %:**	**75th %:**	**90th %:**
79	.23	.33	.45	.66	1.082
# > 90th %:	**Mode:**	**Geo. Mean:**	**Har. Mean:**	**Kurtosis:**	**Skewness:**
84	.45	.476	.33	690.827	25.711

Detection limit is 0.05 ppm - a value of 0.25 ppm has been substituted in calculations and table.

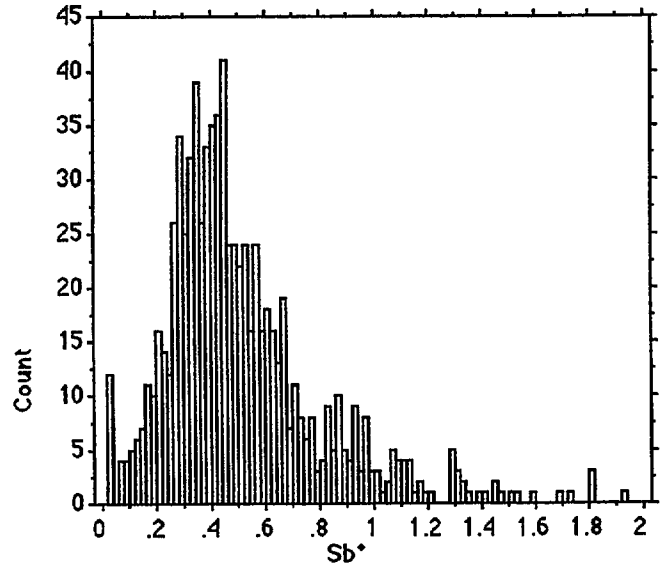

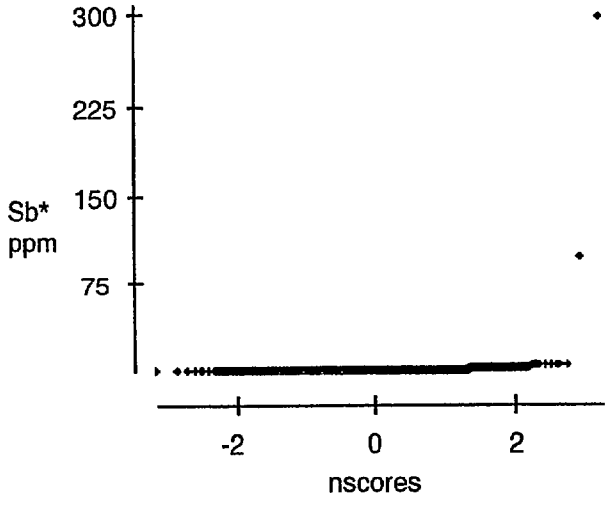

Sb*

Scandium

Mean:	Std. Dev.:	Std. Error:	Variance:	Coef. Var.:	Count:
8.855	4.888	.168	23.891	55.197	843
Minimum:	**Maximum:**	**Range:**	**Sum:**	**Sum of Sqr.:**	**# Missing:**
1	42	41	7465	86221	0
# < 10th %:	**10th %:**	**25th %:**	**50th %:**	**75th %:**	**90th %:**
50	4	5	8	11	15
# > 90th %:	**Mode:**	**Geo. Mean:**	**Har. Mean:**	**Kurtosis:**	**Skewness:**
81	5	7.726	6.707	5.505	1.72

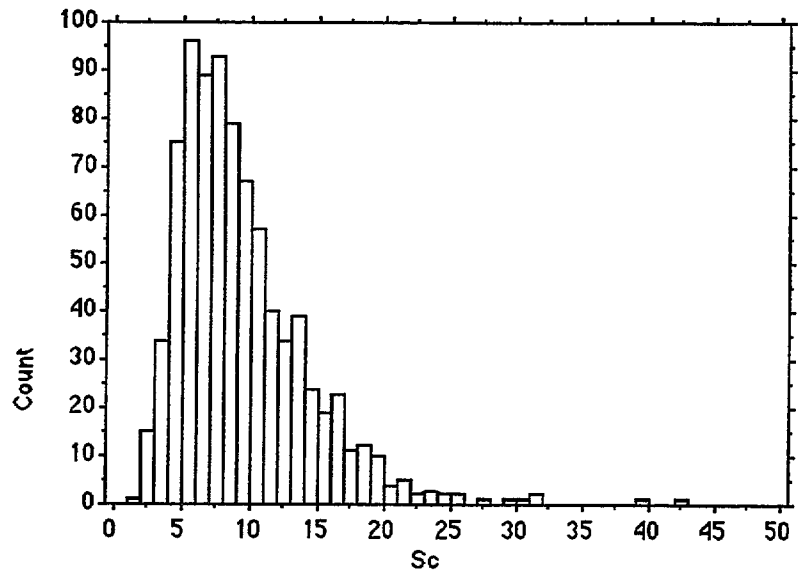

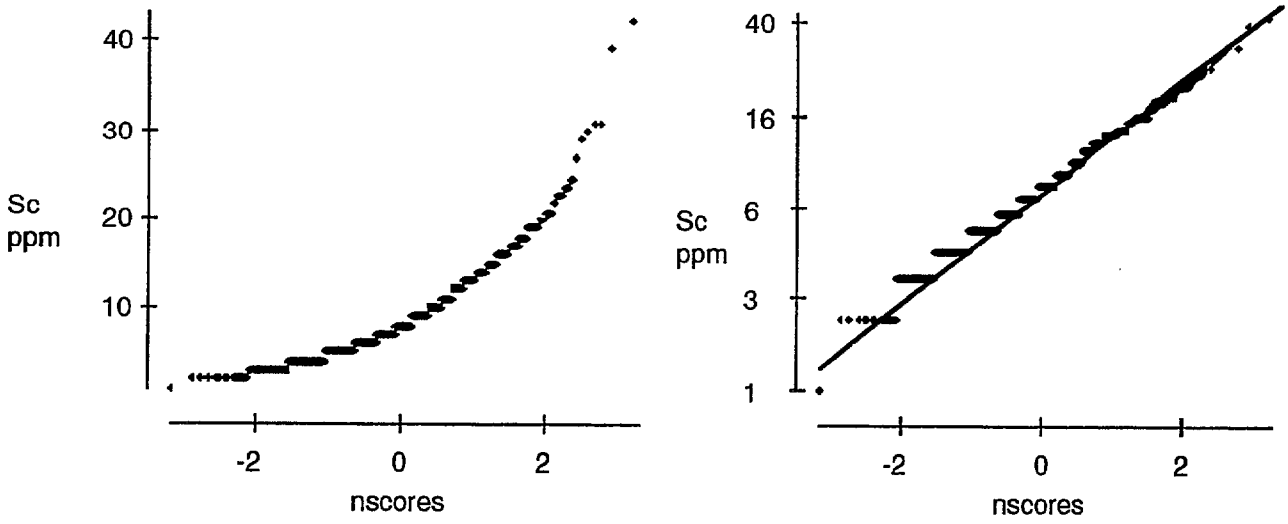

Sc

Tin

Mean:	Std. Dev.:	Std. Error:	Variance:	Coef. Var.:	Count:
33.55	165.004	5.683	27226.386	491.81	843
Minimum:	**Maximum:**	**Range:**	**Sum:**	**Sum of Sqr.:**	**# Missing:**
1	4462	4461	28283	23873523	0
# < 10th %:	**10th %:**	**25th %:**	**50th %:**	**75th %:**	**90th %:**
80	2	4	8	23	64.2
# > 90th %:	**Mode:**	**Geo. Mean:**	**Har. Mean:**	**Kurtosis:**	**Skewness:**
84	1	9.823	4.533	614.633	23.237

Detection limit is 2 ppm - a value of 1 ppm has been substituted in calculations and table.

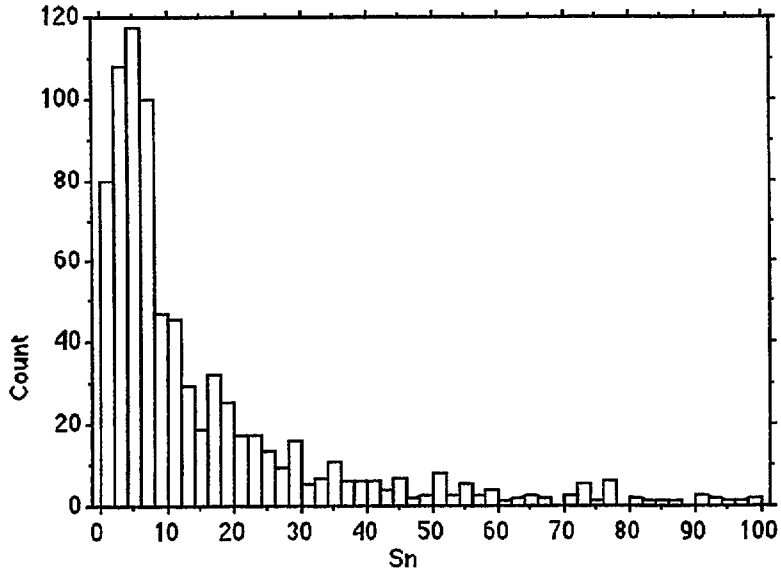

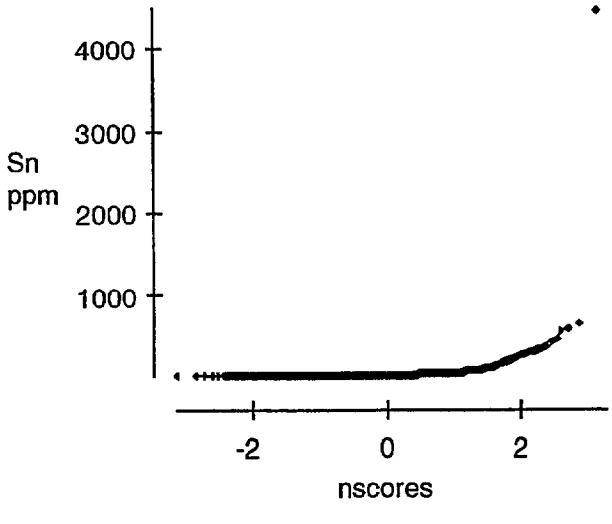

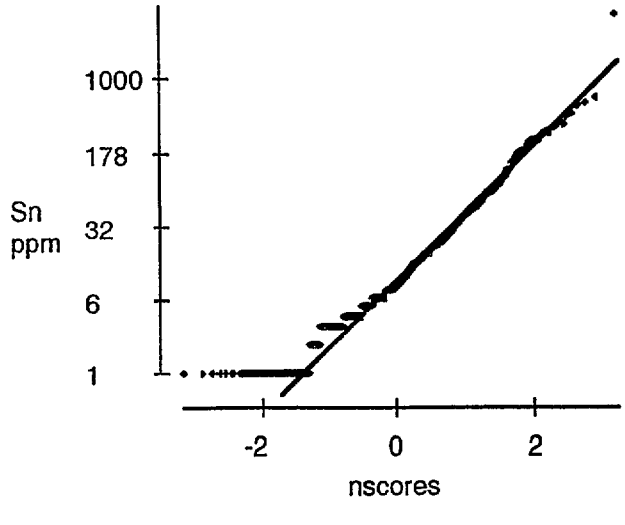

Sn

Strontium

Mean:	Std. Dev.:	Std. Error:	Variance:	Coef. Var.:	Count:
71.364	71.879	2.476	5166.581	100.721	843
Minimum:	**Maximum:**	**Range:**	**Sum:**	**Sum of Sqr.:**	**# Missing:**
6	579	573	60160	8643530	0
# < 10th %:	**10th %:**	**25th %:**	**50th %:**	**75th %:**	**90th %:**
72	13	24	51	89	157.2
# > 90th %:	**Mode:**	**Geo. Mean:**	**Har. Mean:**	**Kurtosis:**	**Skewness:**
84	14	47.296	31.566	7.981	2.429

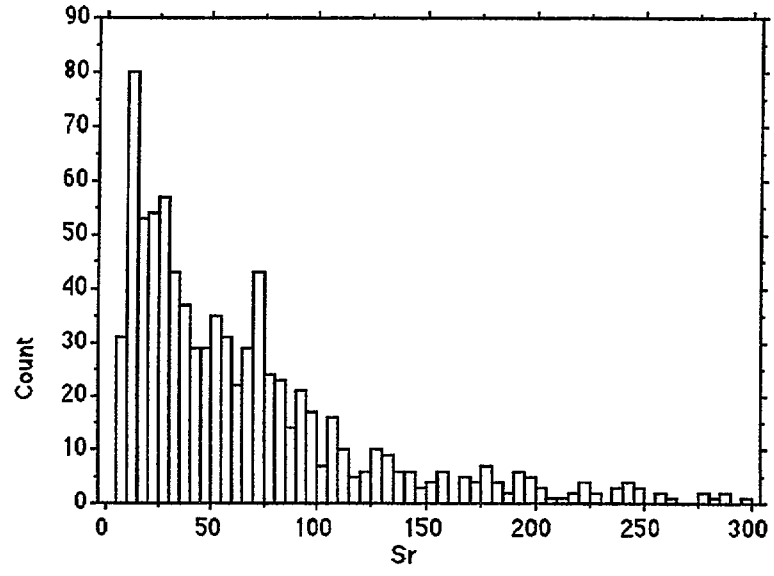

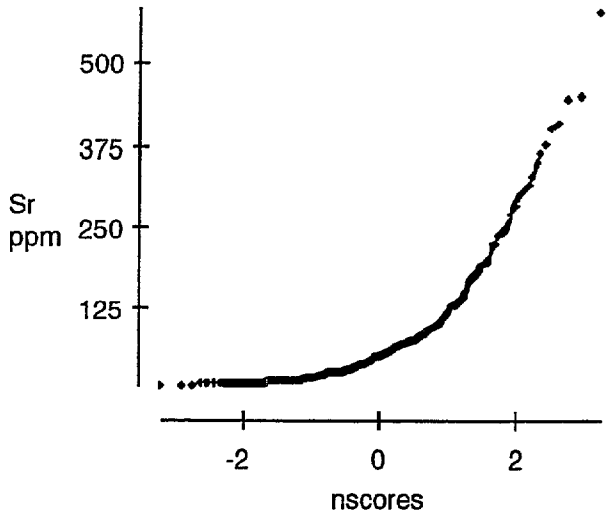

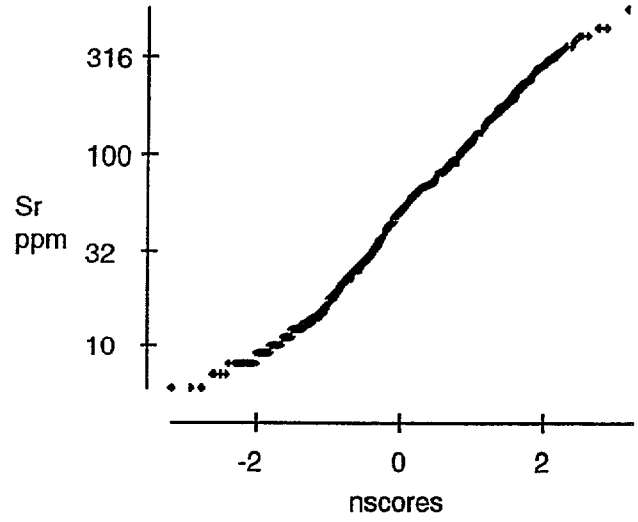

Sr

Thorium

Mean:	Std. Dev.:	Std. Error:	Variance:	Coef. Var.:	Count:
40.121	52.092	1.794	2713.532	129.836	843
Minimum:	**Maximum:**	**Range:**	**Sum:**	**Sum of Sqr.:**	**# Missing:**
2	691	689	33822	3641766	0
# < 10th %:	**10th %:**	**25th %:**	**50th %:**	**75th %:**	**90th %:**
74	9	14	22	46	90.2
# > 90th %:	**Mode:**	**Geo. Mean:**	**Har. Mean:**	**Kurtosis:**	**Skewness:**
84	12	25.673	18.224	39.852	4.853

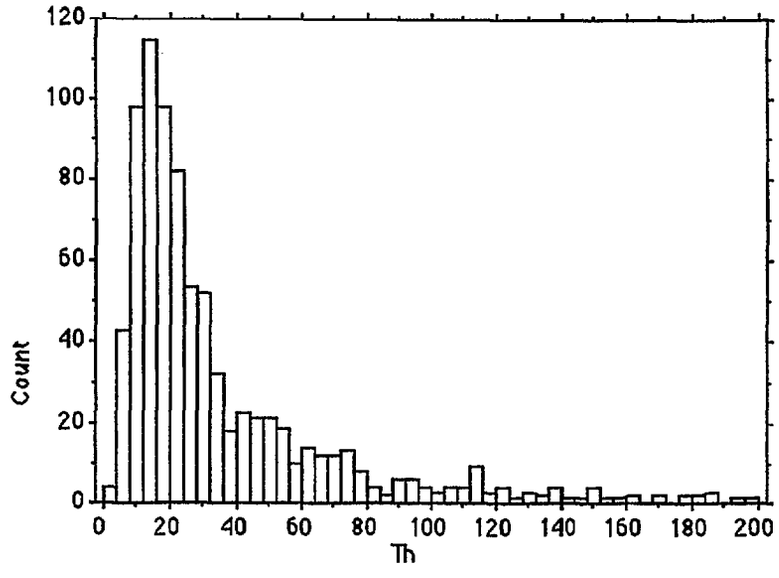

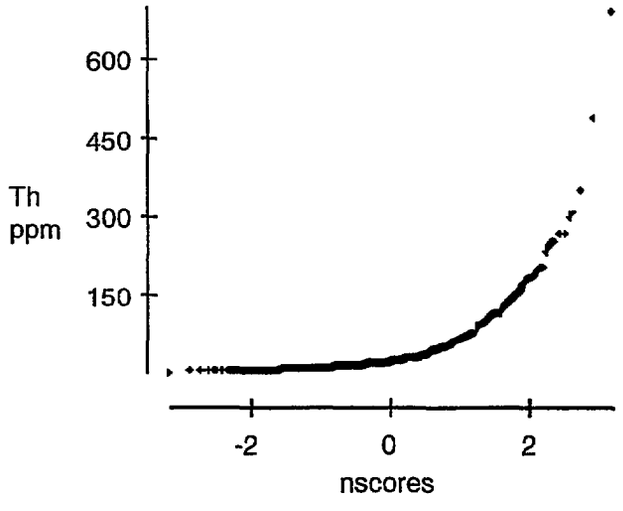

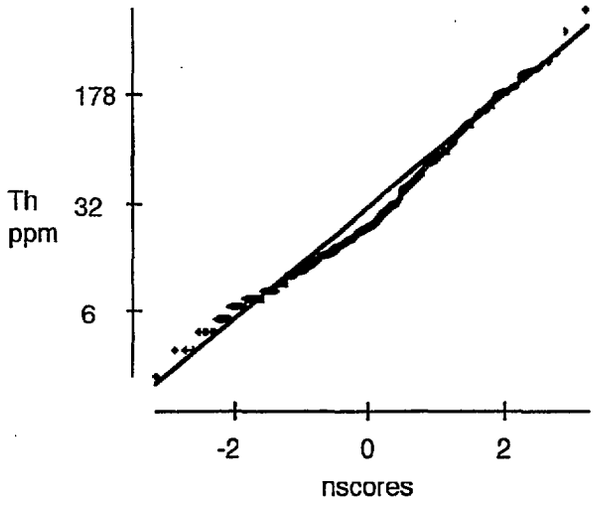

Th

Titanium

Mean:	Std. Dev.:	Std. Error:	Variance:	Coef. Var.:	Count:
8830.044	10752.73	370.344	1.156E8	121.774	843
Minimum:	Maximum:	Range:	Sum:	Sum of Sqr.:	# Missing:
1017	99999	98982	7443727	1.631E11	0
# < 10th %:	10th %:	25th %:	50th %:	75th %:	90th %:
84	2663	3691.25	5438	9319.75	17330.2
# > 90th %:	Mode:	Geo. Mean:	Har. Mean:	Kurtosis:	Skewness:
84	•	6190.121	4882.079	24.689	4.297

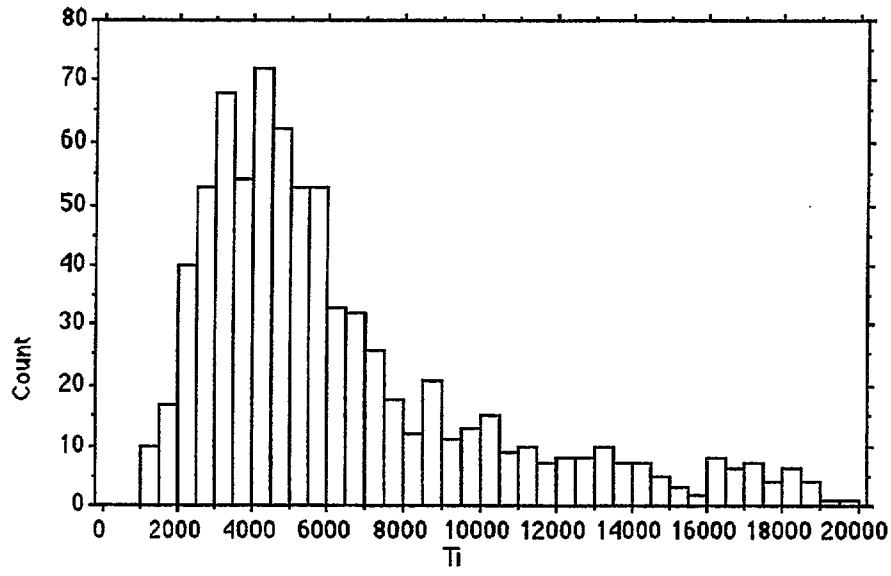

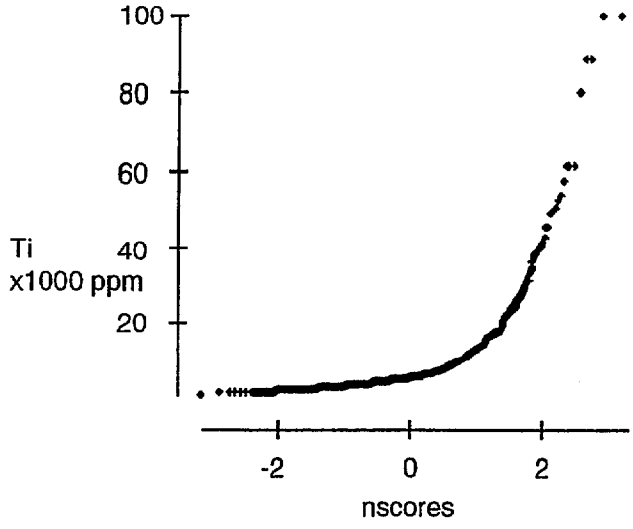

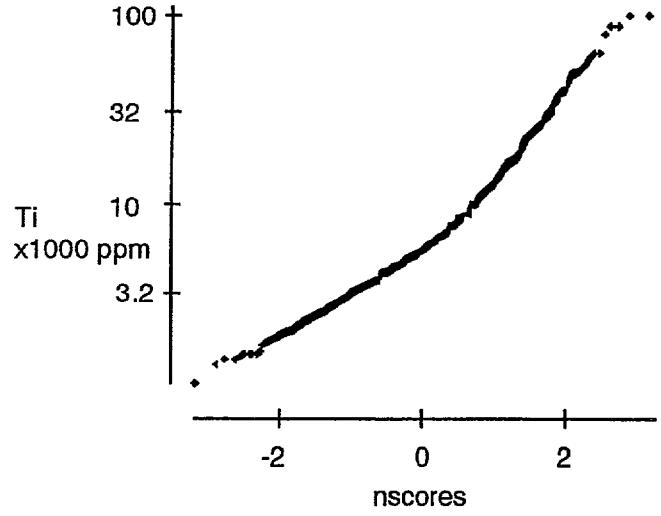

Ti

Thallium

Mean:	Std. Dev.:	Std. Error:	Variance:	Coef. Var.:	Count:
.661	.494	.017	.244	74.742	843
Minimum:	**Maximum:**	**Range:**	**Sum:**	**Sum of Sqr.:**	**# Missing:**
.25	3.39	3.14	557.57	574.555	0
# < 10th %:	**10th %:**	**25th %:**	**50th %:**	**75th %:**	**90th %:**
0	.25	.25	.57	.877	1.32
# > 90th %:	**Mode:**	**Geo. Mean:**	**Har. Mean:**	**Kurtosis:**	**Skewness:**
85	.25	.519	.419	3.595	1.655

Detection limit is 0.5 ppm - a value of 0.25 ppm has been substituted in calculations and table.

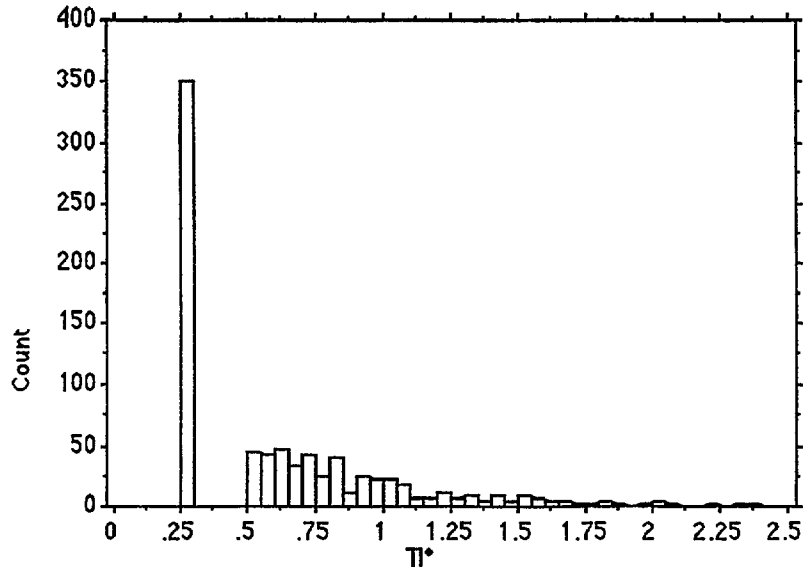

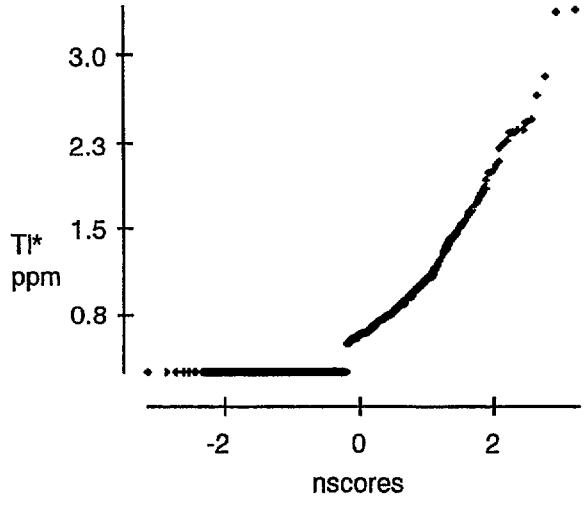

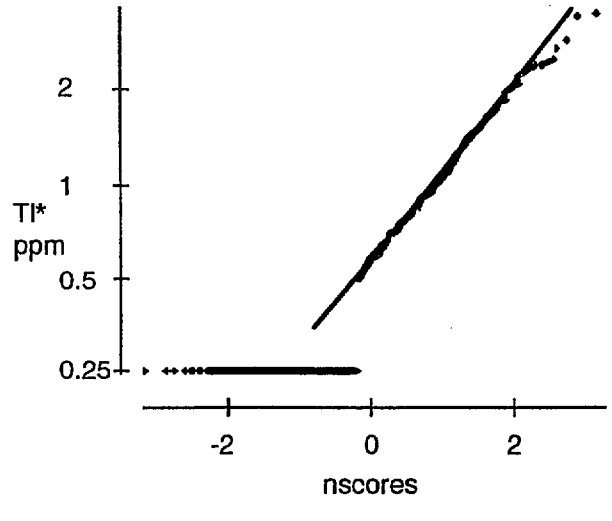

Tl*

Uranium

Mean:	Std. Dev.:	Std. Error:	Variance:	Coef. Var.:	Count:
6.22	5.815	.2	33.814	93.488	843
Minimum:	**Maximum:**	**Range:**	**Sum:**	**Sum of Sqr.:**	**# Missing:**
.25	56	55.75	5243.5	61086.375	0
# < 10th %:	**10th %:**	**25th %:**	**50th %:**	**75th %:**	**90th %:**
77	2	3	4.5	7	12
# > 90th %:	**Mode:**	**Geo. Mean:**	**Har. Mean:**	**Kurtosis:**	**Skewness:**
81	3	4.598	3.241	14.321	3.158

Detection limit is 0.5 ppm - a value of 0.25 ppm has been substituted in calculations and table.

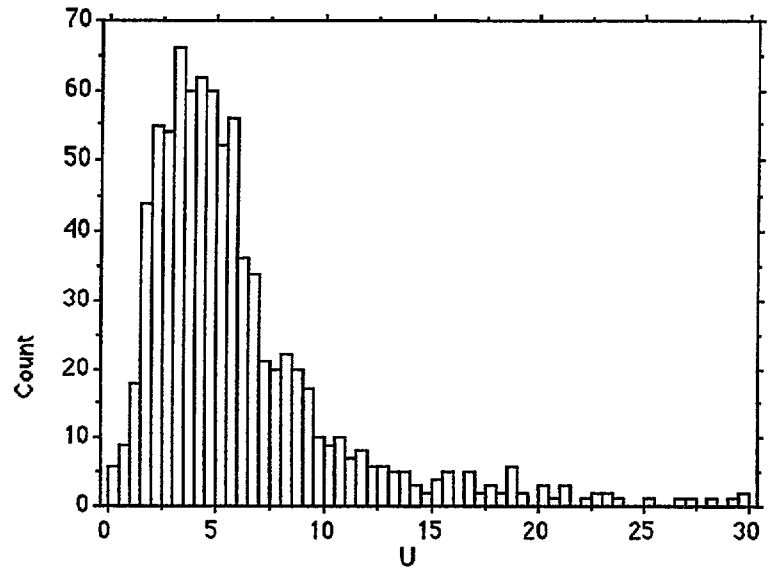

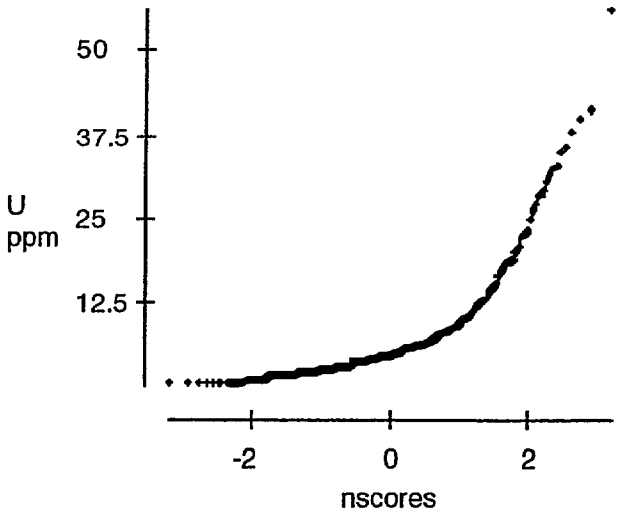

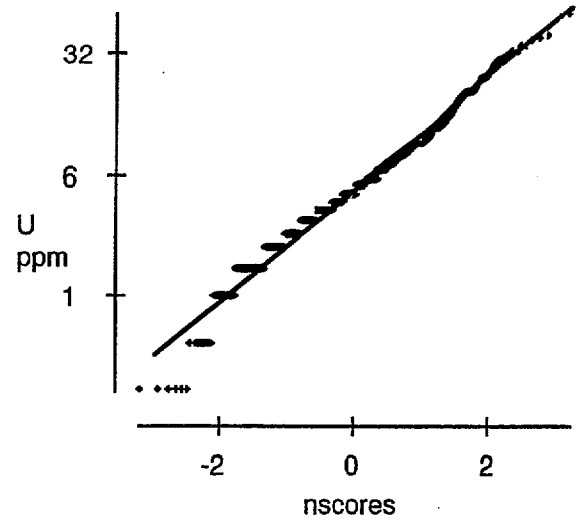

U

Vanadium

Mean:	Std. Dev.:	Std. Error:	Variance:	Coef. Var.:	Count:
67.332	47.182	1.625	2226.132	70.073	843
Minimum:	**Maximum:**	**Range:**	**Sum:**	**Sum of Sqr.:**	**# Missing:**
6	571	565	56761	5696243	0
# < 10th %:	**10th %:**	**25th %:**	**50th %:**	**75th %:**	**90th %:**
84	21.8	36	57	87	122.2
# > 90th %:	**Mode:**	**Geo. Mean:**	**Har. Mean:**	**Kurtosis:**	**Skewness:**
84	•	54.292	42.32	17.77	2.722

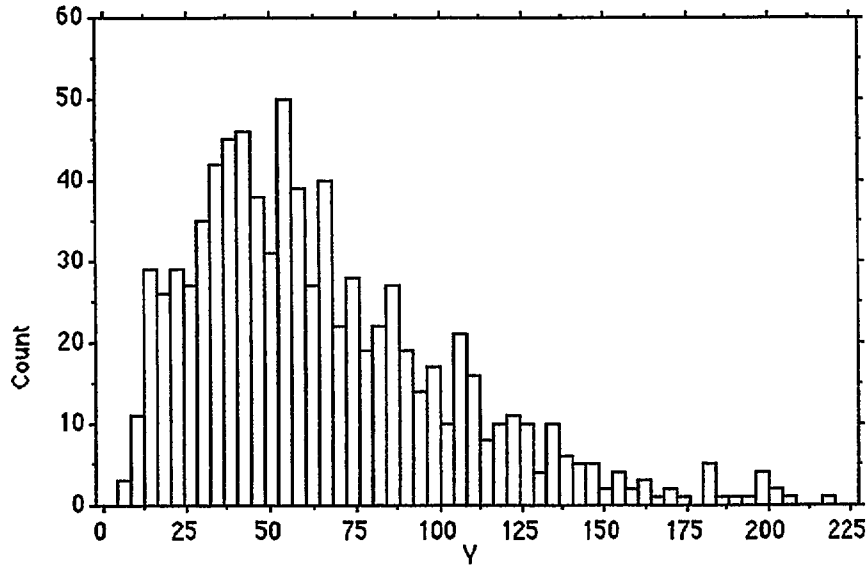

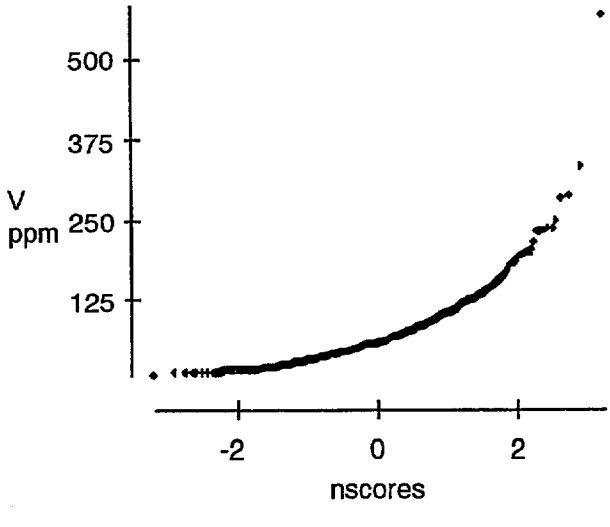

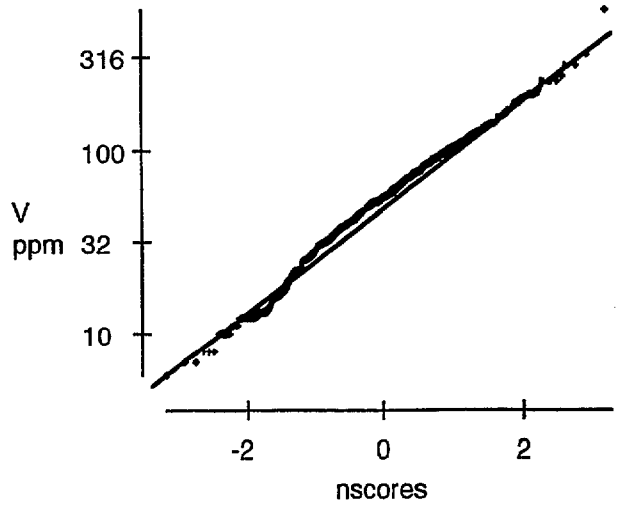

V

Tungsten

Mean:	Std. Dev.:	Std. Error:	Variance:	Coef. Var.:	Count:
6.332	5.074	.175	25.741	80.131	843
Minimum:	**Maximum:**	**Range:**	**Sum:**	**Sum of Sqr.:**	**# Missing:**
1.5	48	46.5	5337.5	55468.25	0
# < 10th %:	**10th %:**	**25th %:**	**50th %:**	**75th %:**	**90th %:**
0	1.5	3	5	8	12
# > 90th %:	**Mode:**	**Geo. Mean:**	**Har. Mean:**	**Kurtosis:**	**Skewness:**
74	1.5	4.79	3.571	10.757	2.467

Detection limit is 3 ppm - a value of 1.5 ppm has been substituted in calculations and table.

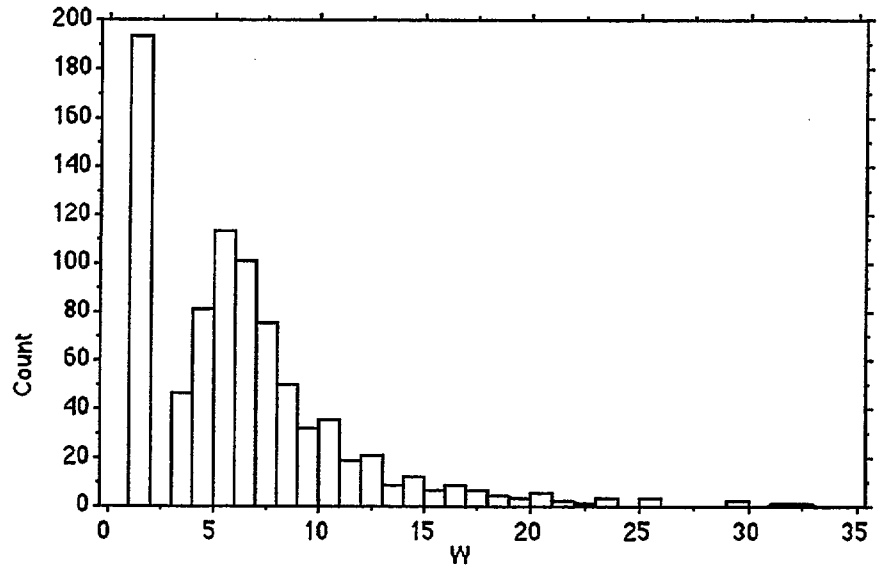

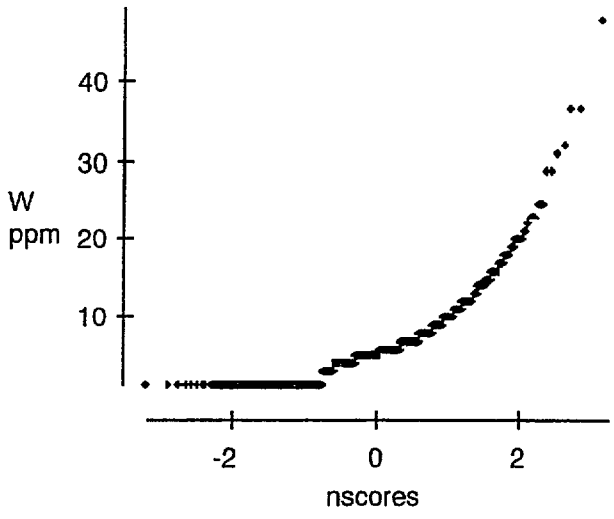

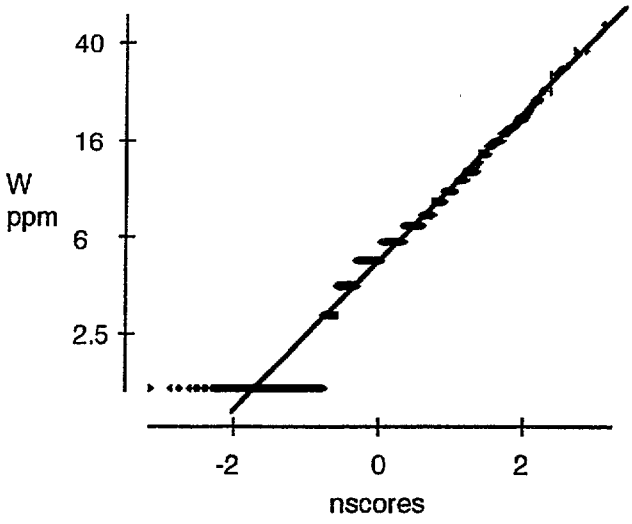

W

Tungsten

Mean:	Std. Dev.:	Std. Error:	Variance:	Coef. Var.:	Count:
2.063	3.815	.131	14.558	184.991	843
Minimum:	**Maximum:**	**Range:**	**Sum:**	**Sum of Sqr.:**	**# Missing:**
.05	59.1	59.05	1738.69	15843.614	0
# < 10th %:	**10th %:**	**25th %:**	**50th %:**	**75th %:**	**90th %:**
79	.22	.53	1.13	2.26	4.134
# > 90th %:	**Mode:**	**Geo. Mean:**	**Har. Mean:**	**Kurtosis:**	**Skewness:**
84	.05	1.064	.52	97.566	8.294

Detection limit is 0.10 ppm - a value of 0.05 ppm has been substituted in calculations and table.

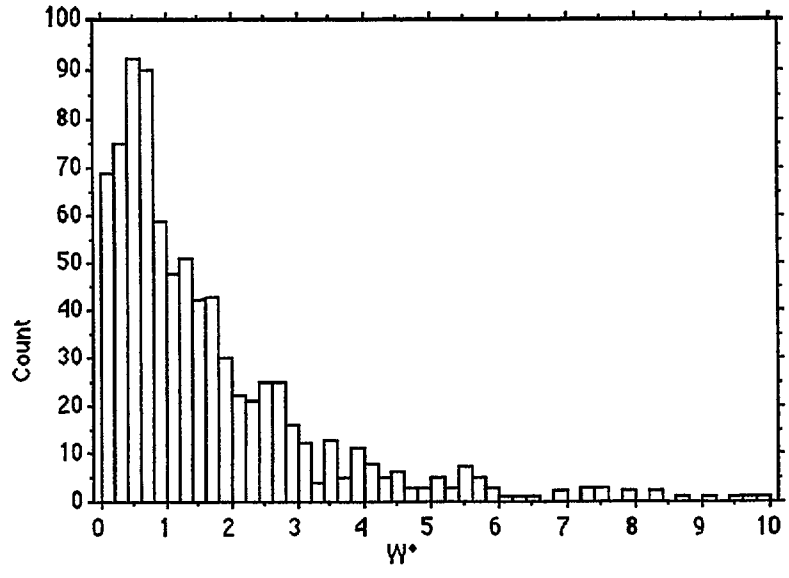

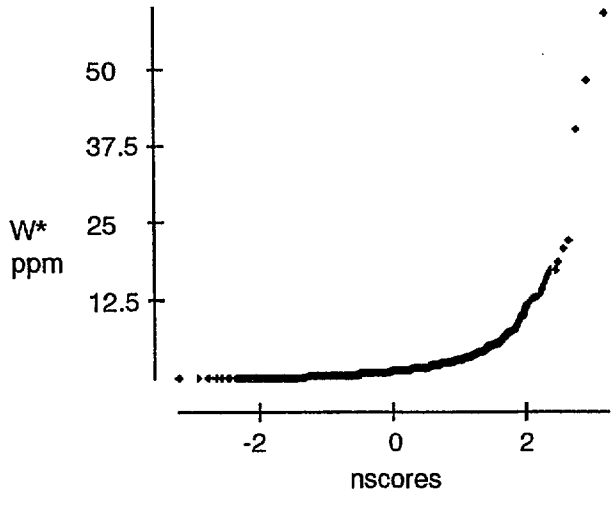

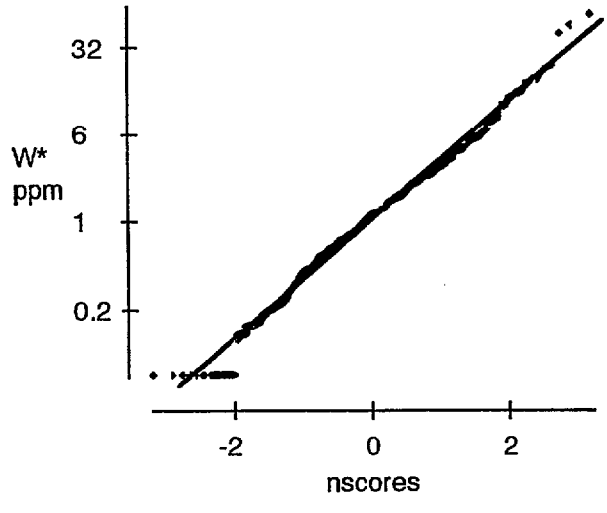

W*

Yttrium

Mean:	Std. Dev.:	Std. Error:	Variance:	Coef. Var.:	Count:
67.05	60.827	2.095	3699.924	90.719	843
Minimum:	**Maximum:**	**Range:**	**Sum:**	**Sum of Sqr.:**	**# Missing:**
7	583	576	56523	6905193	0
# < 10th %:	**10th %:**	**25th %:**	**50th %:**	**75th %:**	**90th %:**
77	23	31	49	76	133.2
# > 90th %:	**Mode:**	**Geo. Mean:**	**Har. Mean:**	**Kurtosis:**	**Skewness:**
84	29	51.359	41.256	13.437	3.061

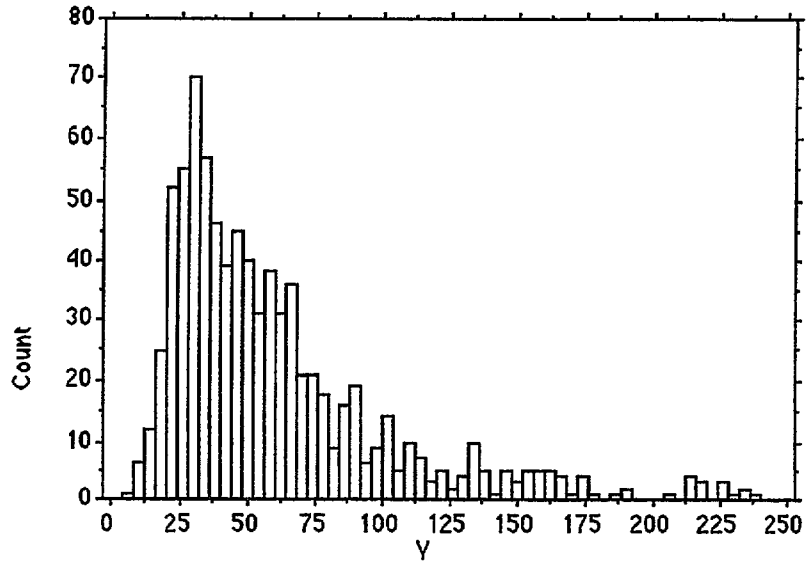

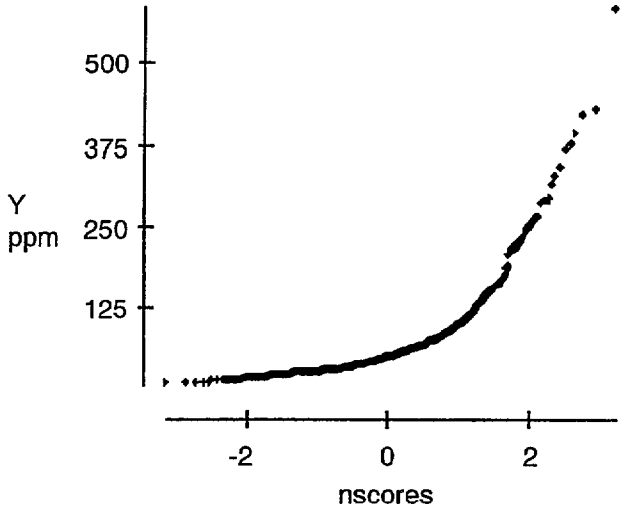

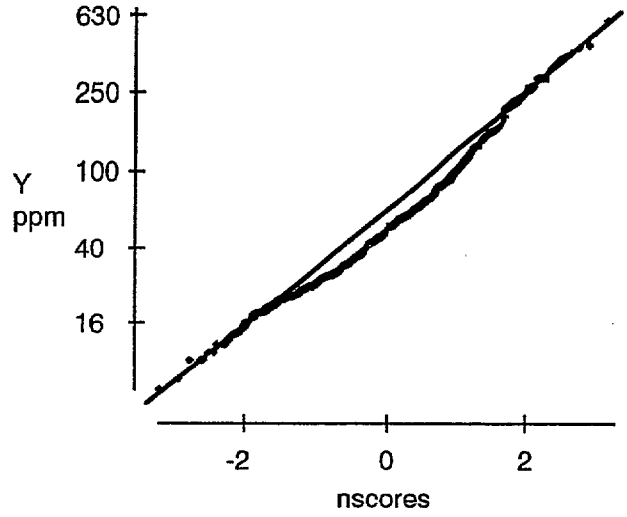

Y

Zinc

Mean:	Std. Dev.:	Std. Error:	Variance:	Coef. Var.:	Count:
35.916	23.565	.812	555.315	65.612	843
Minimum:	**Maximum:**	**Range:**	**Sum:**	**Sum of Sqr.:**	**# Missing:**
4	295	291	30277	1554997	0
# < 10th %:	**10th %:**	**25th %:**	**50th %:**	**75th %:**	**90th %:**
65	11	18	33	47	64
# > 90th %:	**Mode:**	**Geo. Mean:**	**Har. Mean:**	**Kurtosis:**	**Skewness:**
81	16	29.317	23.112	18.62	2.543

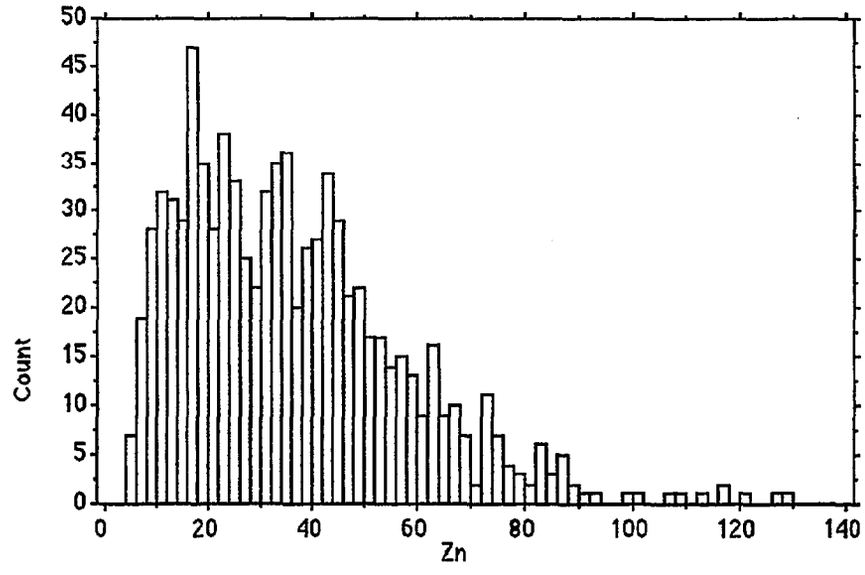

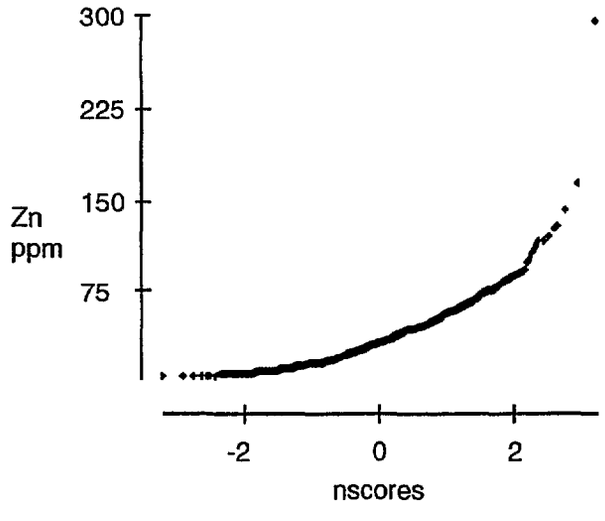

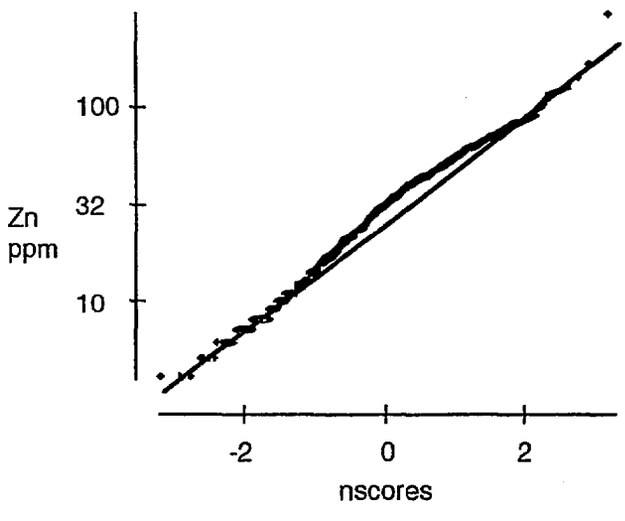

Zn

Zirconium

Mean:	Std. Dev.:	Std. Error:	Variance:	Coef. Var.:	Count:
785.082	629.826	21.692	396681.36	80.224	843
Minimum:	Maximum:	Range:	Sum:	Sum of Sqr.:	# Missing:
121	5844	5723	661824	853591716	0
# < 10th %:	10th %:	25th %:	50th %:	75th %:	90th %:
83	287	391.25	607	942.25	1477.6
# > 90th %:	Mode:	Geo. Mean:	Har. Mean:	Kurtosis:	Skewness:
84	•	630.409	525.353	13.457	2.965

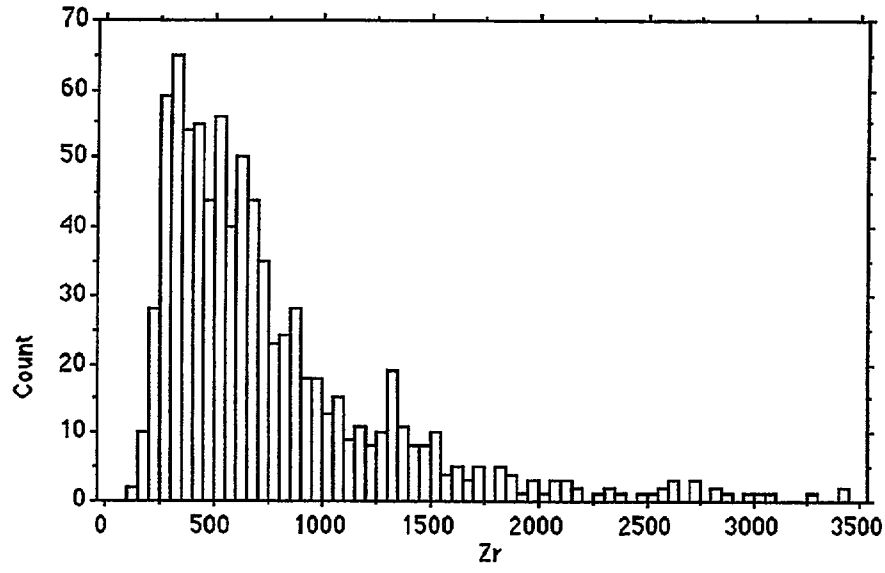

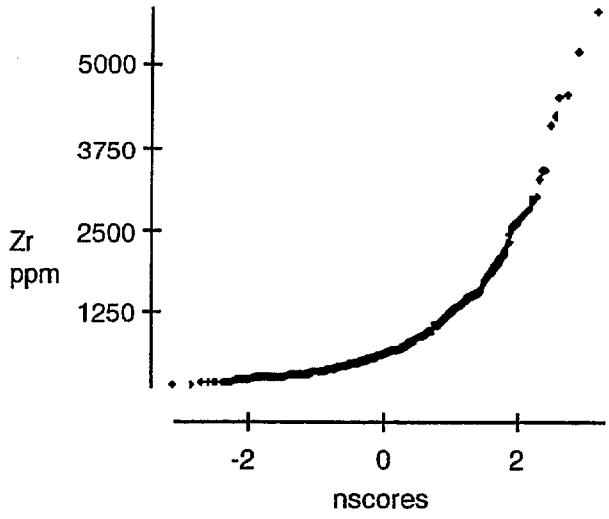

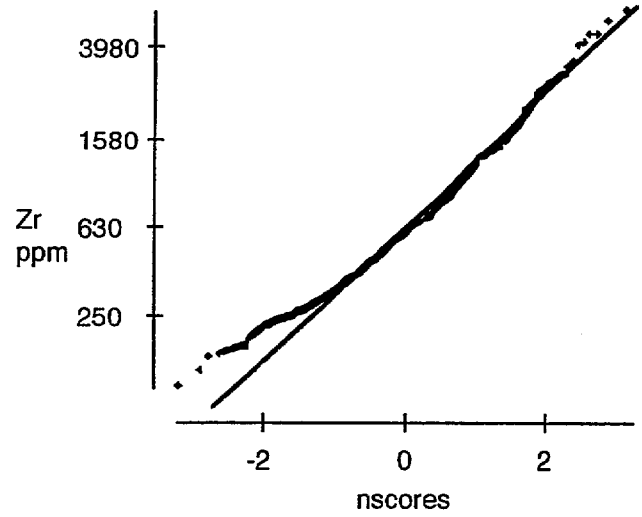

Zr

Appendix C

Table C1. Peason product moment correlation coefficients for RAW DATA and LOG-TRANSFORMED DATA (N=843).

	As	Au#	Ba	Be*	Bi	Bi*	Cd*	Ce	Cr	Cu	Fe	Ga	Ge	Hf	La	Mn	Mo	Mo*	Nb	Nd	Ni
As		0.05	0.14	0.09	0.45	0.36	0.00	0.33	0.00	0.28	0.03	0.04	-.22	0.14	0.32	0.02	0.00	-.05	0.02	0.33	0.01
Au#	0.27		0.11	0.00	-.01	0.03	0.05	0.03	0.05	0.17	0.07	0.02	0.13	-.03	0.03	0.06	0.01	0.00	0.00	0.03	0.06
Ba	0.15	0.19		0.29	0.08	-.02	0.17	0.27	-.17	0.35	0.31	**0.54**	0.16	-.04	0.26	0.38	-.03	0.08	0.18	0.25	0.25
Be*	0.18	0.01	**0.54**		0.14	0.29	0.04	0.10	-.25	0.05	0.01	**0.65**	0.21	0.09	0.07	0.07	-.03	0.27	0.24	0.09	0.05
Bi	0.21	0.10	0.08	0.17		**0.58**	0.04	**0.52**	-.05	0.16	0.09	0.06	-.02	0.45	**0.51**	0.16	0.17	0.01	0.31	**0.52**	-.01
Bi*	0.27	0.05	-.07	0.27	0.42		0.00	0.35	-.07	0.11	-.06	0.11	-.06	0.26	0.35	-.02	0.11	0.16	0.12	0.35	-.08
Cd*	0.07	0.06	0.10	0.08	0.07	0.07		0.06	0.02	0.24	0.25	0.12	0.25	0.00	0.06	0.22	0.02	0.11	0.12	0.05	0.15
Ce	0.19	0.21	**0.57**	0.37	0.32	0.12	0.12		0.00	0.30	0.35	0.08	0.00	0.38	**1.00**	0.44	-.01	-.10	**0.57**	**1.00**	0.11
Cr	0.15	0.15	-.16	-.35	-.08	-.13	0.08	-.02		0.28	0.39	-.09	-.01	-.01	0.01	0.22	0.12	-.13	0.03	0.00	**0.52**
Cu	0.40	0.36	0.44	0.20	0.12	0.09	0.23	0.40	0.46		**0.75**	0.32	0.28	-.17	0.30	**0.62**	0.11	-.07	0.23	0.29	**0.69**
Fe	0.29	0.25	0.43	0.24	0.07	-.07	0.23	0.41	0.48	**0.81**		0.35	0.39	-.06	0.36	**0.90**	0.23	-.08	**0.53**	0.35	**0.73**
Ga	0.22	0.07	**0.60**	**0.68**	0.10	0.20	0.11	0.32	-.12	0.39	**0.52**		0.24	0.02	0.07	0.31	0.09	0.35	0.31	0.07	0.33
Ge	-.21	0.01	0.18	0.26	-.02	-.09	0.18	0.10	0.01	0.18	0.31	0.22		-.12	0.00	0.39	0.02	0.07	0.20	-.01	0.32
Hf	0.02	-.09	-.08	0.00	0.36	0.31	0.02	0.30	-.16	-.30	-.21	-.03	-.15		0.37	0.08	0.46	0.10	0.49	0.38	-.24
La	0.21	0.22	**0.56**	0.34	0.31	0.12	0.12	**0.99**	0.01	0.41	0.43	0.33	0.08	0.29		0.45	0.00	-.11	**0.57**	**1.00**	0.11
Mn	0.17	0.23	**0.67**	0.42	0.13	-.05	0.16	**0.59**	0.14	**0.68**	**0.78**	0.48	0.36	-.10	**0.57**		0.27	-.13	**0.66**	0.44	**0.58**
Mo	0.08	0.03	-.04	-.07	0.19	0.19	0.05	0.00	0.09	0.10	0.19	0.10	0.01	0.28	0.01	0.10		0.07	0.27	-.01	0.04
Mo*	0.07	-.07	0.03	0.27	0.02	0.23	0.06	-.15	-.19	-.13	-.11	0.31	0.05	0.08	-.15	-.20	0.04		0.04	-.10	-.05
Nb	0.08	0.03	0.29	0.30	0.29	0.26	0.15	**0.63**	-.07	0.24	0.42	0.38	0.21	**0.50**	**0.63**	**0.51**	0.25	-.01		**0.57**	0.18
Nd	0.20	0.21	**0.57**	0.37	0.31	0.12	0.12	**0.99**	-.02	0.40	0.41	0.32	0.08	0.29	**0.99**	**0.59**	0.00	-.15	**0.63**		0.10
Ni	0.23	0.25	0.39	0.15	-.03	-.16	0.15	0.24	**0.65**	**0.82**	**0.83**	0.36	0.24	-.41	0.26	**0.65**	0.03	-.14	0.13	0.24	
P*	0.15	0.20	**0.57**	**0.51**	0.20	0.01	0.18	**0.69**	0.11	0.48	0.44	0.38	0.22	-.05	**0.68**	**0.53**	-.13	0.05	0.29	**0.69**	0.45
Pb	0.15	0.06	**0.53**	**0.55**	0.22	0.36	0.12	**0.52**	-.30	0.21	0.16	**0.58**	0.08	0.25	**0.51**	0.37	0.05	0.20	0.46	**0.51**	0.00
Pd#	0.21	0.40	0.03	0.07	0.06	0.02	0.14	0.08	0.24	0.36	0.31	0.03	0.12	-.24	0.08	0.23	0.06	-.05	0.01	0.08	0.34
Pt#	0.18	0.27	-.01	-.03	0.04	0.06	0.05	0.01	0.00	0.10	0.03	-.08	-.13	0.02	0.01	-.03	0.06	-.01	-.03	0.01	-.01
Rb	0.16	0.08	**0.72**	**0.83**	0.16	0.18	0.05	0.47	-.37	0.25	0.29	**0.73**	0.25	0.04	0.45	**0.57**	-.02	0.20	0.39	0.48	0.18
Sb*	0.36	0.11	0.15	0.27	0.12	0.24	0.08	0.11	-.09	0.08	-.09	0.17	-.14	0.05	0.10	-.07	-.07	0.35	-.12	0.11	-.02
Sc	0.27	0.28	0.39	0.23	0.08	0.00	0.22	0.41	**0.50**	**0.78**	**0.90**	**0.53**	0.26	-.13	0.43	**0.69**	0.19	-.08	0.44	0.41	**0.78**
Se	-.04	0.01	-.07	-.05	0.01	-.02	0.05	-.04	0.00	-.02	-.02	0.00	-.01	0.01	-.04	-.07	-.02	0.00	-.01	-.04	-.02
Sn	-.05	-.12	-.17	0.01	0.28	0.47	0.01	0.18	-.13	-.24	-.24	0.00	-.13	**0.60**	0.18	-.21	0.12	0.12	0.29	0.17	-.36
Sr	0.09	0.19	**0.80**	0.44	0.02	-.15	0.09	0.41	0.13	**0.53**	**0.56**	**0.55**	0.28	-.21	0.40	**0.73**	-.04	-.07	0.15	0.41	**0.60**
Ta	0.00	0.04	0.09	0.03	0.06	-.02	0.05	0.09	0.13	0.15	0.21	0.12	0.15	0.03	0.08	0.19	0.06	-.03	0.22	0.08	0.19
Th	0.09	0.11	0.46	0.47	0.35	0.26	0.04	**0.88**	-.16	0.25	0.29	0.39	0.13	0.43	**0.86**	**0.52**	0.06	-.07	**0.70**	**0.87**	0.09
Ti	0.02	0.21	0.14	-.22	0.05	-.12	0.19	0.40	**0.50**	**0.56**	**0.67**	-.01	0.30	0.00	0.42	**0.61**	0.23	-.43	0.49	0.39	**0.55**
Tl*	0.15	0.03	**0.52**	**0.76**	0.16	0.24	0.14	0.30	-.42	0.13	0.13	**0.59**	0.24	0.05	0.26	0.37	-.06	0.37	0.29	0.30	0.04
U	0.16	0.15	0.40	0.47	0.30	0.33	0.07	**0.79**	-.10	0.29	0.32	0.40	0.11	0.38	**0.78**	**0.50**	0.09	-.05	**0.69**	**0.79**	0.12
V	0.21	0.28	0.10	-.18	-.03	-.17	0.18	0.18	**0.77**	**0.75**	**0.81**	0.10	0.21	-.29	0.20	**0.51**	0.15	-.26	0.13	0.17	**0.82**
W	0.09	-.02	0.03	0.19	0.33	0.44	-.06	0.38	-.24	-.08	-.08	0.14	-.12	0.48	0.37	0.04	0.11	0.06	0.41	0.38	-.26
W*	0.29	0.01	0.18	0.40	0.27	**0.52**	-.08	0.16	-.28	-.05	-.07	0.45	-.12	0.30	0.16	-.05	0.14	**0.52**	0.18	0.17	-.18
Y	0.13	0.10	0.36	0.42	0.34	0.36	0.05	**0.79**	-.19	0.14	0.18	0.36	0.04	0.49	**0.78**	0.38	0.09	-.04	**0.66**	**0.80**	-.04
Zn	0.34	0.23	**0.67**	0.47	0.14	0.13	0.23	**0.53**	0.10	**0.71**	**0.78**	**0.66**	0.24	-.08	**0.53**	**0.79**	0.11	0.04	**0.50**	**0.53**	**0.58**
Zr	-.05	-.13	-.16	-.10	0.32	0.26	-.01	0.23	-.16	-.39	-.31	-.16	-.16	**0.96**	0.23	-.22	0.22	0.08	0.42	0.23	-.48
	As	Au#	Ba	Be*	Bi	Bi*	Cd*	Ce	Cr	Cu	Fe	Ga	Ge	Hf	La	Mn	Mo	Mo*	Nb	Nd	Ni

LOG-TRANSFORMED DATA

RAW DATA

P*	Pb	Pd#	Pt#	Rb	Sb*	Sc	Se	Sn	Sr	Ta	Th	Ti	Tl*	U	V	W	W*	Y	Zn	Zr	
0.31	0.10	0.03	0.11	0.03	0.02	0.04	-.02	0.00	-.03	-.03	0.25	-.06	0.07	0.15	0.00	0.16	0.20	0.18	0.10	0.12	As
0.24	0.16	0.17	0.04	0.03	-.01	0.13	-.01	-.02	0.05	0.07	0.03	0.05	0.07	0.07	0.09	-.04	-.01	0.03	0.04	-.04	Au#
0.45	0.44	0.03	0.01	0.32	0.03	0.32	-.04	-.05	**0.62**	0.09	0.21	0.10	0.36	0.19	0.12	0.03	0.08	0.19	**0.54**	-.10	Ba
0.24	0.40	0.00	-.08	**0.79**	0.04	0.04	-.03	-.01	0.12	0.01	0.32	-.18	**0.72**	0.36	-.16	0.34	0.34	0.34	0.21	0.00	Be*
0.38	0.20	0.01	0.00	0.14	0.00	0.08	0.00	0.23	-.01	0.08	**0.51**	0.11	0.14	0.37	0.06	0.46	0.41	0.39	0.11	0.41	Bi
0.34	0.18	-.02	0.01	0.17	0.05	-.02	-.02	0.12	-.07	-.04	0.36	-.07	0.19	0.28	-.09	0.44	**0.51**	0.32	0.06	0.25	Bi*
0.13	0.20	0.20	0.07	0.01	-.03	0.26	0.03	0.02	0.12	0.05	0.00	0.17	0.14	0.02	0.21	-.03	-.03	0.01	0.34	-.01	Cd*
0.69	0.28	0.03	0.00	0.07	0.01	0.31	-.02	0.15	0.08	0.17	**0.84**	0.39	0.04	**0.73**	0.32	**0.50**	0.24	**0.69**	0.28	0.31	Ce
0.04	-.22	0.06	-.03	-.30	-.05	0.38	-.01	-.01	0.08	0.14	-.10	0.27	-.32	-.05	0.46	-.15	-.17	-.10	0.11	0.01	Cr
0.41	0.12	0.35	0.08	-.01	-.02	**0.76**	-.03	-.06	0.29	0.20	0.19	0.46	0.04	0.24	**0.71**	-.01	0.03	0.12	**0.66**	-.24	Cu
0.30	0.04	0.28	0.02	-.02	-.03	**0.93**	-.03	-.06	0.35	0.32	0.23	**0.78**	-.03	0.26	**0.94**	0.01	-.09	0.15	**0.68**	-.17	Fe
0.25	0.47	0.02	-.04	**0.72**	0.07	0.40	-.01	-.04	0.42	0.12	0.27	0.00	**0.65**	0.29	0.13	0.26	0.31	0.29	**0.51**	-.10	Ga
0.14	0.06	0.26	-.07	0.19	-.03	0.37	-.02	-.05	0.21	0.15	0.04	0.34	0.22	0.09	0.34	-.07	-.09	0.02	0.27	-.14	Ge
0.13	0.23	-.17	0.00	0.17	0.02	-.06	0.00	0.36	-.11	0.10	**0.52**	0.13	0.09	0.40	-.07	**0.57**	0.36	0.47	-.04	**0.96**	Hf
0.68	0.26	0.03	0.00	0.05	0.01	0.32	-.02	0.15	0.08	0.17	**0.82**	0.41	0.02	**0.73**	0.33	0.49	0.23	**0.68**	0.28	0.30	La
0.29	0.17	0.21	-.02	0.08	-.01	**0.81**	-.05	-.03	0.40	0.35	0.35	**0.85**	0.06	0.34	**0.82**	0.12	-.04	0.25	**0.68**	-.05	Mn
-.08	0.05	0.03	0.04	-.01	0.06	0.21	-.02	0.15	0.01	0.11	0.06	0.31	-.05	0.06	0.24	0.14	0.21	0.06	0.12	0.39	Mo
-.01	0.22	0.05	0.00	0.27	0.00	-.06	0.03	-.01	-.06	-.03	-.02	-.26	0.37	-.01	-.18	0.14	0.26	0.01	0.14	0.09	Mo*
0.24	0.29	0.00	-.06	0.29	0.01	0.48	-.01	0.16	0.03	0.38	**0.59**	**0.64**	0.20	**0.55**	0.46	0.49	0.14	**0.51**	0.41	0.36	Nb
0.68	0.27	0.02	0.00	0.07	0.01	0.31	-.02	0.14	0.07	0.17	**0.83**	0.39	0.04	**0.73**	0.32	**0.50**	0.24	**0.69**	0.27	0.30	Nd
0.29	-.05	0.24	-.03	0.00	-.04	**0.72**	-.03	-.08	0.40	0.24	0.04	0.38	0.00	0.08	**0.66**	-.16	-.11	-.01	0.47	-.30	Ni
	0.31	0.14	0.01	0.17	-.01	0.37	-.04	0.07	0.35	0.08	**0.65**	0.14	0.18	**0.57**	0.24	0.25	0.23	0.48	0.30	0.09	P*
0.40		-.05	0.01	0.48	0.06	0.06	0.00	0.39	0.22	0.15	0.36	0.00	**0.52**	0.37	-.10	0.36	0.26	0.38	**0.51**	0.16	Pb
0.21	-.06		0.21	-.02	-.01	0.30	-.05	-.07	0.10	0.10	-.01	0.16	0.08	0.07	0.31	-.11	-.08	-.03	0.13	-.20	Pd#
0.02	-.04	0.24		-.14	-.01	0.06	0.06	-.03	0.02	-.03	-.04	-.04	-.10	-.05	0.06	-.01	0.02	-.02	0.06	0.00	Pt#
0.47	**0.62**	0.04	-.13		0.11	0.00	-.04	0.00	0.16	0.04	0.40	-.15	**0.89**	0.43	-.22	0.42	0.40	0.42	0.22	0.06	Rb
0.26	0.24	0.10	0.11	0.19		-.04	0.00	0.01	-.02	-.02	0.04	-.03	0.11	0.03	-.05	0.09	0.10	0.10	0.00	0.02	Sb*
0.47	0.20	0.34	0.08	0.25	-.04		-.02	-.05	0.39	0.29	0.22	**0.67**	-.01	0.26	**0.89**	0.02	-.08	0.16	**0.62**	-.17	Sc
-.05	-.01	-.08	0.05	-.06	0.01	-.01		0.01	-.05	0.03	-.03	-.02	-.03	-.03	-.02	0.00	0.00	-.03	-.02	0.01	Se
-.06	0.29	-.25	0.00	-.01	0.12	-.17	0.05		-.03	0.12	0.17	0.02	-.02	0.15	-.05	0.27	0.11	0.20	-.01	0.37	Sn
0.58	0.38	0.15	-.05	**0.61**	0.09	**0.53**	-.07	-.25		0.12	0.11	0.16	0.14	0.04	0.28	-.06	-.02	0.08	0.34	-.18	Sr
0.05	0.11	0.09	-.05	0.09	-.08	0.19	0.05	-.05	0.14		0.11	0.29	0.05	0.07	0.33	0.04	-.05	0.02	0.21	0.03	Ta
0.62	**0.58**	0.04	-.06	**0.59**	0.11	0.32	-.05	0.27	0.37	0.08		0.27	0.29	**0.85**	0.15	**0.67**	0.49	**0.81**	0.21	0.42	Th
0.23	-.04	0.26	0.00	-.11	-.30	**0.63**	-.03	-.13	0.29	0.20	0.31		-.18	0.31	**0.78**	0.09	-.15	0.22	0.44	0.04	Ti
0.39	**0.56**	0.08	-.09	**0.83**	0.27	0.12	-.02	-.01	0.39	0.07	0.44	-.23		0.33	-.23	0.30	0.36	0.29	0.28	0.00	Tl*
0.52	**0.59**	0.14	-.01	**0.57**	0.11	0.36	-.04	0.28	0.29	0.07	**0.88**	0.33	0.45		0.17	**0.64**	0.36	**0.88**	0.24	0.31	U
0.29	-.17	0.39	0.08	-.18	-.12	**0.79**	-.02	-.28	0.37	0.17	0.03	**0.77**	-.27	0.06		-.07	-.19	0.06	**0.51**	-.17	V
0.08	0.38	-.07	0.05	0.21	0.12	-.01	0.01	0.49	-.10	-.03	0.47	-.03	0.18	**0.51**	-.23		**0.57**	**0.78**	0.10	**0.51**	W
0.10	0.43	-.10	-.01	0.42	0.41	-.01	0.01	0.37	0.03	-.03	0.27	-.41	0.45	0.28	-.33	0.40		0.40	0.08	0.32	W*
0.47	**0.58**	-.01	0.02	**0.50**	0.16	0.24	-.04	0.44	0.23	0.02	**0.86**	0.21	0.37	**0.87**	-.08	**0.63**	0.37		0.19	0.40	Y
0.47	**0.52**	0.17	0.04	**0.59**	0.05	**0.70**	-.03	-.05	**0.62**	0.17	0.42	0.38	0.42	0.45	0.40	0.11	0.21	0.37		-.13	Zn
-.11	0.15	-.28	0.02	-.09	0.03	-.24	0.02	**0.62**	-.32	-.02	0.34	-.04	-.05	0.29	-.33	0.46	0.23	0.42	-.19		Zr
P*	Pb	Pd#	Pt#	Rb	Sb*	Sc	Se	Sn	Sr	Ta	Th	Ti	Tl*	U	V	W	W*	Y	Zn	Zr	

Table C2. Spearmans rank correlation coefficients (N=843).

	As	Au#	Ba	Be*	Bi	Bi*	Cd*	Ce	Cr	Cu	Fe	Ga	Ge	Hf	La	Mn	Mo	Mo*	Nb	Nd	Ni
As		0.31	0.14	0.19	0.12	0.22	0.06	0.16	0.18	0.41	0.36	0.21	-.14	-.02	0.17	0.20	0.10	0.11	0.08	0.17	0.27
Au#			0.19	0.05	0.09	0.00	0.04	0.22	0.12	0.40	0.30	0.03	-.02	-.14	0.22	0.27	0.04	-.08	0.03	0.22	0.30
Ba				**0.58**	0.06	-.10	0.10	**0.60**	-.12	0.42	0.42	**0.61**	0.19	-.09	**0.59**	**0.64**	-.05	0.06	0.31	**0.58**	0.38
Be*					0.17	0.25	0.09	0.44	-.26	0.25	0.26	**0.72**	0.28	-.03	0.41	0.41	-.08	0.29	0.32	0.43	0.22
Bi						0.29	0.07	0.25	-.06	0.10	0.04	0.11	0.02	0.28	0.24	0.09	0.14	0.01	0.26	0.25	-.01
Bi*							0.07	0.07	-.10	0.05	-.08	0.22	-.03	0.27	0.07	-.07	0.16	0.25	0.26	0.07	-.15
Cd*								0.12	0.11	0.21	0.21	0.07	0.19	0.01	0.11	0.15	0.08	0.09	0.15	0.11	0.14
Ce									0.00	0.41	0.40	0.40	0.17	0.24	**0.99**	**0.60**	-.02	-.07	**0.64**	**0.99**	0.29
Cr										0.47	**0.57**	-.04	0.07	-.17	0.03	0.24	0.13	-.14	0.01	0.01	**0.64**
Cu											**0.85**	0.36	0.23	-.35	0.42	**0.74**	0.09	-.08	0.27	0.41	**0.84**
Fe												0.46	0.31	-.30	0.41	**0.79**	0.15	-.04	0.35	0.39	**0.88**
Ga													0.24	0.01	0.39	0.48	0.12	0.39	0.45	0.38	0.35
Ge														-.18	0.16	0.38	0.03	0.12	0.22	0.16	0.29
Hf															0.23	-.20	0.15	0.09	0.43	0.23	-.44
La																**0.58**	0.00	-.08	**0.64**	**0.99**	0.30
Mn																	0.10	-.13	0.49	**0.58**	**0.73**
Mo																		0.07	0.21	-.01	0.05
Mo*																			0.11	-.08	-.11
Nb																				**0.64**	0.16
Nd																					0.28
Ni																					
P*																					
Pb																					
Pd#																					
Pt#																					
Rb																					
Sb*																					
Sc																					
Se																					
Sn																					
Sr																					
Ta																					
Th																					
Ti																					
Tl*																					
U																					
V																					
W																					
W*																					
Y																					
Zn																					
Zr																					
	As	Au#	Ba	Be*	Bi	Bi*	Cd*	Ce	Cr	Cu	Fe	Ga	Ge	Hf	La	Mn	Mo	Mo*	Nb	Nd	Ni

P*	Pb	Pd#	Pt#	Rb	Sb*	Sc	Se	Sn	Sr	Ta	Th	Ti	Tl*	U	V	W	W*	Y	Zn	Zr	
0.15	0.16	0.29	0.22	0.17	0.38	0.32	-.04	0.02	0.13	0.02	0.08	0.05	0.15	0.19	0.26	0.08	0.28	0.15	0.36	-.09	As
0.21	0.04	0.41	0.28	0.08	0.17	0.31	0.01	-.17	0.24	0.03	0.14	0.23	0.03	0.16	0.32	-.01	0.01	0.10	0.28	-.18	Au#
0.60	**0.55**	0.01	-.02	**0.72**	0.19	0.37	-.05	-.18	**0.78**	0.09	**0.50**	0.08	**0.56**	0.40	0.12	0.04	0.20	0.38	**0.64**	-.17	Ba
0.57	**0.57**	0.10	-.02	**0.85**	0.31	0.24	-.03	0.01	0.46	0.04	0.48	-.21	**0.79**	0.48	-.09	0.17	0.44	0.42	0.46	-.12	Be*
0.14	0.20	0.06	0.02	0.15	0.06	0.06	0.03	0.25	0.01	0.05	0.29	0.00	0.15	0.28	-.04	0.32	0.22	0.31	0.12	0.26	Bi
-.06	0.37	0.05	0.06	0.18	0.27	-.01	-.02	**0.50**	-.16	0.00	0.21	-.10	0.25	0.31	-.15	0.40	0.47	0.32	0.07	0.22	Bi*
0.18	0.06	0.13	0.06	0.04	0.12	0.20	0.06	0.01	0.08	0.05	0.05	0.20	0.12	0.05	0.19	-.06	-.10	0.03	0.20	-.02	Cd*
0.71	**0.54**	0.08	-.03	**0.52**	0.14	0.40	-.04	0.14	0.45	0.07	**0.89**	0.35	0.37	**0.81**	0.18	0.35	0.15	**0.79**	**0.54**	0.17	Ce
0.13	-.24	0.23	0.01	-.30	-.03	**0.57**	0.00	-.13	0.17	0.11	-.09	0.49	-.33	-.05	**0.75**	-.19	-.23	-.13	0.21	-.19	Cr
0.54	0.20	0.41	0.10	0.25	0.18	**0.82**	-.02	-.25	**0.57**	0.13	0.30	**0.58**	0.16	0.31	**0.78**	-.06	-.06	0.17	**0.73**	-.44	Cu
0.52	0.14	0.35	0.06	0.27	0.04	**0.90**	-.03	-.28	**0.59**	0.16	0.28	**0.61**	0.14	0.29	**0.87**	-.09	-.10	0.15	**0.78**	-.38	Fe
0.43	**0.64**	0.01	-.06	**0.76**	0.23	0.47	-.01	0.01	**0.53**	0.13	0.45	-.07	**0.66**	0.42	0.12	0.18	**0.51**	0.41	**0.63**	-.12	Ga
0.28	0.11	0.16	-.13	0.26	-.05	0.28	-.02	-.14	0.31	0.14	0.18	0.28	0.26	0.16	0.25	-.11	-.10	0.07	0.27	-.18	Ge
-.12	0.21	-.29	-.01	0.03	0.03	-.23	0.02	**0.60**	-.26	0.00	0.35	-.06	0.03	0.33	-.36	0.46	0.29	0.46	-.16	**0.95**	Hf
0.69	**0.52**	0.07	-.03	0.49	0.13	0.42	-.04	0.14	0.44	0.06	**0.87**	0.36	0.33	**0.79**	0.20	0.34	0.15	**0.78**	**0.54**	0.17	La
0.61	0.35	0.26	-.04	**0.53**	0.01	**0.72**	-.07	-.25	**0.76**	0.16	**0.54**	**0.59**	0.37	0.49	**0.59**	0.01	-.08	0.36	**0.79**	-.30	Mn
-.11	0.02	0.09	0.04	-.03	-.05	0.18	-.02	0.06	-.03	0.03	0.03	0.17	-.05	0.08	0.14	0.09	0.11	0.07	0.10	0.11	Mo
0.03	0.26	-.06	-.04	0.27	0.28	-.02	0.04	0.16	-.08	-.02	-.02	-.31	0.42	0.03	-.19	0.13	**0.54**	0.05	0.09	0.09	Mo*
0.31	0.44	-.01	-.05	0.40	-.06	0.38	-.01	0.27	0.17	0.17	**0.69**	0.41	0.31	**0.68**	0.14	0.40	0.19	**0.67**	0.49	0.35	Nb
0.70	**0.52**	0.08	-.03	**0.51**	0.13	0.40	-.04	0.14	0.44	0.06	**0.88**	0.34	0.36	**0.81**	0.17	0.36	0.16	**0.80**	**0.54**	0.17	Nd
0.53	0.05	0.38	0.02	0.22	0.09	**0.84**	-.03	-.37	**0.65**	0.16	0.19	**0.55**	0.09	0.17	**0.84**	-.21	-.17	0.02	**0.64**	**-.51**	Ni
	0.42	0.25	0.01	**0.52**	0.26	**0.53**	-.05	-.10	**0.64**	0.05	**0.64**	0.30	0.44	**0.55**	0.36	0.08	0.08	0.47	**0.52**	-.18	P*
		-.04	-.05	**0.65**	0.29	0.18	-.02	0.26	0.39	0.08	**0.59**	-.08	**0.57**	**0.58**	-.13	0.39	0.48	**0.59**	0.47	0.11	Pb
			0.22	0.05	0.15	0.37	-.08	-.27	0.19	0.10	0.06	0.30	0.09	0.17	0.42	-.08	-.12	0.01	0.18	-.34	Pd#
				-.14	0.11	0.10	0.05	0.01	-.04	-.05	-.08	0.05	-.09	-.04	0.13	0.04	-.03	-.01	0.03	-.01	Pt#
					0.22	0.23	-.05	-.01	**0.59**	0.09	**0.60**	-.16	**0.87**	**0.58**	-.12	0.20	0.46	**0.50**	**0.55**	-.09	Rb
						0.09	0.00	0.12	0.17	-.07	0.11	-.13	0.26	0.14	-.02	0.12	0.39	0.18	0.11	-.01	Sb*
							-.02	-.23	**0.55**	0.15	0.32	**0.62**	0.12	0.33	**0.85**	-.02	-.04	0.21	**0.69**	-.33	Sc
								0.05	-.08	0.07	-.05	-.02	-.03	-.04	-.02	0.02	0.02	-.04	-.03	0.03	Se
									-.29	-.08	0.22	-.16	0.00	0.26	-.32	0.49	0.40	0.43	-.10	**0.62**	Sn
										0.14	0.42	0.30	0.41	0.32	0.42	-.10	0.01	0.24	**0.63**	-.36	Sr
											0.08	0.12	0.08	0.07	0.12	-.04	-.03	0.01	0.15	-.04	Ta
												0.31	0.46	**0.90**	0.07	0.44	0.23	**0.86**	0.43	0.26	Th
													-.22	0.29	**0.75**	-.05	-.46	0.17	0.35	-.08	Ti
														0.47	-.20	0.17	0.46	0.38	0.41	-.07	Tl*
															0.09	0.49	0.27	**0.87**	0.42	0.24	U
																-.20	-.33	-.05	0.49	-.40	V
																	0.39	**0.61**	0.07	0.44	W
																		0.36	0.16	0.22	W*
																			0.36	0.38	Y
																				-.26	Zn
																					Zr
P*	Pb	Pd#	Pt#	Rb	Sb*	Sc	Se	Sn	Sr	Ta	Th	Ti	Tl*	U	V	W	W*	Y	Zn	Zr	